ESSAYS ON FORECASTING METHODS IN HIGH-FREQUENCY FINANCIAL ECONOMETRICS

by

WEIJIA PENG

A dissertation submitted to the

School of Graduate Studies

Rutgers, The State University of New Jersey

In partial fulfillment of the requirements

For the degree of

Doctor of Philosophy

Graduate Program in Economics

Written under the direction of

Norman Rasmus Swanson

And approved by

_____

_____

_____

_____

New Brunswick, New Jersey

May, 2020

ABSTRACT OF THE DISSERTATION

Essays on Forecasting Methods in High-Frequency Financial Econometrics

By WEIJIA PENG

Dissertation Director:

Norman Rasmus Swanson

This dissertation studies methodologies on forecasting methods in high-frequency financial econometrics. The dissertation consists of three chapters. In the first chapter, I develop novel latent uncertainty measures (i.e., latent factors) using both high dimensional and high frequency financial data as well as multi-frequency macroeconomic data. In particular, I introduce three factors which capture macroeconomic fundamentals, market uncertainty, and financial market stress. These factors are analyzed in a series of forecasting experiments. In the second chapter of my dissertation, I investigate importance of co-jumps for predicting equity return volatility. In particular, using high frequency financial data, I disentangle individual sector jumps and multiple sector co-jumps. Using this information, I construct new jump and co-jump variation measures, which are included in a series of real-time prediction experiments in order to evaluate the importance of co-jumps when predicting stock market return volatility. Finally, in my third chapter, I review recent theoretical and methodological advances in the area of volatility/risk estimation, and in

testing for jumps and co-jumps, using big data.

In chapter 2, we investigate the importance of co-jumps for predicting sector level equity return volatility. For our analysis we use the co-jump tests based on Barndorff-Nielsen and Shephard (2004), Jacod and Todorov (2009), and the jump test introduced in Huang and Tauchen (2005), in order to classify jumps in sector-level S&P500 exchanged-traded funds (ETF) as either idiosyncratic jumps or co-jumps. We find that co-jumps are more densely populated during the 2008 financial crisis and 2011 debt crisis periods. Also, co-jumps occur frequently, and have large magnitudes compared with idiosyncratic jumps. These different types of jumps are analyzed in the context of volatility prediction, using extensions of Heterogeneous Autoregressive models (i.e., HAR-RV-CJ models). Empirical results are promising. There are clear marginal predictive gains associated with including certain types of jumps in HAR regressions; and it is found that the predictive content of co-jumps is higher than that idiosyncratic jumps. This is not surprising, if one assumes that idiosyncratic jumps may be "more" exogenously driven, and hence less useful than co-jumps. In order to shed further light on the estimation of the co-jumps examined in our prediction experiments, we carry out Monte Carlo experiments that are designed to examine the relative performance of the three types of widely used co-jump tests (i.e., the BLT co-jump test of Bollerslev et al. (2008), the JT co-jump test of Jacod and Todorov (2009) and σ thresholding type tests based on bipower variation). Findings indicate that the JT co-jump test and the σ threshold test are more powerful, than the BLT co-jump test. However, there is also a distinct size trade-off when using the alternate tests.

In chapter3, we examine the usefulness of a large variety of machine learning methods for forecasting daily and monthly sector level equity returns. We also examine the usefulness of three new latent risk factors that are designed to capture key forecasting

information associated with financial market stress, market uncertainty, and macroeconomic fundamentals. The factors are variously based on the decomposition (using high frequency financial data) of the quadratic covariation between two assets into continuous and jump components, and the extraction of latent factors from mixed frequency state space models populated with nonparametrically estimated components of quadratic variation and/or low frequency macroeconomic data. In addition to constructing predictions using standard machine learning methods such as random forest, gradient boosting, support vector machine learning, penalized regression, and neural networks, among others, we also investigate the predictive performance of a group of hybrid machine learning methods that combine least absolute shrinkage operator and neural network specification methods. Overall, at the monthly frequency, we find that machine learning methods significantly improve forecasting performance, as measured using mean square forecast error (MSFE) and directional predictive accuracy rate (DPAR), relative to the random walk and linear benchmark alternatives. The "best" method is clearly the random forest method, which "wins" in almost all permutations at the monthly frequency, across all of the "target" variables that we predict. It is also worth noting that our hybrid machine learning methods often outperform individual methods, when forecasting daily data, although predictive gains associated with the use of any machine learning method are substantially reduced when forecasting at a daily versus monthly frequency. Finally, the novel uncertainty factors that we build are present in almost all of our "MSFE-best" and directional "accuracy-best" models, suggesting that the risk factors constructed using both high frequency financial data (e.g., 5-minute frequency S&P500 and sector ETF data) and aggregate low frequency macroeconomic data, are useful for predicting returns.

In recent years, the field of financial econometrics has seen tremendous gains in the amount of data available for use in modeling and prediction. Much of this data is very high frequency, and even 'tick-based', and hence falls into the category of what might

be termed "big data". The availability of such data, particularly that available at high frequency on an intra-day basis, has spurred numerous theoretical advances in the areas of volatility/risk estimation and modeling. In chapter 4, we discuss key such advances, beginning with a survey of numerous nonparametric estimators of integrated volatility. Thereafter, we discuss testing for jumps using said estimators. Finally, we discuss recent advances in testing for co-jumps. Such co-jumps are important for a number of reasons. For example, the presence of co-jumps, in contexts where data has been partitioned into continuous and discontinuous (jump) components, is indicative of (near) instantaneous transmission of financial shocks across different sectors and companies in the markets; and hence represents a type of systemic risk. Additionally, the presence of co-jumps across sectors, say, suggests that if jumps can be predicted in one sector, then such predictions may have useful information for modeling variables such as returns and volatility in another sector. As an illustration of the methods discussed in this paper, we carry out an empirical analysis of DOW and NASDAQ stock price returns.

Acknowledgements

I would like to thank my advisor, Professor Norman R. Swanson, for his enormous invaluable guidance on my research and vigorous support throughout my doctoral studies. I have been very fortunate to have such a great mentor who instructed me to conduct rigorous research and gave me the freedom to explore on my own. His encouragement and assistance are essential to me, especially during those hard times when I lost my ways in the scientific maze.

I am also deeply appreciative of my doctoral committee members: Professor Xiye Yang, Professor Yuan Liao, and Professor John C. Chao for their insights and suggestions on my dissertation. Professor Yang gave me many extraordinary suggestions based on his deep knowledge of econometric theory and finance. Professor Liao broadened my horizons on statistical theory and gave me sincere advice on my career development. I also thank Professor John C. Chao. for his kindness in serving as my outside committee member. I sincerely appreciate their time and efforts for serving on my committee.

I would like to express my thanks to Professor Roger Klein and Professor Marcelle Chauvet for suggestions on my dissertation and the job market. I would also like to thank the administrative staff Linda Zullinger and Janet Budge for their support.

Many thanks go to my friends and classmates in the department of economics at Rutgers for their help and company over the years.

Finally, I want to express my gratitude to my parents and my partner Chun Yao for their infinite support and understanding in the past years.

Dedication

To my parents

Table of Contents

List of Tables

List of Figures

Chapter 1

Introduction

Modeling and analyzing high-frequency financial data have received notable attention in the field of financial econometrics over the past years. As the advent of "big data" era rapidly expands the available information, a group of advanced methods has been evolved to process these "big data". The first part of this dissertation investigates methods for uncovering jump and co-jump activities among high-frequency financial variables, for the purpose of volatility forecasting. The second part of this dissertation focuses on the specification and construction of latent uncertainty measures that are designed to improve the forecasting accuracy of models used to forecast stock return variables.

In the second chapter entitled "Co-jumps, Co-jump Tests and Volatility Prediction Using the S&P 500", I examine the usefulness of jumps and co-jump variation measures for volatility forecasting of sector-level equity ETFs. As is well known, adequately accounting for volatility is crucial for successful portfolio management and risk hedging. Traditional latent volatility forecasting models such as GARCH, ARCH or more recent realized volatility models mainly use univariate information from the forecast target variable in the specification. We instead focus our attention on a new type of cross-sector information called co-jumps, which are based on price co-movements between the forecasting target variable and other assets. In our setup, as is standard in the literature, we assume that the log-price of an asset follows an Ito semi-martingale process, where co-jumps capture simultaneous jumps (discontinuous) components in multiple assets. Such jumps are meant to represent systemic risk across multiple assets, sectors, and markets. These co-jumps may be caused by outside shocks such as big news and changes in economic policy, for example; and they

can be expected to manifest as shocks that can cause financial market stress and thus influence market volatility. To identify co-jumps, I utilize extant jump and co-jump tests from the literature. I additionally carry out Monte Carlo simulations in order to examine relative performance of the currently most widely used co-jump tests. Perhaps not surprisingly, I find that co-jumps become more densely populated during the 2008 financial crisis and the 2011 European debt crisis, affirming the severity of financial stress during crisis periods. Moreover, I show, via a series of forecasting experiments that utilize heterogeneous autoregressive (HAR) models, that volatility forecasting accuracy can be significantly improved when univariate benchmark forecasting models are augments to include co-jump variation measures that quantify the linkages between stocks, industries and markets.

In the third chapter entitled "Forecasting Sector Level Equity Returns with Big Data Factors and Machine Learning Models" (joint with Chun Yao), we empirically explore the usefulness of a variety of machine learning methods for forecasting equity market activity. In particular, we add to the extant empirical finance literature by forecasting the level and direction of equity returns using methods including random forest, gradient boosting, support vector machine learning, penalized regression (shrinkage) and neural network (deep learning) to forecast (equity) returns. We also evaluate related machine learning classifier methods including latent discriminant analysis, naïve Bayes, support vector classifier, k-nearest-neighbors, and gradient boosting. Additionally, we propose and evaluate a group of hybrid two-step machine learning methods that combine the least absolute shrinkage (lasso) and neural networks. More specifically, we are interested in predicting daily and monthly S&P500 and various SPDR sector ETF returns including finance (XLF), technology (XLK), health care (XLV), and consumer discretionary (XLY). Relative performance of our various machine learning methods are compared against random walk and linear benchmark models using conditional Diebold-Mariano tests and Pesaran-Timmermann directional accuracy tests. Results indicate that machine learning models yield significantly lower mean square

forecasting error and higher correct directional forecasting rates than linear benchmark models when forecasting monthly returns for all of the above variables. The random forest model stands out as the overall best performing model in both level and directional forecasting, at a monthly level. Interestingly, deep learning methods (such as deep learning models with three or four hidden layers) outperform shallow learning models (such as deep learning models with one or two hidden layers) for level and directional prediction. Finally, the hybrid machine learning models, outperform many individual methods for both level and directional forecasting.

A key contribution of this paper is our use of big data to construct three latent factors that are designed to capture key forecasting information including macroeconomic fundamentals, market uncertainty, and financial market stress. As an example, our financial market stress factor is based on quantification of correlation between each sector and the S&P 500, which is viewed as critical given that price movements in different sectors tend to show signs of contagion during crisis periods. Our other two factors are constructed using the state-space model setup discussed in Aruoba et al. (2009). Interestingly, we find evidence of substantial forecasting improvements when these factors are included in our different forecasting models, indicating the usefulness of mapping the information in big datasets into a small number of key latent factors when forecasting at the market and sector level. Finally, it is worth noting that we also find that a market correlation index based on discontinuous jump components extracted from our data surges during the 2008 and 2011 financial crisis, and drops when market volatility is relatively low, while a correlation index based on continuous components moves in the opposite direction, except for the energy sector. This finding points to the potential usefulness of information obtained by decomposing returns data into jump and continuous components.

In recent years, the field of financial econometrics has seen tremendous gains in the

amount of data available for use in modeling and prediction. Much of this data is very high frequency, and even "tick-based", and hence falls into the category of what might be termed big data. The availability of such data, particularly that available at high frequency on an intra-day basis, has spurred numerous theoretical advances in the areas of volatility/risk estimation and modeling. In the fourth chapter entitled "Financial Econometrics and Big Data: A Survey of Volatility Estimators and Tests for the Presence of Jumps and Co-jumps" (with Arpita Mukherjee, Norman R. Swanson and Xiye Yang, Handbook of Statistics, Volume 42, 2020), we discuss key such advances, beginning with a survey of numerous nonparametric estimators of integrated volatility. Thereafter, we discuss testing for jumps using said estimators. Finally, we discuss recent advances in testing for co-jumps. Such co-jumps are important for a number of reasons. For example, the presence of co-jumps, in contexts where data has been partitioned into continuous and discontinuous (jump) components, is indicative of instantaneous transmission of financial shocks across different sectors and companies in the markets; and hence represents a type of systemic risk. Additionally, the presence of co-jumps across sectors, say, suggests that if jumps can be predicted in one sector, then such predictions may have useful information for modeling variables such as returns and volatility in another sector. As an illustration of the methods discussed in this paper, we carry out an empirical analysis of DOW and NASDAQ stock price returns.

Chapter 2

Co-Jumps, Co-Jump Tests and Sector Level S&P500 Volatility Prediction

2.1 Introduction

Effective stock volatility prediction remains a key goal for researchers in empirical finance. It is not surprising, thus, that the development of tests and other tools that can aid in said prediction remains at the forefront of theoretical research in the area. An example illustrating the importance of volatility prediction is portfolio management, where agents utilize such predictions when allocating assets and managing risk. Continuous-time models (e.g. stochastic volatility and related models) and discrete-time models (e.g. ARCH-GARCH models) are two important classes of models used to this effect. However, in certain contexts, these models have proven less than adequate for fitting and predicting returns and volatility. From the perspective of volatility prediction, this has led to a new class of models, called Heterogeneous Autoregressive models of Realized Volatility (HAR-RV). These models incorporate lag terms of volatilities over different time horizons, and have seen success in various empirical applications.

In this paper, we further explore the usefulness of these models when realized volatility type measures are decomposed into continuous and discontinuous (jump) components. In particular, we separate continuous from discontinuous (jump) components, and further classify resulting discontinuous components as idiosyncratic (individual asset type) jumps and multiple asset co-jumps. Our impetus for this decomposition is that while idiosyncratic jumps can, in theory, be diversified away in a weighted portfolio, failure to distinguish between idiosyncratic jumps and co-jumps can lead to dire consequences when

managing portfolios. An obvious consequence is analogous to the "correlation problem", where returns previously thought to evolve independently "line up" when large shocks perturb financial markets. Clearly, accurately detecting the number of different co-jumps is important, and disentangling jumps further, into idiosyncratic jumps and co-jumps may yield useful information for volatility prediction and in turn for portfolio allocation. In order to investigate the usefulness of our decomposition, co-jumps and jumps are included in predictive HAR-type regressions, to assess their relative marginal predictive content. Finally, given the importance of co-jump tests in our empirical analysis, we additionally carry out series of Monte Carlo experiments in order to examine the relative performance of a number of widely used co-jump tests.

In the volatility prediction literature, Andersen et al. (2003b) use realized volatility and construct a tri-variate VAR model in order to forecast the volatility of daily exchange rates. Corsi (2004) proposes the HAR-RV model that incorporates multiple frequencies of volatility in a parsimonious forecasting model. Andersen et al. (2007) separate jumps and continuous volatility components, and incorporate jumps in the so-called the HAR-RV-CJ model, for predicting realized volatility. Corsi et al. (2010) introduces the new threshold multipower variation estimator and a new jump test, and find that jumps play a significant role in predicting future volatility. Clements et al. (2014) find that incorporating co-jumps and jump intensities significantly improves predictive accuracy when forecasting realized volatility of a portfolio index. Finally, Duong and Swanson (2015) explore different jump variations, including signed jump power variation and truncated power variation, and find that marginal predictive content varies depending on which estimator is used in prediction experiments.

We add to the above literature on volatility prediction by specifying and estimating different versions of the HAR-RV-CJ model that incorporate both jumps and co-jumps

variables, for the purpose of forecasting S&P 500 sector level ETFs return volatility. Prediction horizons are $h = 1$ (one-day ahead), $h = 5$ (1-week ahead) $h = 22$ (1-month ahead). Our findings indicate that jumps and co-jumps both play important roles in the volatility forecasting. However, models with co-jumps results in higher explanatory power than models with jumps, when carrying out in-sample experiments. Moreover, this result also obtains when carrying out ex ante forecasting experiments, in which mean square forecasting errors (MSFEs) are used to assess the predictive performance of alternative models. These results are robust across all nine sector ETFs in the S&P 500, and also across all prediction horizons. One possible reason for this finding is simply that the magnitude of the variation and the frequency of occurence of co-jumps are both greater than that associated with idiosyncratic (single) jumps. Also, and as might be expected, our findings are consistent with the hypothesis that idiosyncratic jumps may be "more" exogenously driven, than co-jumps. Finally, again as should be expected, the number of co-jumps increased impressively during the 2008 financial crisis and the 2011 European debt crisis, consistent with the great deal of evidence suggesting that correlation across sectors increases during times of crisis.

While univariate jump tests have been researched extensively, the co-jump testing literature used in our empirical analysis is relatively nascent. One strand of the literature identifies co-jump based on the identification of jumps in a portfolio. For example, Bollerslev et al. (2008) use powers of observed returns to construct a test statistic for detecting co-jumps in an equi-weighted index constructed from 40 stocks. Their co-jump test detects the modest-sized common jumps ignored in the Barndorff-Nielsen and Shephard (2004) jump testing approach. Another strand uses univariate jump tests to identify co-jump in multivariate processes (see Gilder et al. (2014)). A third strand develops co-jump tests by direct examination of multiple price processes (see e.g., Jacod and Todorov (2009), Bandi

and Reno (2016), Bibinger and Winkelmann (2015) and Caporin et al. (2017)). For example, Jacod and Todorov (2009) propose co-jump tests based on two null hypotheses: (i) there are common jumps in a bivariate process; (ii) there are disjoint jumps in a bivariate process. Related papers in this literature include: Mancini and Gobbi (2012), Gnabo et al. (2014), Lahaye et al. (2011) and Dungey et al. (2011). As discussed above, we carry out Monte Carlo experiments in order to compare tests from these strands of the literature. These include the JT co-jump test in Jacod and Todorov (2009), BLT co-jump test in Bollerslev et al. (2008), and the σ thresholding type tests based on bipower variation discussed in Barndorff-Nielsen and Shephard (2004). As expected, we find that all co-jump tests perform better (i.e., larger power and more accurate size) under higher sampling frequencies. More importantly, JT co-jump test and the σ threshold test outperform the BLT test in terms of power and size, when there is a moderate number of series in the multivariate data generating process used in our experiments. Finally, it is found that the truncation approach of Mancini (2009), when implemented using prior weekly and monthly data to set the truncation level, mitigates the effects of volatility overestimation (when co-jump intensity is large), and thus mitigates a tendency of tests to under reject, as well as resulting in better sized tests. This finding is most pronounced when examining the finite sample performance of the σ threshold test.

The rest of this paper is organized as follows. Section 2.2 introduces the setup for our empirical analysis. Section 2.3 summarizes the co-jump tests examined in the paper, and Section 2.4 outlines our jump classification methods. Section 2.5 summarizes the setup of our forecasting experiments. Section 2.6 reports the results of our Monte Carlo experiments; and Section 2.7 including a description of the data used in our analysis, and discusses our empirical findings. Concluding remarks are contained in Section 2.8.

2.2 Setup

Let P_t be the log-price of an asset at time t. We assume P_t follows an Itô semimartingale process,

$$P_t = P_0 + \int_0^t b_s ds + \int_0^t \sigma_s dW_s + J_t \tag{2.1}$$

In the above equation, b_s is the drift part. W_s is a standard Brownian motion and J_t is a pure jump process:

$$J_t = \sum_{s \leqslant t} \Delta P_s \tag{2.2}$$

J_t is finite and $\Delta P_s := P_s - P_{s-}$, where $X_{s-} := \lim_{u \to s} X_u$, represents the possible jump of the process P at time s. Jump component J_t follows a compound Poisson process (CPP),

$$J_t = \sum_{i=1}^{N_t} Y_i \tag{2.3}$$

N_t is a Poisson process, representing the number of jumps in the interval [0,t]. The jump magnitudes $Y_i s$ are iid variables.

Consider a finite time horizon, $[0, t]$ that contains n high-frequency observations of the log-price process. A typical time horizon is one day. Let $\Delta = t/n$ be the sampling frequency. The intraday return of equidistant interval is:

$$r_i = P_{i\Delta_n} - P_{(i-1)\Delta_n} \tag{2.4}$$

In the high frequency literature, volatility of log-price is an unobserved variable. Quadratic variation is utilized to measure the variance of the process P_t. It is widely recognized that Realized Volatility (RV) is an error free estimator of quadratic variation. Namely:

$$RV_t \xrightarrow{\text{u.c.p.}} \int_0^t \sigma_s^2 ds + \sum_{s \leq T} (\Delta X_s)^2 = QV_t = IV_t + JV_t, \tag{2.5}$$

where u.c.p. denotes convergence in probability, uniformly in time. σ_s^2 is the intraday instantaneous volatility and Integrated volatility (IV_t) is the variation broken from the continuous component of the quadratic variation. RV is measured by the sum of intraday return square:

$$RV_t = \sum_{i=1}^{M} r_i^2 \tag{2.6}$$

where $RV_{i,t}$ denotes the realized volatility of P_t at day t. There are many estimators of IV and one of the examples is the multipower variations, which as defined as follows:

$$IV_t = \sum_{i=j+1}^{n} |r_i|^{r_1} |r_{i-1}|^{r_2} ... |r_{i-j}|^{r_j}, \tag{2.7}$$

where $r_1, r_2, ..., r_j$ are positive, such that $\sum_{i=1}^{j} r_i = k$. Barndorff-Nielsen and Shephard (2004) propose a bipower variation estimation BPV_t. Namely,

$$BPV_t = (\mu_1)^{-2} \sum_{i=2}^{n} |r_i||r_{i-1}| \tag{2.8}$$

where $\mu_1 = E(|Z|) = 2^{1/2}\Gamma(1)/\Gamma(1/2) = \sqrt{2/\pi}$, with Z a standard normal random variable, and $\Gamma(\cdot)$ denotes the gamma function.

2.3 Co-Jump Tests

In this section, we briefly summarize the jump testing methodology used in the sequel.

2.3.1 BLT Co-Jump Test

Bollerslev et al. (2008) propose a BLT test to detect co-jumps in a large ensemble of stocks. They develop a theoretical foundation which shows how only co-jumps (not idiosyncratic jumps) can be detected in a large equiweighted index. Let M denote the total number of

assets under co-jump detection. The BLT mean cross-product test statistic is defined as:

$$mcp_{t,i} = \frac{2}{M(M-1)} \sum_{j=1}^{M-1} \sum_{l=j+1}^{M} r_i^j r_i^l, i = 1, ..., n, t = 1, ..., T \tag{2.9}$$

where

$$r_i^j = P_{i\Delta_n}^j - P_{(i-1)\Delta_n}^j, \quad for \quad j = 1, ..., M \tag{2.10}$$

Since the mcp-statistic has nonzero mean and is analogous to a U-statistic, the studentized test statistic is:

$$z_{mcp,t,i} = \frac{mcp_{t,i} - \overline{mcp_t}}{s_{mcp,t}}, \quad for \quad i = 1, ..., n \quad and \quad t = 1, ..., T. \tag{2.11}$$

where

$$\overline{mcp_t} = \frac{1}{n} mcp_t = \frac{1}{n} \sum_{i=1}^{n} mcp_{t,i} \tag{2.12}$$

and

$$s_{mcp,t} = \sqrt{\frac{1}{n} \sum_{i=1}^{n} (mcp_{t,i} - \overline{mcp_t})^2} \tag{2.13}$$

The null distribution under the null hypothesis of no jump is derived from bootstrapping the test statistics $z_{mcp,t,i}$ using Monte Caro simulations.

2.3.2 JT Co-Jump Test

Jacod and Todorov (2009) construct two test statistics to identify co-jumps under two different null hypothesis: i. There is at least one common jump under the null hypothesis; ii. There is at least one disjoint jump under the null hypothesis. The test statistics are proposed for detecting co-jumps on bivariate processes for the path of $s \longrightarrow P_s$ on $[0, t]$. Co-jumps among multivariate processes can be detected from the combination of bivariate

processes. The test statistics of the common jump $\Phi_n^{(j)}$ and disjoint jump $\Phi_n^{(d)}$ are defined as:

$$\Phi_n^{(j)} = \frac{V(f, k\Delta_n)_t}{V(f, \Delta_n)_t} \tag{2.14}$$

$$\Phi_n^{(d)} = \frac{V(f, \Delta_n)_t}{\sqrt{V(g_1, \Delta_n)_t V(g_2, \Delta_n)_t}} \tag{2.15}$$

where k is an integer greater than 1, and $\Delta_n = \frac{t}{n}$ is the length of equispaced intra-daily time interval. $V(f, k\Delta_n)_t$ is defined as:

$$V(f, k\Delta_n)_t = \sum_{i=1}^{[t/k\Delta_n]} f(P_{i\Delta_n} - P_{(i-1)\Delta_n}) \tag{2.16}$$

Where the functions for $f(x)$, $g_1(x)$ and $g_2(x)$ are defined as:

$$f(x) = (x_1 x_2)^2, g_1(x) = (x_1)^4, g_2(x) = (x_2)^4 \tag{2.17}$$

They propose asymptotic properties and central limit theorems of these two test statistics when the mesh Δ_n approaches 0. They show that the test statistics for the null hypothesis with disjoint jumps $\Phi_n^{(d)}$ converges stably in law to 0 on $\Omega_T^{(d)}$ and the null hypothesis with common jumps $\Phi_n^{(j)}$ converges stably in law to 1 on $\Omega_T^{(d)}$. Here $\Omega_T^{(j)}$ and $\Omega_T^{(d)}$ are defined as:

$$\Omega_T^{(j)} = \{\omega\text{: on } [0,t] \text{ the process } r_i^1 r_i^2 \text{ is not identically } 0\} \tag{2.18}$$

$$\begin{aligned}\Omega_T^{(j)} = \{\omega\text{: on } [0,t] \text{ the processes } r_i^1 \text{ and } r_i^2 \text{ are} \\ \text{not identically 0, but the process } r_i^1 r_i^2 \text{ is}\}\end{aligned} \tag{2.19}$$

Where $r_i^j = P_{i\Delta_n}^j - P_{(i-1)\Delta_n}^j$, for $j = 1, 2$ and $i = 1, ..., n$. The authors construct critical regions of the two statistics as:

$$C_n^{(j)} = \{|\Phi_n^{(j)} - 1| \geq c_n^{(j)}\} \tag{2.20}$$

$$C_n^{(d)} = \{\Phi_n^{(d)} \geq c_n^{(d)}\} \tag{2.21}$$

where $c_n^{(j)} = \hat{V}_n^{(j)}/\sqrt{\alpha}$ and $c_n^{(d)} = \hat{V}_n^{\prime(d)}/\alpha$. α is the significance level in the test. $\hat{V}_n^{(j)}$ is defined as:

$$\hat{V}_n^{(j)} = \frac{\sqrt{\Delta_n(k-1)\hat{F}_t^{\prime n}}}{V(f, \Delta_n)_t} \tag{2.22}$$

where $\hat{F}_t^{\prime n}$ is:

$$\hat{F}_t^{\prime n} = \frac{2}{k_n \Delta_n} \sum_{i=1+k_n}^{[t/\Delta_n]-k_n-1} \sum_{m \in I_n(i)} (r_i^1)^2 (r_i^2)^2 \times (r_i^1 r_m^2 + r_m^1 r_i^2)^2 1_{\{|r_i| > \alpha\Delta_n^\omega, |r_m| \leq \alpha\Delta_n^\omega\}} \tag{2.23}$$

where $I_n(i) = I_{n,-}(i) \cup I_{n,+}(i)$ and $I_{n,-} = i - k_n, i - k_n + 1, ..., i - 1$ if $i > k_n$ and $I_{n,+}(i) = i + 2, i + 3, ..., i + k_n + 1$. $\hat{V}_n^{(\prime d)}$ is defined as:

$$\hat{V}_n^{(\prime d)} = \frac{\Delta_n \hat{F}_t^n + \hat{A}_T^{\prime n}}{V(g_1, \Delta_n)_t V(g_2, \Delta_n)_t} \tag{2.24}$$

where $\hat{F}_t^n$ is:

$$\hat{F}_t^n = \frac{2}{k_n \Delta_n} \sum_{i=1+k_n}^{[t/\Delta_n]-k_n-1} \sum_{m \in I_n(i)} ((r_i^1)^2 (r_m^2)^2 + (r_m^1)^2 (r_i^2)^2) \times 1_{\{|r_i| > \alpha\Delta_n^\omega, |r_m| \leq \alpha\Delta_n^\omega\}} \tag{2.25}$$

and $\hat{A}_t^{\prime n}$ is:

$$\hat{A}_t^{\prime n} = \frac{1}{\Delta_n} \sum_{i=1}^{t/\Delta_n} f(r_i) 1_{\{|r_i| \leq \alpha\Delta_n^\omega\}} \tag{2.26}$$

The local window $k_n = 1/\sqrt{\Delta_n}$ and the truncation level of $\alpha\Delta_n^\omega = 0.03 \times \Delta_n^{0.49}$.

2.3.3 σ Threshold Co-Jump Test

Integrated volatility is used to construct thresholds to detect jumps in each univariate process. To measure integrated volatility , bipower variation is widely used in the literature. The standardized realized Bipower variation (BPV), introduced by Barndorff-Nielsen and Shephard (2004), is denoted as:

$$BV_t(\Delta) \equiv \mu_1^{-2} \sum_{j=2}^{1/\Delta} \mid r_j \mid\mid r_{j-1} \mid \tag{2.27}$$

where $\mu_1 \equiv \sqrt{2/\pi}$ is the mean of the absolute value of standard normally distributed random variable and $\Delta = \frac{1}{n}$. Threshold σ is defined as:

$$\sigma_t = \sqrt{\frac{1}{(\frac{1}{\Delta} - 1)} \times BV_t} \tag{2.28}$$

$$\tag{2.29}$$

We use σ_t to calculate the averaged daily standard deviation threshold:

$$\sigma = \frac{1}{T} \sum_{t=1}^{T} \sigma_t \tag{2.30}$$

where T is the number of replications of the sample path. In terms of choosing optimal threshold level, we apply 5σ to identify jumps in each univariate process and then identify co-jumps among multivariate processes.

2.3.4 Truncation

When applying co-jump tests on simulated price series with co-jumps, we need to pay special attention to the simulation cases with notably large co-jump intensity. Under large co-jump intensity, one problem is how to estimate volatility level, which can be overestimated and lead to under rejection of the null of no co-jumps. The truncation approach introduced here, by incorporating previous weekly or monthly data to set the truncation

level, can solve the over-estimated volatility problem. To determine the truncation level of α_n, we use the following iteration procedure in Mancini (2009):

- Use Bipower variation to obtain an initial estimate of integrated volatility (IV)
- Set the initial truncation value of α_n as

$$\alpha_n^{(0)} = C \times (\frac{1}{t} I\hat{V}_t^{(0)})^{1/2} \times \Delta_n^{\omega} \tag{2.31}$$

  Here C is a tuning parameter range around $[1, 6]$ and should be kept as small as possible to get the optimal truncation level. ω is set to 0.49.

- With $\alpha_n^{(i-1)}$ determined, use the truncated version of Bipower variation to obatain new estimate of IV, denoted by $I\hat{V}_i^{(i)}$. Then let

$$\alpha_n^{(i)} = C \times (\frac{1}{t} I\hat{V}_t^{(i)})^{1/2} \times \Delta_n^{\omega} \tag{2.32}$$

- Repeat last step until $\mid I\hat{V}_t^{(i)} - I\hat{V}_t^{(i-1)} \mid$ is smaller than $0.05 I\hat{V}_t^{(i-1)}$.

2.4 Jump and Co-Jump Classification and Measurement

2.4.1 Jump and Co-Jump Classification

The S&P 500 index has over 500 stock components and most of them are traded on NYSE and NASDAQ. It can be seen as one of the most common financial indicators of the U.S. economy. Based on Global Industry Classification Standard(GICS), the S&P 500 index has 11 sectors according to constituent classifications, including consumer discretionary sector, consumer staples sector, energy sector, financial sector, financial service sector, health care sector, industrials sector, materials sector, real estate sector, technology sector and utilities sector. Each sector is composed of different stocks in S&P 500. Table 2.6 shows details about the 11 sectors in S&P 500 and the number of constituents in each sector.

In the high-frequency financial econometrics, the return of S&P500 index can be further decomposed into a continuous component and a jump (discontinuous) component. The continuous part is usually driven by some fundamental trends in the business cycle, and the jump part is usually caused by some outside shocks, such as the release of unexpected economic policy. Müller et al. (1993) propose the Heterogeneous Market Hypothesis, which argues that variation from jump components are caused by the heterogeneity reaction of the agents among different markets.

In this paper, we want to further classify the heterogeneity reactions of agents based on the connection between different markets, and study their effects on the market volatility separately. Therefore, we classify the jump in each sector as either a co-jump or a single jump. Co-jumps are defined as jumps occurring simultaneously on more than or equal to two sectors returns of the S& P 500 index. Single jumps are defined as jumps happening in only one sector return of the S&P 500 during the intraday time interval. Co-jumps among different sectors can be viewed as a market 'lining up', which is usually driven by the systemic risk among markets. Co-jumps is a measurement of the correlation among different connected sectors. Single jumps represent sector individual shocks, which is usually driven by the idiosyncratic risks in each sector. The co-jumps and single jumps cover different types of risks, and thus influence the market in different channels. Also, since S&P 500 has 11 sectors, we can identify co-jumps among the different number of sectors, ranging from two sectors co-jumps to 11 sectors co-jumps.

2.4.2 Jump and Co-Jump Measurement

Barndorff-Nielsen and Shephard (2004) prove integrated variance can be estimated by realized bipower variation(BPV) under special cases and the quadratic variation of the jump can be calculated by the difference of RV and realized BPV. Followed Andersen et al.

(2007), the realized bipower variation in general form is:

$$BV = \mu_r^{-1}\mu_{2-r}^{-1}\{r_n^j\}^{[r,2-r]} \tag{2.33}$$

where

$$\mu_r = 2^{r/2}\frac{\Gamma(\frac{1}{2}(r+1))}{\Gamma(\frac{1}{2})} \tag{2.34}$$

In this paper, we focus on the special case when $r = 1$, then,

$$BPV_t = (\mu_1)^{-2}\sum_{i=2}^{n}|r_i||r_{i-1}| \tag{2.35}$$

where $\mu_1 = E(|Z|) = 2^{1/2}\Gamma(1)/\Gamma(1/2) = \sqrt{2/\pi}$. The realized bipower variation is an asymptotic estimation of continuous component variation. Then the jump component variation is:

$$J_t = RV_t - BV_t \tag{2.36}$$

Since the sampling interval in the empirical analysis is finite ($\Delta>0$), J_t can be negative in some cases. Andersen et al. (2007) suggest to exclude the negative value of the estimates and truncate the jump measurements at 0,

$$J_t = max[RV_t - BV_t, 0] \tag{2.37}$$

The theoretical framework for jump measurement is based on the increasingly finer sampling interval. Under the finite sampling intervals, there will be some measurement errors. Andersen et al. (2007) proposes a theoretical framework that treats small jumps as a continuous component, leaving only large jumps in jump measurement. They identify jumps variations with the newly proposed method as:

$$J_t \equiv I[Z_t>\Phi_\alpha]\cdot[RV_t - BV_t], \tag{2.38}$$

and new continuous component variations as:

$$C_{i,t} \equiv I[Z_t \leqslant \Phi_\alpha] \cdot RV_t + I[Z_t > \Phi_\alpha] \cdot BV_t \tag{2.39}$$

where Φ_α is the critical value for the ratio-statistic $Z_t$for the joint bivariate distribution from Huang and Tauchen (2005),

$$Z_t \equiv \Delta^{-1/2} \times \frac{[RV_t - BV_t]RV_t^{-1}}{[(\mu_1^{-4} + 2\mu_1^{-2} - 5)max\{1, TQ_t BV_t^{-2}\}]^{1/2}} \tag{2.40}$$

where Δ is the intraday time interval and TQ_t denotes standardized realized tripower quarticity measure:

$$TQ_t \equiv \Delta^{-1}\mu_{4/3}^{-3} \sum_{j=1}^{M-2} \mid r_j \mid^{4/3} \mid r_{j+1} \mid^{4/3} \mid r_{j+2} \mid^{4/3} \tag{2.41}$$

We further classify co-jump and single jumps variations by applying 5σ co-jump test. Thus, we generate indicators for co-jumps and single jumps as $I_{co-jump}$ and I_{sjump}. Co-jumps variations are defined as:

$$J_t^{co-jump} = J_t * I_{co-jump} \tag{2.42}$$

And single jumps variation are defined as:

$$J_t^{sump} = J_t * I_{sjump} \tag{2.43}$$

The ratio of co-jumps contributions to total variations is calculated as:

$$ratio^{co-jump} = \frac{J_t^{co-jump}}{RV_t} \tag{2.44}$$

And the ratio of single jumps contributions to total variations is calculated as:

$$ratio^{co-jump} = \frac{J_t^{sjump}}{RV_t} \tag{2.45}$$

2.5 Experimental Setup and Forecasting Methods

Müller et al. (1997) construct a HARCH model from the Heterogeneous Market Hypothesis. Based on this idea, Corsi (2004) proposes HAR-RV models incorporating different kinds of market volatilities over different time horizons. One simple version of the HAR-RV model is:

$$RV_{t+1d}^{(d)} = c + \beta^{(d)} RV_t^{(d)} + \beta^{(\omega)} RV_t^{(\omega)} + \beta^{(m)} RV_t^{(m)} + \omega_{t+1d}, \tag{2.46}$$

Andersen et al. (2007) separate jumps from continuous part and design a new HAR-RV-CJ prediction model that incorporates jumps and lag terms of realized volatilities and jumps over different time horizons. The multiperiod jump measurement is defined as the average value of jumps over time h:

$$J_{t,t+h} = h^{-1}[J_{t+1} + J_{t+2} + ... + J_{t+h}] \tag{2.47}$$

The multiperiod continuous part measurement is defined as the average value of continuous component over time h:

$$C_{t,t+h} = h^{-1}[C_{t+1} + C_{t+2} + ... + C_{t+h}] \tag{2.48}$$

The HAR-RV-CJ model is shown as:

$$\begin{aligned} RV_{t,t+h} = \beta_0 + \beta_{cd} C_t + \beta_{cw} C_{t-5,t} + \beta_{cm} C_{t-22,t} + \beta_{jd} J_t \\ + \beta_{jw} J_{t-5,t} + \beta_{jm} J_{t-22,t} + \epsilon_{t,t+h} \end{aligned} \tag{2.49}$$

where C_t is the continues component and J_t is the discontinuous part for jumps. C_t, $C_t - 5$ and $C_t - 22$ are lag term estimators for $h = 1$, $h = 5$ and $h = 22$.

In this paper, we extend the HAR-RV-J model by classifying co-jumps (CJ_t) and single jumps (SJ_t), and then incorporated co-jumps and single jumps into the HAR-RV-CJ models.

Specification 1: HAR-RV-CJ model with co-jumps (CJ_t):

$$RV_{t,t+h} = \beta_0 + \beta_{cd}C_t + \beta_{cw}C_{t-5,t} + \beta_{cm}C_{t-22,t} + \beta_{jd}CJ_t + \beta_{jw}CJ_{t-5,t} + \beta_{jm}CJ_{t-22,t} + \epsilon_{t,t+h}$$

Specification 2: HAR-RV-SJ model with single jumps (SJ_t):

$$RV_{t,t+h} = \beta_0 + \beta_{cd}C_t + \beta_{cw}C_{t-5,t} + \beta_{cm}C_{t-22,t} + \beta_{jd}SJ_t + \beta_{jw}SJ_{t-5,t} + \beta_{jm}SJ_{t-22,t} + \epsilon_{t,t+h}$$

Specification 3: HAR-RV-SJ model with single jumps (SJ_t) and co-jumps (CJ_t):

$$\begin{aligned} RV_{t,t+h} = \beta_0 + \beta_{cd}C_t + \beta_{cw}C_{t-5,t} + \beta_{cm}C_{t-22,t} + \beta_{jd}SJ_t + \beta_{jw}SJ_{t-5,t} + \beta_{jm}SJ_{t-22,t} \\ +\beta_{jd}CJ_t + \beta_{jw}CJ_{t-5,t} + \beta_{jm}CJ_{t-22,t} + \epsilon_{t,t+h} \end{aligned}$$

To explore casualty effects of jumps, lag terms of jumps are incorporated into the HAR-RV-CJ model. The lag terms for co-jumps are CJ_t, CJ_{t-5} and CJ_{t-22}. The lag terms for single jumps are SJ_t, SJ_{t-5} and SJ_{t-22}. These lag terms are added into HAR-RV-CJ model, which explains daily, weekly and monthly lag regression terms. Standard deviation and logarithmic form are also used under prediction horizons h=1 for one day, 5 for one week and 22 for one month. We use a rolling window size 200 to estimate MSFEs in each sector constituents in the S&P 500 market.

2.6 Monte Carlo Experiments

Monte Carlo experiments were carried out in order to evaluate the finite sample properties of: (i) The BLT co-jump test under the null of co-jumps; (ii) The 5σ threshold under the null hypothesis of co-jumps; (iii) The JT[1] test under the null hypothesis of co-jumps; and (vi) All three co-jump tests with truncation approach under the null hypothesis of co-jumps.

[1]We choose test statistic Φ_n^d in the JT test

The Data Generating Process (DGP)[2] of each component is specified as :

$$dlnX_t^{(i)} = \mu dt + \sqrt{V_t^{(i)}} dW_{1,t}^{(i)} + dJ_t^{(i)}, \tag{2.50}$$

$$dV_t^{(i)} = \kappa_v(\theta_v - V_t^{(i)})dt + \zeta\sqrt{V_t^{(i)}} dW_{2,t}^{(i)} \tag{2.51}$$

where in the expression above the volatility is described as a square-root process. Leverage effects for $X^{(i)}$ are characterized by $corr(dW_1^{(i)}, dW_2^{(i)}) = \rho$. The jump component $J_t^{(i)}$ is simulated as a compound Poisson process N_t with intensity λ_i:

$$J_t^{(i)} = \sum_{j=1}^{N_t} Y_j \tag{2.52}$$

where Y_j are independently and identically drawn from a normal distribution. We also consider the microstruction noise in our Monte Carlo experiments. Following Zhang et al. (2005), the observed return process is assumed to be in the form:

$$Y_{t_i} = X_{t_i} + \epsilon_{t_i} \tag{2.53}$$

where X_t is the real price of an asset. ϵ_{t_i} is independent identically distributed with $E\epsilon_{t_i} = 0$ and $var(\epsilon_{t_i}) = E\epsilon^2$. We also assume ϵ_{t_i} is independent with $X_t^{(i)}$ process. The modeling setup does not require ϵ_{t_i} existing for every t_i. Therefore, we only add noise with observations under specific sampling frequency. Under the null hypothesis of co-jumps, we simulate a single jump and add it to all simulated asset prices as co-jumps among multiple assets prices.

Table 2.1 shows the parameter settings in the Monte Carlo experiments. We follow the parameter settings from Huang and Tauchen (2005) and Corradi et al. (2015), with larger jump intensity. This is because jump intensity varies largely before and post-financial crisis and one of our Monte Carlo simulation objectives is to compare these test performances

[2]We simulate observations using the Milstein discretization scheme.

before and after this period. Table 2.2 shows details for each data generating process with 1000 replications. We simulate $N = 10$ processes for each DGP. The two intra-daily sampling frequencies: $\Delta = 1/78$ and $\Delta = 1/390$ represent 5-minute and 1-minute sampling frequencies.

Table 2.3 shows the empirical power of co-jump tests. The significance level is set as 10% for all co-jump tests. The σ threshold method and the JT co-jump test have larger powers compared to the BLT co-jump test. As noted in the table 2.3, the range of empirical power of the BLT test is from 0.996 to 0.910, while the range of σ threshold is from 1.000 to 0.968 and the JT test is from 1.000 to 0.995. Jump intensity affects the empirical power of the co-jump tests negatively. In BLT co-jump test, σ threshold, and JT co-jump test, increasing jump intensity lowers the empirical power of co-jump tests. For example in DGP 1 and 2, as jump intensity λ increases from 0.3 to 2.0, the empirical power of BLT co-jump test drops from 0.983 to 0.963, and σ threshold drops from 1.000 to 0.999, and JT test drops from 1.000 to 0.997. Adding microstructure noise into the DGP process generally reduces the empirical power. For example, the power of the BLT co-jump test with microstructure noise (e.g. DGP 2) is slightly larger than the DGPs without microstructure noise(e.g. DGP 18). Additionally, the empirical power of all co-jump tests is positively associated with jump magnitude (e.g DGPs 5 and 7, DGPs 6 and 8). Table 2.14 shows the empirical power of three co-jump tests under the truncation approach. The truncation approach does not affect the power of the JT co-jump test, and generally increases the empirical power of σ threshold method.

Table 2.5 shows the empirical size of co-jump tests. The nominal size is set as 10% for all three co-jump tests. The BLT test has the largest size compared with all other co-jump tests under all DGPs. For example in DGP12, the empirical size for the BLT test is 0.0613, which is the largest value compared with the empirical size of 0.0002 in the σ threshold,

and 0.0000 in the JT co-jump test. Jump intensity affects the empirical size of the co-jump tests in different directions. In the BLT co-jump test, increasing jump intensity lowers the empirical size of co-jump tests, while the effect is reversed in the σ threshold and JT co-jump test. Adding microstructure noise into the DGP process increases the empirical size in most cases. For example, the size of the BLT co-jump test without microstructure noise (e.g. DGP 17) is smaller than the DGPs with microstructure noise(e.g. DGP 1). Additionally, the empirical power of all co-jump tests is negatively associated with jump magnitude (e.g DGPs 5 and 7, DGPs 6 and 8). Table 2.6 shows the empirical size of co-jump tests with the truncation approach. The truncation approach does not affect the empirical size of the JT co-jump test, but it lowers the empirical size of the σ threshold method.

2.7 Empirical Findings

2.7.1 Data Description

The data for SPDR S&P 500 ETF and 9 sectors ETFs cover the periods from January 1st, 2006 to December 31st, 2013 for a total of 2013 days. For measuring the price variation of the S&P 500 index, SPDR S&P 500 ETF is selected. The sources of 9[3] sectors ETFs daily observations and SPDR S&P 500 ETF are from Trade and Quote Database (TAQ) through Wharton Research Data Service(WRDS). We select trade data ranging from 9:30 am to 4 pm on a regular day and ignore time outside this range. Outliers are eliminated from our dataset.

[3]Data from Financial Service and Real Estate sector are not available from WRDS.

For sampling frequency, the current literature discussed the performance under sampling of different frequencies. Hansen and Lunde (2006) demonstrates a kernel-based estimator for integrated variance dominates realized volatility for considering the characteristics of market microstructure noise. Bandi and Russell (2008) shows market microstructure noise bias can be reasonably reduced by variance reduction from appropriately high-frequency sampling. We use the 30-second sampling frequency and the total observations for a day with 30-second sampling frequency is 780. We clean the high-frequency data and apply the truncation approach in section 2.3.4 to eliminate the microstructure noise. The previous tick method derived from Gençay et al. (2001) is used to filter out price data.

2.7.2 Co-Jumps in the S&P 500

Table 2.7 shows summary statistics for single jumps and co-jumps over nine sectors in the S&P 500, including material sector (XLB), energy sector (XLE), financial sector (XLF), industrial sector (XLI), technology sector (XLK), consumer staple sector (XLP), utility sector (XLU), health care sector (XLV), and consumer discretionary sector (XLY). The second and fifth rows show proportions of single jumps and co-jumps[4] over total numbers of single jumps and co-jumps. It is noteworthy that proportions for co-jumps are always larger than single jumps among all sectors. The financial sector (XLF) has the largest proportions of 67.18% which suggests the financial sector has closer linkage with other sectors. The utility sector has the smallest proportions of 54.79%. Co-jump magnitudes are also larger than single jumps, based on the mean and standard deviations of co-jumps and single jumps variations. This is consistent since co-jumps are usually caused by larger shocks happening simultaneously among multiple sectors. Single jumps are usually caused by relatively smaller shocks. In this way, co-jumps usually have larger magnitude compared with single

[4]The proportions exclude those negative values to ensure all of the estimates for single jump and co-jumps parts are nonnegative.

jumps in terms of shock sizes. The financial sector has both the largest magnitude and proportion for co-jumps.

Multiple sectors in S&P 500 market become closely correlated in recent times. The 2008-2009 financial crisis and the 2011 European debt crisis are examples to show these market linkages. Figure 2.1 shows total co-jump numbers in S&P 500 market from 2006 to 2013. From top to bottom panels are the number of three-sector co-jumps, four-sector co-jumps, five-sector co-jumps, six-sector co-jumps, seven-sector co-jumps, eight-sector co-jumps, and nine-sector co-jumps. We can see clearly that 2008 and 2011 have the largest number of co-jumps compared with other periods. This confirms the observations that co-jumps happen more frequently during crisis periods when markets become more correlated.

Figure 2.2 plots co-jump and single jump contribution to total variation from the year 2006 to 2013 for each sector[5]. We identify co-jumps variation between the post and pre-financial crisis periods and further find co-jumps are more linked with the 2008 financial crisis and 2011 European debt crisis. Co-jumps have larger variation when compared with single jumps among all nine sectors. Co-jumps also have higher total variation during the 2008 financial crisis and the 2011 European Debt crisis, which also reflects market correlation increasing during crisis periods. These sector co-jumps tend to happen when the market is influenced by some large exogenous shocks.

2.7.3 Co-Jumps in Realized Volatility Prediction

Table 2.9-2.17 shows the in-sample HAR-RV-CJ prediction regressions with co-jumps and single jumps over different sectors in S&P 500 market. We only report the tables for energy, financial and technology sectors here. For coefficients of the continuous part variations, most coefficients are statistically significant for β_{cd}, β_{cw} and β_{cm}. For coefficients of single

[5]We use a 21-day moving average to smooth out the variations

jumps variations, most of the coefficients are statistically insignificant for β_{jd} and β_{jm}. The coefficient of co-jumps variations β_{jd} is statistically significant for all models at prediction horizon $h = 1$. In comparing R^2, the logarithmic model fits better than standard deviation modes. Standard deviation models fit better than linear models. R-square in our sector ETFs prediction regression is significantly high, even most cases are over 0.7. R-square for HAR models with co-jumps is larger than HAR models with single jumps. This suggests that co-jumps are relatively more important in the context of volatility prediction when compared with single jumps. Co-jumps reflect market co-movement which is not contained in individual single jumps and therefore contains more market information. The financial sector has the largest in sample R-square compared with other sectors, which suggests the financial market is more connected with other sectors in the S&P 500 market.

Tables 2.18, 2.19 and 2.20 show the square root of mean forecasting error (MSFE), In-Sample R^2 and Out-of-Sample R^2 for HAR-RV-CJ models with co-jumps and single jumps. Rolling window size 200 is used to estimate MSFEs in each sector constituents in S&P 500 market. Results show that HAR models with co-jumps outperform HAR models with single jumps over all sectors, in terms of MSFEs, regardless of prediction horizon and model formation. The MSFE difference between co-jumps and single jumps is larger in the financial sector compared with other sectors, which indicates the co-jumps are more densely populated among the financial sector and also with a larger magnitude. Square root model wins over the linear model and the log model based on the MSFEs. Linear models outperform the log models.

2.8 Concluding Remarks

In this paper, I investigate the importance of co-jumps for predicting equity return volatility. In particular, using high-frequency financial data, I disentangle individual sector jumps

and multiple sector co-jumps. Using this information, I construct new jumps and co-jumps variation measures, which are included in a series of real-tome prediction experiments to evaluate the importance of co-jumps when prediction stock market return volatility. Additionally, Monte Calor simulations are utilized to conduct power and size analysis to evaluate the performance of three widely used co-jump tests. Different scenarios including various jump intensities, jump magnitudes, microstructure noise, and significance levels are discussed in the paper. The co-jump test is further utilized to identify co-jumps and single jumps among nine sectors in the S&P 500 market, using the sectors ETFs price data. We extend the HAR-RV forecasting models by including co-jumps and single jumps variations and show the usefulness of co-jumps variation in the context of volatility prediction. These interesting findings provide a guideline for design trading strategies in the stock markets.

Table 2.1: Monte Carlo Experiments - Parameter Settings*

Jump Intensity	$\lambda = \{0.3, 2.0\}$
Microstructure Noise	$\epsilon \sim i.i.d. \quad N(0, 0.0005^2)$
Leverage Effect	$\rho = \{0, -0.5\}$
Jump Distribution	$\sigma_{jump} = \{0.5, 2.5\}$
Sampling Frequency	$\Delta_n = \{\frac{1}{78}, \frac{1}{390}\}$
Other Parameters	$\mu, \kappa_v, \theta_v, \zeta, N = \{0.05, 5, 0.16, 0.5, 10\}$

*Notes: N is the number of simulation series. $\frac{1}{78}$ is five-minute sampling frequency and $\frac{1}{390}$ is one-minute sampling frequency. See section 2.6 for complete details.

Table 2.2: Monte Carlo Experiments -Data Generating Process*

	ϵ	λ	ρ	σ_{jump}	Δ_n	μ	κ_v	θ_v	ζ	N
DGP1	+	0.3	-0.5	0.5	$\frac{1}{390}$	0.05	5	0.16	0.5	10
DGP2	+	2.0	-0.5	0.5	$\frac{1}{390}$	0.05	5	0.16	0.5	10
DGP3	+	0.3	-0.5	2.5	$\frac{1}{390}$	0.05	5	0.16	0.5	10
DGP4	+	2.0	-0.5	2.5	$\frac{1}{390}$	0.05	5	0.16	0.5	10
DGP5	+	0.3	0.0	0.5	$\frac{1}{390}$	0.05	5	0.16	0.5	10
DGP6	+	2.0	0.0	0.5	$\frac{1}{390}$	0.05	5	0.16	0.5	10
DGP7	+	0.3	0.0	2.5	$\frac{1}{390}$	0.05	5	0.16	0.5	10
DGP8	+	2.0	0.0	2.5	$\frac{1}{390}$	0.05	5	0.16	0.5	10
DGP9	+	0.3	0.0	0.5	$\frac{1}{78}$	0.05	5	0.16	0.5	10
DGP10	+	2.0	0.0	0.5	$\frac{1}{78}$	0.05	5	0.16	0.5	10
DGP11	+	0.3	0.0	2.5	$\frac{1}{78}$	0.05	5	0.16	0.5	10
DGP12	+	2.0	0.0	2.5	$\frac{1}{78}$	0.05	5	0.16	0.5	10
DGP13	+	0.3	-0.5	0.5	$\frac{1}{78}$	0.05	5	0.16	0.5	10
DGP14	+	2.0	-0.5	0.5	$\frac{1}{78}$	0.05	5	0.16	0.5	10
DGP15	+	0.3	-0.5	2.5	$\frac{1}{78}$	0.05	5	0.16	0.5	10
DGP16	+	2.0	-0.5	2.5	$\frac{1}{78}$	0.05	5	0.16	0.5	10
DGP17	-	0.3	-0.5	0.5	$\frac{1}{390}$	0.05	5	0.16	0.5	10
DGP18	-	2.0	-0.5	0.5	$\frac{1}{390}$	0.05	5	0.16	0.5	10
DGP19	-	0.3	-0.5	2.5	$\frac{1}{390}$	0.05	5	0.16	0.5	10
DGP20	-	2.0	-0.5	2.5	$\frac{1}{390}$	0.05	5	0.16	0.5	10
DGP21	-	0.3	0.0	0.5	$\frac{1}{390}$	0.05	5	0.16	0.5	10
DGP22	-	2.0	0.0	0.5	$\frac{1}{390}$	0.05	5	0.16	0.5	10
DGP23	-	0.3	0.0	2.5	$\frac{1}{390}$	0.05	5	0.16	0.5	10
DGP24	-	2.0	0.0	2.5	$\frac{1}{390}$	0.05	5	0.16	0.5	10
DGP25	-	0.3	0.0	0.5	$\frac{1}{78}$	0.05	5	0.16	0.5	10
DGP26	-	2.0	0.0	0.5	$\frac{1}{78}$	0.05	5	0.16	0.5	10
DGP27	-	0.3	0.0	2.5	$\frac{1}{78}$	0.05	5	0.16	0.5	10
DGP28	-	2.0	0.0	2.5	$\frac{1}{78}$	0.05	5	0.16	0.5	10
DGP29	-	0.3	-0.5	0.5	$\frac{1}{78}$	0.05	5	0.16	0.5	10
DGP30	-	2.0	-0.5	0.5	$\frac{1}{78}$	0.05	5	0.16	0.5	10
DGP31	-	0.3	-0.5	2.5	$\frac{1}{78}$	0.05	5	0.16	0.5	10
DGP32	-	2.0	-0.5	2.5	$\frac{1}{78}$	0.05	5	0.16	0.5	10

*Notes: + denotes the Monte Carlo experiments with microstructure noise and - denotes the Monte Carlo experiments without microstructure noise. We simulate $N = 10$ processes for the Data Generating Process (DGP). Simulated jumps are added to 10 processes at the same interval as co-jumps. There are a total of 36 DGPs.

Table 2.3: Monte Carlo Experiments - Co-jump Test (Empirical Power)*

	BLT Test	σ Threshold	JT Test
DGP1	0.980	1.000	1.000
DGP2	0.950	0.999	0.997
DGP3	0.993	1.000	1.000
DGP4	0.959	1.000	0.998
DGP5	0.980	1.000	1.000
DGP6	0.954	0.999	0.995
DGP7	0.993	1.000	1.000
DGP8	0.957	1.000	0.998
DGP9	0.959	1.000	1.000
DGP10	0.881	0.968	0.999
DGP11	0.976	1.000	1.000
DGP12	0.916	0.999	1.000
DGP13	0.969	1.000	1.000
DGP14	0.876	0.969	1.000
DGP15	0.973	1.000	1.000
DGP16	0.898	0.999	1.000
DGP17	0.980	1.000	1.000
DGP18	0.951	0.999	0.995
DGP19	0.993	1.000	1.000
DGP20	0.960	1.000	0.998
DGP21	0.980	1.000	1.000
DGP22	0.953	0.999	1.000
DGP23	0.993	1.000	1.000
DGP24	0.957	1.000	0.998
DGP25	0.959	1.000	1.000
DGP26	0.880	0.968	0.999
DGP27	0.976	1.000	1.000
DGP28	0.894	0.999	1.000
DGP29	0.969	1.000	1.000
DGP30	0.876	0.969	1.000
DGP31	0.973	1.000	1.000
DGP32	0.898	0.999	1.000

*Notes: Table 2.3 shows the empirical power of BLT, JT and σ threshold co-jump tests. The significance level is set as 10% for all co-jump tests. In all experiments, we perform 1000 Monte Carlo replications. For complete details, refer to Section 2.6.

Table 2.4: Monte Carlo Experiments - Co-jump Test (Empirical Power) with Truncation Approach*

	BLT Test	σ Threshold	JT Test
DGP1	0.973	1.000	1.000
DGP2	0.952	0.9995	0.997
DGP3	0.993	1.000	1.000
DGP4	0.961	1.000	0.998
DGP5	0.973	1.000	1.000
DGP6	0.957	0.999	0.995
DGP7	0.990	1.000	1.000
DGP8	0.958	1.000	1.000
DGP9	0.952	1.000	1.000
DGP10	0.879	0.969	0.999
DGP11	0.983	1.000	1.000
DGP12	0.928	0.999	1.000
DGP13	0.959	1.000	1.000
DGP14	0.884	0.972	1.000
DGP15	0.976	1.000	1.000
DGP16	0.905	0.999	1.000
DGP17	0.973	1.000	1.000
DGP18	0.953	0.9995	0.995
DGP19	0.993	1.000	1.000
DGP20	0.961	1.000	1.000
DGP21	0.973	1.000	1.000
DGP22	0.957	0.999	0.997
DGP23	0.990	1.000	1.000
DGP24	0.958	1.000	0.998
DGP25	0.952	1.000	1.000
DGP26	0.880	0.970	0.999
DGP27	0.980	1.000	1.000
DGP28	0.906	0.999	1.000
DGP29	0.959	1.000	1.000
DGP30	0.883	0.972	1.000
DGP31	0.973	1.000	1.000
DGP32	0.905	0.999	1.000

*Notes: See notes in Table 2.3. Table 2.3 shows the empirical power of BLT, JT and σ threshold co-jump tests with the truncation approach. All Monte Carlo simulation data are truncated based on the truncation approach in section 2.3.4.

Table 2.5: Monte Carlo Experiments - Co-jump Test (Empirical Size)*

	BLT Test	σ Threshold	JT Test
DGP1	0.0805	0.0000	0.0000
DGP2	0.0358	0.00001	0.0000
DGP3	0.0817	0.0000	0.0000
DGP4	0.0349	0.00001	0.0000
DGP5	0.0809	0.0000	0.0000
DGP6	0.0361	0.00001	0.0000
DGP7	0.0822	0.0000	0.0000
DGP8	0.0351	0.00001	0.0000
DGP9	0.0849	0.0000	0.0000
DGP10	0.0366	0.00002	0.0000
DGP11	0.0864	0.0000	0.0000
DGP12	0.0613	0.00002	0.0000
DGP13	0.0858	0.0000	0.0000
DGP14	0.0376	0.00002	0.0000
DGP15	0.0870	0.0000	0.0000
DGP16	0.0353	0.00002	0.0000
DGP17	0.0805	0.0000	0.0000
DGP18	0.0359	0.00001	0.0000
DGP19	0.0817	0.0000	0.0000
DGP20	0.0349	0.00001	0.0000
DGP21	0.0810	0.0000	0.0000
DGP22	0.0362	0.00001	0.0000
DGP23	0.0822	0.0000	0.0000
DGP24	0.0352	0.00001	0.0000
DGP25	0.0848	0.0000	0.0000
DGP26	0.0366	0.00002	0.0000
DGP27	0.0864	0.0000	0.0000
DGP28	0.0351	0.00002	0.0000
DGP29	0.0857	0.0000	0.0000
DGP30	0.0376	0.00002	0.0000
DGP31	0.0870	0.0000	0.0000
DGP32	0.0353	0.00002	0.0000

*Notes: Table 2.5 shows the empirical size of BLT, JT and σ threshold co-jump tests. The nominal size is set as 10% for all co-jump tests. In all experiments, we perform 1000 Monte Carlo replications. For complete details, refer to Section 2.6.

Table 2.6: Monte Carlo Experiments - Co-jump Test (Empirical Size) with Truncation Approach*

	BLT Test	σ Threshold	JT Test
DGP1	0.0820	0.0000	0.0000
DGP2	0.0358	0.00001	0.0000
DGP3	0.0761	0.0000	0.0000
DGP4	0.0354	0.00001	0.0000
DGP5	0.0822	0.0000	0.0000
DGP6	0.0361	0.00001	0.0000
DGP7	0.0765	0.0000	0.0000
DGP8	0.0356	0.00001	0.0000
DGP9	0.0844	0.0000	0.0000
DGP10	0.0368	0.00002	0.0000
DGP11	0.0898	0.0000	0.0000
DGP12	0.0612	0.00001	0.0000
DGP13	0.0850	0.0000	0.0000
DGP14	0.0375	0.00002	0.0000
DGP15	0.0910	0.0000	0.0000
DGP16	0.0350	0.00002	0.0000
DGP17	0.0820	0.0000	0.0000
DGP18	0.0358	0.00001	0.0000
DGP19	0.0762	0.0000	0.0000
DGP20	0.0354	0.00001	0.0000
DGP21	0.0822	0.0000	0.0000
DGP22	0.0362	0.00001	0.0000
DGP23	0.0765	0.0000	0.0000
DGP24	0.0357	0.00001	0.0000
DGP25	0.0845	0.0000	0.0000
DGP26	0.0369	0.00002	0.0000
DGP27	0.0898	0.0000	0.0000
DGP28	0.0348	0.00002	0.0000
DGP29	0.0850	0.0000	0.0000
DGP30	0.0375	0.00002	0.0000
DGP31	0.0907	0.0000	0.0000
DGP32	0.0350	0.00002	0.0000

*Notes: See notes in Table 2.5. Table 2.6 shows the empirical size of BLT, JT and σ threshold co-jump tests with the truncation approach. All Monte Carlo simulation data are truncated based on the truncation approach in section 2.3.4.

Table 2.7: Sectors Classification in S&P500 Index*

Sector Classification	number of constituents
Consumer Discretionary (GICS Consumer Discretionary Sector)	87
Consumer Staples (GICS Consumer Staples Sector)	36
Energy (GICS Energy Sector)	38
Financial (GICS Financials Sector)	92
Financial Services (GICS Financials Sector excluding the Real Estate Industry Group, but including Mortgage REITs)	64
Health Care (GICS Health Care Sector)	56
Industrials (GICS Industrials Sector)	68
Materials (GICS Materials Sector)	26
Real Estate (GICS Real Estate Industry Group excluding Mortgage REITs)	28
Technology (GICS Information Technology Sector & Telecommunication Services Sector)	68 & 5
Utilities (GICS Utilities Sector)	29

*Notes: Number of constituents denotes the number of stocks in each sector.

Table 2.8: Descriptive Statistics for Single Jumps and Co-jumps*

Sector		XLB	XLE	XLF	XLI	XLK	XLP	XLU	XLV	XLY
Single jump	Prop.	0.3936	0.3327	0.3282	0.3861	0.3664	0.4354	0.4521	0.4318	0.4005
	Mean	0.0487	0.0451	0.0533	0.0482	0.0430	0.0471	0.0484	0.0453	0.0447
	St. dev.	0.0526	0.0517	0.0635	0.0446	0.0445	0.0814	0.0423	0.0346	0.0411
Co-jump	Prop.	0.6064	0.6673	0.6718	0.6139	0.6336	0.5646	0.5479	0.5682	0.5995
	Mean	0.0886	0.0984	0.1291	0.0917	0.0820	0.0833	0.0930	0.0837	0.0812
	St. dev.	0.1314	0.1858	0.2039	0.1170	0.1152	0.0814	0.1171	0.0877	0.1163

*Notes: Single jump and co-jump are detected through a 5σ threshold test. Prop denotes proportions of each jump/co-jump type over the total number of co-jumps and jumps. Mean and St. dev denotes mean and standard deviation for single jumps and co-jumps variations. XLB is material select sector ETF; XLE is energy select sector ETF; XLF is financial select sector EFT; XLI is industrial select sector EFT; XLK is technology select sector EFT; XLP is consumer staples select sector EFT; XLU is utility sector ETF; XLV is health care sector ETF and XLY is consumer discretionary sector ETF.

Table 2.9: Energy Sector Prediction Regression Results with Co-jumps*

	$RV_{t,t+h}$			$RV_{t,t+h}^{1/2}$			$log(RV_{t,t+h})$		
h	h=1	h=5	h=22	h=1	h=5	h=22	h=1	h=5	h=22
β_0	0.014	0.023	0.026	0.017	0.035	0.044	-0.123	-0.227	-0.358
	(0.006)	(0.014)	(0.030)	(0.009)	(0.019)	(0.046)	(0.032)	(0.066)	(0.157)
β_{cd}	0.476	0.308	0.177	0.422	0.298	0.137	0.375	0.282	0.122
	(0.061)	(0.063)	(0.089)	(0.041)	(0.043)	(0.052)	(0.030)	(0.036)	(0.039)
β_{cw}	0.273	0.256	0.084	0.419	0.369	0.107	0.389	0.273	0.040
	(0.111)	(0.113)	(0.201)	(0.077)	(0.100)	(0.139)	(0.049)	(0.082)	(0.103)
β_{cm}	0.170	0.325	0.675	0.098	0.240	0.701	0.159	0.308	0.619
	(0.076)	(0.130)	(0.178)	(0.060)	(0.097)	(0.145)	(0.040)	(0.078)	(0.122)
β_{jd}	0.234	0.191	0.118	0.085	0.074	0.058	0.573	0.364	0.304
	(0.067)	(0.084)	(0.087)	(0.018)	(0.031)	(0.023)	(0.114)	(0.185)	(0.176)
β_{jw}	0.359	0.314	0.308	0.040	-0.009	0.038	0.455	0.455	0.824
	(0.160)	(0.180)	(0.110)	(0.039)	(0.063)	(0.068)	(0.248)	(0.395)	(0.435)
β_{jm}	-0.072	-0.067	-0.338	0.072	0.089	-0.136	-0.004	0.134	-0.667
	(0.104)	(0.204)	(0.186)	(0.036)	(0.064)	(0.084)	(0.175)	(0.392)	(0.531)
R^2	0.780	0.627	0.371	0.761	0.621	0.406	0.769	0.632	0.427
$adjR^2$	0.779	0.626	0.369	0.760	0.619	0.404	0.769	0.631	0.425

*Notes: Table 2.9 shows the in-sample regression results with co-jumps for the energy sector (XLE). Entries in parenthesis show the corresponding t statistics of the coefficients. Results are reported for linear, square root and log HAR-RV-CJ models at daily ($h = 1$), weekly ($h = 5$) and monthly ($h = 22$) prediction horizons. See sections 2.4 and 2.5 for further details.

Table 2.10: Energy Sector Prediction Regression Results with Single Jumps*

	$RV_{t,t+h}$			$RV_{t,t+h}^{1/2}$			$log(RV_{t,t+h})$		
h	h=1	h=5	h=22	h=1	h=5	h=22	h=1	h=5	h=22
β_0	-0.046	-0.034	-0.005	-0.045	-0.021	0.032	0.082	-0.055	-0.362
	(0.016)	(0.026)	(0.032)	(0.020)	(0.033)	(0.051)	(0.053)	(0.081)	(0.112)
β_{cd}	0.519	0.345	0.182	0.448	0.321	0.146	0.392	0.294	0.126
	(0.071)	(0.065)	(0.081)	(0.043)	(0.044)	(0.053)	(0.031)	(0.037)	(0.039)
β_{cw}	0.570	0.495	0.261	0.496	0.391	0.160	0.456	0.326	0.106
	(0.154)	(0.155)	(0.218)	(0.081)	(0.094)	(0.145)	(0.050)	(0.079)	(0.106)
β_{cm}	0.215	0.364	0.518	0.186	0.344	0.590	0.181	0.339	0.573
	(0.101)	(0.123)	(0.195)	(0.059)	(0.082)	(0.130)	(0.042)	(0.071)	(0.113)
β_{jd}	-0.006	0.121	0.004	0.031	0.035	0.023	0.241	0.448	0.116
	(0.072)	(0.101)	(0.116)	(0.017)	(0.020)	(0.023)	(0.249)	(0.269)	(0.283)
β_{jw}	-0.066	-0.456	0.373	-0.014	-0.045	-0.015	0.083	-0.268	-0.148
	(0.370)	(0.634)	(0.928)	(0.040)	(0.072)	(0.083)	(0.784)	(1.240)	(1.603)
β_{jm}	0.112	1.340	3.035	-0.001	0.112	0.308	0.343	2.084	7.163
	(0.693)	(1.459)	(1.473)	(0.077)	(0.143)	(0.179)	(1.313)	(2.704)	(3.655)
R^2	0.666	0.551	0.378	0.732	0.605	0.413	0.746	0.616	0.429
$adjR^2$	0.666	0.549	0.377	0.731	0.604	0.411	0.745	0.615	0.427

*Notes:See notes to table 2.9.

Table 2.11: Energy Sector Prediction Regression Results with Single Jumps and Co-jumps*

	$RV_{t,t+h}$			$RV_{t,t+h}^{1/2}$			$log(RV_{t,t+h})$		
h	h=1	h=5	h=22	h=1	h=5	h=22	h=1	h=5	h=22
β_0	0.012	0.018	0.016	0.014	0.029	0.035	-0.166	-0.307	-0.520
	(0.006)	(0.143)	(0.030)	(0.009)	(0.020)	(0.048)	(0.036)	(0.072)	(0.127)
β_{cd}	0.473	0.305	0.164	0.421	0.295	0.131	0.373	0.279	0.117
	(0.061)	(0.061)	(0.079)	(0.041)	(0.042)	(0.049)	(0.030)	(0.036)	(0.038)
β_{cw}	0.270	0.248	0.076	0.412	0.359	0.097	0.387	0.272	0.040
	(0.108)	(0.111)	(0.179)	(0.076)	(0.099)	(0.134)	(0.048)	(0.082)	(0.102)
β_{cm}	0.149	0.280	0.581	0.085	0.219	0.667	0.148	0.285	0.571
	(0.073)	(0.116)	(0.178)	(0.057)	(0.094)	(0.147)	(0.040)	(0.076)	(0.121)
β_{jd}^{sjump}	0.095	0.204	0.054	0.056	0.055	0.039	0.450	0.591	0.240
	(0.055)	(0.120)	(0.112)	(0.017)	(0.023)	(0.025)	(0.229)	(0.289)	(0.290)
β_{jw}^{sjump}	0.220	-0.217	0.541	0.001	-0.039	-0.012	0.521	0.143	0.278
	(0.225)	(0.534)	(0.881)	(0.032)	(0.063)	(0.078)	(0.569)	(1.067)	(1.525)
β_{jm}^{sjump}	0.463	1.727	2.910	0.100	0.205	0.297	1.055	3.141	7.315
	(0.376)	(1.138)	(1.311)	(0.059)	(0.140)	(0.179)	(0.965)	(2.322)	(3.382)
$\beta_{jd}^{co-jump}$	0.233	0.190	0.099	0.090	0.079	0.060	0.580	0.369	0.266
	(0.067)	(0.080)	(0.072)	(0.018)	(0.029)	(0.022)	(0.110)	(0.179)	(0.152)
$\beta_{jw}^{co-jump}$	0.357	0.286	0.282	0.040	-0.015	0.034	0.443	0.384	0.668
	(0.158)	(0.173)	(0.095)	(0.038)	(0.059)	(0.063)	(0.242)	(0.368)	(0.387)
$\beta_{jm}^{co-jump}$	-0.043	0.011	-0.189	0.090	0.123	-0.083	0.075	0.329	-0.225
	(0.102)	(0.181)	(0.119)	(0.035)	(0.063)	(0.078)	(0.175)	(0.359)	(0.411)
R^2	0.637	0.636	0.406	0.764	0.627	0.418	0.771	0.637	0.441
$adjR^2$	0.635	0.635	0.403	0.763	0.625	0.415	0.770	0.635	0.439

*Notes:See notes to table 2.9.

Table 2.12: Financial Sector Prediction Regression Results with Co-jumps*

	$RV_{t,t+h}$			$RV_{t,t+h}^{1/2}$			$log(RV_{t,t+h})$		
h	h=1	h=5	h=22	h=1	h=5	h=22	h=1	h=5	h=22
β_0	0.007	0.012	0.027	0.013	0.020	0.044	-0.143	-0.192	-0.326
	(0.004)	(0.009)	(0.021)	(0.006)	(0.014)	(0.031)	(0.032)	(0.071)	(0.152)
β_{cd}	0.548	0.355	0.307	0.506	0.287	0.253	0.434	0.215	0.214
	(0.060)	(0.096)	(0.080)	(0.039)	(0.062)	(0.057)	(0.029)	(0.042)	(0.042)
β_{cw}	0.380	0.428	0.022	0.355	0.410	0.050	0.327	0.388	0.079
	(0.107)	(0.145)	(0.238)	(0.065)	(0.108)	(0.166)	(0.046)	(0.082)	(0.123)
β_{cm}	0.060	0.198	0.609	0.112	0.270	0.638	0.142	0.273	0.507
	(0.072)	(0.128)	(0.294)	(0.048)	(0.090)	(0.197)	(0.036)	(0.073)	(0.136)
β_{jd}	0.254	0.055	0.029	0.087	0.019	0.025	0.568	0.143	0.103
	(0.060)	(0.068)	(0.057)	(0.019)	(0.022)	(0.019)	(0.107)	(0.128)	(0.123)
β_{jw}	0.001	0.018	0.012	0.008	0.028	0.006	0.016	0.134	-0.038
	(0.083)	(0.166)	(0.204)	(0.022)	(0.060)	(0.085)	(0.157)	(0.338)	(0.532)
β_{jm}	0.123	0.211	0.126	0.043	0.032	-0.035	0.320	0.486	0.611
	(0.093)	(0.220)	(0.347)	(0.032)	(0.079)	(0.146)	(0.198)	(0.457)	(0.677)
R^2	0.818	0.686	0.532	0.847	0.740	0.591	0.848	0.752	0.611
$adjR^2$	0.817	0.685	0.530	0.846	0.739	0.590	0.848	0.751	0.610

*Notes:See notes to table 2.9.

Table 2.13: Financial Sector Prediction Regression Results with Single Jumps*

	$RV_{t,t+h}$			$RV_{t,t+h}^{1/2}$			$log(RV_{t,t+h})$		
h	h=1	h=5	h=22	h=1	h=5	h=22	h=1	h=5	h=22
β_0	-0.014	0.002	0.031	-0.013	0.011	0.069	0.022	-0.038	-0.167
	(0.006)	(0.009)	(0.017)	(0.009)	(0.015)	(0.029)	(0.032)	(0.057)	(0.105)
β_{cd}	0.655	0.365	0.298	0.560	0.295	0.267	0.467	0.222	0.218
	(0.065)	(0.095)	(0.083)	(0.042)	(0.061)	(0.055)	(0.030)	(0.042)	(0.042)
β_{cw}	0.474	0.473	0.043	0.400	0.453	0.054	0.359	0.417	0.085
	(0.131)	(0.151)	(0.210)	(0.074)	(0.100)	(0.150)	(0.048)	(0.076)	(0.116)
β_{cm}	0.068	0.306	0.699	0.112	0.276	0.602	0.152	0.303	0.557
	(0.098)	(0.133)	(0.206)	(0.056)	(0.085)	(0.153)	(0.038)	(0.066)	(0.119)
β_{jd}	0.019	0.030	-0.111	0.019	0.016	-0.016	0.335	0.157	-0.311
	(0.102)	(0.114)	(0.077)	(0.021)	(0.024)	(0.024)	(0.218)	(0.262)	(0.262)
β_{jw}	0.034	-0.094	-0.169	0.021	0.001	0.060	0.171	-0.269	0.208
	(0.236)	(0.282)	(0.466)	(0.035)	(0.052)	(0.077)	(0.603)	(0.832)	(1.230)
β_{jm}	-0.431	-0.817	-1.519	-0.017	-0.057	-0.275	0.472	-0.134	-2.717
	(0.277)	(0.476)	(1.071)	(0.041)	(0.079)	(0.167)	(0.803)	(1.477)	(3.132)
R^2	0.788	0.679	0.539	0.835	0.737	0.597	0.838	0.746	0.609
$adjR^2$	0.787	0.678	0.537	0.835	0.737	0.596	0.838	0.745	0.608

*Notes:See notes to table 2.9.

Table 2.14: Financial Sector Prediction Regression Results with Single Jumps and Co-jumps*

	$RV_{t,t+h}$			$RV_{t,t+h}^{1/2}$			$log(RV_{t,t+h})$		
h	h=1	h=5	h=22	h=1	h=5	h=22	h=1	h=5	h=22
β_0	0.007	0.017	0.039	0.011	0.026	0.069	-0.153	-0.191	-0.302
	(0.004)	(0.008)	(0.022)	(0.007)	(0.037)	(0.029)	(0.032)	(0.073)	(0.152)
β_{cd}	0.542	0.345	0.290	0.503	0.285	0.254	0.433	0.213	0.213
	(0.061)	(0.093)	(0.078)	(0.039)	(0.056)	(0.055)	(0.030)	(0.042)	(0.042)
β_{cw}	0.378	0.430	0.028	0.350	0.411	0.045	0.323	0.391	0.002
	(0.107)	(0.143)	(0.219)	(0.064)	(0.161)	(0.150)	(0.046)	(0.082)	(0.121)
β_{cm}	0.069	0.218	0.648	0.124	0.267	0.625	0.147	0.272	0.504
	(0.072)	(0.126)	(0.275)	(0.048)	(0.205)	(0.153)	(0.036)	(0.073)	(0.135)
β_{jd}^{sjump}	0.152	0.063	-0.097	0.056	0.025	-0.008	0.606	0.231	-0.275
	(0.100)	(0.114)	(0.082)	(0.020)	(0.027)	(0.024)	(0.210)	(0.277)	(0.274)
β_{jw}^{sjump}	-0.060	-0.120	-0.183	-0.005	0.058	0.060	-0.074	-0.363	0.093
	(0.185)	(0.274)	(0.451)	(0.032)	(0.072)	(0.077)	(0.504)	(0.814)	(1.212)
β_{jm}^{sjump}	-0.181	-0.626	-1.424	-0.013	-0.273	-0.275	0.712	-0.004	-2.624
	(0.210)	(0.412)	(1.004)	(0.034)	(0.168)	(0.167)	(0.669)	(1.340)	(3.109)
$\beta_{jd}^{co-jump}$	0.262	0.059	0.025	0.095	0.019	0.023	0.611	0.160	0.079
	(0.061)	(0.069)	(0.058)	(0.019)	(0.020)	(0.023)	(0.107)	(0.131)	(0.123)
$\beta_{jw}^{co-jump}$	-0.003	0.011	-0.001	0.006	0.003	-0.015	0.013	0.113	-0.069
	(0.083)	(0.167)	(0.198)	(0.023)	(0.085)	(0.083)	(0.160)	(0.343)	(0.527)
$\beta_{jm}^{co-jump}$	0.118	0.201	0.107	0.035	-0.020	0.308	0.284	0.493	0.662
	(0.094)	(0.221)	(0.332)	(0.035)	(0.149)	(0.179)	(0.198)	(0.465)	(0.655)
R^2	0.849	0.687	0.541	0.848	0.598	0.597	0.838	0.752	0.613
$adjR^2$	0.849	0.686	0.539	0.847	0.596	0.413	0.746	0.751	0.611

*Notes:See notes to table 2.9.

Table 2.15: Technology Sector Prediction Regression Results with Co-jumps*

	$RV_{t,t+h}$			$RV_{t,t+h}^{1/2}$			$log(RV_{t,t+h})$		
h	h=1	h=5	h=22	h=1	h=5	h=22	h=1	h=5	h=22
β_0	0.003	0.010	0.023	0.005	0.019	0.052	-0.116	-0.219	-0.432
	(0.005)	(0.012)	(0.027)	(0.009)	(0.020)	(0.044)	(0.055)	(0.116)	(0.282)
β_{cd}	0.576	0.273	0.223	0.486	0.248	0.157	0.403	0.232	0.117
	(0.059)	(0.114)	(0.088)	(0.040)	(0.060)	(0.058)	(0.031)	(0.038)	(0.044)
β_{cw}	0.426	0.614	0.285	0.410	0.482	0.232	0.360	0.315	0.164
	(0.097)	(0.280)	(0.240)	(0.059)	(0.155)	(0.164)	(0.047)	(0.104)	(0.112)
β_{cm}	0.023	0.107	0.463	0.108	0.249	0.547	0.158	0.326	0.484
	(0.081)	(0.189)	(0.176)	(0.051)	(0.119)	(0.130)	(0.042)	(0.094)	(0.123)
β_{jd}	0.119	0.049	0.014	0.037	0.026	0.016	0.459	0.155	0.180
	(0.045)	(0.046)	(0.036)	(0.014)	(0.015)	(0.014)	(0.146)	(0.147)	(0.132)
β_{jw}	0.063	-0.007	0.108	0.022	-0.024	0.025	0.241	0.288	0.403
	(0.128)	(0.211)	(0.160)	(0.025)	(0.055)	(0.048)	(0.300)	(0.569)	(0.623)
β_{jm}	0.077	0.131	-0.222	0.017	0.030	-0.122	0.158	0.275	-0.205
	(0.105)	(0.245)	(0.345)	(0.028)	(0.068)	(0.106)	(0.281)	(0.693)	(1,038)
R^2	0.721	0.573	0.353	0.744	0.603	0.399	0.736	0.597	0.405
$adjR^2$	0.721	0.572	0.351	0.743	0.602	0.397	0.736	0.595	0.403

*Notes:See notes to table 2.9.

Table 2.16: Technology sector Prediction Regression Results with Single Jumps*

	$RV_{t,t+h}$			$RV_{t,t+h}^{1/2}$			$log(RV_{t,t+h})$		
h	h=1	h=5	h=22	h=1	h=5	h=22	h=1	h=5	h=22
β_0	-0.015	-0.002	0.028	-0.020	0.004	0.065	0.068	-0.061	-0.360
	(0.006)	(0.011)	(0.015)	(0.011)	(0.020)	(0.030)	(0.045)	(0.088)	(0.152)
β_{cd}	0.631	0.298	0.227	0.509	0.265	0.166	0.424	0.238	0.121
	(0.065)	(0.118)	(0.089)	(0.042)	(0.061)	(0.061)	(0.032)	(0.038)	(0.044)
β_{cw}	0.535	0.637	0.372	0.453	0.467	0.260	0.407	0.353	0.217
	(0.120)	(0.223)	(0.240)	(0.066)	(0.131)	(0.167)	(0.047)	(0.089)	(0.119)
β_{cm}	0.041	0.184	0.303	0.127	0.287	0.425	0.174	0.354	0.470
	(0.090)	(0.168)	(0.237)	(0.057)	(0.104)	(0.162)	(0.043)	(0.078)	(0.111)
β_{jd}	0.028	0.036	0.017	0.025	0.012	0.010	0.460	0.236	0.139
	(0.047)	(0.056)	(0.035)	(0.014)	(0.018)	(0.015)	(0.243)	(0.317)	(0.238)
β_{jw}	-0.084	0.048	-0.300	-0.029	-0.014	-0.062	-0.713	-0.729	-1.581
	(0.099)	(0.203)	(0.241)	(0.023)	(0.040)	(0.060)	(0.555)	(0.921)	(1.266)
β_{jm}	0.165	-0.030	0.435	0.052	0.056	0.104	1.514	1.602	4.147
	(0.123)	(0.249)	(0.526)	(0.031)	(0.062)	(0.153)	(0.707)	(1.390)	(2.598)
R^2	0.711	0.570	0.352	0.740	0.603	0.397	0.731	0.595	0.408
$adjR^2$	0.710	0.569	0.350	0.739	0.602	0.395	0.730	0.593	0.406

*Notes:See notes to table 2.9.

Table 2.17: Technology Sector Prediction Regression Results with Single Jumps and Co-jumps*

	$RV_{t,t+h}$			$RV_{t,t+h}^{1/2}$			$log(RV_{t,t+h})$		
h	h=1	h=5	h=22	h=1	h=5	h=22	h=1	h=5	h=22
β_0	0.001	0.009	0.021	-0.001	0.013	0.046	-0.150	-0.247	-0.480
	(0.005)	(0.011)	(0.024)	(0.009)	(0.019)	(0.039)	(0.057)	(0.122)	(0.306)
β_{cd}	0.578	0.276	0.220	0.487	0.247	0.154	0.405	0.231	0.114
	(0.059)	(0.113)	(0.088)	(0.040)	(0.060)	(0.060)	(0.030)	(0.037)	(0.044)
β_{cw}	0.425	0.608	0.302	0.402	0.480	0.239	0.361	0.319	0.179
	(0.098)	(0.277)	(0.238)	(0.058)	(0.154)	(0.163)	(0.046)	(0.103)	(0.112)
β_{cm}	0.017	0.106	0.453	0.118	0.254	0.545	0.150	0.317	0.465
	(0.082)	(0.189)	(0.178)	(0.051)	(0.119)	(0.129)	(0.042)	(0.094)	(0.124)
β_{jd}^{sjump}	0.071	0.055	0.021	0.045	0.024	0.018	0.643	0.295	0.203
	(0.241)	(0.059)	(0.038)	(0.015)	(0.019)	(0.016)	(0.243)	(0.323)	(0.242)
β_{jw}^{sjump}	-0.0001	0.080	-0.271	-0.019	-0.020	-0.057	-0.482	-0.729	-1.344
	(0.101)	(0.213)	(0.281)	(0.023)	(0.040)	(0.068)	(0.541)	(0.948)	(1.375)
β_{jm}^{sjump}	0.137	-0.009	0.354	0.045	0.060	0.086	1.563	1.734	4.114
	(0.117)	(0.260)	(0.583)	(0.031)	(0.062)	(0.159)	(0.672)	(1.407)	(2.770)
$\beta_{jd}^{co-jump}$	0.124	0.053	0.015	0.047	0.031	0.019	0.514	0.179	0.193
	(0.046)	(0.047)	(0.036)	(0.015)	(0.016)	(0.015)	(0.149)	(0.152)	(0.136)
$\beta_{jw}^{co-jump}$	0.060	-0.004	0.090	0.019	-0.027	0.013	0.189	0.239	0.286
	(0.132)	(0.215)	(0.170)	(0.026)	(0.057)	(0.055)	(0.311)	(0.584)	(0.660)
$\beta_{jm}^{co-jump}$	0.089	0.134	-0.203	0.015	0.033	-0.109	0.261	0.386	0.046
	(0.107)	(0.251)	(0.365)	(0.029)	(0.070)	(0.111)	(0.289)	(0.714)	(1.110)
R^2	0.722	0.570	0.354	0.746	0.604	0.400	0.739	0.598	0.410
$adjR^2$	0.721	0.551	0.351	0.744	0.602	0.398	0.737	0.596	0.407

*Notes:See notes to table 2.9.

Table 2.18: rMSFEs of HAR-RV-CJ models*

		rMSFEs								
Sector		Linear Models			Square Root Models			Log Models		
	Case	h=1	h=5	h=22	h=1	h=5	h=22	h=1	h=5	h=22
XLB	I	0.0442	0.0588	0.0708	0.0486	0.0619	0.0734	0.2277	0.2813	0.3397
	II	0.0469	0.0610	0.0727	0.0488	0.0624	0.0757	0.2304	0.2843	0.3464
	III	0.0438	0.0587	0.0713	0.0485	0.0624	0.0744	0.2272	0.2820	0.3424
XLE	I	0.0476	0.0647	0.0772	0.0525	0.0667	0.0792	0.2309	0.2913	0.3552
	II	0.0552	0.0704	0.0805	0.0524	0.0673	0.0809	0.2349	0.2960	0.3617
	III	0.0472	0.0647	0.0785	0.0522	0.0673	0.0808	0.2303	0.2923	0.3585
XLF	I	0.0486	0.0664	0.0789	0.0517	0.0662	0.0804	0.2349	0.2956	0.3640
	II	0.0523	0.0692	0.0833	0.0520	0.0669	0.0826	0.2391	0.2988	0.3691
	III	0.0488	0.0679	0.0842	0.0517	0.0668	0.0831	0.2349	0.2972	0.3707
XLI	I	0.0480	0.0619	0.0742	0.0505	0.0635	0.0782	0.2470	0.3026	0.3794
	II	0.0499	0.0628	0.0750	0.0509	0.0636	0.0788	0.2495	0.3053	0.3844
	III	0.0475	0.0619	0.0762	0.0502	0.0635	0.0792	0.2451	0.3029	0.3839
XLK	I	0.0380	0.0486	0.0584	0.0450	0.0559	0.0665	0.2339	0.2859	0.3495
	II	0.0393	0.0494	0.0594	0.0451	0.0559	0.0687	0.2360	0.2887	0.3511
	III	0.0380	0.0490	0.0599	0.0449	0.0561	0.0676	0.2333	0.2869	0.3520
XLP	I	0.0302	0.0351	0.0421	0.0406	0.0470	0.0553	0.2372	0.2740	0.3245
	II	0.0328	0.0359	0.0410	0.0428	0.0474	0.0548	0.2522	0.2802	0.3243
	III	0.0299	0.0346	0.0413	0.0399	0.0464	0.0547	0.2343	0.2705	0.3225
XLU	I	0.0422	0.0489	0.0583	0.0467	0.0541	0.0648	0.2413	0.2794	0.3391
	II	0.0429	0.0496	0.0614	0.0472	0.0543	0.0673	0.2463	0.2817	0.3448
	III	0.0420	0.0499	0.0614	0.0464	0.0547	0.0666	0.2405	0.2820	0.3459
XLV	I	0.0353	0.0427	0.0521	0.0435	0.0517	0.0640	0.2386	0.2841	0.3495
	II	0.0372	0.0434	0.0514	0.0451	0.0522	0.0639	0.2477	0.2886	0.3498
	III	0.0351	0.0426	0.0515	0.0434	0.0515	0.0637	0.2371	0.2830	0.3467
XLY	I	0.0401	0.0526	0.0647	0.0464	0.0589	0.0729	0.2392	0.2957	0.3716
	II	0.0411	0.0530	0.0634	0.0466	0.0585	0.0729	0.2407	0.2962	0.3707
	III	0.0396	0.0521	0.0637	0.0460	0.0588	0.0722	0.2372	0.2937	0.3693

*Notes: Table 2.18 reports the Root mean square forecasting errors for different sectors using the HAR-RV-CJ models. Linear models, square root models and log models over horizon h=1, h=5 and h=22 are compared in this table. I is the case with only co-jumps; II is with only single jumps; III is with both co-jumps and single jumps. Forecasting errors for models with only co-jumps(case I) are always smaller than models with single jumps(case II). The ranking of forecasting errors with both co-jumps and single jumps(case III) changes among different sectors when compared with other cases.

Table 2.19: In-Sample R^2 of HAR-RV-CJ models*

		In-Sample R^2								
Sector		Linear Models			Square Root Models			Log Models		
	Case	h=1	h=5	h=22	h=1	h=5	h=22	h=1	h=5	h=22
XLB	I	0.785	0.631	0.399	0.787	0.651	0.451	0.777	0.2813	0.467
	II	0.759	0.617	0.395	0.779	0.648	0.444	0.769	0.2843	0.466
	III	0.788	0.633	0.403	0.790	0.653	0.452	0.779	0.2820	0.469
XLE	I	0.780	0.650	0.371	0.761	0.621	0.406	0.769	0.632	0.427
	II	0.666	0.646	0.378	0.732	0.605	0.413	0.746	0.616	0.429
	III	0.783	0.651	0.406	0.764	0.627	0.418	0.771	0.637	0.441
XLF	I	0.818	0.686	0.532	0.847	0.740	0.611	0.848	0.752	0.611
	II	0.788	0.679	0.539	0.835	0.737	0.597	0.838	0.746	0.609
	III	0.818	0.687	0.541	0.848	0.740	0.598	0.849	0.752	0.613
XLI	I	0.765	0.620	0.407	0.781	0.651	0.451	0.769	0.644	0.449
	II	0.753	0.618	0.402	0.777	0.651	0.447	0.764	0.644	0.449
	III	0.768	0.623	0.407	0.784	0.654	0.453	0.773	0.649	0.452
XLK	I	0.721	0.573	0.353	0.744	0.603	0.399	0.736	0.597	0.405
	II	0.711	0.570	0.352	0.740	0.603	0.397	0.731	0.595	0.408
	III	0.722	0.574	0.354	0.746	0.604	0.400	0.739	0.598	0.410
XLP	I	0.710	0.547	0.316	0.718	0.589	0.383	0.697	0.590	0.401
	II	0.689	0.527	0.319	0.699	0.581	0.388	0.672	0.577	0.410
	III	0.713	0.553	0.328	0.725	0.599	0.391	0.704	0.601	0.418
XLU	I	0.737	0.582	0.334	0.739	0.607	0.384	0.713	0.593	0.393
	II	0.727	0.0496	0.329	0.731	0.608	0.378	0.701	0.594	0.391
	III	0.740	0.586	0.336	0.743	0.610	0.384	0.717	0.599	0.394
XLV	I	0.673	0.534	0.314	0.697	0.572	0.358	0.691	0.568	0.369
	II	0.652	0.526	0.317	0.681	0.565	0.365	0.672	0.559	0.374
	III	0.676	0.536	0.323	0.701	0.576	0.367	0.696	0.573	0.382
XLY	I	0.783	0.653	0.471	0.799	0.681	0.505	0.786	0.676	0.512
	II	0.766	0.640	0.454	0.792	0.680	0.510	0.780	0.673	0.513
	III	0.785	0.657	0.478	0.802	0.687	0.514	0.791	0.682	0.522

*Notes: Table 2.19 shows In-sample R^2 of HAR-RV-CJ models. I is the case with only co-jumps; II is with only single jumps; III is with both co-jumps and single jumps. In-Sample R^2 for HAR models with only co-jumps is usually larger than with only single jumps.

Table 2.20: Out-of-Sample R^2 of HAR-RV-CJ models*

Sector		Out-of-Sample R^2								
		Linear Models			Square Root Models			Log Models		
	Case	h=1	h=5	h=22	h=1	h=5	h=22	h=1	h=5	h=22
XLB	I	0.6548	0.3816	0.0679	0.6574	0.4375	0.1818	0.6655	0.4846	0.2285
	II	0.6106	0.3333	0.0150	0.6539	0.4288	0.1304	0.6573	0.4732	0.1976
	III	0.6595	0.3834	0.0531	0.6581	0.4297	0.1598	0.6668	0.4820	0.2161
XLE	I	0.6372	0.3266	0.0031	0.6188	0.3804	0.1264	0.6558	0.4496	0.1815
	II	0.5134	0.2031	-0.0401	0.6202	0.3702	0.0896	0.6438	0.4317	0.1512
	III	0.6434	0.3270	0.0121	0.6222	0.3698	0.0903	0.6576	0.4456	0.1662
XLF	I	0.6415	0.3279	0.0564	0.6501	0.4234	0.1530	0.6707	0.4763	0.2070
	II	0.5852	0.2692	-0.0517	0.6462	0.4116	0.1044	0.6589	0.4647	0.1845
	III	0.6385	0.2968	-0.0756	0.6503	0.4136	0.0947	0.6707	0.4703	0.1775
XLI	I	0.6028	0.3400	0.0554	0.6484	0.4453	0.1585	0.6626	0.4930	0.2038
	II	0.5709	0.3189	0.0341	0.6426	0.4423	0.1460	0.6557	0.4836	0.1830
	III	0.6110	0.3383	0.0032	0.6535	0.4451	0.1382	0.6676	0.4917	0.1849
XLK	I	0.5637	0.2804	-0.0301	0.5879	0.3587	0.0957	0.6047	0.4050	0.1152
	II	0.5330	0.2564	-0.0688	0.5855	0.3593	0.0367	0.5978	0.3935	0.1071
	III	0.5641	0.2684	-0.0850	0.5903	0.3548	0.0659	0.6069	0.4012	0.1025
XLP	I	0.4774	0.2934	-0.0127	0.4997	0.3264	0.0693	0.5176	0.3546	0.0931
	II	0.3830	0.2611	0.0400	0.4426	0.3144	0.0836	0.4546	0.3250	0.0941
	III	0.4891	0.3131	0.0257	0.5167	0.3443	0.0877	0.5290	0.3706	0.1041
XLU	I	0.4196	0.2171	-0.1134	0.4847	0.3065	-0.0040	0.5086	0.3384	0.0171
	II	0.3990	0.1967	-0.2355	0.4733	0.2995	-0.0836	0.4882	0.3276	-0.0162
	III	0.4244	0.1867	-0.2355	0.4921	0.2915	-0.0596	0.5119	0.3260	-0.0225
XLV	I	0.5674	0.3644	0.0558	0.5881	0.4153	0.1052	0.5938	0.4226	0.1249
	II	0.5180	0.3431	0.0809	0.5562	0.4038	0.1086	0.5622	0.4044	0.1236
	III	0.5701	0.3662	0.0796	0.5899	0.4206	0.1148	0.5989	0.4272	0.1391
XLY	I	0.6398	0.3793	0.0679	0.6545	0.4430	0.1527	0.6542	0.4707	0.1697
	II	0.6212	0.3691	0.1066	0.6518	0.4510	0.1546	0.6499	0.4689	0.1739
	III	0.6488	0.3908	0.0972	0.6604	0.4463	0.1703	0.6600	0.4781	0.1801

*Notes: Table 2.20 shows Out-of-sample R^2 of HAR-RV-CJ models. I is the case with only co-jumps; II is with only single jumps; III is with both co-jumps and single jumps. In-Sample R^2 for HAR models with only co-jumps is usually larger than with only single jumps.

Figure 2.1: Number of Daily Sector Co-jump*

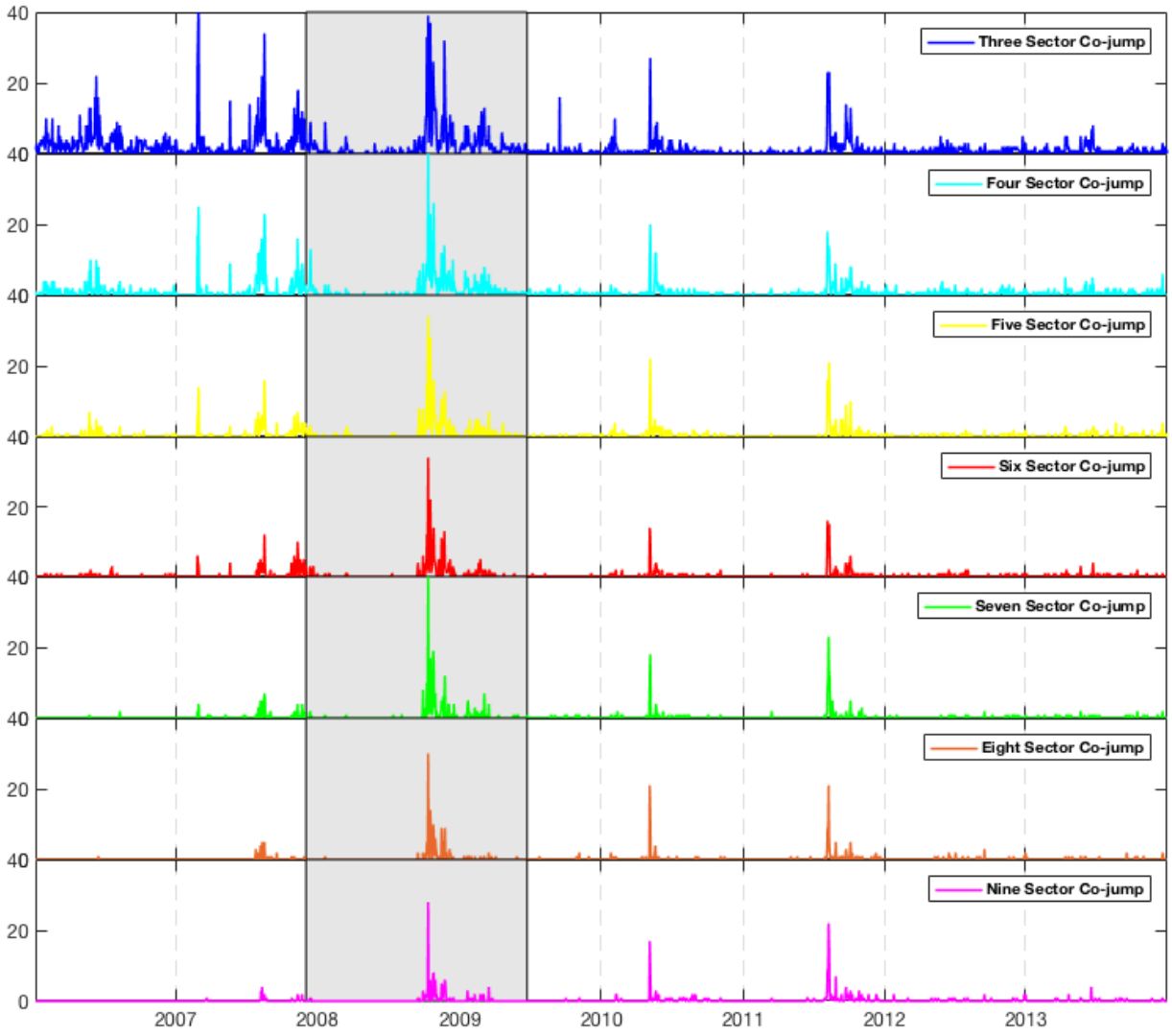

*Notes: Figure 2.1 shows the number of different sectors co-jumps from the year 2006 to 2013. The co-jump test is carried out using a significance level of $\alpha = 0.1$. From top to bottom panels are the number of three-sector co-jumps, four-sector co-jumps, five-sector co-jumps, six-sector co-jumps, seven-sector co-jumps, eight-sector co-jumps, and nine-sector co-jumps. The number of sector co-jumps is in the range from 0 to 40. The shadowed period in the figure is known as the 2007-2008 financial crisis.

Figure 2.2: Co-jump and Single Jump Contribution to Total Variation*

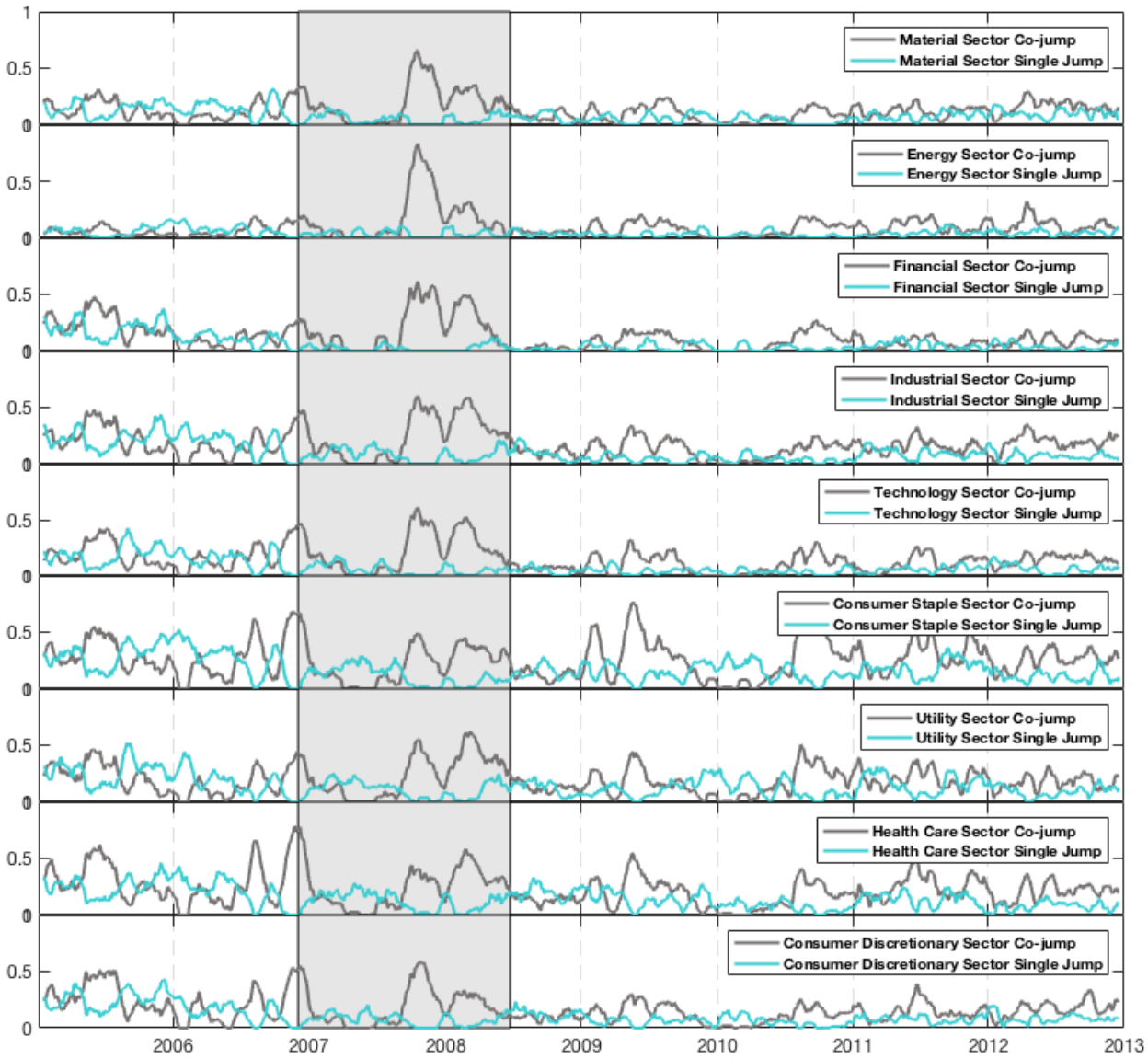

*Notes: Figure 2.2 shows co-jumps and single jumps contribution to total variations among each sector in S&P 500 market. The results are taken a 22-day (monthly) moving average. The co-jump test is carried out using a significance level of $\alpha = 0.1$. From top to bottom panels are the material sector, energy sector, financial sector, industrial sector, technology sector, consumer staple sector, utility sector, health care sector and consumer staple sectors. The shadowed period in the figure is known as the 2007-2008 financial crisis.

Chapter 3

Forecasting Sector Level Equity Returns Using Big Data Factors and Machine Learning Models

3.1 Introduction

The equity risk premium is one of the most widely studied topics in finance, and is crucial to both the understanding of the financial market and portfolio management. A small group of early key works in this area include Fama and French (1992), Fama and French (2015), Welch and Goyal (2007) and Rapach and Zhou (2013), who identify characteristics that have correlation with the equity returns and develop time series models useful for forecasting equity risk premia.

Since the advent of the "big data" era, research into this field of empirical finance has grown ever more rapidly, and numerous researchers have developed and championed the use of ever more sophisticated models for understanding the equity risk premium. In this paper, we add to this nascent literature by examining the marginal predictive content of a large number of machine learning methods for daily and monthly market and sector level equity returns. The novel feature of the modeling approach that we take in this paper is that we not only utilize multi-frequency and multi-dimensional datasets, but we also create a group of latent economic factors including market correlation indices, volatility risk measures, and macro risk factors. This paper, thus, adds to the literature on equity returns forecasting in two ways. First, we build on the work of Aruoba et al. (2009), Bloom (2009), Jurado et al. (2015), Aït-Sahalia and Xiu (2016) and others by introducing a class of multi-frequency macroeconomic/financial volatility risk factors and market correlation risk indices that are aimed at measuring market uncertainty. Our state space models are

specified in one of two ways, referring to Yao (2019). First, volatility risk factors are specified and estimated using a state space model that includes latent components of quadratic variation, including realized variance (RV_t), truncated realized variance (TRV_t), bi-power variation (BPV_t), and jump variation (JV_t); and also mixed frequency macroeconomic indicators.[1] Alternatively, macroeconomic risk factors are specified and estimated using a state space model that only includes mixed frequency macroeconomic indicators such as interest rates, employment, and production. Finally, we also construct and evaluate market correlation risk indices (or "correlation risk" factors), which are based on estimates of quadratic covariation constructed using high frequency market and sector level returns data. The construction of these indices follows Aït-Sahalia and Xiu (2016), who decompose the quadratic covariation between two assets into continuous and jumps components using high-frequency asset price data, and construct the continuous correlation indices by measuring the correlation between continuous returns, and jump correlation indices using the correlation between jump returns. [2]

Second, we utilize a large number of potentially interesting machine learning methods to allow for a rich variety of model specifications, when forecasting returns. We thus build on previous literature that discusses the difficulties in predicting equity returns, particularly at higher frequencies, such as daily returns (see e.g. Christoffersen and Diebold (2006)). In general, a large machine learning related literature has developed in recent years in the field of financial econometrics. For instance, Hutchinson et al. (1994) develop a nonparametric method for estimating the pricing formula of a derivative asset using neural network models. Rapach et al. (2013) applies adaptive elastic net estimation to predict monthly stock returns

[1] All of our measures of integrated volatility are extracted from high frequency S&P500 data.

[2] Related papers that utilize mixed-frequency state space models include Mariano and Murasawa (2003), Frale et al., Aruoba et al. (2009) and Marcellino et al. (2016). None of these papers, however, include multiple frequencies of the same latent variable, as is done in this paper. Additionally, see Ghysels et al. (2007) for an introduction to the alternative approach of using MIDAS for mixed frequency modeling.

in industrialized countries. Other related work includes, but not limit to, Harvey and Liu (2018), Kim and Swanson (2016) and Swanson and Xiong (2017). More recently, in an interesting paper, Gu et al. (2018) conduct a comprehensive study using machine learning methods to predict individual stock risk premia and construct investment portfolios.

More specifically, we evaluate machine learning methods including random forest, gradient boosting, support vector machine, penalized regressions and neural network (deep learning). Additionally, we evaluate machine learning classifier models including latent discriminant analysis, naive Bayes, support vector classifier, k-nearest-neighbors, random forest, and deep learning. Finally, we propose a group of hybrid machine learning models based on a two-step method that combines the least absolute shrinkage operator (lasso) and neural network methods. As discussed above, our objective is to forecast returns and indicators of directional change. Specifically, we predict both level and directional changes of daily and monthly returns for a variety of target variables, including the S&P500 (SPY) and four SPDR sector ETFs: financials (XLF), technology (XLK), health care (XLV), and consumer discretionary (XLY).[3] The predictors that we use in our analysis include both a small set of mixed frequency variables (for use in our state space models) as well as a variety of other predictors that have been examined previously by Neely et al. (2014), Fama and French (2015) and Welch and Goyal (2007).

Our experimental findings are based on the construction of 1-day and 1-month ahead predictions, formed using rolling and recursive estimation window strategies, for the sample period from 2009 - 2017. Our one-month-ahead forecasts are calculated by aggregating daily forecasts for each month. We also construct two types of directional forecasts. The first type is derived from our returns forecasts, in the sense that returns forecasts are classified

[3]The SPY is the largest exchange-traded fund in the world which is designed to track the S&P 500 stock market index. The XLF, XLK, XLV, and XLY are designed to represent the financial sector, technology sector, healthcare sector, and consumer discretionary sector of the S&P 500 index. The four selected sectors are the largest four S&P 500 sectors, by market cap, as of April 2019, according to Fidelity Research.

as "upward signals" if forecasts are positive, and are otherwise classified as "downward signals". The second type is constructed by utilizing machine learning classifiers to directly generate directional predictions. Our main findings are summarized as follows.

First, based on mean square forecasting error (MSFE) and directional predictive accuracy rates (DPAR), machine learning models yield forecasts that are significantly superior to the random walk and linear regression benchmark forecasts, when predicting monthly returns. Not surprisingly, though, daily results indicate little to choose between our alternative models. Indeed, it is only when we aggregate daily predictions to form monthly predictions, that machine learning methods dominate, for all target assets (i.e. different sector returns), regardless of estimation window strategy.

Second, the random forest method is clearly the preferred machine learning approach. These results are statistically significant (when forecasting monthly returns), and prevail for all of our target variables and estimation strategies. Moreover, these results continue to hold regardless of the set of predictor variables utilized in our different models (we evaluate predictor sets both with and without the latent uncertainty factors discussed above).

Third, "deep" learning models outperform "shallow" learning models. For instance, deep learning models with two to four hidden layers have statistically smaller MSFEs and higher DPARs than shallow learning models with only one hidden layer. Again, this result holds across all windowing strategies used to estimate our models, and for all targets and predictor sets.

Fourth, hybrid machine learning models, which combine lasso and neural network models, often outperform individual models based on both the MSFE and the DPAR. For example, these models usually yield smaller MSFEs and higher DPARs than models based on solely the lasso or neural networks.

Fifth, all three novel risk factors, including market correlation indices, volatility risk

factors, and macro risk factors, are shown to contain significant marginal predictive content. In particular, "MSFE-best" and "DPAR-best" forecasting models yield significantly smaller MSFEs and higher DPARs than models without risk factors. Moreover, for the majority of our machine learning models that are not "MSFE-best" or "DPAR-best" best, these three types of factors also prove to be useful.

Sixth, the market as well as all of the sectors that we analyze have different levels of sensitivity to input information, in the form of the predictor set used when constructing the "MSFE-best" or "DPAR-best" model. For the S&P500, a broad range of predictor sets, including sets consisting of (i) all variables, (ii) all variables except macro variables, and (iii) all variables except one of our uncertainty factors have marginal predictive content, when used as machine learning inputs. The exception is our set of "technical variables", which includes trading volume and price trend indicators. When these variables are excluded from the set of predictor variables, MSFEs and DPARs generally improve, for all of our target variables. This may be because useful predictive information contained in our technical variables is also included in our latent uncertainty factors. However, even if this is the case, it is clear from our findings that our latent uncertainty factors have further information embedded in them that is also useful for predicting returns.

Finally, it is worth noting that our correlation indices based on jump variation surges during 2008 and 2011, and drops when market volatility is stable, while our correlation indices based on continuous variation moves in the opposite direction, except for the energy sector. This suggests that the rise in correlation across markets and sectors is largely driven by co-jump behavior. Moreover, When exiting the financial crisis period around 2008, volatility risk factors generally move together across all of the sectors that we analyze in our experiments, including the market (i.e., the S&P500).

The rest of this paper is organized as follows. Section 3.2 summarizes our setup, including a discussion of the latent uncertainty factors that we examine. Section 3.3 discusses our experiment setup and briefly outlines all of the machine learning methods used in the sequel. Finally, Section 3.4 contains a description of the data used in our experiments, and summarizes our empirical findings, and Section 3.5 concludes.

3.2 Market Correlation Indices, Volatility Risk Factors, and Macroeconomic Risk Factors

In this section, we outline the methodology used in the construction of risk factors[4] and market correlation indices analyzed in the sequel. We first introduce the measurements of high-frequency volatility and continuous and jump volatility parts, and layout the construction of correlation indices. We then turn to the state space framework used to estimate our volatility risk and macroeconomic risk factor, and address temporal aggregation and missing observations problems while working with mixed-frequency series.

3.2.1 High frequency measures of volatility and jump risk

Let X_t be the log-price of an asset at time t. Assume that the log-price process follows a jump-diffusion model (hence, almost surely, its paths are right continuous with left limits). Namely,

$$X_t = X_0 + \int_0^t b_s ds + \int_0^t \sigma_s dB_s + \sum_{s \leq t} \Delta X_s. \tag{3.1}$$

In the above expression, B is a standard Brownian motion and $\Delta X_s := X_s - X_{s-}$, where $X_{s-} := \lim_{u \uparrow s} X_u$, represents the possible jump of the process X, at time s.

[4] We use the notation and setup as in Yao (2019)

Consider a finite time horizon, $[0,t]$ that contains n high-frequency observations of the log-price process. A typical time horizon is one day. Let $\Delta_n = t/n$ be the sampling frequency. Then intra-daily returns can be expressed as $r_{i,n} = X_{i\Delta_n} - X_{(i-1)\Delta_n}$.

A well-established result in the high frequency econometrics literature is that realized volatility is a consistent estimator of the total quadratic variation. Namely,

$$RV_t = \sum_{i=1}^{n} r_{i,n}^2 \xrightarrow{\text{u.c.p.}} \int_0^t \sigma_s^2 ds + \sum_{s \leq T} (\Delta X_s)^2 = QV_t = IV_t + JV_t, \tag{3.2}$$

where $\xrightarrow{\text{u.c.p.}}$ denotes convergence in probability, uniformly in time. There are many estimators of integrated volatility (IV_t), which is the variation due to the continuous component of quadratic variation (QV_t). For example, multipower variations are defined as follows:

$$V_t = \sum_{i=j+1}^{n} |r_{i,n}|^{r_1} |r_{i-1,n}|^{r_2} ... |r_{i-j,n}|^{r_j}, \tag{3.3}$$

where $r_1, r_2, ..., r_j$ are positive, such that $\sum_{i=1}^{j} r_i = k$, say. An important special case of this estimator is bipower variation (BPV_t), which was introduced by Barndorff-Nielsen and Shephard (2004). Namely,

$$BPV_t = (\mu_1)^{-2} \sum_{i=2}^{n} |r_{i,n}||r_{i-1,n}| \tag{3.4}$$

where $\mu_1 = E(|Z|) = 2^{1/2}\Gamma(1)/\Gamma(1/2) = \sqrt{2/\pi}$, with Z a standard normal random variable, and where $\Gamma(\cdot)$ denotes the gamma function. Another useful estimator is truncated bipower variation ($TBPV_t$), which combines the truncation method proposed by Mancini (2009) and the bipower variation (BPV_t) estimator discussed above. Namely,

$$TBPV_t = (\mu_1)^{-2} \sum_{i=2}^{n} |\overline{r}_{i,n}||\overline{r}_{i-1,n}|, \quad \overline{r}_{i,n} = r_{i,n} 1_{\{|r_{i,n}| < \alpha_n\}}, \tag{3.5}$$

where $\alpha_n = \alpha \Delta_n^{\varpi}, \varpi \in (0, \frac{1}{2})$. Similarly, truncated realized variance (TRV_t) is defined as

$$TRV_t = \sum_{i=1}^{n} \overline{r}_{i,n}^2. \tag{3.6}$$

Finally, jump variation (JV_t) can be estimated as $JV_t = RV_t - BPV_t$ or $JV_t = RV_t - TBPV_t$, for example. In the sequel, we shall utilize RV_t, TRV_t, BPV_t and $JV_t = RV_t - BPV_t$.

Under certain regularity conditions [5], BPV_t, $TBPV_t$ and TRV_t are consistent estimators of unobserved integrated volatility $\text{IV}_t := \int_0^t \sigma_s^2 ds$, and JV_t is the consistent estimator of jump volatility. Moreover, it is also well-established that these estimators converge stably in law at the rate $\sqrt{1/\Delta_n}$, or equivalently, $\sqrt{n}$. Let T be the total number of such representative finite time horizon $[0, t]$ (e.g., day, week, month or quarter). If $\Delta_n T \to 0$, then the impact of estimating the latent volatility and jump risk factors are asymptotically negligible, since the parameters in our state space model converge at rate $\sqrt{T}$.

3.2.2 Market correlation indices

In the high frequency literature, previous research focusing on covariation under multivariate settings has focused mainly on solving three challenges: i) High frequency data tends to be severely contaminated with the microstructure noise; ii) non-synchronous high frequency data lead to estimation bias when constructing covariation measures; and iii) covariation matrices must be positive semi-definite in order to guarantee the existence of stable inverses thereof. Notably, Aït-Sahalia and Xiu (2016) address these issues, and develop estimators to decompose quadratic covariation between two assets into continuous and jump components.

Following Aït-Sahalia and Xiu (2016), the quadratic covariation between X_i and X_j is equal to the sum of continuous component quadratic covariation and jump component

[5] See papers cited above and Jacod and Protter (2011) and Aït-Sahalia and Jacod (2014) for details about regularity conditions.

covariation:

$$[X_i, X_j]_t = [X_i, X_j]_t^c + [X_i, X_j]_t^d, \tag{3.7}$$

where $[X_i, X_j]_t$ is the quadratic covariation between X_i and X_j, $[X_i, X_j]_t^c$ is the continuous quadratic covariation component, and $[X_i, X_j]_t^d$ is the quadratic covariation associated with the discontinuous (jump) component of a process. Andersen et al. (2003b) propose realized measures of quadratic covariation, named realized covariance, that are based on the sum of the product of intra-day returns between two assets:

$$cov_{i,j}(t; n) = \sum_{k=1}^{n} r_{i,k,t} \times r_{j,k,t} \tag{3.8}$$

where $cov_{i,j}(t; n)$ denotes the realized covariance between asset i and asset j, at day t. Here, $r_{i,k,t}$ is the intra-daily return of asset i at time interval k, during day t. Realized covariance is an error free estimator of quadratic covariation $[X_i, X_j]_t$, when the length of each intra-daily interval approaches 0 (i.e. the number of intra-daily intervals $n \to \infty$). Namely,

$$\lim_{n\to\infty} cov_{i,j}(t; n) = [X_i, X_j]_t \tag{3.9}$$

In Aït-Sahalia and Xiu (2016), the correlation, $\rho_{i,j}^c$, between asset X_i and asset X_j, which is derived from the continuous component is:

$$\rho_{i,j}^c = \frac{[X_i, X_j]^c}{\sqrt{[X_i, X_i]}\sqrt{[X_j, X_j]}} \tag{3.10}$$

The correlation, $\rho_{i,j}^d$, between asset X_i and asset X_j, which is derived from the jump component is:

$$\rho_{i,j}^d = \frac{[X_i, X_j]^d}{\sqrt{[X_i, X_i]}\sqrt{[X_j, X_j]}} \tag{3.11}$$

where $[X_i, X_i]$ and $[X_j, X_j]$ denote the quadratic variations of assets X_i and X_j, respectively. The quadratic variation in the above formulae is estimated using realized volatility,

as in equation (2). The jump component of quadratic covariation, $[X_i, X_j]^d$, is equal to $\sum_{s \leq t} \Delta X_{i,s} \Delta X_{j,s}^T$, where $\Delta X_{i,s}$ represents the jump in X_i, at time s.

In our empirical experiments, we estimate $[X_i, X_j]^d$ using a "jump-test" approach. Namely, the realized covariance associated with jumps is:

$$cov_{i,j}(t;n)^d = \sum_{k=1}^{n} (r_{i,k,t} * I_{jump,i,k,t}) \times (r_{j,k,t} * I_{jump,j,k,t}). \tag{3.12}$$

The jump indicators, $I_{jump,i,k,t}$ and $I_{jump,j,k,t}$, are identified using the Lee and Mykland (2007) jump test. More specifically, Lee and Mykland (2007) use the ratio of realized returns to estimated instantaneous volatility, and construct a nonparametric jump test to identify the exaxt timing of jumps at the intra-day level. The test statisic which identifies whether there is a jump during the interval $(t + l/n, t + (l+1)/n)$ is:

$$L_{(t+(l+1)/n)} = \frac{X_{t+(l+1)/n} - X_{t+l/n}}{\widehat{\sigma_{t+(l+1)/n}}}, \tag{3.13}$$

where

$$\widehat{\sigma_{t+(l+1)/n}}^2 \equiv \frac{1}{K-2} \sum_{i=l-K+1}^{l-2} |X_{t+(i+1)/n} - X_{t+i/n} \mid\mid X_{t+i/n} - X_{t+(i-1)/n}|. \tag{3.14}$$

Here K is the window size of a local movement of the process. We choose K = 10 and use the 5-minute sampling frequency (i.e., the number of intra-day observations, n, equals 78). These authors show that

$$\frac{max_{l \in \bar{A}_n} |L_{(t+(l+1)/n)}| - C_n}{S_n} \to \varepsilon, \quad as \;\; \Delta t \to 0, \tag{3.15}$$

where ε has a cumulative distribution function $P(\varepsilon \leq x) = exp(-e^{-x})$,

$$C_n = \frac{(2logn)^{1/2}}{c} - \frac{log\pi + log(logn)}{2c(2logn)^{1/2}} \quad and \quad S_n = \frac{1}{c(2logn)^{1/2}} \tag{3.16}$$

c ≈ 0.7979 and $\bar{A}_n$ is the set of $l \in \{0, 1, ..., n\}$, so that there are no jumps in $(t + l/n, t + (l+1)/n]$. We choose a 10% significance level when applying this test. If the test statistic,

$L_{(t+(l+1)/n)}$, lies in the critical region of the null distribution at 10% significance level, then we reject the null hypothesis that there is no jump during $(t + l/n, t + (l + 1)/n]$, and the jump indicator, I_{jump}, is set equal to 1. Otherwise, the jump indicator is set equal to 0.

Finally, the continuous component of quadratic covariation is estimated as the difference between realized covariance and discontinuous (jump) realized covariance. Namely,

$$cov_{i,j}(t;n)^c = cov_{i,j}(t;n) - cov_{i,j}(t;n)^d \tag{3.17}$$

3.2.3 Volatility risk factors

Using the state space model setup in Yao (2019), the variable $y_t = (y_t^1, y_t^2, y_t^3, y_t^4)$ corresponding to data measured at 4 different time horizons, including daily (denoted by d), bi-daily (denoted by $2d$), tri-daily (denoted by $3d$), and weekly (denoted by w). In our setup, y_t is alternately set equal to TRV_t. The latent risk factor that we are interested in extracting is called MF_t^{vol}. Finally, the elements of y_t, which are aggregated, are flow variables. Therefore, we include three aggregated state variables, i.e., C_t^1, C_t^2 and C_t^3, to address the aggregation issues discussed above. The state space model is:

Observation Equation:

$$\begin{pmatrix} y_t^d \\ y_t^{2d} \\ y_t^{3d} \\ y_t^w \end{pmatrix} = \begin{pmatrix} \beta_1 & 0 & 0 & 0 & 1 & 0 & 0 & 0 \\ 0 & \beta_2 & 0 & 0 & 0 & 1 & 0 & 0 \\ 0 & 0 & \beta_3 & 0 & 0 & 0 & 1 & 0 \\ 0 & 0 & 0 & \beta_4 & 0 & 0 & 0 & 1 \end{pmatrix} \begin{pmatrix} MF_t^{vol} \\ C_t^1 \\ C_t^2 \\ C_t^3 \\ u_t^1 \\ u_t^2 \\ u_t^3 \\ u_t^4 \end{pmatrix}$$

State Equation:

$$\begin{pmatrix} MF_{t+1}^{vol} \\ C_{t+1}^1 \\ C_{t+1}^2 \\ C_{t+1}^3 \\ u_{t+1}^1 \\ u_{t+1}^2 \\ u_{t+1}^3 \\ u_{t+1}^4 \end{pmatrix} = \begin{pmatrix} \rho & 0 & 0 & 0 & 0 & 0 & 0 & 0 \\ \rho & \psi_{t+1}^1 & 0 & 0 & 0 & 0 & 0 & 0 \\ \rho & 0 & \psi_{t+1}^2 & 0 & 0 & 0 & 0 & 0 \\ \rho & 0 & 0 & \psi_{t+1}^3 & 0 & 0 & 0 & 0 \\ 0 & 0 & 0 & 0 & \eta_1 & 0 & 0 & 0 \\ 0 & 0 & 0 & 0 & 0 & \eta_2 & 0 & 0 \\ 0 & 0 & 0 & 0 & 0 & 0 & \eta_3 & 0 \\ 0 & 0 & 0 & 0 & 0 & 0 & 0 & \eta_4 \end{pmatrix} \begin{pmatrix} MF_t^{vol} \\ C_t^1 \\ C_t^2 \\ C_t^3 \\ u_t^1 \\ u_t^2 \\ u_t^3 \\ u_t^4 \end{pmatrix}$$

$$+ \begin{pmatrix} 1 & 0 & 0 & 0 & 0 \\ 1 & 0 & 0 & 0 & 0 \\ 1 & 0 & 0 & 0 & 0 \\ 1 & 0 & 0 & 0 & 0 \\ 0 & 1 & 0 & 0 & 0 \\ 0 & 0 & 1 & 0 & 0 \\ 0 & 0 & 0 & 1 & 0 \\ 0 & 0 & 0 & 0 & 1 \end{pmatrix} \begin{pmatrix} e_t^1 \\ e_t^2 \\ e_t^3 \\ e_t^4 \\ e_t^5 \end{pmatrix},$$

where the error terms $e_t^i \overset{i.i.d}{\sim} N(0, \sigma_i^2)$, with $i = 1, ..., 5$.

As mentioned above, the three aggregated variables in the state vector, C_t^1, C_t^2 and C_t^3, are designed to handle bi-daily, tri-daily and weekly updating of our volatility series, respectively. Also, ψ_1, ψ_2 and ψ_3 are binary-valued parameters for the aggregated state variables, and are defined as follows:

$$\psi_t^1 = \begin{cases} 0, & \text{if t is an odd number} \\ 1, & \text{otherwise,} \end{cases},$$

for the bi-daily updating series;

$$\psi_t^2 = \begin{cases} 0, & \text{if t is the first day of every three days} \\ 1, & \text{otherwise,} \end{cases},$$

for the tri-daily updating series; and

$$\psi_t^3 = \begin{cases} 0, & \text{if t is the first day of every week} \\ 1, & \text{otherwise,} \end{cases}$$

for the weekly series.

In the above observation equation, only the highest frequency variable, y_t^d, is directly connected with the factor, MF_t^{vol}, via β_1. The three other volatility variables are connected with MF_t^{vol} via the aggregated state variables (i.e, C_t^1, C_t^2 and C_t^3) and via β_2, β_3 and β_4. Coupled with the setup of the binary-valued parameters (i.e., ψ_1, ψ_2 and ψ_3) in the state equation, this ensures the proper inter-temporal aggregation of the flow variables in the system. and refreshes the quantity at the beginning of each period. Finally, the u_t are stochastic disturbance terms, and are assumed to follow autoregressive processes, as in Aruoba et al. (2009). In the state equation, the first four state variables are connected with MF_t^{vol} via ρ. Of these four state variables, the last three (i.e., C_t^1, C_t^2 and C_t^3) are defined such that their previous values are added to ρMF_t^{vol} whenever flow aggregation is required.

3.2.4 Macroeconomic risk factors

We again begin with $y_t = (y_t^1, y_t^2, y_t^3, y_t^4)$. In this section, the data are measured at daily (denoted by d), weekly (denoted by w), monthly (denoted by m), and quarterly (denoted by w) frequencies. This allows us to construct a "benchmark" risk factor corresponding to the business conditions index analyzed by Aruoba et al. (2009). In particular, following Aruoba et al. (2009), we use four macroeconomic variables with different sampling frequencies, including: (1) the daily yield curve spread (y_t^1), defined to be the difference between the 10-year U.S. Treasury bond yield and the 3-month Treasury bill yield; (2) weekly initial claims for unemployment insurance (y_t^2); (3) nonfarm payroll employment (y_t^3); and (4) quarterly gross domestic product (y_t^4). The corresponding state-space model used to extract

our risk factor, called MF_t^{mac} is: *Observation equation:*

$$\begin{pmatrix} y_t^1 \\ y_t^2 \\ y_t^3 \\ y_t^4 \end{pmatrix} = \begin{pmatrix} \beta_1 & 0 & 0 & 1 \\ 0 & \beta_2 & 0 & 0 \\ \beta_3 & 0 & 0 & 0 \\ 0 & 0 & \beta_4 & 0 \end{pmatrix} \begin{pmatrix} MF_t^{mac} \\ C_t^1 \\ C_t^2 \\ u_t^1 \end{pmatrix} + \begin{pmatrix} 0 & 0 & 0 \\ \gamma_2 & 0 & 0 \\ 0 & \gamma_3 & 0 \\ 0 & 0 & \gamma_4 \end{pmatrix} \begin{pmatrix} y_{t-W}^2 \\ y_{t-M}^3 \\ y_{t-Q}^4 \end{pmatrix} + \begin{pmatrix} 0 \\ w_t^2 \\ w_t^3 \\ w_t^4 \end{pmatrix}.$$

State equation:

$$\begin{pmatrix} MF_{t+1}^{mac} \\ C_{t+1}^1 \\ C_{t+1}^2 \\ u_{t+1}^1 \end{pmatrix} = \begin{pmatrix} \rho & 0 & 0 & 0 \\ \rho & \psi_{t+1}^1 & 0 & 0 \\ \rho & 0 & \psi_{t+1}^2 & 0 \\ 0 & 0 & 0 & \gamma_1 \end{pmatrix} \begin{pmatrix} MF_t^{mac} \\ C_t^1 \\ C_t^2 \\ u_t^1 \end{pmatrix} + \begin{pmatrix} 1 & 0 \\ 1 & 0 \\ 1 & 0 \\ 0 & 1 \end{pmatrix} \begin{pmatrix} e_t^1 \\ e_t^2 \end{pmatrix},$$

where the error terms $e_t^i \overset{i.i.d}{\sim} N(0, \sigma_i^2)$, with $i = 1, 2$.

The variables in this model include observed variables, the y_t; our latent risk factor, MF_t^{mac}; aggregate state variables, C_t^1 and C_t^2; and stochastic disturbance terms, u_t^1, w_t^2, w_t^3, and w_t^4. Note that in this model, only y_t^2 and y_t^4 are flow variables in this model, and hence there are only two aggregate state variables. Accordingly, we also define two binary-valued variables ψ_1 and ψ_2 for these aggregated state variables. Namely,

$$\psi_t^1 = \begin{cases} 0, & \text{if t is the first day of the week} \\ 1, & \text{otherwise,} \end{cases}$$

and

$$\psi_t^2 = \begin{cases} 0, & \text{if t is the first day of the quarter} \\ 1, & \text{otherwise.} \end{cases}$$

3.2.5 Technical indicators

Technical indicators have been widely used by practitioners in asset pricing applications. Two key papers discussing different technical indicators include Fama and Blume (1966)

and Brock et al. (1992). These papers explore the usefulness of various technical indicators, including filter rules, moving averages, and momentum, when designing trading strategies. Neely et al. (2014) shows the usefulness of technical indicators for predicting the equity risk premium. These authors analyze 14 common technical indicators.

In our experiments, we use two types of technical indicators, including moving average indicators and volume-based trend indicators, following Neely et al. (2014). The moving average technical indicators are derived by using moving-average (MA) rules to generate long or short signals at the end of each trading day, t. Namely, define:

$$D_t = \begin{cases} 1 & \text{if } P_t^{MA(k)} \geqslant P_t^{MA(s)} \\ 0 & \text{otherwise} \end{cases} \tag{3.18}$$

where

$$P_t^{MA(q)} = \frac{1}{q} \sum_{i=0}^{q-1} P_{t-i} \quad \text{for} \quad q = k, s \tag{3.19}$$

Here $D_t = 1$ represents the long signal and $D_t = 0$ represents the short signal at day t. We use 30-, 90-, and 120-day moving-averages of asset prices, P_t, in our experiments.[6] This allows us to obtain potentially useful price trend indicators. The values for q are thus set equal to $30, 90, 120$, representing monthly, quarterly, and semiannually time periods, and yielding three price trend indicators. Table 3.1A lists the technical indicators in detail.

Our volume-based trend indicators are constructed by combining trading volume and prices in order to identify volume trends in the market. The daily "net "" volume is defined as:

$$V_{net,t} = V_t \times S_t \tag{3.20}$$

[6]Here P_t is the asset price, measured at the end of each trading day, t

where V_t is the trading volume at day, t. The dummy variable, S_t, is:

$$S_t = \begin{cases} 1 & \text{if } P_t \geqslant P_{t-1} \\ -1 & \text{otherwise.} \end{cases} \tag{3.21}$$

We use the "net" volume, $V_{net,t}$, to generate the trading signals D_t, where:

$$D_t = \begin{cases} 1 & \text{if } V_{net,t}^{MA(k)} \geqslant V_{net,t}^{MA(s)} \\ 0 & \text{otherwise} \end{cases} \tag{3.22}$$

with

$$V_{net,t}^{MA(q)} = \frac{1}{q} \sum_{i=0}^{q-1} V_{net,t-i} \quad \text{for} \quad q = k, s \tag{3.23}$$

Here $D_t = 1$ represents the "long" signal and $D_t = 0$ represents the "short" signal, on day t. We utilize 30-, 90-, and 120-day moving averages of the "net" volume in order to construct our volume-based trend indicators. The parameters q is thus set as $30, 90, 120$ to represent monthly, quarterly, and semiannually time periods.

3.3 Experiment Setup

In this section, we introduce our experimental setups and models used to predict asset returns. First, we detail the splitting of sample data into validation, training and test parts. The validation dataset is established to estimate hyperparameters in machine learning models and avoid potential overfitting problem. Second, we show specific setups of forecasting models we use in the experiment. For example, in machine learning models, we discuss the tuning process of hyperparameter, the objective function of the model, and parameter estimation algorithm or solver.

In our empirical experiment, forecast targets are the return of the following financial assets: SPY (SPDR S&P 500 ETF Trust), XLF (Financial Select Sector SPDR Fund), XLK

(Technology Select Sector SPDR Fund), XLV (Health Care SPDR), and XLY (Consumer Discretionary SPDR). The SPY is the largest exchange-traded fund in the world which is designed to track the S&P 500 stock market index. The XLF, XLK, XLV and XLY are designed to represent the financial sector, technology sector, healthcare sector, and consumer discretionary sector of the S&P 500 index. We forecast one-day-ahead daily returns and directional changes for each target asset using both rolling and recursive estimation windows. The rolling window size is $T = 500$. We denote daily returns of targeted assets at day t as $r_{i,t}$, where i corresponds to one of the five sectors mentioned earlier. We also calcualte one-month-ahead forecasts by aggregating daily forecasts. Finally, as as mentioned above, we also construct two types of directional forecasts. The first type is derived from our returns forecasts, in the sense that returns forecasts are classified as "upward signals" if forecasts are positive, and are otherwise classified as "downward signals". The second type is constructed by utilizing machine learning classifiers to directly generate directional predictions.

3.3.1 Linear models

We use a random walk model as our main benchmark. Namely, forecasts are constructed using:

$$r_{t+1} = a + \epsilon_{t+1} \tag{3.24}$$

where ϵ_{t+1} is a stochastic disturbance term, and a is constant. In our experiments, a is estimated under both rolling and recursive data windows. For the rolling scheme, the window size $T = 500$. For the recursive scheme, a is constructed using asset returns from $t = 251^{th} - t^*$, where t^* denotes the last trading day prior to the period being forecasted. We also estimate linear models with the following specification:

$$r_{t+1} = c + \alpha' W_t + \epsilon_{t+1}, \tag{3.25}$$

where $r_{i,t+1}$ is the "target" forecast variable of interest (i.e. daily returns for SPY, XLF, XLK, XLV, and XLY), and the forecast horizon is one-day-ahead. W_t contains explanatory variables at time t, and α is a conformably defined coefficient vector. W_t consists one-day-lagged returns, $r_{i,t}$, and exogenous variables including macroeconomic and financial volatility (risk) factors, and market correlation indeices; as well as the macroeconomic and technical indicators outlined in Table 3.1A. For details regarding the variables in W_t, refer to Table 3.2. Models are estimated using least squares.

3.3.2 Penalized linear models

We utilize two varieties of penalized regression - ridge regression and Least absolute shrinkage operator (lasso)type regression.

Ridge regression

Ridge regression is introduced by Hoerl and Kennard (1970). Estiamtion involves solving the following problem:

$$minL(\lambda, \alpha) = \sum_{t=1}^{T} [r_{t+1} - c - \alpha' W_t]^2 + \lambda |\alpha'|^2 + \lambda c^2 \tag{3.26}$$

where $\alpha = (\alpha_1, ..., \alpha_p)$ and $\lambda \geq 0$. Here $|\alpha'|^2 = \sum_{j=1}^{p} \alpha_j^2$. The tuning parameter, λ, controls the amount of shrinkage.

Lasso regression

Lasso regression is introduced by Tibshirani (1996). Estimation involves solving the following problem:

$$minL(\lambda, \alpha) = \sum_{t=1}^{T} [r_{t+1} - c - \alpha' W_t]^2 + \lambda |\alpha'| + \lambda |c| \tag{3.27}$$

where $\alpha = (\alpha_1, ..., \alpha_p)$ and $\lambda \geq 0$. Here $|\alpha'| = \sum_{j=1}^{p} |\alpha_j|$. We optimize the tuning parameter, λ, using the training' sample, as discussed above.

3.3.3 Logistic regression

Logistic regression is used in several areas including, for example, the bioassay, epidemiology, and machine learning fields. In a key paper, Cox (1966) introduces the multinomial logistic regression model. The purpose of these models is to estimate the probability that categorical response variables, say r_{t+1}, belong to a particular category via use of a linear probability model. In particular, probabilities based on logistic regression are calculated using the logistic function:

$$\begin{aligned} P(r_{t+1} = m|W_t) &= \frac{exp(c_m + \alpha'_m W_t)}{1 + \sum_{n=1}^{M-1} exp(c_n + \alpha'_n W_t)}, m = 1, ..., M-1, \\ P(r_{t+1} = M|W_t) &= \frac{1}{1 + \sum_{n=1}^{M-1} exp(c_n + \alpha'_n W_t)}, \end{aligned} \tag{3.28}$$

where $M = 2$ in our directional prediction accuracy experiments. Maximum likelihood is used to estimate $\theta = \{c_1, \alpha'_1\}$; and the likelihood function is

$$l(\theta) = \prod_t P(r_{t+1} = 1|W_t) \prod_t (1 - P(r_{t+1} = 2|W_t)) \tag{3.29}$$

To maximize this likelihood function, we use the *liblinear* algoritm discussed in Fan et al. (2008).

3.3.4 Linear discriminant analysis

Linear discriminant analysis (LDA) was introduced by Fisher (1936). LDA is useful because it is more stable than logistic regression, when the distribution of predictors, $W_t = \{W_{1,t}, ..., W_{p,t}\}$, is approximately normal. The idea is to model the distribution of W_t from each class of response variable, $r_{j,t+1}$, say (in our experiments, $j = 1, ..., 5$ as

discussed above), separately and then use Bayes theorem to update $P(r_{j,t+1} = m|W_t)$. Suppose that π_m represents the prior probability of $r_{j,t+1}$ belonging to the class, m, where $\sum_{m=1}^{M} \pi_m = 1$. The probability density function of W_t belonging to class m is $f_m(W_t)$. Bayes' theorem then implies that:

$$P(r_{j,t+1} = m|W_t) = \frac{f_m(W_t)\pi_m}{\sum_{m=1}^{M} f_m(W_t)\pi_m}, \tag{3.30}$$

Linear discriminant analysis models the density function $f_m(W_t)$ as a multivariate Gaussian process. Namely:

$$f_m(W_t) = \frac{1}{(2\pi)^{(p/2)}|\Sigma_m|^{1/2}} e^{-\frac{1}{2}(W_t-\mu_m)^T\Sigma_m^{-1}(W_t-\mu_m)} \tag{3.31}$$

where μ_m is the mean of W_t for the m^{th} class, and Σ_m is the covariance matrix common to all m classes. Finally, it is worth noting that the log-ratio of the conditional probability density function between two classes is:

$$\begin{aligned} log\frac{P(r_{j,t+1} = l|W_t)}{P(r_{k,t+1} = m|W_t)} &= log\frac{f_l(W_t)}{f_m(W_t)} + log\frac{\pi_l}{\pi_m} \\ &= log\frac{\pi_l}{\pi_m} - \frac{1}{2}(\mu_l + \mu_m)^T\Sigma^{-1}(\mu_l + \mu_m) \\ &+ W_t^T\Sigma^{-1}(\mu_k - \mu_l), \end{aligned} \tag{3.32}$$

which is linear in W_t.

3.3.5 Naive Bayes classifier

The Naive Bayes classifier was first introduced in the pattern recognition field by Duda (1973). More recent machine learning papers in the area include Langley (1993) and Friedman et al. (1997). The naive Bayes model assumes input variables $W_t = \{W_{t,1}, ..., W_{t,p}\}$ are independent in each class of the response variable $r_{j,t+1} = 1, ..., M$. Namely:

$$f_m(W_t) = \prod_{k=1}^{p} f_{mk}(W_{t,k}), \tag{3.33}$$

where $f_m(W_t)$ is the probability density function of W_t in class $r_{j,t+1} = m$. As the LDA model, the log-ratio of the conditional probability density function between two classes is:

$$log\frac{P(r_{t+1}=l|W_t)}{P(r_{t+1}=m|W_t)} = log\frac{\pi_l f_l(W_t)}{\pi_m f_m(W_t)} = log\frac{\pi_l \prod_{k=1}^{p} f_{lk}(W_{t,k})}{\pi_m \prod_{k=1}^{p} f_{mk}(W_{t,k})} = log\frac{\pi_l}{\pi_m} + \sum_{k=1}^{p} log\frac{f_{lk}(W_{t,k})}{f_{mk}(W_{t,k})}. \tag{3.34}$$

3.3.6 Support vector machines

Support vector machines (SVMs) were first proposed by Vapnik and Chervonenkis (1964). A key recent paper in this area is Cortes and Vapnik (1995). A key impetus for this machine learning method is that linearity is a strict assumption, and may yield poor approximations in high-dimensional and high-frequency data environments. This has led to the introduction of various "learning methods", of which SVMs are an example.

SVMs utilize hyperplanes in order to delineate boundaries for the separation of observations into different categories. The idea is to find "optimal" separating boundaries that effectively categorize data and maximize the distance from the closest observations to the boundary. While several other techniques such as the Latent Dirichlet allocation (LDA) also incorporate a similar idea, support vector machine/regression models are interesting because estimation only requires a small percentage of the data (i.e., to construct so-called "support vectors"). Rather than depending on all sample data, as in the case of LDA, optimization hinges on the use of these support vectors, which are easy to construct using big data and are robust to overfitting problems.

Without loss of generality, define a hyperplane for a p-dimensional dataset as:

$$c + \alpha_1 W_{t,1} + \cdots + \alpha_p W_{t,p} = 0,$$

where $W_t = (W_{t,1}, \cdots, W_{t,p})'$, for observations $t = 1, ..., T$. These hyperplanes are used in

the following classification rule:

$$If \quad c + \alpha_1 W_{t,1} + \cdots + \alpha_p W_{t,p} > 0, \quad then \quad d_t = 1$$

and

$$If \quad c + \alpha_1 W_{t,1} + \cdots + \alpha_p W_{t,p} < 0, \quad then \quad d_t = -1$$

Optimal separating boundaries are obtained by maximizing the margin around the boundary, say M. Under separability, M denotes a certain "minimal distance" of data points from the boundary. Under nonseparability, a small number of data points may be misclassified, in the sense that they reside on the other side of the boundary. In this setup, ξ_t is defined to be the magnitude of any miscalssification. If there is none, then $\xi_t = 0$. Otherwise, $\xi_t =$ equals the distance from the data points to the hypoerplane, with $\xi_t \geqslant 0$. An additional constraint "$\sum_{i=1}^{N} \xi_t \leqslant constant$" controls the level of missclassification allowed. The objective function used to estimate the parameters in a support vector machine is:

$$\begin{aligned} &\underset{c,\alpha,||\alpha,c||=1}{max} M \\ &s.t. \quad d_t(c + \alpha_1 W_{t,1} + \cdots + \alpha_p W_{t,p}) \geq M(1 - \xi_t), \end{aligned} \tag{3.35}$$

where $||\cdot||$ denotes the Euclidean norm. Support vector regression extends the idea of support vector machines into a regression framework. Rather than focusing on the distance of support vectors to hyperplanes, under, support vector regression minimizes the error between fitted and true observational values. For example, using the simplest linear regression where $f(W_t) = c + \alpha_1 W_{t,1} + \cdots + \alpha_p W_{t,p}$, support vector regression incorporates the error term $r_{j,t+1} - f(W_t)$ into its objective function. Following Cortes and Vapnik (1995), the objective function for support vector regression can be written as:

$$\underset{c,\alpha}{min} \sum_{i=1}^{N} V(r_{j,t+1} - f(W_t)) + \lambda|\alpha|^2 + \lambda c^2 \tag{3.36}$$

where λ is a tuning parameter. Here:

$$V_m(\varepsilon) = \begin{cases} 0, & \text{if } |\varepsilon| < m \\ |\varepsilon| - m, & \text{otherwise.} \end{cases} \tag{3.37}$$

Notably, regardless of the specification of $V_m(\varepsilon)$, solutions for the optimal values of c and α are a linear combination of kernel functions, $K(W_t, W_t') = \sum_{n=1}^{p} h_n(W_t)h_n(W_t')$. We utilize three different kernels in our experiments, including:

- linear kernel: $K(W_t, W_t') = \sum_{n=1}^{p} W_{t,n}W_{t,n}$
- polynomial kernel: $K(W_t, W_t') = (1 + \sum_{n=1}^{p} W_{t,n}W_{t,n})^d$
- radial kernel: $K(W_t, W_t') = exp(-\gamma||W_t - W_t'||^2)$

Therefore, the hyperparameters that we estimate with our training dataset include: 1) λ in linear kernel; 2) λ and d in polynomial kernel; and 3)λ and γ in radial kernel.[7]

3.3.7 Random forest methods

The random forest machine learning method was first introduced by Breiman (2001). Like other tree-based statistical learning techniques, it is based on specifying "subsections" of the predictor space, W_t. Tree-based methods use the mean of response of variable $r_{j,t}$ under each subsection to construct forecasts. The procedure used to develop subsections resembles the structure of the tree, and each subsection of data is therefore also called a tree node.

The first step of tree-based methods involves bootstrapping the sample data. Then, within each bootstrapped sample, the tree-based algorithm tries to find the best "split"

[7] All machine learning methods utilized in our experiments involve three distinct sample periods, including: (i) a training dataset (used for the estiamtion of hypoerparameters), (ii) a forecasting model estimation period, and (iii) and ex-ante forecasting period.

of the predictor W_t using the criteria of least squares. Hence, the space of predictors and response variable is partitioned into $m = 1, 2, \cdots$, M regions/tree nodes. More specifically, for each tree node, $R_1(m, c) = \{W_{t,m} | W_{t,m} < c\}$ and $R_2(m, c) = \{W_{t,m} | W_{t,m} \geq c\}$, the parameters m and c are determined by solving the following problem:

$$min \sum_{t:W_t \in R_1(m,c)} (r_{j,t+1} - \hat{r}_{R_1})^2 + \sum_{t:W_t \in R_2(m,c)} (r_{j,t+1} - \hat{r}_{R_2})^2 \tag{3.38}$$

where $\hat{r}_{R1}$ is predicted value of response variable $r_{j,t+1}$ and equals the mean of $r_{j,t+1}$ in the sample data associated with R_1. Here, $\hat{r}_{R2}$ is defined analogously.

The major difference between random forest and other tree-based methods, in particular bagging, is the additional constraint requiring the choice of m from only a subset of the p predictors, which is randomly chosen, and usually consists of $\sqrt{p}$ of the original predictors. This design avoids the problem of correlation among fitted trees, when one or a few predictors dominate other predictors. For further discussion, see Friedman et al. (2001).

The algorithm that we utilize in order to carry out random forest regression is:

1. Draw B bootstrap samples from the data.

2. For each bootstrap sample b, where $b = 1, 2, \cdots, B$*:*

(a) Choose a subset of variables from the p predictors.

(b) Find the optimal variable m and corresponding cutoff value c that yield the lowest sum squared prediction error.

(c) Partition the data at W_t *with cutoff value c.*

(d) Recursively repeat the above procedures until a minimal tree node size, say n_{min} *is reached.*

3. Make predictions based on developed trees, called $T_b(W_t)$*, using:*

$$\hat{r}^B(W_t) = \frac{1}{B} \sum_{b=1}^{B} T_b(W_t).$$

Within each boostrap, observations are independently drawn from the training sample, with replacement. The number of observations in each boostrap is the same as in the traning sample. We use a validation (training) dataset to conduct cross validation and tune the hyperparameter B, for values of $B = \{100, 200, 300, 400\}$.

In a classification setting, the objective loss function is different than in the regression framework above. Classification models often use an alternative approach based on the "classification error rate", which measures the fraction of training observations which are not classified as belonging to the majority class, within a specific region. However, use of the Gini index for model specification is preferable in our context, because classification error rates are not sufficiently sensitive for our tree-based model. The Gini index is denoted as:

$$L = \sum_{n=1}^{N} \hat{p}_{mn}(1 - \hat{p}_{mn}) \tag{3.39}$$

where $\hat{p}_{mn}$ is the proportion of training observations in the m^{th} region that belongs to the n^{th} class ($n = 1, 2, \cdots, \mathrm{N}$). Under the binary classification case, N=2.

Hyperparameters that we estimate for our random forests are the maximum depth of the tree, the minimum number of samples required to split an internal node, the minimum number of bootstrap samples required to be at a tree node, the number of predictors to consider when looking for the best split, and the number of trees.

3.3.8 Gradient tree boosting

The gradient boosting method is developed in Friedman (2001) for regression and classification. The objective loss function[8][9] is:

$$L(\hat{f}) = \sum_{i=1}^{N} L(r_{t+1}, f(W_t)) \tag{3.40}$$

Here we use l_2 penalty for the loss function $L(.)$. $f(.)$ is a sum of regression trees:

$$f_M(W_t) = \sum_{m=1}^{M} K(W_t; \kappa) \tag{3.41}$$

Where each $K(W_t; \kappa)$ represents a regression tree and κ is the parameter in the model. One solution to this loss function is to estimate the tree $K(W_t; \kappa)$ at mth iteration to fit the negative gradient:

$$\hat{\kappa}_m = \underset{\kappa}{argmin}(-g_m - K(W_t; \kappa))^2 \tag{3.42}$$

where the components of the gradient g_m are:

$$g_{im} = [\frac{\partial L(r_{t+1}, f(W_t))}{\partial f(W_t)}]_{f(W_t)=f_{m-1}(W_t)}, i = 1, ..., N \tag{3.43}$$

The following summarizes the gradient tree boosting algorithm:

1. Start $f_0(W_t) = argmin_\theta \sum_{i=1}^{N} L(r_{t+1}, \theta)$.

2. For $m = 1$ to M:

   (a). For $i = 1, 2, ..., N$ compute:

$$s_{im} = -[\frac{\partial L(r_{t+1}, f(W_t))}{\partial f(W_t)}]_{f=f_{m-1}} \tag{3.44}$$

---

[8] We use the notation in Friedman et al. (2001)

[9] The loss function for gradient boosting classification is same as in the random forest.

(b). Train a regression tree with target s_{im} to get the terminal regions S_{jm}, $j = 1, 2, ...J_m$.

(c). For $j = 1, 2, ...J_m$ compute:

$$\hat{\theta}_{jm} = \underset{\theta}{argmin} \sum_{W_t \in S_{jm}} L(r_{t+1}.f_{m-1}(W_t) + \theta) \tag{3.45}$$

(d). Update $f_m(W_t) = f_{m-1}(W_t) + \lambda \sum_{j=1}^{J_m} \theta_{jm} I(W_t \in S_{jm})$

3. Output $\hat{f}(W_t) = f_M(W_t)$

In the hyperparameter estimation, the learning rate λ shrinks the contribution of each tree. M captures the number of booting stages in the estimation. We also tune other variables including min_sample_split[10], min_samples_leaf[11] and max_depth[12] during the cross-validation.

3.3.9 Neural networks

Neural network models build on a set of nonlinear functions mimicking the neural architecture of brains. The earliest neural networks trace back to Rosenblatt (1958) and McCulloch and Pitts (1943), where propositional logic models and probabilistic models are proposed to describe nervous system activity, information storage, and organization in the brain. Since these early papers, neural networks and their applications have been studied extensively across numerous disciplines. A key paper in this area is Hornik et al. (1989), who prove that multilayer feed-forward networks are "universal approximators", in the sense that as long as the complexity of the network is allowed to grow (i.e., increasing the number of so-called

[10]The minimum number of samples required to split an internal node.

[11]The minimum number of samples required to be at a leaf node.

[12]The maximum number of nodes in the tree.

"hidden units") with the sample size, then a network can estimate an arbitrary function, arbitrarily well. Not surprisingly, given this result, recent work shows that networks with multiple hidden layers are often better approximators than models with one hidden layer (see e.g, He et al. (2016)). IN this paper we utilize the traditional "feed-forward" neural network model of the variety discussed in Hornik et al. (1989).

Let W_t denote the "inputs" to the neural network. A hidden layer is defined as:

$$G_m = f(c + \alpha' W_t), \tag{3.46}$$

where $W_t = (W_{t,1}, ..., W_{t,p})$. The nonlinear function, $f(\cdot)$, is called the activation function, and we utilize four such functions in our experiments, with choice amongst them carried out using cross validation. These include:

Identity Function:$f(W_t) = W_t$

Sigmoid Function:$f(W_t) = 1/(1 + exp(-W_t))$

Hyperbolic Tan Function:$f(W_t) = tanh(W_t)$

Rectified Linear Unit Function:$f(W_t) = max(0, W_t)$

The output $r_{j,t+1}$ given as:

$$r_{j,t+1} = g(\theta_{0s} + \theta_s^M G), \quad m = 1, ..., M \tag{3.47}$$

where $G = (G_1, G_2, ..., G_M)$. We incorporate up to four hidden layers in our experiments, and the number of neurons (variables) in each layer is selected according to the geometric pyramid rule (see Masters (1993)).

In our classification variant of this model, we use cross-entropy, L, as the loss function, where:

$$L = -\sum_{m=1}^{M} \hat{p}_{mn} log \hat{p}_{mn}, \tag{3.48}$$

with $\hat{p}_{mn}$ defined to be the proportion of training observations in the m^{th} region arising from the n^{th} class. The output function, $g(\cdot)$, in our classification method is the *Softmax* function[13]. For parameter estimation, we use least squares with quasi-Newton numerical optimization, and the parameter α is tuned during cross-validation.

3.3.10 K-nearest-neighbor classifiers

The nearest neighbor classification method was first proposed by Cover and Hart (1967) in the field of pattern recognition. This nonparametric method performs clustering based on minimum distance measures. Given an unclassified point, W_0, and k points, W_t, $t = 1, ..., N$, in a training dataset are selected based on the closest distance to W_0, and then the point W_0 is classified. Distance, d_l is measured using the standard Euclidean norm:

$$d_l = \|W_t - W_0\| \tag{3.49}$$

The number of neighbors, k, is dependent on a tuning parameter which is calibrated using cross-validation.

3.3.11 Hybrid machine learning methods

We also explore the usefulness of a hybrid class of models that combines the lasso with neural networks. These hybrid models are based on a two step specification method. In the first step, the lasso is utilized to predict the forecasting target using the model:

$$r_{j,t+1} = c + \alpha' W_t + \epsilon_{t+1} \tag{3.50}$$

with specification achieved by minimizing the following function:

$$L(\lambda, \alpha) = |r_{t+1} - c - \alpha' W_t|^2 + \lambda |\alpha'|^2. \tag{3.51}$$

[13]See Bridle (1990).

In the second step, the residual, ϵ_{t+1}, estimated using this minimizer is deployed as our forecasting target, and neural networks are estimated. In this step, we carry out two types of experiments, based on the use different input variables, W_t. In the first type, W_t is the same as that used in the lasso. In the second type, Z_t is instead used as the input into the networks, where Z_t is the subset of W_t obtained by utilizing the lasso as a variable selection device.

3.3.12 Experimental setup and forecast evaluation

All forecasting models are estimated using three difference rolling window sizes, and all models and parameters are re-estimated/re-specified prior to the construction of each new daily forecast.[14] Additionally, and as discussed above, monthly forecasts are formed by aggregating daily forecasts. Forecasting performance is evaluated using mean squareforecast error (MSFE), where $MSFE = \frac{1}{T}\sum_{t=1}^{T}(r_{j,t} - \hat{r}_{j,t})^2$, with $\hat{r}_{j,t}$ denoting a prediction. Comparative model accuracy is evaluated using the Diebold and Mariano (DM) test (see Diebold and Mariano (1995)). The null hypothesis of equal predictive accuracy of two forecasting models, say f and g, in this test is:

$$H_o : E[l(\epsilon^f_{t+h})] - E[l(\epsilon^g_{t+h})] = 0, \tag{3.52}$$

where ϵ^f_{t+h} is the prediction error in model f, ϵ^g_{t+h} is the prediction error in model g, and $l(\cdot)$ is the quadratic loss function. If we assume there is no parameter estimation error(i.e., $P/R \to 0$, where $P + R = T$, P denotes the number of ex-ante forecasts, and R is the length of the rolling window, or the initial length of the recursive window), and also under an assumption that the models are nonnested, then $DM_P = \frac{\bar{d}}{\hat{\sigma}_{\bar{d}}}$, where $\bar{d} = P^{-1}\sum_{t=1}^{P} d_t$ has a standard normal limiting distribution (here $\hat{\sigma}_{\bar{d}_t}$ is a heteroskedasticity and autocorrelation

[14] Papers discussing the use of rolling and recursive estimation windows include Clark and McCracken (2009), Rossi and Inoue (2012), and the papers cited therein.

robust estimator of the standard deviation of $\bar{d}$), and $d_t = (\hat{\epsilon}_t^f)^2 - (\hat{\epsilon}_t^g)^2$ are estimates of true forecasting errors ϵ_{t+h}^f and ϵ_{t+h}^g. Details concerning appropriate critical values for cases in which parameter estiamtion error is not assumed to be negligible, asympotitcally, and/or in which models are nested are contained in Corradi and Swanson (2006) and McCracken (2000).

We adopt the Pesaran and Timmermann (1992) test to check the independence of our directional forecasts (namely, we construct classical chi-square tests of independence). In this context, we consider confusion matrices defined as follows:[15]

		Predicted	
		up	down
Actual	up	n_1	n_2
	down	n_3	n_4

(3.53)

Here n_1 (n_4) is the number of correct forecasts of upward (downward) return forecasts and n_2 (n_3) is the number of incorrect forecasts of upward (downward) movement in returns. Next, define:

$$p_{actu} = \frac{n_1 + n_2}{n_1 + n_2 + n_3 + n_4}, q_{actu} = \frac{p_{actu}(1 - p_{actu})}{n_1 + n_2 + n_3 + n_4}, \tag{3.54}$$

$$p_{pred} = \frac{n_1 + n_3}{n_1 + n_2 + n_3 + n_4}, q_{pred} = \frac{p_{pred}(1 - p_{pred})}{n_1 + n_2 + n_3 + n_4}, \tag{3.55}$$

The null hypothesis of Peseran-Timmermann (PT) test is that the model provides no value in directional forecasting. The test statistic is:

$$PT = \frac{p_{true} - p}{\sqrt{v - w}} \to N(0, 1), \tag{3.56}$$

where

$$p_{true} = \frac{n_1 + n_4}{n_1 + n_2 + n_3 + n_4}, p = p_{actu}p_{pred} + (1 - p_{actu})(1 - p_{pred}) \tag{3.57}$$

[15]See Swanson and White (1997) for details.

and

$$v = \frac{p(1-p)}{n_1+n_2+n_3+n_4}, w = (2p_{pred}-1)^2 q_{actu} + (2p_{actu}-1)^2 q_{pred} + 4q_{actu}q_{pred}. \quad (3.58)$$

The PT test is a one-sided test and the critical region is the upper tail of the standard normal distribution.

In addition, we report point direction forecasting performance using directional predictive accuracy rates (DPAR). The DPAR is defined as:

$$DPAR = \frac{\text{Number of correct forecasts}}{\text{Totol number of forecasts}} = \frac{n_1+n_4}{n_1+n_2+n_3+n_4} \quad (3.59)$$

We impose a simple "filter" on our forecasts in order to address the occasional occurrence of so-called "nonsense" forecasts, as discussed in Swanson and White (1997). Namely, if the one day change associated with a daily prediction exceeds the 90% percent of the average change observed during the past 22 trading days (i.e., one month), then the forecast from random walk model in Section 3.2 is used in place of the associated model based prediction.

Finally, correlation indices, macro risk factors, and volatility risk factors are 30-day moving averages. This smoothing was found to yield superior results relative to the use of un-smoothed uncertainty measures in our experiments.[16]

3.4 Empirical Results

3.4.1 Data

Our analysis is based on the use of 4 different datasets: 5-minute frequency equity price data, trading volume data, widely used macroeconomic predictors (as detailed in Welch

[16]In the prediction of SPY, all correlation indices are incorporated in the model. In the prediction of XLF, XLK, XLY, and XLV, only corresponding correlation indices are incorporated in the prediction model. See Data Section for further detials.

and Goyal (2007)), and additional macroeconomic variables. Table 3.1A and Table 3.1B summarize the predictors and the prediction targets. Technical indicators, correlation indices, volatility risk factor, and all forecasting targets are derived from the 5-minute high-frequency price dataset, which is extracted from Trade and Quote (TAQ) database.[17] The trading volume dataset used to compute technical indicators is obtained from Yahoo Finance. The macroeconomic predictors include book to market ratio of the Dow Jones Industrial Average, net equity expansion and dividend-price ratios for S&P 500 index are from the dataset detailed in Welch and Goyal (2007). Our additional macroeconomic variables, including, for example, default spreads, term spreads, and the consumer price index are obtained from the FRED-MD database of Federal Reserve Bank of St.Louis.

More specifically, the macroeconomic variables that are used to build our macro risk factor, MF_t^{mac}, are obtained from the FRED-MD database of Federal Reserve Bank of St.Louis, and include (1) the daily yield curve spreads, defined as the difference between the 10-year U.S. Treasury bond yield and the 3-month Treasury bill yield; (2) weekly initial claims for unemployment insurance; (3) the monthly number of nonfarm payroll employees; and (4) quarterly gross domestic product. All of these variables are log differenced in all calculations, in order to ensure stationarity, and are then standardized, with the exception of yield spreads, which are standardized, but not log-differenced. The fourth row in Table 3.1A and the third row in Table 3.1B show the transformations used in conjunction with our macroeconomic variables.

The daily financial variable log-returns that make up our target set of variables to be forecasted include: SPY (SPDR S&P 500 ETF Trust), XLF (Financial Select Sector SPDR Fund), XLK (Technology Select Sector SPDR Fund), XLY (Consumer Discretionary SPDR), and XLV (Health Care SPDR). All data cover the period from Jan 03, 2006 to

[17]Data obtained from Wharton Research Data Service (WRDS).

Dec 31, 2017, with high frequency financial variables measured at intra-day and daily frequencies, and macroeconomic data measures at daily, weekly, monthly, and quarterly frequencies.

3.4.2 Forecasting results

Table 3.1C lists all forecasting models in the experiments, both for level and directional prediction. Table 3.2 and Table 3.3 report 1-step-ahead daily relative MSFEs of all forecasting models, using a rolling and a recursive window. The random walk model is used as a benchmark to generate relative MSFEs for all machine learning models. The monthly aggregate relative MSFEs of all forecasting models are tabulated in Table 3.4 (rolling window) and Table 3.5 (recursive window). We calculate the monthly aggregate return by summing over all 1-step-ahead daily return predictions. Table 3.6 (rolling window) and Table 3.7 (recursive window) contain the directional predictive accuracy rate based on 1-step-ahead daily level forecasting results. The directional accuracy rate based on monthly aggregate level forecasting results are shown in Table 3.8 (rolling window) and Table 3.9. Notably, direction forecasting results in Table 3.6-3.9 are directly derived from level prediction results. For example, returns forecasts are classified as "upward signals" if forecasts are positive, and are otherwise classified as "downward signals". The forecasting period of all tables is from Jun 2009 - Dec 2017 with a total of 2129 observations. We summarize the main empirical findings in the following:

First, machine learning models yields significantly smaller MSFEs and higher DPARs than the benchmark random walk model at monthly frequency. For example, monthly relative MSFEs results in Table 3.4 and Table 3.5 suggest most machine learning models outperform benchmark in all scenarios. Similarly, in Table 3.8 and Table 3.9, in terms of DPARs at a monthly frequency, machine learning models also stand out to be the best

"DPARs" model. It is also noteworthy that some entries in Tables 3.4, 3.5, 3.8 and 3.9 are starred, especially for random forest and boosting models, indicating these machine learning models are statistically significantly different from benchmark, based on application of DM test and PT test discussed in Section 3.2. However, in Tables 3.2, 3.3, 3.6 and 3.7 at daily frequency, machine learning models show little improvement in terms MSFEs, and they perform slightly better under the measurement of DPARs, as for each given forecasting target and predictors, the best DPARs models are always machine learning models.

Second, the random forest model "wins" over other machine learning and benchmark models in both level and directional forecasting at monthly frequency. Evidently, almost all entries in bold [18] are listed under the random walk models in Tables 3.4, 3.5, 3.8 and 3.9. In terms of level forecasting, random forest stands out to be the best MSFEs model in 19 of 30 cases (Table 3.4) and 14 of 30 cases (Table 3.5). Also in terms of direction forecasting, random forest dominates other machine learning and benchmark models in 23 of 30 cases (Table 3.8), and 19 over 30 cases (Table 3.9). In particular, the lowest relative MSFEs for random forest model reaches 0.5503 (Table 3.5), and the highest DPARs achieves 0.8350 (Table 3.8). Note that other machine learning models including boosting and support vector regressions also prove to be the MSFEs and DPARs best models a few times in the forecasting "horse race".

Third, deep learning models outperform shallow learning models in both level and direction predictions. In Tables 3.2-3.5, deep learning models with 2-4 hidden layers have lower MSFEs than shallow learning models with only one hidden layer across different choices of predictors and forecasting targets. In Tables 3.6-3.9, DPARs of deep learning models with 2-4 hidden layers are significantly higher than the DPARs of shallowing learning models with one hidden layer. Deep learning models are more efficient in capturing the

[18] The entires with smallest relative MSFEs and largest DPARs in each row are denoted in bold

data pattern and more accurate in forecasting the target variable.

Fourth, hybrid machine learning models, which combine lasso and neural network models, outperform individual models in both level and direction forecasting. As shown in Table 3.4 and Table 3.5, at monthly frequency, hybrid models have smaller MSFEs than individual lasso or neural network models in 23 of 30 cases (Table 3.4), and in 17 of 30 cases (Table 3.5). Moreover, directional prediction results show hybrid models "win" over individual lasso or neural network models in 22 of 30 cases (Table 3.8), and 19 of 30 cases (Table 3.9).

Fifth, all three risk factors, including market correlation indices, volatility risk factors, and macro risk factors, have significant marginal predictive content. In Figure 3.8, adding the volatility factor to our forecasting models reduces relative MSFEs by 3.2%-18.3% for different forecasting targets (SPY, XLF, XLK, XLY, and XLV). Adding the macro factor reduces relative MSFEs by 0.8%-22.5%, for the different target variables. Finally, adding the correlation indices leads to relative MSFE reductions of 1.7%-28.8%. These findings hold when monthly aggregate relative directional predictive accuracy rates (DPARs) are analyzed, as shown in Figure 3.9. In Figure 3.9, we see that adding the volatility factor leads to 1.3%-10.3% DPAR increases, while adding the macro factor increases DPARs by 1.3%-11.4%. Finally, adding correlation indices increase DPARs by 1.3%-8.9%, with an exception of SPY, for which no gains are noted.

Sixth, each sector generally has a different sensitivity to the input information. We evaluate the contribution of different inputs by comparing MSFEs and DPARs using the leave-one-out scheme within each type of model. Each round, we leave one of the following five categories of predictors out of the model: 1) macro variables 2) technical variables 3) volatility risk factors 4) macro risk factors and 5) market correlation indices. Details about the predictors in each category can be found in Table 3.1B. First examining Tables 3.4-3.5, under the MSFEs best model- random forest, for the SPY, leaving inputs such as macro

variables, factors for uncertainty, market correlation and macroeconomic condition, induces larger MSFEs than original model having all variables, except technical indicators. This evidence is also confirmed in terms of DPARs results shown in Tables 3.8-3.9, with only one exception for correlation index. For XLF and XLY, as shown in Tables 3.4, 3.5, 3.8 and 3.9, leaving any type of inputs yields larger MSFEs and lower DPARs than original model having all variables. For XLK, removing macro variables or macro condition factor leads to larger MSFEs (Tables 3.4-3.5), and removing macro variables, technical variables or macro condition factor yields lower DPARs (Tables 3.8-3.9). Finally, for XLV, leaving macro variables and technical variables leads to larger MSFEs (Tables 3.4-3.5), and removing any type of inputs induces lower DPARs (Tables 3.8-3.9).

Figure 3.1-3.3 show the continuous component correlation indices and the jump component correlation indices of energy sector (XLE) and S&P500 (SPY), finance sector (XLF) and SPY, industrial sector (XLI) and SPY, technology sector (XLK) and SPY, health care sector (XLV) and SPY, and consumer discretionary sector (XLY) and SPY from 2006:01 - 2017:12. The jump correlation index surges during the 2008 and 2011 financial crisis, and drops when the market volatility is low. However, the energy market correlation index behaves differently comparing with the other four sectors. One sensible explanation is energy market depends more on the balance of supply and demand in energy commodities while less related to the financial market condition. Interestingly, the correlation index based on the continuous part behaves oppositely to the correlation index calculated by jump components.

Figure 3.4 depicts the volatility risk factors of the S&P 500 market (MF_t^{TRV}), financial sector (MF_t^{XLF}), technology sector (MF_t^{XLK}), health care sector (MF_t^{XLV}), and consumer discretionary sector (MF_t^{XLY}). During the Great Recession, the financial sector volatility risk factor positions higher than risk factors of all other sectors, and shows a

unique two-peak shape corresponding to the period of December 2008 and April 2009. The second peak is extremely contrasting since volatility factors calmed down significantly among all other sectors during the time. These two peaks can match back to historical events, as the first peak points to the big market tumble at the beginning of December 2008, with S&P 500 down 9% and financial sector fell the most by 17%, and the second peak relates to a big bull market rally from March to May 2009 with financial stocks strikingly went up 150%, explaining the unique second peak in the financial section volatility risk factor.

3.5 Concluding Remarks

In this paper, we extensively study the performance of machine learning individual models, as well as hybrid machine learning models, in the sector-level equity return forecasting, including random forest, boosting, support vector machine, penalized regression, logistic regression, latent discriminant analysis, naive Bayes classifier, k-nearest-neighbor classifier, neural network, and hybrid models. The impetus of our study is to analyze a number of new finance and macro-oriented latent measures of uncertainty, and to assess their marginal predictive content. These measures are constructed using high frequency and high dimensional financial data, as well as mixed frequency macroeconomic indicators. Out-of-sample forecasting experiments are carried out for the following financial assets: SPY (SPDR S&P 500 ETF Trust), XLF (Financial Select Sector SPDR Fund), XLK (Technology Select Sector SPDR Fund), XLV (Health Care SPDR), and XLY (Consumer Discretionary SPDR). We analyze both level and directional predictions at daily and monthly frequencies. Results from our empirical experiments are promising. Machine learning models, especially the random forest model, achieve significantly higher directional accuracy rates and lower mean square forecasting errors than the random walk benchmark. Moreover, various of

our new latent uncertainty measures deliver significant marginal predictive content, which is particularly useful for forecasting at a monthly frequency. All categories of predictors show contributions to both level and directional forecasting.

Table 3.1A: Predictor Variables*

Predictor Name	**Category**	**Description**	X_t	**Frequency**
T10Y3M	Macro Variables	term spread: 10-year treasury constant maturity minus 3-month treasuty constant maturity	X_t	Daily
defauspr		default spread: the difference between BAA and AAA-rated corporate bond yields	X_t	Daily
b/m		ratio of book value to market value of the Dow Jones Industrial Average	X_t	Monthly
ntis		Net Equity Expansion: the ratio of 12-month moving sums of net issues by NYSE listed stocks divided by the total end-of-year market capitalization of NYSE stocks.	X_t	Monthly
Diff_CPIAUCSL		Consumer Price Index	$ln(X_t) - ln(X_{t-1})$	Monthly
D/P		Dividend Price ratio of S&P 500 index	$x_t = log(D_t) - log(P_t)$	Daily
indi_30_90	Technical Indicators	30-day trading volume indicator	X_t	Daily
indi_90_120		90-day trading volume indicator	X_t	Daily
indi_30_120		120-day trading volume indicator	X_t	Daily
MA_30_90		30-day price trend indicator	X_t	Daily
MA_90_120		90-day price trend indicator	X_t	Daily
MA_30_120		120-day price trend indicator	X_t	Daily
XLECorr_ma	Correlation Index	continuous part price correlation index between enery sector(XLE) and SPY	X_t	Daily
XLFcorr_ma		continuous part price correlation between financial sector(XLF) and SPY	X_t	Daily
XLICorr_ma		continuous part price correlation index between industry sector(XLI) and SPY	X_t	Daily
XLKCorr_ma		continuous part price correlation index between technology sector(XLK) and SPY	X_t	Daily
XLVCorr_ma		continuous part price correlation index between health care sector(XLV) and SPY	X_t	Daily
XLYCorr_ma		continuous part price correlation index between consumer discretionary sector(XLY) and SPY	X_t	Daily
XLEJump_ma		Jump part price correlation index between enery sector(XLE) and SPY	X_t	Daily
XLFJump_ma		Jump part price correlation between financial sector(XLF) and SPY	X_t	Daily
XLIJump_ma		Jump part price correlation index between industry sector(XLI) and SPY	X_t	Daily
XLKJump_ma		Jump part price correlation index between technology sector(XLK) and SPY	X_t	Daily
XLVJump_ma		Jump part price correlation index between health care sector(XLV) and SPY	X_t	Daily
XLYJump_ma		Jump part price correlation index between consumer discretionary sector(XLY) and SPY	X_t	Daily
MF^{TRV}	Volatility Risk Factor	Multi-frequency financial volatility risk factor	X_t	Daily
MF_t^{mac}	Macro Risk Factor	Macroeconomic factor	X_t	Daily
Return_lag	Lag Term	lag one day of prediction target return	X_{t-1}	Daily

*Note: Table 3.1A shows all predictors in the forecasting models for the period 2006:01-2017:12. All predictors are divided into six categories, which is shown in the second column. Data transformations used in forecasting experiments are given in the fourth column of the table. See Section 3.2 and 3.3 for further details.

Table 3.1B: Target Forecast Variables*

Target Name	**Description**	X_t	**Frequency**
SPY	SPDR S&P 500 ETF Trust	$ln(X_t) - ln(X_{t-1})$	Daily
XLF	Financial Sector SPDR Fund	$ln(X_t) - ln(X_{t-1})$	Daily
XLK	Technology Sector SPDR Fund	$ln(X_t) - ln(X_{t-1})$	Daily
XLY	Consumer Discretionary SPDR	$ln(X_t) - ln(X_{t-1})$	Daily
XLV	Health Care SPDR	$ln(X_t) - ln(X_{t-1})$	Daily

*Notes: This table reports the prediction targets. Data transformations used in forecasting experiments are given in the third column of the table. See Section 3.3 for further details.

Table 3.1C: Models Used in Forecasting Experiments*

	Method	Description
Level Forecasting	Benchmark	Random Walk
	Linear	Linear regression
	SVR_rbf	Support vector regresion with radial basis function kernel
	SVR_lin	Support vector regresion with linear kernel
	SVR_poly	Support vector regresion with polynomial kernel
	RanForest	Random forest regression
	Boosting	Gradient boosting regression
	Lasso	Lasso regression
	Ridge	Ridge regression
	Nnet1	Neural network regression with one hidden layer
	Nnet2	Neural network regression with twp hidden layers
	Nnet3	Neural network regression with three hidden layers
	Nnet4	Neural network regression with four hidden layers
	Hybrid1	A hybrid mode of Lasso and Nnet1 with selected variables
	Hybrid2	A hybrid mode of Lasso and Nnet2 with selected variables
	Hybrid3	A hybrid mode of Lasso and Nnet3 with selected variables
	Hybrid4	A hybrid mode of Lasso and Nnet4 with selected variables
	Hybrid5	A hybrid mode of Lasso and Nnet1 with All variables
	Hybrid6	A hybrid mode of Lasso and Nnet2 with All variables
	Hybrid7	A hybrid mode of Lasso and Nnet3 with All variables
	Hybrid8	A hybrid mode of Lasso and Nnet4 with All variables
Direction Forecasting	Logit	Logistic regression
	LDA	Linear discriminant analysis
	NB	Naive bayes classifier
	SVC_RBF	Support vector classification with radial basis function kernel
	SVC_lin	Support vector classification with linear kernel
	SVC_poly	Support vector classification with polynomial kernel
	KNN	K-nearest neighbors algorithm
	Boosting	Gradient boosting classification
	RanForest	Random forest classification
	Nnet1	Neural network classification with one hidden layer
	Nnet2	Neural network classification with two hidden layers
	Nnet3	Neural network classification with three hidden layers
	Nnet4	Neural network classification with four hidden layers

*Notes: This table reports the models in forecasting experiments. Complete details for all models are given in Section 3.3.

Table 3.2: 1-Step-Ahead Daily Relative MSFEs of All Forecasting Models (Rolling Window)*

		Linear	SVRrbf	SVRlin	SVRpoly	RanForest	boosting	lasso	ridge	NN1	NN2	NN3	NN4	hybrid1	hybrid2	hybrid3	hybrid4	hybrid5	hybrid6	hybrid7	hybrid8
SPY	All Variables	1.2077***	1.7704***	1.1303***	1.2676***	1.0366***	1.1504***	0.9995	1.0541***	1.5332***	1.3431***	1.0253***	0.9993	1.0037	1.0079	1.0009	**0.9987**	1.1088***	1.0129	1.0046	0.9998
	Drop Macro Variables	1.1528***	1.0984***	1.095***	1.2324***	1.0314**	1.2492***	0.9995	1.0344***	1.2886***	1.2190***	1.0025	1.0007*	1.0124**	1.0089*	1.0061	0.9994	1.1604***	1.0973***	**0.9989**	1.0000
	Drop technical Variables	1.1869***	1.0644***	1.1026***	1.0516***	1.0856***	1.5325***	**0.9995**	1.0326***	1.3756***	1.1605***	1.0085*	1.8679***	1.0029	1.0072	1.0054	1.0018	1.0516***	1.0213**	1.0016	1.2696***
	Drop Volatility factor	1.1987***	1.0897***	1.1193***	1.1592***	1.0200**	1.1308***	**0.9994**	1.0515***	4.2393***	1.279***	1.0138***	1.3581***	1.0132**	1.0060*	1.0069**	1.0068	1.9241***	1.0394***	1.0039	1.0518**
	Drop Macro Factor	1.1991***	1.7923***	1.1525***	1.1309***	1.0183**	1.4545***	1.0002	1.0481***	1.6493***	1.3019***	1.0141***	0.9998	1.0059**	1.0168***	**0.9972**	1.0007*	1.1324***	1.0224***	1.0004	0.9994
	Drop Correlation index	1.1680***	1.1115***	1.0959***	1.06***	1.0223**	1.2094***	0.9995	1.0529***	1.6683***	1.1513***	1.0115**	0.9998	1.0141***	1.0070*	1.0024	1.0003	1.2129***	1.0204**	0.9999	**0.9987**
XLF	All Variables	1.2234***	1.0897***	1.0849***	1.0626***	1.0525***	1.1453***	**1.0017**	1.0781***	1.1496***	1.2958***	1.0463***	1.1017***	1.0227***	1.0275***	1.0062**	1.0084**	1.0524***	1.1137***	1.0214**	1.0226***
	Drop Macro Variables	1.0932***	1.0779***	1.0661***	1.1795***	1.028***	1.1493***	**1.0017**	1.0607***	1.0734***	1.0277***	1.0239***	1.1391***	1.0141***	1.0070**	1.0042*	1.0200***	1.0344***	1.0047	1.0097**	1.0423***
	Drop technical Variables	1.1324***	1.0338***	1.0367***	1.0226***	1.0904***	1.1737***	**1.0005**	1.0312***	1.0756***	1.0713***	1.0023	1.0604***	1.0077*	1.0042	1.0079***	1.0070**	1.0366***	1.0249**	1.0081**	1.0094**
	Drop Volatility factor	1.2243***	1.2762***	1.0803***	1.2180***	1.0309***	1.1586***	1.0003	1.0782***	1.0979***	1.0557***	**0.9996**	1.1466***	1.0157***	1.0100**	1.0010	1.0183***	1.059***	1.0212***	1.0003	1.0211**
	Drop Macro Factor	1.2139***	1.0819***	1.0760***	1.0596***	1.0313***	1.1528***	1.0028**	1.0822***	1.1366***	1.0839***	1.0435***	2.7153**	1.0208***	1.0184***	**1.0005**	1.0182***	1.0301**	1.0330***	1.0295***	1.1065***
	Drop Correlation index	1.2058***	1.0876***	1.0800***	1.0631***	1.0246***	1.1374***	1.0017	1.0763***	1.0698***	1.0231**	1.1251***	1.0272***	1.0106**	1.0055	1.0209***	**0.9978**	1.0325***	1.0106*	1.0187***	1.0193***
XLK	All Variables	1.1195***	1.0637***	1.0737***	1.039***	1.0196***	1.2742***	1.0002	1.0608***	1.2355***	1.207***	1.0064**	**0.9995**	1.0018	1.0006	0.9998	1.0003	1.0265***	1.0750***	1.0012	0.9998
	Drop Macro Variables	1.0652***	1.0489***	1.0421***	1.0294***	1.024***	1.1828***	1.0002	1.0413***	1.0639***	1.0965***	1.0060	1.0000	1.0064	0.9999	**0.9994**	1.0003	1.0100*	1.0114**	1.0013	1.0004
	Drop technical Variables	1.0651***	1.0257***	1.0397***	1.0161**	1.0245***	1.1583***	1.0002	1.0184***	1.0575***	1.0988***	1.0042	1.001	**0.9995**	1.0066**	1.0005	1.0002	1.0111**	1.0356***	1.0054**	0.9999
	Drop Volatility factor	1.1177***	1.0440***	1.0516***	1.0314***	1.0213***	1.2149***	**1.0001**	1.0567***	1.1596***	1.0768***	1.0006	1.0015***	1.0110*	1.0018	1.0017	**1.0001**	1.0219***	1.0174***	1.0047**	**1.0001**
	Drop Macro Factor	1.1126***	1.0573***	1.0731***	1.0392***	1.0175***	1.4152***	1.0000	1.0581***	1.2087***	1.2515***	1.0023	1.1242***	1.0008	1.0012	**0.9995**	1.0022	1.0188***	1.0434***	1.0027**	1.0023
	Drop Correlation index	1.1138***	1.0621***	1.0693***	1.1387***	1.0529***	1.3824***	1.0002	1.0608***	1.1406***	1.1016***	1.0357***	1.1165***	1.0084**	1.0027	**0.9989**	1.0292***	1.0189***	1.0192***	**0.9989**	1.0191***
XLY	All Variables	1.1453***	1.0769***	1.1102***	1.0737***	1.0465***	1.1069***	1.0010	1.0724***	1.2696***	1.1585***	1.0587***	**0.9994**	1.0170***	1.0154***	1.0022	1.0011*	1.1153***	1.0253***	1.0078*	1.0011
	Drop Macro Variables	1.0537***	1.0663***	1.0478***	1.0401***	1.0735***	1.1008***	1.0010	1.0433***	1.0843***	1.0771***	1.0123***	**1.0002**	1.0100**	1.0119***	1.0035*	1.0011*	1.0138**	1.0139***	**1.0002**	1.0012*
	Drop technical Variables	1.0799***	1.0351***	1.0610***	1.0307***	1.0192***	1.0994***	1.0005	1.0246***	1.2612***	1.0887***	1.1074***	**1.0002**	1.0096***	1.0006	1.0140**	1.0004	1.0690***	1.0310***	1.0102**	1.0003
	Drop Volatility factor	1.1477***	1.0642***	1.1014***	1.0615***	1.0253***	1.0991***	1.0006	1.0714***	1.8243***	1.1428***	1.0062**	1.2808***	1.0108*	1.0079***	**0.9998**	1.0518***	1.2371***	1.0157**	1.0016	1.0581***
	Drop Macro Factor	1.1374***	1.0622***	1.1144***	1.0622***	1.0421***	1.0883***	**1.0006**	1.0719***	1.2166***	1.1413***	1.1840***	1.0002	1.0112***	1.0032	1.0010	1.0008	1.0200***	1.0201***	1.0456***	1.0013**
	Drop Correlation index	1.1430***	1.0752***	1.1019***	1.0740***	1.0294***	1.1325***	**1.0010**	1.0725***	1.1388***	1.0933***	1.0139***	1.2876***	1.0065*	1.0105***	1.0035*	1.0100***	1.0317***	1.0179***	1.0054*	1.0477***
XLV	All Variables	1.0904***	1.0499***	1.0596***	1.1656***	1.0251***	1.1955***	1.0000	1.0426***	2.5925***	1.4951***	1.0005	1.0004	1.0012*	1.0011	1.0001	1.0000	**0.9999**	1.0016	1.0001	**0.9999***
	Drop Macro Variables	1.0622***	1.0459***	1.0333***	1.0269***	1.0325***	1.1757***	1.0000	1.038***	1.1325***	1.0622***	1.0155***	1.0003	1.0012*	1.0011	1.0001	1.0000	**0.9999**	1.0016	1.0001	**0.9999***
	Drop technical Variables	1.0584***	1.0238***	1.0176**	1.0154**	1.0301***	1.1875***	1.0000	1.0154***	1.2394***	1.0946***	1.0091**	1.0653***	1.0012*	1.0011	1.0001	1.0000	**0.9999**	1.0016	1.0001	**0.9999***
	Drop Volatility factor	1.0847***	1.0493***	1.036***	1.0339***	1.0555***	1.2246***	1.0000	1.0371***	1.2447***	1.121***	1.0079***	**0.9996**	1.0012*	1.0011	1.0001	1.0000	0.9999	1.0016	1.0001	0.9999*
	Drop Macro Factor	1.0936***	1.0475***	1.0502***	1.022***	1.0355***	1.2327***	1.0000*	1.0397***	1.2465***	2.4683***	1.0082***	1.0007*	1.0012*	1.0011	1.0001	1.0000	**0.9999**	1.0016	1.0001	**0.9999***
	Drop Correlation index	1.0762***	1.2771***	1.0365***	1.1761***	1.0323***	1.2265***	1.0000	1.0415***	1.1636***	1.0452***	1.0191***	1.0465***	1.0012*	1.0011	1.0001	1.0000	**0.9999**	1.0016	1.0001	**0.9999***

*Notes: See notes to Table 3.1A. Table 3.2 reports the 1-step-ahead relative mean square forecasting error (MSFE) of market sector ETFs with rolling window size 500. Forecasts are daily, for the period 2009:6-2017:12. Tabulated relative MSFEs are calculated such that numerical values less than unity indicates the alternative model has lower point MSFE than the random walk benchmark model. Entries in bold denote models with lowest relative MSFE for a given forecasting target and predictors. Starred entries denote rejection of the null of equal predictive accuracy, based on the application of Diebold and Mariano (1995) (DM) test. All machine learning models are tested against the random walk benchmark, based on MSFE loss. Significance levels for the test are reported as $***p < 0.01$, $**p < 0.05$, and $*p < 0.1$, where p is the $p-$value corresponding to DM test statistics.

Table 3.3: 1-Step-Ahead Daily Relative MSFEs of All Forecasting Models (Recursive Window)*

		Linear	SVRrbf	SVRlin	SVRpoly	RanForest	boosting	lasso	ridge	NN1	NN2	NN3	NN4	hybrid1	hybrid2	hybrid3	hybrid4	hybrid5	hybrid6	hybrid7	hybrid8
SPY	All Variables	1.1616***	1.7658***	1.0666***	1.221***	1.0094*	1.0455***	0.9991	1.0404***	1.3753***	1.2400***	1.0219***	1.0003	1.0016	1.0076**	1.0067*	**0.9989**	1.2382***	1.0969***	1.0181***	0.9993
	Drop Macro Variables	1.0805***	1.0588***	1.0463***	1.1630***	1.0064*	1.0656***	0.9991	1.019***	1.5325***	1.4164***	1.036***	1.0007	1.1077***	1.0455***	1.0081*	**0.9986**	1.2673***	1.2595***	1.0182***	1.0007
	Drop technical Variables	1.1531***	1.0438***	1.0610***	1.0283***	1.0658***	1.4103***	**0.9991**	1.0311***	1.2795***	1.1489***	1.0183***	1.8884***	1.0031	1.0064	1.0085**	1.0099***	1.1486***	1.0604***	1.0174***	1.3809***
	Drop Volatility factor	1.1592***	1.0537***	1.0592***	1.0923***	1.0026	1.0471***	**0.9991**	1.0337***	3.4572***	1.3582***	1.0005	1.1905***	1.0774***	1.0413***	1.0019	1.0404***	2.7528***	1.2012***	1.0167***	1.1285***
	Drop Macro Factor	1.1534***	1.7902***	1.0719***	1.0881***	1.0017	1.3266***	1.0003***	1.0338***	2.1067***	1.2658***	1.0113**	1.0001	1.0030	1.0062**	**0.9990**	1.0001	1.1328***	1.0271***	0.9994	0.9999
	Drop Correlation index	1.1270***	1.0726***	1.0435***	1.0232***	1.0056*	1.0661***	0.9991	1.0358***	1.5577***	1.1924***	1.0251***	0.9990	1.1031***	1.0319***	1.0042	**0.9984**	1.4183***	1.1044***	1.007*	0.9988
XLF	All Variables	1.1840***	1.0586***	1.0534***	1.037***	1.0538***	1.0630***	**1.0018***	1.0689***	1.1587***	1.3453***	1.1048***	1.0638***	1.0108**	1.0253***	1.0045**	1.0176***	1.0348***	1.1682***	1.0190**	1.0188***
	Drop Macro Variables	1.0491***	1.0493***	1.0392***	1.1066***	1.0086***	1.0569***	**1.0016**	1.0429***	1.0961***	1.0614***	1.0389***	1.0918***	1.0023	1.0170***	1.0027	1.0382***	1.0487***	1.0059	1.0103**	1.0124
	Drop technical Variables	1.1118***	1.0261***	1.0252***	1.0182***	1.0813***	1.0998***	**1.0009**	1.0287***	1.1098***	1.0513***	1.0189***	1.0137***	1.0102**	1.0094**	1.0048**	1.0074*	1.0600***	1.0547***	1.0035	1.0043
	Drop Volatility factor	1.1809***	1.2085***	1.0517***	1.2064***	1.0155***	1.0746***	1.0005	1.0665***	1.1476***	1.1086***	1.0027	1.0648***	1.0243***	1.0049	**0.9986**	1.0082	1.0671***	1.0170**	1.0029	1.0493***
	Drop Macro Factor	1.1778***	1.0578***	1.0486***	1.0392***	1.0171***	1.0830***	**1.0025*** **	1.0666***	1.1085***	1.1244***	1.0591***	1.3106***	1.0162***	1.0107**	1.0044**	1.0113***	1.0650***	1.0615***	1.0201***	1.1819***
	Drop Correlation index	1.1687***	1.0582***	1.0462***	1.0373***	1.0035	1.0757***	**1.0018***	1.0673***	1.0897***	1.0585***	1.0489**	1.0038	1.0128***	1.0126***	1.0239***	1.0122***	1.0373***	1.0250***	1.0170***	1.0105***
XLK	All Variables	1.0696***	1.0339***	1.0374***	1.0165***	1.0034	1.1304***	**1.0001****	1.0247***	1.1609***	1.4002***	1.0050	1.0009*	1.0015	1.0019	1.0002	1.0003**	1.0195***	1.0514***	1.0013	1.0004*
	Drop Macro Variables	1.0243***	1.0313***	1.0197***	1.0168***	1.0078***	1.0500**	1.0001**	1.0162***	1.0682***	1.1659***	1.0145***	1.0000	1.0027	1.0023	1.0012	1.0002	1.0119***	1.0057	1.0020	**0.9999**
	Drop technical Variables	1.0486***	1.0167**	1.0152**	1.0072	1.0025	1.0658***	**1.0001****	1.0121***	1.0997***	1.0685***	1.0099***	1.0312***	1.0031**	1.0021	1.0013	1.0004	1.0147***	1.0130**	1.0026*	1.0001
	Drop Volatility factor	1.0682***	1.0306***	1.0229***	1.0131**	1.0072***	1.092***	1.0000	1.0237***	1.1590***	1.1779***	1.0169***	1.0014***	1.0022	1.0024**	**0.9992**	1.0003	1.0304***	1.0165***	1.0000	0.9999
	Drop Macro Factor	1.0677***	1.0325***	1.0354***	1.0144***	1.0033	1.2668***	1.0001***	1.0234***	1.1008***	1.1787***	1.0133***	1.087***	1.0012***	1.0005***	0.9998	1.0009**	1.0055*	1.0170*	**0.9994**	1.0095
	Drop Correlation index	1.0689***	1.0370***	1.0318***	1.0834***	1.0576***	1.1796***	**1.0001****	1.0250***	1.1549***	1.0475***	1.0445***	1.0955***	1.0034**	1.0039**	1.0011	1.0118***	1.0126**	1.0119**	1.0051*	1.0149**
XLY	All Variables	1.0860***	1.0493***	1.0604***	1.0311***	1.0443***	1.0381***	1.0005	1.0360***	1.4131***	1.1167***	1.1025***	**0.9993**	1.0144***	1.0046	1.0019	1.0004	1.1698***	1.0172***	1.0154***	1.0009*
	Drop Macro Variables	1.0284***	1.0346***	1.0246**	1.0177**	1.0559***	1.0407***	1.0004	1.0216***	1.1148***	1.1730***	1.0228***	1.0005	1.0065**	0.9997	**0.9984**	1.0003	1.0132**	1.0156**	1.0020	1.0004
	Drop technical Variables	1.0582***	1.0193***	1.0312***	1.0136**	1.0032	1.0400***	1.0004	1.0164***	1.2477***	1.1056***	1.0720***	1.0018***	1.0087***	**0.9996**	1.0027	1.0003	1.0981***	1.0313***	1.0161**	0.9999
	Drop Volatility factor	1.0838***	1.0374***	1.0619***	1.0260***	1.0065	1.0347***	**0.9999**	1.0346***	1.5831***	1.1435***	1.0076***	1.1433***	1.0053	1.0025	1.0009	1.0350***	1.2985***	1.0511***	1.0036*	1.0396***
	Drop Macro Factor	1.0836***	1.0409***	1.0579***	1.0271***	1.0323***	1.0451***	1.0005*	1.0347***	1.1708***	1.1666***	1.4072***	1.0000	1.0017	1.0054**	**1.0004**	1.0006*	1.0248***	1.0046	1.0203***	1.0005
	Drop Correlation index	1.0919***	1.0468***	1.0511***	1.0318***	1.0104**	1.0568***	**1.0005**	1.0416***	1.1296***	1.1119***	1.0087**	1.0701***	1.0041*	1.0019	1.0007	1.0028	1.0332***	1.0134***	1.0084***	1.0429***
XLV	All Variables	1.0513***	1.0231***	1.0237***	1.0894***	1.0058**	1.0761***	**0.9997**	1.0191***	2.0021***	1.5009***	1.0089**	0.9999	**0.9997**	**0.9997**	**0.9997**	**0.9997**	**0.9997**	**0.9997**	**0.9997**	**0.9997**
	Drop Macro Variables	1.0260***	1.0219***	1.0058*	1.0043	1.0114***	1.1138***	**0.9997**	1.0149***	1.1256***	1.1804***	1.0111**	1.0010	**0.9997**	**0.9997**	**0.9997**	**0.9997**	**0.9997**	**0.9997**	**0.9997**	**0.9997**
	Drop technical Variables	1.0440***	1.0060	1.0107*	1.0050	1.0059*	1.0794***	**0.9997**	1.0090**	1.2063***	1.1386***	1.0098**	1.0289***	**0.9997**	**0.9997**	**0.9997**	**0.9997**	**0.9997**	**0.9997**	**0.9997**	**0.9997**
	Drop Volatility factor	1.0489***	1.0153**	1.0192***	1.0131**	1.0520***	1.0786***	**0.9997**	1.0177***	1.1400***	1.1987***	1.0056*	1.0005	**0.9997**	**0.9997**	**0.9997**	**0.9997**	**0.9997**	**0.9997**	**0.9997**	**0.9997**
	Drop Macro Factor	1.0531***	1.0191***	1.0178***	1.0078	1.0167***	1.0814***	**0.9997**	1.0180***	1.1165***	1.8097***	1.0048	0.9998	**0.9997**	**0.9997**	**0.9997**	**0.9997**	**0.9997**	**0.9997**	**0.9997**	**0.9997**
	Drop Correlation index	1.0453***	1.1823***	1.0171**	1.0969***	1.0074*	1.092***	**0.9997**	1.0187***	1.1471***	1.0324***	1.0140***	1.0166***	**0.9997**	**0.9997**	**0.9997**	**0.9997**	**0.9997**	**0.9997**	**0.9997**	**0.9997**

*Notes: See notes in table 3.2. Recursive window size 500.

Table 3.4: Monthly Aggregate Relative MSFEs of All Forecasting Models (Rolling Window)*

		Linear	SVRrbf	SVRlin	SVRpoly	RanForest	boosting	lasso	ridge	NN1	NN2	NN3	NN4	hybrid1	hybrid2	hybrid3	hybrid4	hybrid5	hybrid6	hybrid7	hybrid8
SPY	All Variables	1.7483***	0.8873***	1.1617***	0.9068***	**0.7677*** **	0.9405***	0.9748*	1.2326***	1.3868***	1.2175***	1.0273**	1.0027	0.9634	0.9687*	0.9831	0.9967	1.1062**	1.006	1.0035	0.9868
	Drop Macro Variables	1.2639***	0.9889***	0.8629***	0.8879***	0.8048***	**0.5709*** **	0.9748*	0.9726***	0.9959***	1.0992***	1.0007	1.0009	0.9801	0.969	1.0213**	0.9831	1.0051***	1.0923	1.0119	0.9849
	Drop technical Variables	1.8221***	1.0555***	1.2425***	1.0566***	**0.6262*** **	0.7587***	0.9748*	1.1983***	1.1527***	1.1437***	1.0475	1.0038***	0.9719	1.0121	0.9798	0.9839	1.0158**	0.9678	0.9924	1.1093**
	Drop Volatility factor	1.6141***	0.8772***	1.107***	0.887***	**0.7921*** **	0.9105***	0.9638**	1.243***	2.6349***	1.2478***	1.0216**	0.9687***	0.9569**	0.9436	1.0256	0.9671	1.4345***	1.1083*	0.971	0.946
	Drop Macro Factor	1.8599***	0.8122***	1.2382***	0.8328***	0.8202***	**0.7496*** **	1.0031**	1.1774**	1.4029***	1.1068***	1.0262	1.0026	1.0061***	1.0353***	1.0025	1.0032***	0.9373***	0.9991**	0.9969*	1.0038
	Drop Correlation index	2.49***	0.9818***	1.3913***	1.0922***	**0.8292* **	0.9451***	0.9748*	1.3533***	0.996***	1.1156***	0.9946**	1.0056	0.9942***	0.9271	0.9951	0.994	0.8969***	0.9989*	0.9883	0.9798
XLF	All Variables	3.099***	1.0838***	1.2804***	1.2063***	**0.6448*** **	0.8643***	1.0061	1.6261***	1.2243***	1.1551***	1.0017	1.0397**	1.0986**	1.0483	1.0178*	1.0291	1.1412***	1.1386*	1.0066	1.0179*
	Drop Macro Variables	1.4752***	1.1046***	1.1567***	0.8887***	**0.8056* **	0.9705***	1.0061	1.3305***	1.0023***	0.994	1.0346	1.0608***	1.0593*	1.0362	1.0157	1.0748**	1.0516**	1.0073*	0.9984	1.0565**
	Drop technical Variables	2.2144***	0.9684***	0.9947**	0.9555***	**0.6043*** **	1.0068***	0.9776	1.2519***	0.8767***	1.0276***	1.0008**	1.0098***	0.9876	0.9715	0.9909	0.9724	0.9904	0.9582	0.9904	0.9809
	Drop Volatility factor	3.1517***	0.9783***	1.2784***	0.9667***	**0.7103*** **	0.9502***	0.9790	1.6939***	1.1423***	1.0099***	1.0039	0.9828***	1.0868*	0.998	0.9864	0.9849	1.153***	0.9668	0.9855	0.9998
	Drop Macro Factor	3.1485***	0.9962***	1.1717***	1.1858***	**0.6957** **	1.0179***	1.0377**	1.7524***	0.964***	1.0581**	1.014**	1.7497***	1.208**	1.0697*	1.0347	1.2017***	1.112	1.0969	1.0252*	1.3216***
	Drop Correlation index	3.2623***	1.0604***	1.2862***	1.2242***	**0.7691*** **	0.9230***	1.0061	1.6155***	1.0802***	0.9242	1.0045**	1.0002***	1.0539	1.0408*	1.0637	1.0263	1.081*	1.0503	1.0011**	1.0024*
XLK	All Variables	1.7044***	0.8886***	1.1048***	1.0398***	0.8423*	**0.7639*** **	0.9876	1.3904***	1.1089***	0.9331***	0.9848	0.9982***	0.9888	0.9924	0.9958	0.9895	1.0169***	1.0592**	0.9884	0.9879
	Drop Macro Variables	1.3333***	1.0526***	1.1428***	1.0932***	0.9527***	**0.7625*** **	0.9876	1.2627***	1.1250**	1.0593***	1.013***	0.9998	1.0101**	0.9924	1.0018*	0.9925	1.0034**	0.9802	0.9960	0.9884
	Drop technical Variables	1.4983***	0.8304*	1.0297***	0.9009	0.8569***	**0.7406*** **	0.9876	1.0661***	0.9699**	1.0506**	1.0107	1.0004	0.991	0.9879	0.9926	0.9914	1.0336**	0.9594	0.9949	0.9888
	Drop Volatility factor	1.7496***	0.982***	1.0792***	1.0228***	0.8017***	**0.7876*** **	0.9856	1.4733***	1.2542***	1.0244**	0.9946	0.9998	0.9837	0.9621	0.986	0.9919	1.0268***	0.9702*	1.006**	0.989
	Drop Macro Factor	1.726***	0.9079***	1.1431***	1.0093***	0.8521*	**0.7989*** **	1.0011	1.4353***	1.0806***	1.1249***	1.0051	0.9868**	1.0016	1.0012	0.9965*	1.0081	0.9406*	0.9953***	1.0022**	0.9906
	Drop Correlation index	1.7010***	0.9152***	1.2148***	0.9635***	**0.6808*** **	0.8260***	0.9876	1.4094***	1.0847***	1.0001***	1.0045**	1.0239***	0.9813	0.9854	0.9857	0.9690	1.0026	0.9793*	0.9772*	1.0147**
XLY	All Variables	1.9525***	1.2327***	1.7358***	1.615**	**0.6864*** **	0.9469**	1.0039**	1.7071***	1.1996***	0.992***	1.0255***	1.0007	1.0687*	1.0094**	1.0011	0.9992	0.9918***	1.0293**	0.9817	0.9973
	Drop Macro Variables	1.2435***	1.0929**	1.3126**	1.2753**	**0.801*** **	0.8964***	1.0039**	1.3240**	1.0950***	1.097**	1.0039*	1.0009	1.0005	0.9798	1.0096	1.0029	1.0126	0.9716	1.0019	0.9972**
	Drop technical Variables	1.6683***	1.0035***	1.3086***	1.1205***	**0.8449**	0.9455***	0.9932*	1.2081*	1.2139***	0.9679	1.015***	0.9998	0.9873	0.9916	1.0011**	0.9933	0.9897***	0.9406**	0.9889	0.9947
	Drop Volatility factor	2.1121***	1.323***	1.6931***	1.5638**	**0.8077**	0.9571*	0.9968	1.8705***	1.7701***	1.1164***	1.0002	1.1238***	1.0383*	0.9849	0.9884	1.0456	1.1911***	0.9968*	0.9942	1.0756**
	Drop Macro Factor	2.063***	1.2558***	1.8644***	1.5697***	**0.7739** **	0.9409***	1.0091*	1.7579***	1.4218***	0.9893***	1.0016***	1.0018	1.0572	1.0295	1.0113	1.0053	1.0099	1.0521*	0.9775	1.0076
	Drop Correlation index	2.0376***	1.2363***	1.6822***	1.5612**	**0.7667* **	0.9291***	1.0039**	1.6987***	1.076***	1.0547***	1.0017	1.1186***	1.0254	0.9952*	0.9899	1.0743*	1.0587***	0.9467*	0.9868	0.9763***
XLV	All Variables	1.3759***	0.8621***	1.1091***	1.0236***	0.8885***	**0.8131*** **	1.0000*	1.1223***	2.3288***	1.4233***	1.0000	0.9972	1.0017**	0.9998**	0.9999	1.0001	0.997	1.0176**	0.9999**	0.9998
	Drop Macro Variables	1.2741***	0.91***	1.0541***	1.0096***	0.8939***	**0.6793*** **	1.0000*	1.1034***	1.0395***	1.0102***	1.0114	1.0026	1.0017**	0.9998**	0.9999	1.0001	0.997	1.0176**	0.9999**	0.9998
	Drop technical Variables	1.3406***	0.9177*	1.011**	0.9671**	0.8529***	**0.7487*** **	1.0000*	1.0365**	1.1495***	1.0012**	0.9864*	1.0092	1.0017**	0.9998**	0.9999	1.0001	0.9970	1.0176**	0.9999**	0.9998
	Drop Volatility factor	1.3607***	0.9791***	0.9702**	1.0172**	**0.7275*** **	0.8929***	1.0000*	1.1463***	1.1242***	1.1446***	0.9932	0.9995	1.0017**	0.9998**	0.9999	1.0001	0.9970	1.0176**	0.9999**	0.9998
	Drop Macro Factor	1.4677***	0.8734***	1.1071***	0.8639	**0.7806** **	0.8591***	1.0000*	1.1205***	1.1533***	1.1805***	1.0100*	1.006**	1.0017**	0.9998**	0.9999	1.0001	0.9970	1.0176**	0.9999**	0.9998
	Drop Correlation index	1.3237***	0.8424***	0.9701***	1.0138***	0.8536*	**0.7947*** **	1.0000*	1.111***	1.0608***	1.0251***	1.0011**	1.0068	1.0017**	0.9998**	0.9999	1.0001	0.9970	1.0176**	0.9999**	0.9998

*Notes: See notes in Table 3.2. We calcualte the one-month-ahead forecasting results by aggregating daily forecasts during each month, i.e., summing all daily forecasting results within the same month to generate monthly forecasts. Table 3.4 reports aggregate monthly relative MSFEs of all forecasting models, comparing with the random walk benchmark.

Table 3.5: Monthly Aggregate Relative MSFEs of All Forecasting Models (Recursive Window)*

		Linear	SVRrbf	SVRlin	SVRpoly	RanForest	boosting	lasso	ridge	NN1	NN2	NN3	NN4	hybrid1	hybrid2	hybrid3	hybrid4	hybrid5	hybrid6	hybrid7	hybrid8
SPY	All Variables	1.9681***	0.8833***	0.9901***	1.0111***	**0.8542**	0.8708	0.9709	1.3027***	1.2143***	1.1665***	1.001*	1.0025*	0.9742	1.0006	0.9917	0.9815	1.2746***	0.9868***	1.0184*	0.9769
	Drop Macro Variables	1.272***	0.9329***	0.9279***	0.8272***	0.8977	**0.7821****	0.9709	1.0239**	1.2364***	1.1399***	0.9701	0.9986	1.1602***	0.9988**	0.992	0.9877	1.1481***	1.0659***	1.0204**	0.9876
	Drop technical Variables	2.0196***	1.0371***	0.9898***	1.0002**	**0.6678*****	1.1757***	0.9709	1.3048***	0.979***	1.0239***	0.9999	1.4895***	0.9643	1.0265	1.0065	0.9651	1.0006***	0.9985***	0.9485	1.0378***
	Drop Volatility factor	2.1402***	**0.8054*****	1.0078***	0.8201***	0.9139	0.9217*	0.9626	1.2509***	2.4901***	1.2854***	1.0039**	1.0283*	1.1142***	0.9454	0.9808	0.9728	2.2817***	0.9384***	0.9836***	0.9907
	Drop Macro Factor	1.9558***	**0.7929*****	1.0047***	0.8779***	0.9228	0.7932***	1.0031**	1.221**	1.7081***	1.2742***	0.9989***	1.0029	1.0286**	1.0016	1.0007	1.0041***	0.9654**	1.0523**	0.9897	1.0035
	Drop Correlation index	2.5***	**0.8749*****	1.0022**	0.9772**	0.9392*	1.0503	0.9709	1.4531***	1.5625***	1.0748***	1.0135	0.9967	1.0652***	1.0759**	0.9926	0.989	1.0905***	1.0423***	0.9595	0.981
XLF	All Variables	3.4172***	1.1973***	1.2687***	1.2315***	**0.6482*****	0.9754	1.0101	1.9073***	1.328***	1.159***	1.098***	1.018	1.1792**	1.1414***	1.0191	1.0715***	1.1125	1.0738***	1.032*	1.0319
	Drop Macro Variables	1.6088***	1.067***	1.1449***	1.091***	**0.9687**	1.0436***	1.0154	1.5658***	1.1494***	1.0893***	1.082***	0.9522***	1.0553	0.9977	1.0125	1.133*	1.0966***	1.0357**	1.0669	1.0106**
	Drop technical Variables	2.1866***	1.0298**	1.0206**	1.0268***	**0.5503*****	0.9247**	0.9894	1.297***	0.9492**	1.0018**	1.0233	0.9953	1.0091	0.987	0.9995	0.9855*	0.9817***	0.9627**	0.9984	0.9923
	Drop Volatility factor	3.3743***	0.978***	1.3112***	1.088***	**0.7939***	0.8742**	0.9837	1.8959***	1.2773***	1.0765***	0.9932	0.9896**	1.0616**	1.0067	0.985*	1.0005*	1.1601***	1.064**	0.9912	1.0119
	Drop Macro Factor	3.3947***	1.1572***	1.3094***	1.2388***	**0.8363***	1.0022**	1.0303**	1.9457***	1.3884***	1.0384***	1.1048**	1.6947***	1.2049***	1.0367	1.0452**	1.1877**	1.2393***	1.2078***	1.0289	1.3555***
	Drop Correlation index	3.4324***	1.1755***	1.2549***	1.2602***	0.9109	**0.8559*****	1.0101	1.9036***	1.1143***	1.0365***	1.0335	1.0045	1.0371	1.0218	1.0644**	1.0084*	1.0671***	0.9779	1.0396	1.0156
XLK	All Variables	1.5220***	**0.8708****	1.0934***	0.9974	0.948	0.9317***	0.9992	1.2491***	1.1656***	1.1179***	1.0223	1.0013	0.9893	0.9976	0.9981	0.9999	0.9279*	0.9955	0.9938	0.9993*
	Drop Macro Variables	1.2517**	0.9799***	0.9743**	1.0062**	0.9818**	**0.9027*****	0.9992	1.22**	1.1047**	1.0603***	0.9656	1.0005*	1.0032*	0.9942	1.002	0.9995	0.965	0.9955	0.9932	1.0002**
	Drop technical Variables	1.2645***	0.8654**	0.9821	0.8782*	0.9343	**0.8222****	0.9992	1.0819***	1.0475***	1.0613	0.9955	0.9958	0.9948	1.0033	0.9995	0.9988	1.0295**	0.9884**	1.0082	1.0013
	Drop Volatility factor	1.5860***	0.9533***	1.0267***	0.9842**	0.9536	**0.9382*****	0.9980	1.2934***	1.2783***	1.2113***	1.0230***	1.0005**	1.0171*	0.9963	0.9988	0.9982	1.0246***	0.9861	0.9964	0.9993
	Drop Macro Factor	1.7095***	0.9769***	1.0286***	0.9313*	0.9523	**0.7848*****	1.001***	1.3137***	1.1496***	1.1982***	1.0255**	1.0066	1.0084***	1.0020	1.0019	1.0028	1.0180	1.0287	1.0045	1.0048
	Drop Correlation index	1.6708***	0.898**	1.0887	0.8555***	**0.6804*****	0.8291***	0.9992	1.2568***	1.1443***	0.9979	1.0614*	1.0489***	0.999	0.9969	1.0052**	0.9999	1.0279	0.9924	1.001	1.016*
XLY	All Variables	1.8408***	1.247**	1.4264***	1.2182*	**0.7092*****	1.0117	0.996	1.4409***	1.3534***	0.9925***	1.0879***	1.0005	1.0358	1.0055	1.0095*	0.9972	1.3947***	0.9633	0.9973	1.0014**
	Drop Macro Variables	1.4291*	1.1673***	1.3200	1.2383	**0.8173*****	0.9661	0.9971	1.4108*	1.2135***	1.0906***	1.0117	1.0017	1.0008	0.9978	0.9927	0.9974	0.9833	0.9909**	1.0214	0.9957
	Drop technical Variables	1.5498**	0.9578*	1.0905	0.9874	0.9136	**0.9025****	0.9958	1.1403**	1.0781***	1.0088	1.0577***	1.0019*	1.0134	1.0018	0.9843*	0.9937	1.029***	0.9831**	0.9915**	1.0009
	Drop Volatility factor	1.8591***	1.1862	1.4617***	1.2741*	**0.8657**	0.993	0.9886	1.5085***	1.1874***	1.0351***	0.9740	1.1356***	1.0255	0.9942	0.9883	1.0374	1.3065***	1.1439***	1.0038***	0.9725**
	Drop Macro Factor	1.9584***	1.2437***	1.4269***	1.2023*	**0.7152**	1.0108	1.0061	1.4936**	1.1139***	1.1534***	1.1574***	0.9982	1.0154	0.9985	1.0006	1.0027	1.0222***	0.9720	1.1087	1.0042*
	Drop Correlation index	1.8895***	1.2432***	1.2797**	1.1906*	**0.8684**	0.9070	0.9960	1.5130***	1.3423***	1.0424***	1.0063	1.1475***	0.9809	1.0275	1.0024	1.0159	1.1031**	1.0059	1.0163**	1.0321***
XLV	All Variables	1.2423***	**0.8312*****	0.9675*	0.9169***	0.9525	0.8542***	1.0072	1.0179***	1.7498***	1.1977***	1.0334**	1.0066	1.0072	1.0072	1.0072	1.0072	1.0072	1.0072	1.0072	1.0072
	Drop Macro Variables	1.1639***	0.9274***	0.9506	0.9449	0.9414***	**0.8815*****	1.0072	1.0673***	1.0983***	1.2340***	1.0010	1.0017	1.0072	1.0072	1.0072	1.0072	1.0072	1.0072	1.0072	1.0072
	Drop technical Variables	1.2367***	0.8732	0.9604*	**0.8502**	0.9637	0.8748***	1.0072	1.009*	1.0065***	1.0218***	0.9790	1.0077	1.0072	1.0072	1.0072	1.0072	1.0072	1.0072	1.0072	1.0072
	Drop Volatility factor	1.1876***	0.8643***	0.9080	0.8853	**0.7271*****	0.8821***	1.0072	1.009***	1.0662***	1.1857***	0.9798	1.0032	1.0072	1.0072	1.0072	1.0072	1.0072	1.0072	1.0072	1.0072
	Drop Macro Factor	1.3455***	**0.7981*****	0.9466	0.8646	0.8776**	0.9106	1.0072	1.0427***	1.0530***	1.4495***	0.9957	0.9985	1.0072	1.0072	1.0072	1.0072	1.0072	1.0072	1.0072	1.0072
	Drop Correlation index	1.2112***	**0.8075*****	0.8876	0.8921***	0.9425	0.8690	1.0072	1.0343***	1.1448***	1.0012**	1.0105	1.0123	1.0072	1.0072	1.0072	1.0072	1.0072	1.0072	1.0072	1.0072

*Notes: See notes in Table 3.4. Recursive window size 500.

Table 3.6: Directional Predictive Accuracy Rate Based on 1-Step-Ahead Daily Level Forecasting Results (Rolling Window)*

		RandomWalk	Linear	SVRrbf	SVRlin	SVRpoly	RanForest	boosting	lasso	ridge	NN1	NN2	NN3	NN4	hybrid1	hybrid2	hybrid3	hybrid4	hybrid5	hybrid6	hybrid7	hybrid8
SPY	All Variables	0.5303	0.5082	0.4899	0.5233	0.5228	0.5092	0.512	0.542	0.4951	0.4847	0.4974	0.4941	0.5369	0.5378	0.535	0.5369	0.5420	0.5416	0.5355	0.5420	**0.5444**
	Drop Macro Variables	0.5303	0.4941	0.5082	0.5129	0.5106	0.5228	0.4979	0.542	0.5021	0.4984	0.4852	0.5223	0.5317	0.5326	0.5425	0.5359	**0.5430**	0.5270	0.5326	0.5378	0.5383
	Drop technical Variables	0.5303	0.5106	0.5242	0.5294*	0.5355	0.5059	0.5049	**0.5420**	0.4998	0.5106	0.5190*	0.5209	0.5115	0.5364	0.5364	0.5378	0.5416	0.5326	0.5406	0.5355	0.5322
	Drop Volatility factor	0.5303	0.5031	0.5167	0.5195	0.5176	0.5298	0.5153	**0.5402**	0.4913	0.5040	0.4974	0.5078	0.5059	0.5373	**0.5402**	0.5345	0.5383	0.5359	0.5312	0.5392	0.5359
	Drop Macro Factor	0.5303	0.5035	0.4984	0.5214	0.5181	0.5195	0.5035	0.5303	0.5002	0.5012	0.5101	0.5031	0.5233	0.5317	0.5331	**0.5364**	0.5303	0.5355	0.5336	0.5355	0.5298
	Drop Correlation index	0.5303	0.5129	0.5218	0.5364**	0.5322	0.5171	0.5073	**0.5420**	0.4951	0.5049	0.4937	0.504	0.5275	0.5369	0.5373	0.5388	0.5406	0.5411	0.5359	0.5373	0.5402
XLF	All Variables	0.5045	0.5124	0.5012	0.5073	0.5101	0.4782	0.5106	0.5059	0.5007	0.4847	0.4951	0.4913	0.4814	0.5073	0.5031	0.5087	**0.5204**	0.5148	0.5139	0.5129	0.5092
	Drop Macro Variables	0.5045	0.4955	0.4838	**0.5134**	0.5016	0.4988	0.4927	0.5059	0.5007	0.4974	0.5110	0.4918	0.4927	0.5012	0.5059	0.5031	0.5110	0.5101	0.5157	0.5096	0.5106
	Drop technical Variables	0.5045	0.5134	0.5035	0.5049	0.5002	0.4819	0.4979	0.5054	0.5087	0.5031	0.5096	0.5073	0.4965	0.5148	0.5059	0.5045	0.5096	0.5049	**0.5228**	0.5082	0.5054
	Drop Volatility factor	0.5045	0.5162	0.4918	0.5016	0.4984	0.4890	0.5026	0.5049	0.4984	0.4941	0.4960	**0.5308***	0.5021	0.5082	0.5063	0.5087	0.5068	0.5162	0.5129	0.5124	0.5073
	Drop Macro Factor	0.5045	0.4998	0.4890	0.5106	0.5068	0.4852	0.4998	0.5040	0.4885	0.4984	0.5012	0.4922	0.4674	0.4998	0.5054	0.5059	0.5045	**0.5157**	0.5106	0.5134	0.5016
	Drop Correlation index	0.5045	0.5204	0.4937	0.5181	0.5068	0.5040	0.5059	0.5059	0.5035	0.5106	**0.5247**	0.4988	0.5021	0.5026	0.5092	0.5049	0.511	0.5143	0.5195	0.5016	0.5002
XLK	All Variables	0.5406	0.5237*	0.5279	0.5524***	0.5270	0.5200	0.4960	0.5434	0.5298	0.5002	0.5087	0.5171	0.5388	0.5402	0.5458	0.5425	0.5449	**0.5552****	0.543	0.5383	0.5420
	Drop Macro Variables	0.5406	0.5157	0.5186	0.5218	0.5228	0.5115	0.5087	0.5434	0.5233	0.5181	0.4937	0.5237	0.5411	0.5373	0.5416	0.5416	0.5444	0.5439	0.5420	**0.5463**	0.5439
	Drop technical Variables	0.5406	0.5355***	0.5364*	0.5345**	0.5251	0.5195	0.5073	0.5434	0.5171	0.5233	0.5059	0.5350	0.5378	0.5430	0.5416	0.5463	0.5420	0.5463	0.5378	**0.5481**	0.5383
	Drop Volatility factor	0.5406	0.5218	0.5265	0.5317**	0.5176	0.5139	0.5167	0.5434	0.5284*	0.5106	0.5124	0.5247	0.5397	0.5434	0.5406	0.5406	**0.5467**	0.5444	0.5449	0.5420	0.5388
	Drop Macro Factor	0.5406	0.5195	0.5359*	0.5383***	0.5341*	0.5294	0.5092	0.5406	0.5308	0.4927	0.5002	0.5383	0.5322	0.5458	0.5402	0.5434	0.543	0.5481	0.5449	0.5425	**0.5463**
	Drop Correlation index	0.5406	0.5261	0.5265	**0.5486*****	0.5204	0.5223	0.511	0.5434	0.5345*	0.5007	0.5120	0.5143	0.4927	0.5388	0.5425	0.5420	0.5430	**0.5486**	0.5420	0.5463	0.5420
XLY	All Variables	0.5355	0.5303**	0.5176	0.5303*	0.5289	0.5087	0.5096	0.5369	0.5148	0.5176	0.4829	0.5153	0.5355	0.5326	0.5284	0.5355	0.5383	0.5373	0.5308	**0.5392**	0.5341
	Drop Macro Variables	0.5355	0.5218	0.5153	0.519	0.5233	0.5209	0.5101	0.5369	0.5153	0.5073	0.5124	0.5082	0.5308	0.5341	0.5308	0.5373	**0.5392**	0.5294	0.5383	0.5303	0.5378
	Drop technical Variables	0.5355	0.5289**	0.5204	0.519	0.5157	0.5153	0.5167	0.5312	0.5129	0.4941	0.5054	0.5115	0.5373	0.5261	**0.5364**	0.5322	0.5331	0.5326	0.5279	0.5303	0.5317
	Drop Volatility factor	0.5355	0.5223	0.5190	0.5157	0.5312	0.5265	0.5162	**0.5373**	0.5195	0.4998	0.4857	0.5237	0.5002	0.5322	0.5341	**0.5373**	0.5308	0.5336	0.5359	0.535	0.5322
	Drop Macro Factor	0.5355	0.5223*	0.5214	0.5110	0.5218	0.5101	0.5120	0.5378	0.5063	0.4974	0.4979	0.5082	0.5317	0.5359	0.5378	0.5345	**0.5383**	0.5364	0.5364	0.5341	0.5364
	Drop Correlation index	0.5355	0.5326**	0.5218	0.5289	0.5242	0.5162	0.5233*	0.5369	0.5148	0.5101	0.5016	0.5171	0.5016	**0.5359**	0.5336	0.5303	0.5341	0.5270	0.5416	0.5303	0.5303
XLV	All Variables	0.5228	0.5082	0.4866	0.5082	0.4852	0.504	0.5045	0.5228	0.4852	0.4908	0.4861	**0.5359***	0.5148	0.5214	0.5228	0.5228	0.5228	0.5233	0.5223	0.5228	0.5228
	Drop Macro Variables	0.5228	0.4932	0.5035	0.4918	0.5016	0.5045	0.5012	0.5228	0.4941	0.5031	0.5063	0.5124	**0.5242**	0.5214	0.5228	0.5228	0.5228	0.5233	0.5223	0.5228	0.5228
	Drop technical Variables	0.5228	0.5031	0.504	0.5204	0.5068	0.5059	0.5087	0.5228	0.5021	0.5021	0.5059	**0.5279**	0.5186	0.5214	0.5228	0.5228	0.5228	0.5233	0.5223	0.5228	0.5228
	Drop Volatility factor	0.5228	0.5031	0.4998	0.5078	0.4974	0.5007	0.5031	0.5228	0.4904	0.5181	0.5134	0.5148	**0.5298**	0.5214	0.5228	0.5228	0.5228	0.5233	0.5223	0.5228	0.5228
	Drop Macro Factor	0.5228	0.5124	0.4922	0.5082	0.5016	0.5045	0.5162	0.5228	0.4899	0.4974	0.5049	0.5073	0.5195	0.5214	0.5228	0.5228	0.5228	**0.5233**	0.5223	0.5228	0.5228
	Drop Correlation index	0.5228	0.5082	0.5176	0.5148	0.489	0.5068	0.4960	0.5228	0.4838	0.4955	0.5054	0.5195	0.5176	0.5214	0.5228	0.5228	0.5228	**0.5233**	0.5223	0.5228	0.5228

*Notes: Table 3.6 reports the 1-step-head directional predictive accuracy rate (DPAR) of market sector ETFs With rolling window size 500, for the period 2009:6-2017:12. All DPARs are derived from level forecasting results. If the forecasted return is positive, then it is classified as an upward direction, otherwise as a downward direction. Entries in bold denote models with highest directional accuracy rate for a given forecasting target and predictors. Starred entries denote rejection of the null of no information about the direction of change forecasting, based on Pesaran and Timmermann (1992) (PT) test. Significance levels for the test are reported as $***p < 0.01$, $**p < 0.05$, and $*p < 0.1$, where p is the $p-$value corresponding to PT test statistics.

Table 3.7: Directional Predictive Accuracy Rate Based on 1-Step-Ahead Daily Level Forecasting Results (Recursive Window)*

		RandomWalk	Linear	SVRrbf	SVRlin	SVRpoly	RanForest	boosting	lasso	ridge	NN1	NN2	NN3	NN4	hybrid1	hybrid2	hybrid3	hybrid4	hybrid5	hybrid6	hybrid7	hybrid8
SPY	All Variables	0.4988	0.4951	0.4937	0.5242	0.5256	**0.5378**	0.5364*	0.5129	0.4908	0.4946	0.496	0.4852	0.4979	0.5106	0.5218	0.5129	0.5181	0.496	0.5228	0.5214	0.5171
	Drop Macro Variables	0.4988	0.4814	0.5068	0.5265	0.5012	**0.5289**	0.5045	0.5129	0.4946	0.5124*	0.4918	0.4861	0.4843	0.5040	0.5106	0.5181	0.5251	0.5073	0.5092	0.5021	0.5045
	Drop technical Variables	0.4988	0.5059	**0.5388****	0.5355	0.5350	0.5298**	0.5242*	0.5129	0.5082	0.5087	0.4725	0.5035	0.4969	0.5200	0.5214	0.5200	0.4998	0.5209	0.5106	0.5139	0.5171
	Drop Volatility factor	0.4988	0.4819	0.5139	0.5237	0.5181	**0.5331**	0.5326	0.5139	0.4852	0.5007	0.4965	0.511	0.4927	0.5167	0.5063	0.5186	0.5176	0.5298	0.5026	0.5176	0.5157
	Drop Macro Factor	0.4988	0.4937	0.4974	0.5195	0.5237	**0.5388**	0.5218*	0.4988	0.4890	0.4843	0.4955	0.5059	0.5087	0.5021	0.5035	0.5002	0.4984	0.5063	0.5031	0.5073	0.4993
	Drop Correlation index	0.4988	0.4955	0.5026	0.5171	0.5209	0.5153	0.5181	0.5129	0.4767	0.5012	0.5129	0.4730	0.4988	0.5186	0.5143	**0.5270**	0.5214	0.5092	0.5054	0.5190	0.5204
XLF	All Variables	0.4998	0.5021	0.5082	0.5016	0.5049	0.4791	**0.5148**	0.4974	0.4979	0.4852	0.5002	0.4908	0.4918	0.4998	0.5026	0.4965	0.4960	0.5012	0.5026	0.4979	0.5021
	Drop Macro Variables	0.4998	0.5026	0.4951	0.4984	0.5049	0.5035	**0.5134**	0.4974	0.5063	0.4937	0.5035	0.5054	0.4974	0.5007	0.4899	0.4998	0.4960	0.4993	0.5012	0.4871	0.4993
	Drop technical Variables	0.4998	0.5031	0.5087	0.4946	0.4974	0.4829	0.4965	0.4974	0.4904	**0.5068**	0.5026	0.4871	0.4946	0.5026	0.4974	0.5035	0.5007	0.4960	0.5059	0.5040	0.4979
	Drop Volatility factor	0.4998	0.5035	0.5078	0.5049	0.4969	0.5040	**0.5134**	0.4974	0.5002	0.4955	0.5016	0.4960	0.5031	0.5007	0.4988	0.5026	0.4988	0.4941	0.5063	0.4960	0.5026
	Drop Macro Factor	0.4998	0.4998	0.4908	0.5007	0.5031	0.4969	0.5082	0.504	0.5016	**0.5106**	0.4937	0.4984	0.4829	0.4932	0.5059	0.4922	0.4988	0.5002	0.4965	0.5016	0.5021
	Drop Correlation index	0.4998	0.5045	0.5101	0.5045	0.5115	0.5124	0.5078	0.4974	0.5035	**0.5181**	0.4922	0.5016	0.5092	0.4927	0.5016	0.4998	0.4993	0.5082	0.5115	0.4984	0.4965
XLK	All Variables	0.5369	0.5223	0.5256	0.5251	0.5303	0.5477	0.5265	0.5359	0.5218	0.5171	0.4899	0.5204	0.5326	0.5425	0.5430	0.5458	0.5364	0.5416	**0.5500**	0.5463	0.5350
	Drop Macro Variables	0.5369	0.4998	0.5265	0.5355	0.5420	0.5265	0.5228	0.5359	0.5031	0.5063	0.4979	0.5162	0.5289	0.5458	0.5383	0.5420	0.5369	0.5420	**0.5472**	0.5458	0.5364
	Drop technical Variables	0.5369	0.5237	0.5373	0.5406	0.5312	**0.5458**	0.5364	0.5359	0.5124	0.4998	0.5200	0.5242	0.5331	0.5406	0.5378	0.5350	0.5392	0.5449	0.5430	0.5439	0.5350
	Drop Volatility factor	0.5369	0.5294	0.5275	0.5233	0.5115	0.5463	0.5223	0.5359	0.5214	0.4937	0.4876	0.4984	0.5350	0.5392	0.5434	0.5411	0.5373	0.5434	0.5402	**0.5486**	0.5463
	Drop Macro Factor	0.5369	0.5016	0.5317	0.5115	0.5265	**0.5458**	0.4960	0.5369	0.5082	0.5298**	0.5026	0.4974	0.5350	0.5359	0.5359	0.5388	0.5388	0.5411	0.5449	0.5402	0.5383
	Drop Correlation index	0.5369	0.5214	0.527	0.5265	0.5242	0.5251	0.5031	0.5359	0.5157	0.4899	0.5063	0.5120	0.4941	0.5453	0.5359	0.5378	0.5430	0.5481	0.5449	**0.551**	0.5500
XLY	All Variables	0.5294	0.5195	0.5186	0.5200	0.5265	0.5162	0.5383	0.5294	0.5167	0.5031	0.5124	0.5167	0.5279	0.5265	0.5284	0.5279	0.5317	**0.5388**	0.5345	0.5326	0.5275
	Drop Macro Variables	0.5294	0.5303**	0.5228	0.5326	0.5345	0.5284**	0.5294	0.5298	0.5209	0.4941	0.4974	0.4955	0.5265	0.5270	0.5326	0.5308	0.5294	**0.5397**	0.5341	0.5345	0.5275
	Drop technical Variables	0.5294	0.5087	0.5298	0.5298	0.5298	0.5341	0.5336	0.5294	0.5035	0.5007	0.4988	0.5284	0.5190	0.5350	0.5265	**0.5350**	0.5303	0.5308	0.5284	**0.5350**	0.5312
	Drop Volatility factor	0.5294	0.5204	0.52	0.5223	0.5223	0.5336	0.535	0.5294	0.5124	0.5209*	0.5026	0.5078	0.4908	0.5322	0.5294	0.5303	0.535	0.5303	0.5308	0.527	**0.5406**
	Drop Macro Factor	0.5294	0.5162	0.5096	0.5153	0.5223	0.5261	0.5373	0.5294	0.5096	0.5031	0.5031	0.5026	0.5233	0.5364	0.5359	0.5308	0.5275	0.5350	**0.5392**	0.5364	0.5303
	Drop Correlation index	0.5294	0.5317**	0.5251	0.5284	0.5317	0.5312	0.5256	0.5294	0.5148	0.5162	0.5261**	0.5181	0.5129	0.5308	0.5242	0.5308	0.5312	**0.5383**	0.5289	0.5317	0.5284
XLV	All Variables	0.5228	0.5045	0.5045	0.5035	0.4955	**0.5275**	0.5261	0.5186	0.5063	0.4969	0.4918	0.5002	0.5115	0.5186	0.5186	0.5186	0.5186	0.5186	0.5186	0.5186	0.5186
	Drop Macro Variables	**0.5228**	0.4857	0.5096	0.4984	0.5040	0.5087	0.5021	0.5186	0.4904	0.4984	0.5101	0.5040	0.5106	0.5186	0.5186	0.5186	0.5186	0.5186	0.5186	0.5186	0.5186
	Drop technical Variables	0.5228	0.5007	0.511	0.5186	0.5242	**0.5247**	0.5214	0.5186	0.5171	0.5035	0.4984	0.5045	0.512	0.5186	0.5186	0.5186	0.5186	0.5186	0.5186	0.5186	0.5186
	Drop Volatility factor	0.5228	0.5026	0.512	0.5134	0.5139	0.5049	0.5214	0.5186	0.504	0.5186	0.5059	**0.5256**	0.5171	0.5186	0.5186	0.5186	0.5186	0.5186	0.5186	0.5186	0.5186
	Drop Macro Factor	0.5228	0.4922	0.5209	0.5101	0.5101	**0.5233**	**0.5233**	0.5186	0.4974	0.5115	0.4927	0.519	0.52	0.5186	0.5186	0.5186	0.5186	0.5186	0.5186	0.5186	0.5186
	Drop Correlation index	0.5228	0.5153	0.5110	**0.5237**	0.5031	0.5181	0.5214	0.5186	0.5087	0.5087	0.5026	0.5143	0.5167	0.5186	0.5186	0.5186	0.5186	0.5186	0.5186	0.5186	0.5186

*Notes: See notes to Table 3.6. Recursive window size 500.

Table 3.8: Directional Predictive Accuracy Rate Based on Monthly Aggregate Level Forecasting Results (Rolling Window)*

		RandomWalk	Linear	SVRrbf	SVRlin	SVRpoly	RanForest	boosting	lasso	ridge	NN1	NN2	NN3	NN4	hybrid1	hybrid2	hybrid3	hybrid4	hybrid5	hybrid6	hybrid7	hybrid8
SPY	All Variables	0.5922	0.6117***	0.7184***	0.6117**	0.6214**	**0.7573*** **	0.6408***	0.6019	0.5825*	0.5049	0.5534	0.6019	0.5922	0.6019	0.6117	0.5922	0.6117	0.5922	0.5825	0.5922	0.6117
	Drop Macro Variables	0.5922	0.6117**	0.6602***	0.6505***	0.6019*	0.6893***	**0.7476*** **	0.6019	0.5825	0.5825*	0.5049	0.6117	0.5922	0.6214	0.6117	0.5922	0.6117	0.5922	0.5534	0.6019	0.6019
	Drop technical Variables	0.5922	0.5922**	0.6796***	0.6699***	0.6796***	**0.8058*** **	0.7573***	0.6019	0.6117**	0.5534	0.5243	0.5825	0.4854	0.6117	0.6019	0.6214	0.6117	0.6019	0.6408*	0.5922	0.5728
	Drop Volatility factor	0.5922	0.6117***	0.6602***	0.6214**	0.6311**	**0.7476*** **	0.6602***	0.6117	0.6019**	0.4466	0.5437	0.6214	0.5534	0.6214	0.6019	0.5825	0.6117	0.6019	0.5825	0.6019	0.5922
	Drop Macro Factor	0.5922	0.5922**	0.7379***	0.6602***	0.6602***	0.6796***	**0.7379*** **	0.5922	0.5728	0.5243	0.5146	0.6019	0.6019	0.6019	0.5922	0.5922	0.6019	0.6117	0.5825	0.5922	0.5922
	Drop Correlation index	0.5922	0.6117***	0.6408***	0.5922	0.6019	**0.7864*** **	0.767***	0.6019	0.5534	0.5922	0.5631	0.6019	0.6019	0.6117	0.6117	0.6117	0.6019	0.5922	0.6019	0.5825	0.6019
XLF	All Variables	0.6019	0.6311***	0.6505***	0.5922**	0.534	**0.835*** **	0.7087***	0.6019	0.5825*	0.5437	0.6019*	0.6311**	0.5922	0.6214	0.6019	0.6019	0.5922	0.6214	0.6408*	0.5534	0.6311*
	Drop Macro Variables	0.6019	0.5534	0.6505***	0.5728	**0.6602*** **	0.6408*	**0.6602*** **	0.6019	0.5243	0.5922*	0.5534	0.5534	0.5146	0.6311*	0.6505**	0.5922	0.5825	0.6019	0.6214	0.5922	0.6019
	Drop technical Variables	0.6019	0.5825**	0.699***	0.5825**	0.5825**	**0.7864*** **	0.5922*	0.6019	0.6019**	0.6214**	0.5825	0.6214	0.5534	0.6408**	0.6214	0.6117	0.5728	0.6505**	0.6699***	0.6117	0.6214
	Drop Volatility factor	0.6019	0.6019**	0.6214*	0.5631	0.5922	**0.7573*** **	0.6699***	0.6019	0.5534	0.5922	0.6408**	0.5728	0.6214**	0.6214*	0.5825	0.5922	0.6214*	0.6117	0.6214	0.6019	0.5825
	Drop Macro Factor	0.6019	0.5922**	0.6311**	0.5631	0.5825	**0.7767*** **	0.6893***	0.6117	0.5534	0.5437	0.5825	0.6117	0.4951	0.6602**	0.6408*	0.6117	0.6505**	0.6505**	0.6408*	0.5922	0.6117
	Drop Correlation index	0.6019	0.5728*	0.6311**	0.6019**	0.5534	**0.7670*** **	0.6796***	0.6019	0.6019**	0.5049	0.5825	0.5534	0.5631	0.6505**	0.6214*	0.6214*	0.6214	0.6408**	0.6311*	0.6019	0.6019
XLK	All Variables	0.6117	0.6311***	0.6699***	0.6699***	0.6699***	0.7087***	**0.7184*** **	0.6311	0.6408***	0.6117*	0.5728	0.6505	0.6117	0.6214	0.6214	0.6408	0.6311	0.6408	0.6699*	0.6505	0.6311
	Drop Macro Variables	0.6117	0.5534	0.6408*	0.6214	0.6311*	0.6408*	**0.6990*** **	0.6311	0.5631	0.5534	0.5728	0.6602*	0.6214	0.6311	0.6214	0.6311	0.6311	0.6505	0.6408	0.6408	0.6311
	Drop technical Variables	0.6117	0.6214**	0.6311	0.699***	0.6602***	0.6990***	**0.7184*** **	0.6311	0.5728*	0.5825	0.6311	0.6311	0.6311	0.6311	0.6311	0.6311	0.6311	0.6408	0.6408	0.6117	0.6311
	Drop Volatility factor	0.6117	0.5922**	0.6214*	0.6311***	0.6311***	**0.7184*** **	**0.7184*** **	0.6311	0.5825*	0.5243	0.6214	0.6408	0.6214	0.6311	0.6311	0.6311	0.6311	0.6311	0.6408	0.6408	0.6311
	Drop Macro Factor	0.6117	0.6602***	0.6505**	**0.7184*** **	0.6117	0.699***	0.6408***	0.6214	0.6311*	0.534	0.5146	0.6505	0.5825	0.6214	0.6117	0.6117	0.6311	0.6602	0.6408	0.6311	0.6602
	Drop Correlation index	0.6117	0.6214**	0.6602**	0.6699***	0.6602***	**0.7476*** **	0.6893***	0.6311	0.6311**	0.5728	0.6019	0.5728	0.5825	0.6117	0.6311	0.6214	0.6214	0.6505	0.6602	0.6408	0.6214
XLY	All Variables	0.5922	0.534	0.5534	0.5728	0.534	**0.7573*** **	0.6408***	0.5728	0.534	0.5825	0.5728	0.5631	0.5922	0.5825	0.5922	0.5922	0.5728	0.6117	0.6019	0.5922	0.5922
	Drop Macro Variables	0.5922	0.5243	0.5534	0.6019	0.5825	**0.7184*** **	0.7087***	0.5728	0.5243	0.5922	0.5825	0.6019	0.5922	0.5922	0.5825	0.5825	0.5728	0.5922	0.5825	0.5922	0.5728
	Drop technical Variables	0.5922	0.5728	0.5534	0.5631	0.5534	**0.6893*** **	0.6796***	0.5825	0.5631	0.534	0.5825	0.5049	0.5922	0.5922	0.6117	0.5922	0.5825	0.6019	0.6117	0.6019	0.5825
	Drop Volatility factor	0.5922	0.5437	0.5728	0.534	0.5243	**0.7087*** **	0.6699***	0.5728	0.5049	0.5534	0.5728	0.5922	0.5728	0.5922	0.5922	0.5922	0.5922	0.6019	0.6019	0.5728	0.6311
	Drop Macro Factor	0.5922	0.5922**	0.5437	0.5922*	0.5631	**0.7379*** **	0.6408***	0.5922	0.4951	0.5534	0.5631	0.6019	0.5922	0.5631	0.5922	0.5728	0.5825	0.5728	0.5825	0.5922	0.5825
	Drop Correlation index	0.5922	0.5146	0.5437	0.5437	0.5437	**0.7087*** **	0.6893***	0.5728	0.5243	0.5825	0.5534	0.5728	0.5534	0.5922	0.6019	0.5728	0.5728	0.5825	0.6311	0.6019	0.5825
XLV	All Variables	0.6214	0.6505***	0.6699**	0.6699***	0.6505**	**0.7670*** **	0.7282***	0.6214	0.6311**	0.466	0.5631	0.6505	0.6505	0.6214	0.6214	0.6214	0.6214	0.6214	0.6117	0.6214	0.6214
	Drop Macro Variables	0.6214	0.5243	0.6505	0.6214	0.6602**	**0.6990*** **	0.6602**	0.6214	0.5922	0.6699***	0.6214	0.5631	0.6408	0.6214	0.6214	0.6214	0.6214	0.6214	0.6117	0.6214	0.6214
	Drop technical Variables	0.6214	0.6214*	0.6699*	0.6505*	0.6311	**0.7573*** **	0.7476***	0.6214	0.6602***	0.6311*	0.6408*	0.6505	0.6408	0.6214	0.6214	0.6214	0.6214	0.6214	0.6117	0.6214	0.6214
	Drop Volatility factor	0.6214	0.6311**	0.6311	0.6214	0.5437	**0.7476*** **	0.7282***	0.6214	0.6408**	0.5534	0.5437	0.6214	0.6505	0.6214	0.6214	0.6214	0.6214	0.6214	0.6117	0.6214	0.6214
	Drop Macro Factor	0.6214	0.6117***	0.699***	0.6214*	0.5631	**0.7573*** **	0.7282***	0.6214	0.6214**	0.5631	0.5825*	0.6214	0.6214	0.6214	0.6214	0.6214	0.6214	0.6214	0.6117	0.6214	0.6214
	Drop Correlation index	0.6214	0.6311**	0.699***	0.6408*	0.6311**	**0.7573*** **	0.7087***	0.6214	0.6311**	0.5825	0.5825	0.6117	0.6019	0.6214	0.6214	0.6214	0.6214	0.6214	0.6117	0.6214	0.6214

*Notes: See notes to Table 3.6. We calcualte the one-month-ahead forecasting results by aggregating daily forecasts during each month, i.e., summing all daily forecasting results within the same month to generate monthly forecasts. All DPARs are derived from monthly aggregate results. If the monthly aggregate return is positive, then it is classified as an upward direction, otherwise as a downward direction.

Table 3.9: Directional Predictive Accuracy Rate Based on Monthly Aggregate Level Forecasting Results (Recursive Window)*

		RandomWalk	Linear	SVRrbf	SVRlin	SVRpoly	RanForest	boosting	lasso	ridge	NN1	NN2	NN3	NN4	hybrid1	hybrid2	hybrid3	hybrid4	hybrid5	hybrid6	hybrid7	hybrid8
SPY	All Variables	0.5146	0.4951	**0.6893*** **	0.6019	0.6602***	0.6796***	0.6699***	0.5437	0.5728**	0.4757	0.3883	0.5728**	0.5243	0.5728	0.5243	0.5922	0.5631	0.4951	0.5146	0.5049	0.5437
	Drop Macro Variables	0.5146	0.5049	0.6505***	0.6117	0.5922	0.6408**	**0.6796*** **	0.5437	0.5340	0.4951	0.5049	0.5340	0.5049	0.5340	0.5534	0.5146	0.5631	0.5534	0.4951	0.5049	0.5243
	Drop technical Variables	0.5146	0.5146	0.6117*	0.6311*	0.6117	**0.8155*** **	0.6699***	0.5437	0.5922***	0.5825**	0.5049	0.4563	0.4757	0.5825	0.5534	0.5534	0.5728	0.5437	0.4951	0.534	0.5146
	Drop Volatility factor	0.5146	0.4660	**0.6699*** **	0.6311**	0.6505***	0.6408**	**0.6699*** **	0.5437	0.5534**	0.4369	0.4563	0.4757	0.5437	0.5049	0.5049	0.5437	0.5534	0.6019*	0.5728	0.5340	0.5631
	Drop Macro Factor	0.5146	0.4757	**0.7184*** **	0.5922	0.6505**	0.6019	0.6893***	0.5146	0.5728**	0.5437*	0.4951	0.5243	0.5146	0.5146	0.5243	0.5049	0.5146	0.5243	0.5146	0.5146	0.5146
	Drop Correlation index	0.5146	0.4563	**0.6602*** **	0.5728	0.6019	0.6214	0.6408**	0.5437	0.4854	0.4757	0.5437	0.5146	0.5146	0.4757	0.5631	0.5728	0.5534	0.5437	0.5146	0.5243	0.5728
XLF	All Variables	0.5243	0.5243	0.4951	0.5340	0.5437	**0.8058*** **	0.6019	0.5243	0.4466	0.5243	0.6019***	0.5049	0.5728	0.5437	0.5340	0.534	0.5728	0.5146	0.5340	0.5437	0.5437
	Drop Macro Variables	0.5243	0.5049	0.5825	0.5922	**0.6505** **	0.6408***	0.6505***	0.5243	0.4466	0.5049	0.4466	0.4466	0.5728*	0.5340	0.5146	0.5243	0.5049	0.5146	0.5146	0.4951	0.5437
	Drop technical Variables	0.5243	0.5437	0.5631	0.5340	0.5243	**0.7767*** **	0.5243	0.5243	0.534	0.4563	0.4563	0.5146	0.4854	0.5243	0.5631	0.5340	0.5534	0.5728	0.5146	0.5437	0.534
	Drop Volatility factor	0.5243	0.5243	0.6408***	0.5631	0.6602***	**0.699*** **	0.6019	0.5243	0.4369	0.4757	0.4466	0.534	0.5631	0.5437	0.5340	0.534	0.5146	0.5243	0.5243	0.5340	0.5243
	Drop Macro Factor	0.5243	0.5049	0.4563	0.534	0.5631	**0.6893*** **	0.5728	0.5340	0.4272	0.4951	0.5437	0.4563	0.4660	0.5146	0.5437	0.5146	0.5049	0.4854	0.5243	0.5437	0.5049
	Drop Correlation index	0.5243	0.4854	0.5146	0.5243	0.5631*	**0.5922**	0.5825	0.5243	0.4563	0.4854	0.4466	0.5340	0.5922**	0.5437	0.5534	0.5534	0.5146	0.5146	0.5243	0.5534	0.5437
XLK	All Variables	0.6117	0.5437	**0.6699*** **	0.5922	0.6214	0.6602	0.6602**	0.6311	0.4660	0.6019*	0.5340	0.6019	0.6117	0.6408	0.6311	0.6311	0.6311	0.6505	0.6214	0.5922	0.6408
	Drop Macro Variables	0.6117	0.4660	0.6505	0.6602	**0.6699***	0.6505	0.699***	0.6311	0.4272	0.5534	0.4563	0.6408	0.6214	0.6214	0.6117	0.6117	0.6311	0.6311	0.6408	0.6117	0.6214
	Drop technical Variables	0.6117	0.5631	0.6408*	0.6214	0.6311	**0.6893*** **	**0.6893*** **	0.6311	0.5437	0.5922*	0.5243	0.6019	0.6019	0.6311	0.6214	0.6408	0.6214	0.6505	0.6408	0.6214	0.6019
	Drop Volatility factor	0.6117	0.5243	0.6214*	0.5728	0.5728	**0.6699***	0.6117	0.6311	0.4563	0.4369	0.466	0.5922	0.6214	0.6311	0.6408	0.6311	0.6311	0.6408	0.6117	0.6117	0.6408
	Drop Macro Factor	0.6117	0.5049	0.6796***	0.5534	0.6117	0.6699*	**0.6893*** **	0.6117	0.4563	0.5825	0.5825	0.6214	0.5631	0.6117	0.6117	0.6117	0.6214	0.6408	0.6311	0.6117	0.6214
	Drop Correlation index	0.6117	0.4757	0.6505**	0.6117	0.6699***	**0.7670*** **	0.6796***	0.6311	0.4951	0.4854	0.5631	0.5049	0.6408**	0.6408	0.6214	0.6311	0.6408	0.6019	0.6699*	0.6505	0.6408
XLY	All Variables	0.5825	0.5437	0.5243	0.5534	0.5825	**0.767*** **	0.6019	0.5728	0.5049	0.5437	0.5049	0.5340	0.5922	0.5728	0.5631	0.5825	0.5728	0.5728	0.6117	0.5631	0.5631
	Drop Macro Variables	0.5825	0.4369	0.5631	0.5437	0.5534	**0.699*** **	0.6408*	0.5728	0.4175	0.5340	0.5146	0.5534	0.5728	0.5728	0.5631	0.5728	0.5728	0.6117	0.6019	0.5728	0.5631
	Drop technical Variables	0.5825	0.5922*	0.5631	0.5825	0.6117	**0.6505***	0.6214	0.5728	0.5631	0.5340	0.5049	0.5825	0.5631	0.5825	0.5825	0.5728	0.5728	0.5922	0.6214	0.6019	0.5631
	Drop Volatility factor	0.5825	0.5631	0.5146	0.534	0.5534	**0.6311**	0.6019	0.5728	0.4951	0.5631	0.5243	0.6019	0.5049	0.5825	0.5728	0.5534	0.5825	0.5825	0.5728	0.5534	0.5922
	Drop Macro Factor	0.5825	0.5049	0.5049	0.6019	0.5631	**0.7379*** **	0.5534	0.5728	0.5146	0.4563	0.4466	0.4757	0.5728	0.5922	0.5922	0.5825	0.5728	0.6019	0.6019	0.5922	0.5728
	Drop Correlation index	0.5825	0.4854	0.5631	**0.6311***	0.5631	**0.6311**	0.6214	0.5728	0.5049	0.4466	0.5437	0.5631	0.5146	0.5728	0.5534	0.5728	0.5825	0.5825	0.5825	0.5631	0.5631
XLV	All Variables	0.6214	0.6019	0.7087***	0.6408**	0.6602**	**0.7282*** **	0.7087**	0.6117	0.5922	0.5243	0.534	0.6117	0.6019	0.6117	0.6117	0.6117	0.6117	0.6117	0.6117	0.6117	0.6117
	Drop Macro Variables	0.6214	0.5146	0.6505	0.6019	0.5922	0.6602	**0.6699**	0.6117	0.5437	0.5534	0.5146	0.6214	0.6019	0.6117	0.6117	0.6117	0.6117	0.6117	0.6117	0.6117	0.6117
	Drop technical Variables	0.6214	0.5728	0.6408*	0.6602**	0.6311	**0.7087** **	0.699*	0.6117	0.6408**	0.5340	0.5728	0.5922	0.5728	0.6117	0.6117	0.6117	0.6117	0.6117	0.6117	0.6117	0.6117
	Drop Volatility factor	0.6214	0.5922	0.6699**	0.6214	0.5922	**0.7573*** **	0.7087**	0.6117	0.6117*	0.5825	0.6311*	0.6602*	0.6311	0.6117	0.6117	0.6117	0.6117	0.6117	0.6117	0.6117	0.6117
	Drop Macro Factor	0.6214	0.5437**	0.7282***	0.6214**	0.6019	**0.7282*** **	0.7184***	0.6117	0.6214***	0.5631	0.4660	0.5922	0.6117	0.6117	0.6117	0.6117	0.6117	0.6117	0.6117	0.6117	0.6117
	Drop Correlation index	0.6214	0.6408*	0.6505**	0.6796***	0.6602**	0.6990*	**0.7087** **	0.6117	0.6214	0.5146	0.5631	0.6214	0.6117	0.6117	0.6117	0.6117	0.6117	0.6117	0.6117	0.6117	0.6117

*Notes: See notes to Table 3.8. Recursive window size 500.

Figure 3.1: Sector Continuous Component Correlation Index with S&P 500 Market*

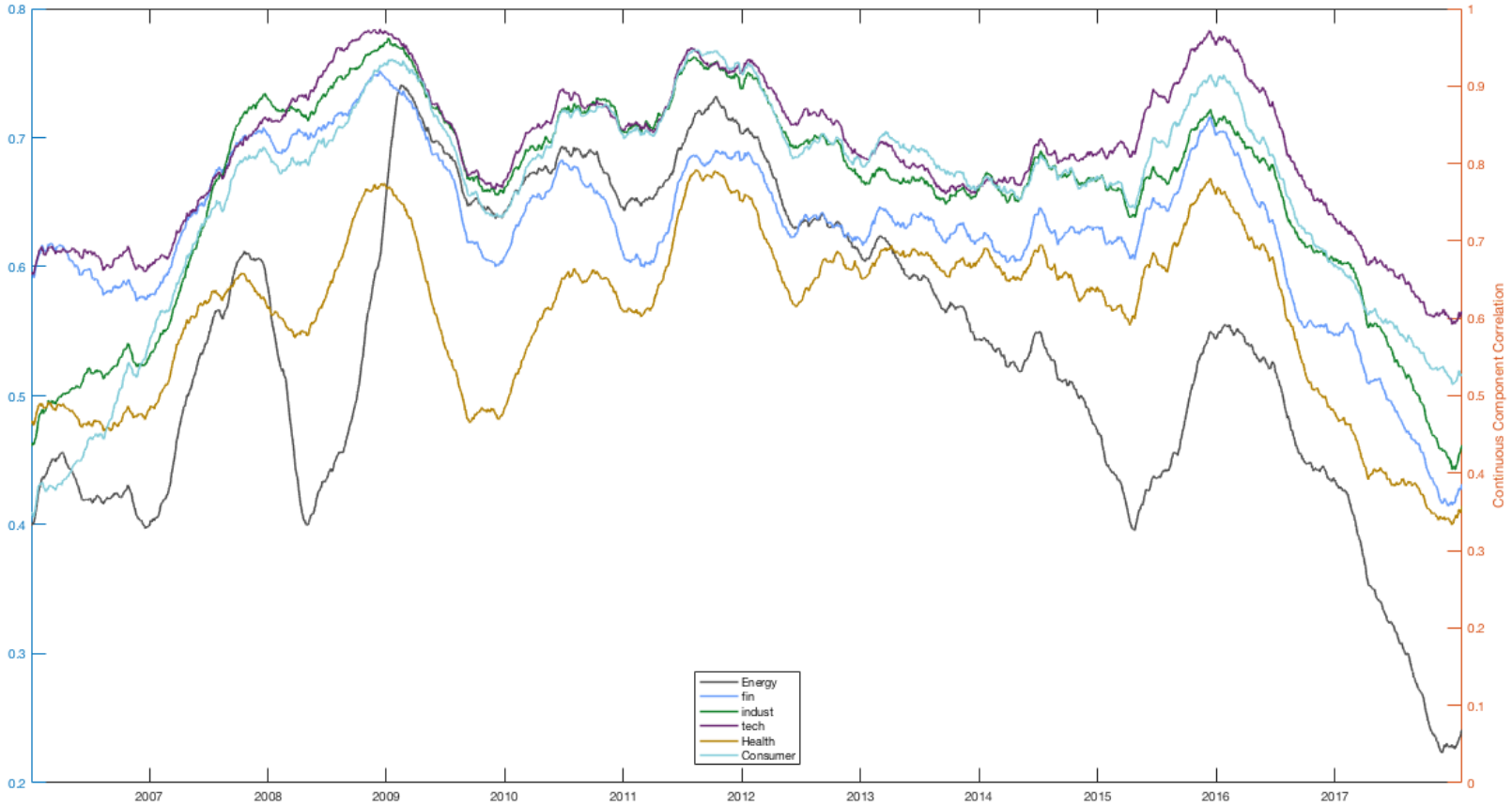

*Notes: This figure depicts the continuous component correlation indices of energy sector (XLE) and S&P 500(SPY), finance sector (XLF) and S&P 500(SPY), industrial sector (XLI) and S&P 500(SPY), technology sector (XLK) and S&P 500(SPY), health care sector (XLV) and S&P 500(SPY), and consumer discretionary sector (XLY) and S&P 500(SPY) from 2006:01 - 2017:12. All correlation indices are measured within [0,1] scale.

Figure 3.2: Sector Jump Component Correlation Index with S&P 500 Market*

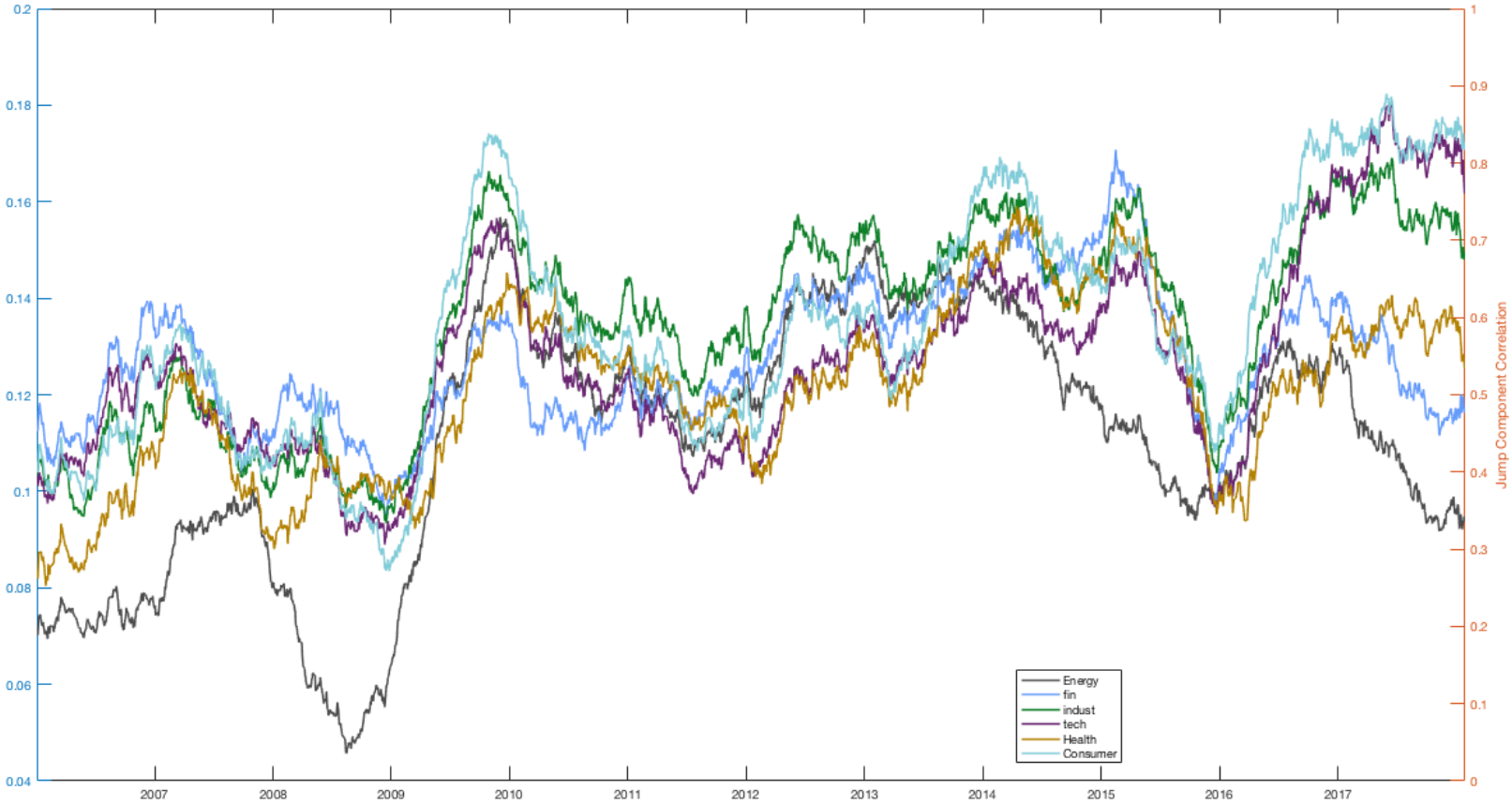

*Notes: See notes in Figure 3.1. Figure 3.2 depicts the jump component correlation indices of energy sector (XLE) and S&P 500(SPY), finance sector (XLF) and S&P 500(SPY), industrial sector (XLI) and S&P 500(SPY), technology sector (XLK) and S&P 500(SPY), health care sector (XLV) and S&P 500(SPY), and consumer discretionary sector (XLY) and S&P 500(SPY) from 2006:01 - 2017:12.

Figure 3.3: Comparison between jump part correlation index and continuous part correlation index*

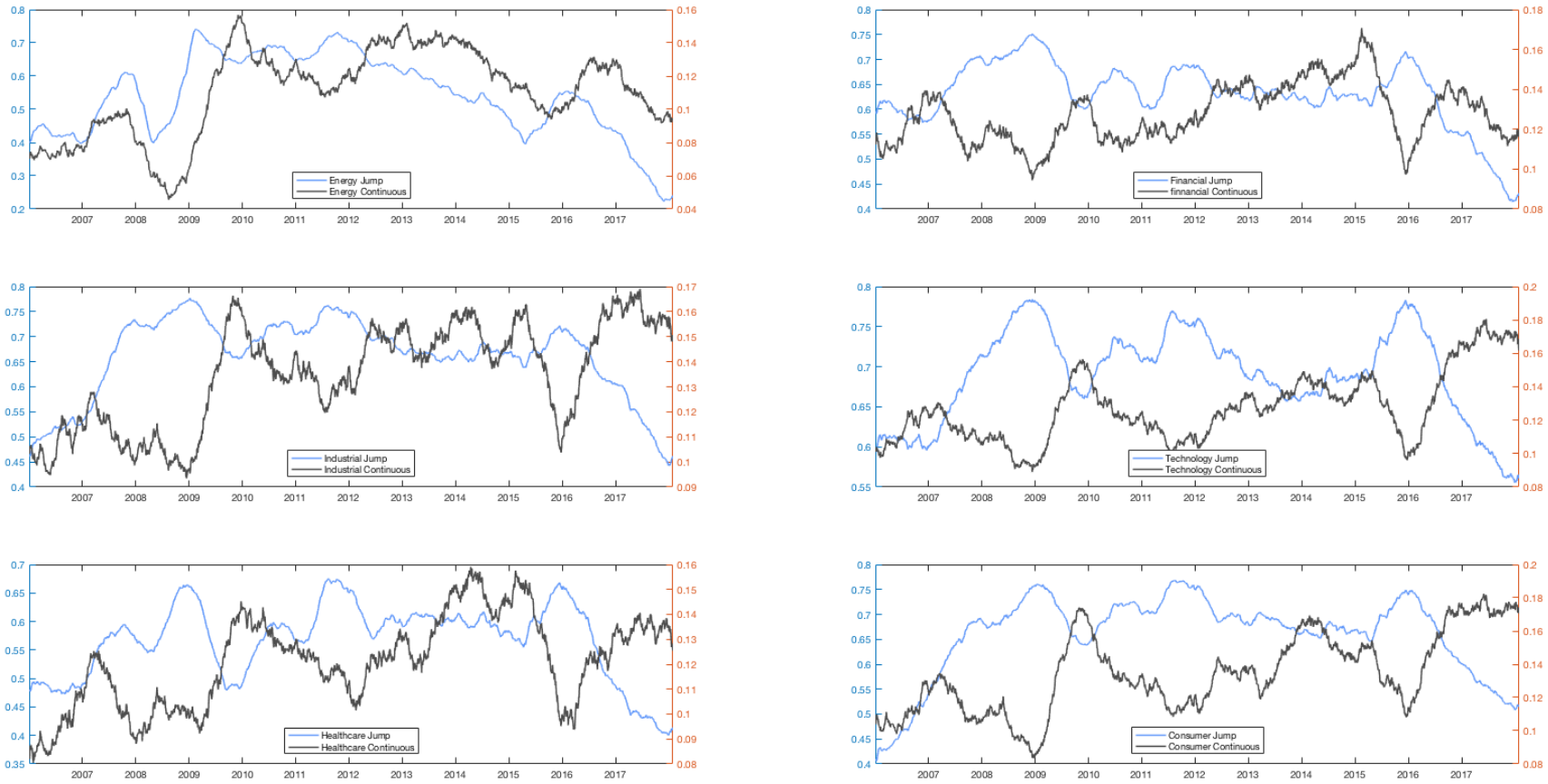

*Notes: This figure compares the jump part correlation index with continuous part correlation index of energy sector (XLE) and S&P500(SPY), finance sector (XLF) and S&P500(SPY), industrial sector (XLI) and S&P500(SPY), technology sector (XLK) and S&P500(SPY), health care sector (XLV) and S&P500(SPY), and consumer discretionary sector (XLY) and S&P500(SPY) from 2006:01 - 2017:12.

Figure 3.4: Macroeconomic Factor and Macroeconomic Series*

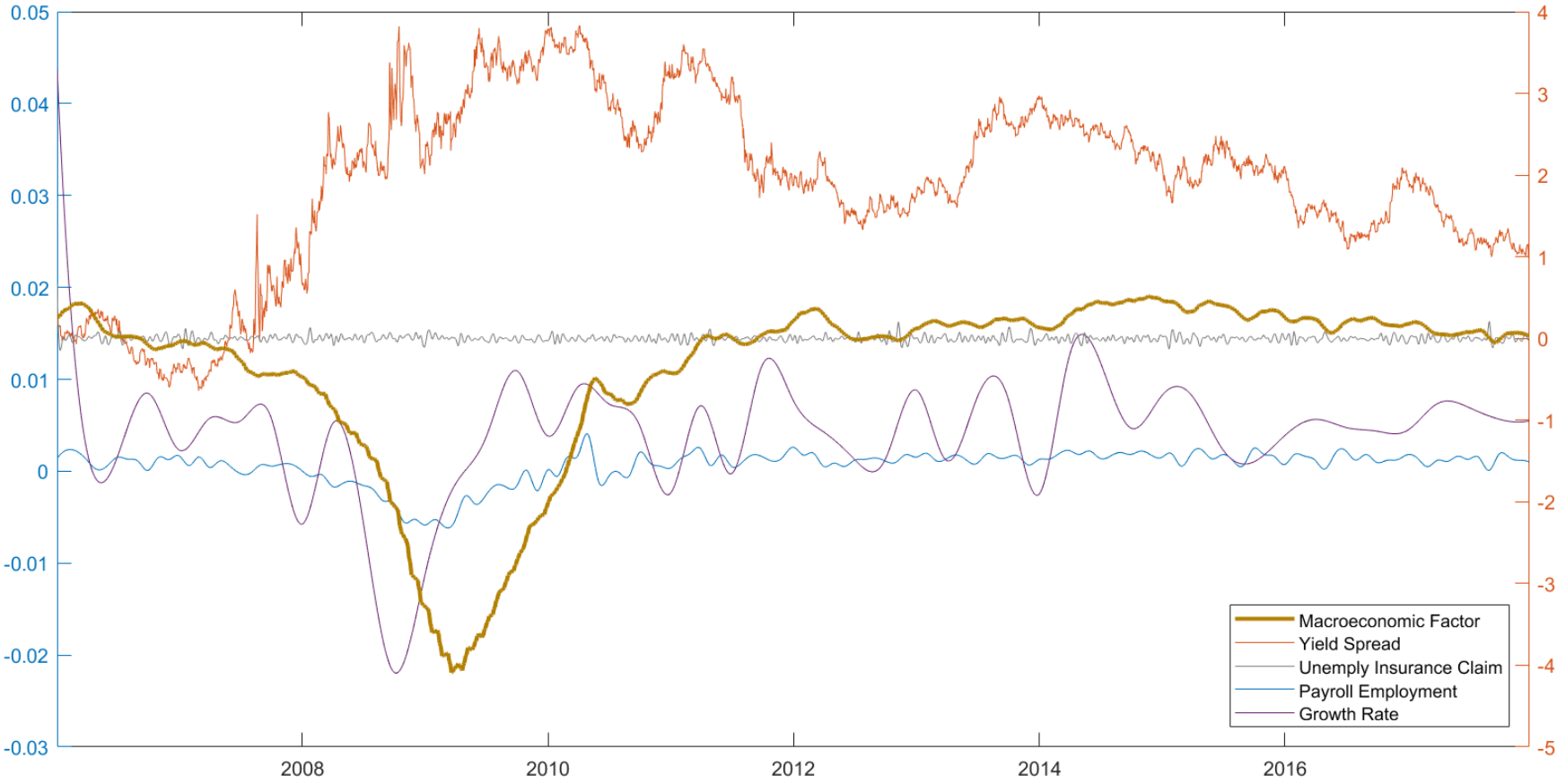

*Notes: We plot logged differenced value of original unemployment insurance claim, payroll employment and growth rate data. Y-axis on the right-hand side corresponds to the macroeconomic risk factor (MF_t^{mac}), yield spread and unemployment insurance claim. Y-axis on the right-hand side is for payroll employment and growth rate.

Figure 3.5: Volatility Factors*

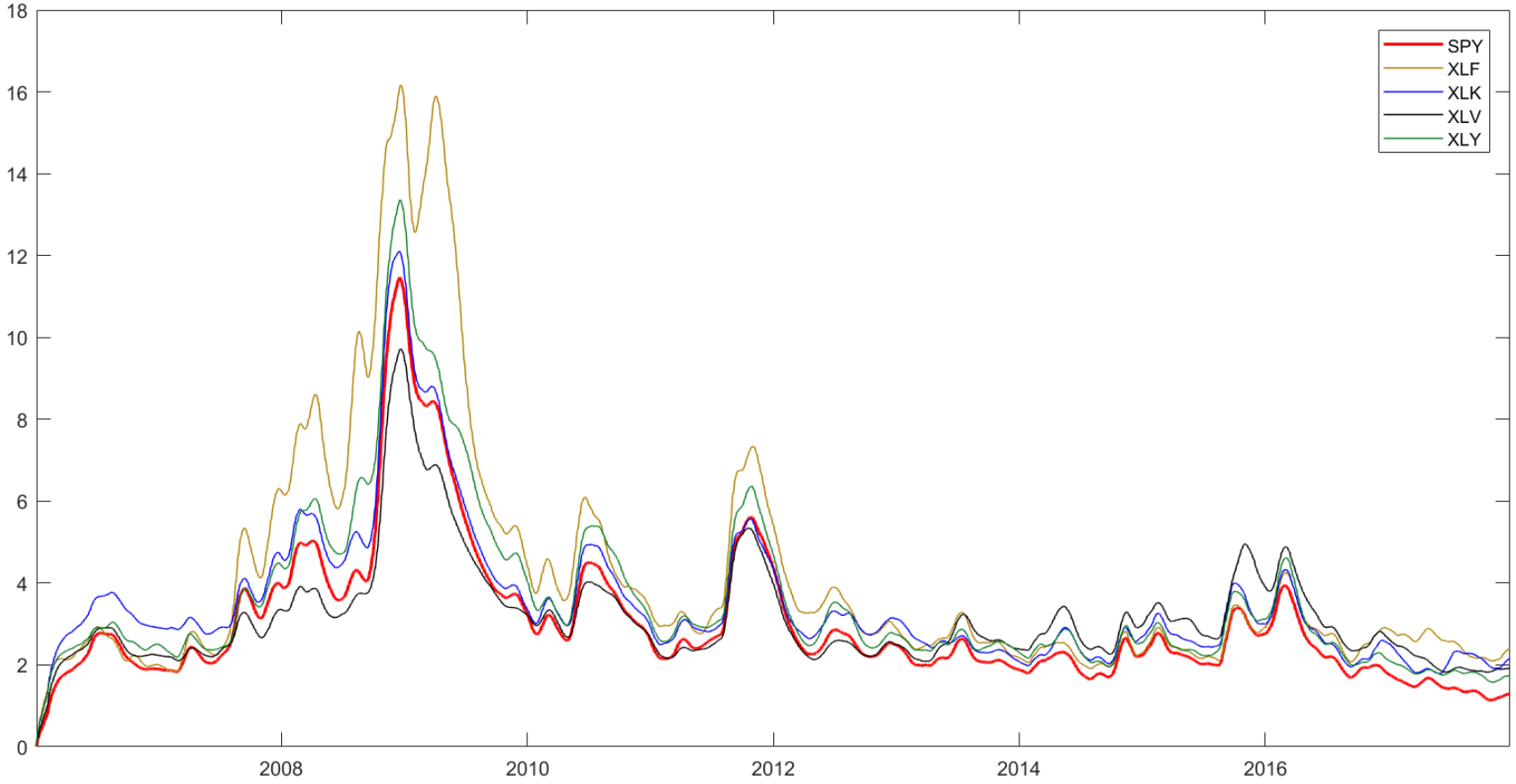

*Notes: We plot volatility risk factors for the S&P 500 market (MF_t^{TRV}), financial sector (MF_t^{XLF}), technology sector (MF_t^{XLK}), health care sector (MF_t^{XLV}), and consumer discretionary sector (MF_t^{XLY}).

Figure 3.6: Monthly Aggregate Relative MSFEs For Machine Leaning Models (Rolling Window Size)*

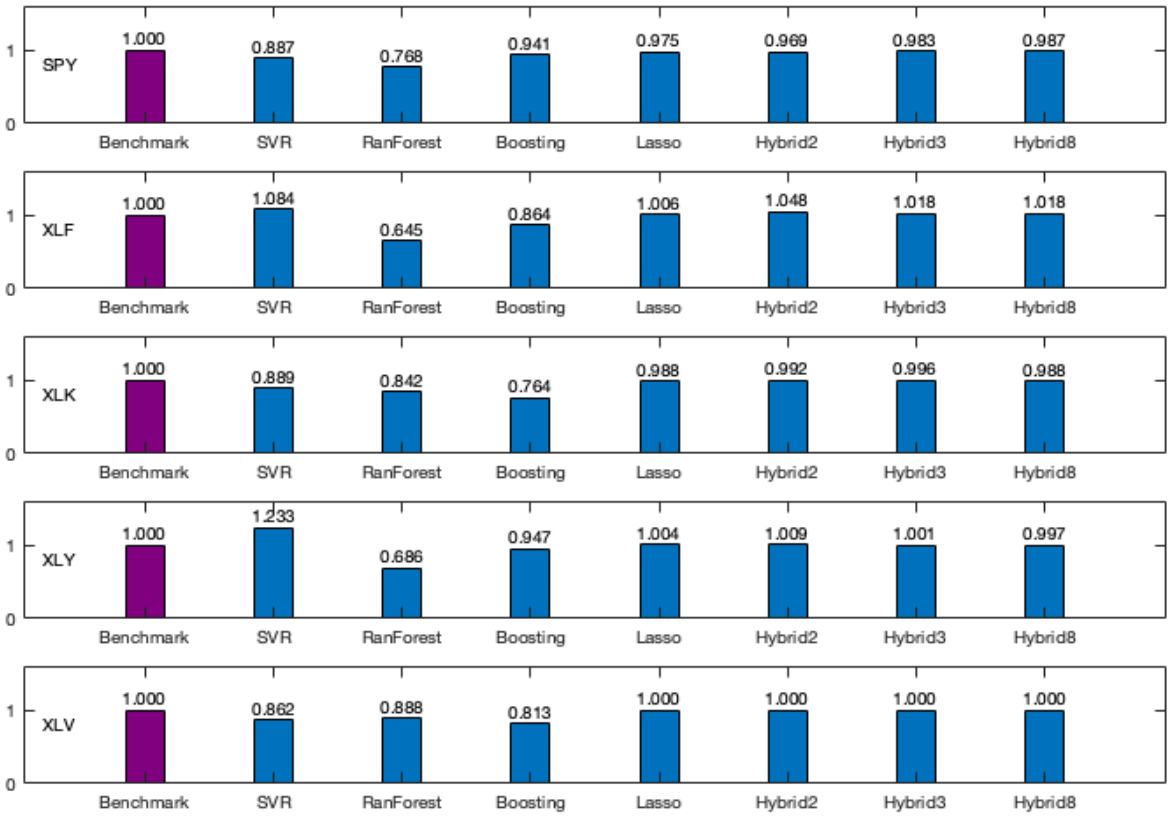

*Notes: Figure 3.6 shows the relative mean square forecasting error (MSFE) for machine learning models. Relative MSFEs are calculated such that numerical values less than unity indicates the alternative model has lower point MSFE than the random walk benchmark model. The panels from top to bottom display different forecasting targets including SPY (S&P 500 ETF), XLF (financial sector ETF), XLK (technology sector ETF), XLY (consumer discretionary sector ETF), and XLV (health care sector ETF). Results in each panel are obtained in Table 3.4 under the row of All Variables.

Figure 3.7: Monthly Aggregate Relative DPARs for Machine Leaning Models (Rolling Window Size)*

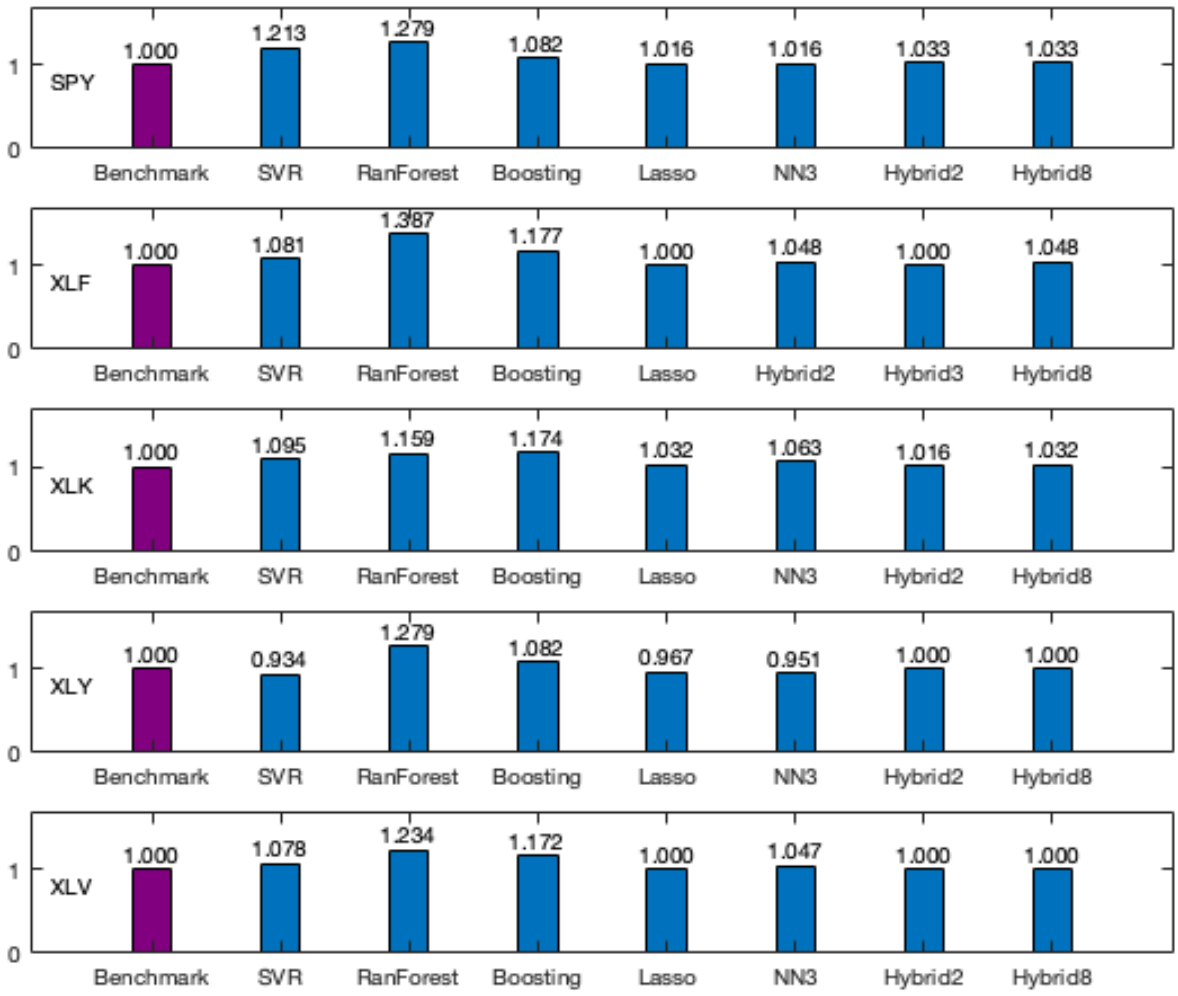

*Notes: Figure 3.7 shows the relative directional prediction accuracy rate (DPARs) for machine learning models. Relative DAPRs are calculated such that numerical values less than unity indicates the alternative model has lower DPAR than the random walk benchmark model. The panels from top to bottom display different forecasting targets including SPY (S&P 500 ETF), XLF (financial sector ETF), XLK (technology sector ETF), XLY (consumer discretionary sector ETF), and XLV (health care sector ETF). Results in each panel are obtained in Table 3.8 under the row of All Variables.

Figure 3.8: Monthly Aggregate Relative MSFEs Due to the Factors (Recursive Window Size)*

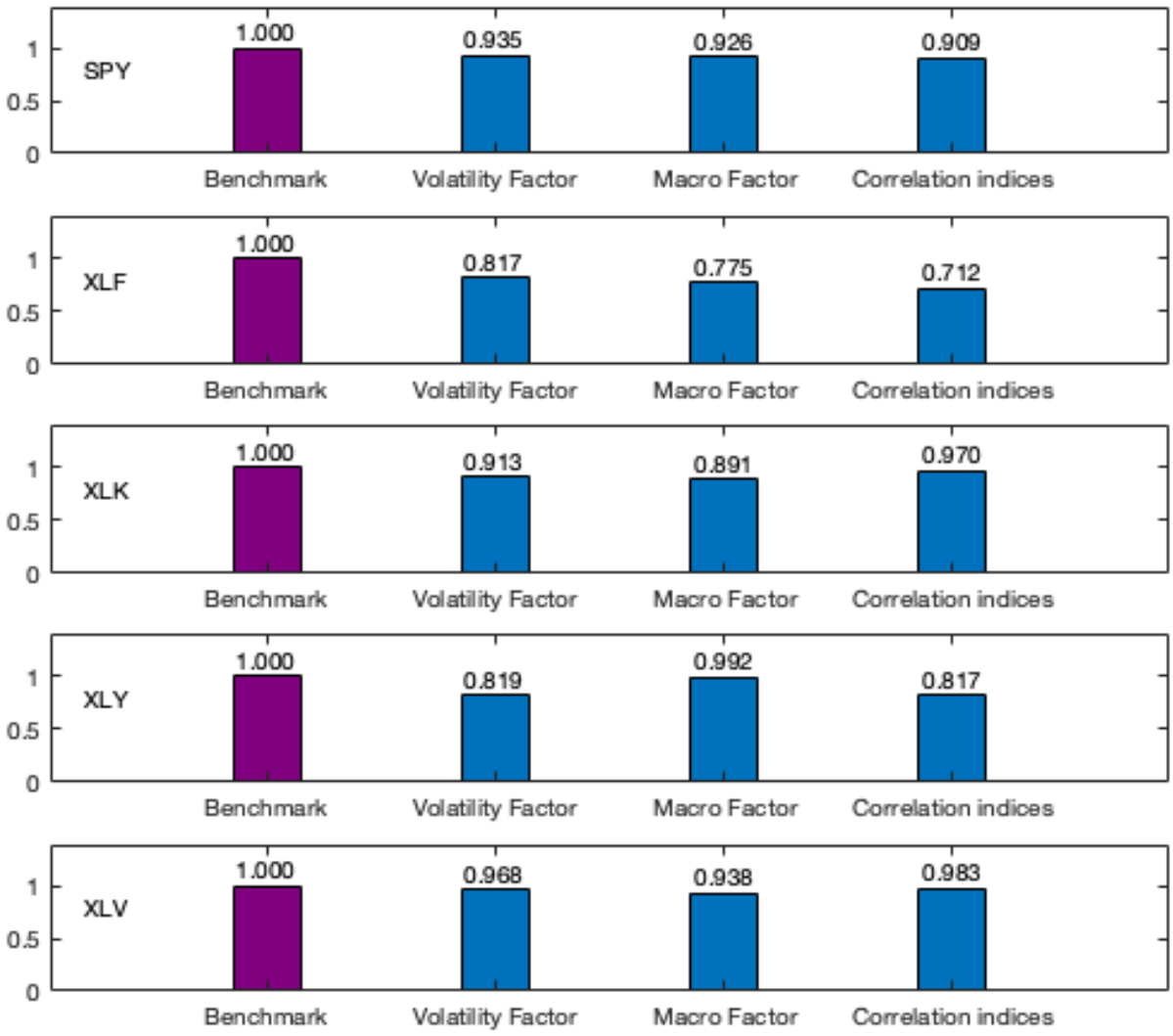

*Notes: See notes to Figure 3.6. Figure 3.8 shows the relative mean square forecasting error (MSFE) of forecasting models with factors. The benchmark model is the same forecasting models but without factors. The results in each panel are obtained from Table 3.5. Within each forecasting target (SPY, XLF, XLK, XLY, and XLV), we navigate to the MSFEs best machine learning model and further analyze the contribution of adding each factor.

Figure 3.9: Monthly Aggregate Relative DPARs Due to the Factors (Rolling Window Size)*

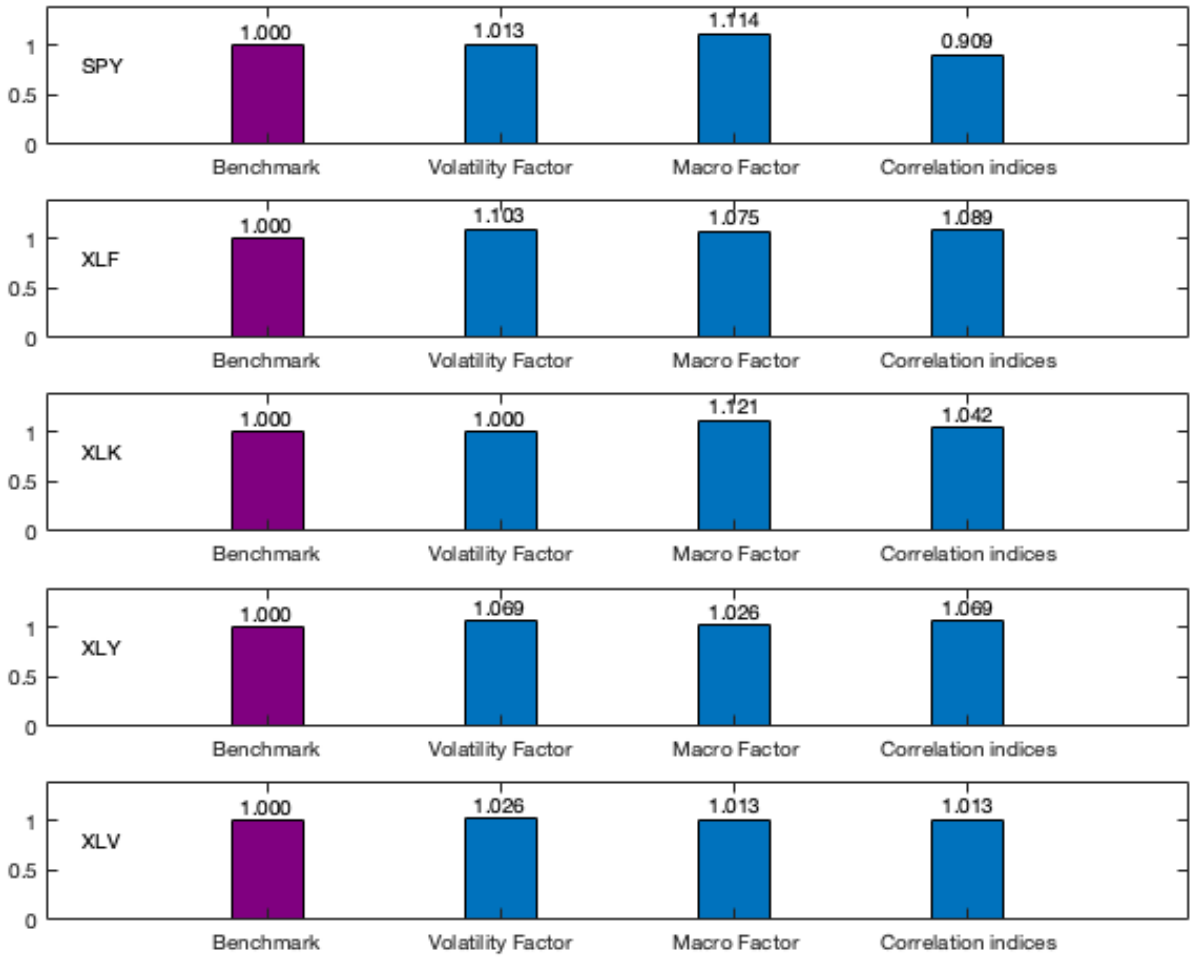

*Notes: See notes in Figure 3.7. Figure 3.9 shows the relative directional prediction accuracy rate (DPARs) of forecasting models with factors. The benchmark model is the same forecasting models but without factors. The results in each panel are obtained from Table 3.9. Within each forecasting target (SPY, XLF, XLK, XLY, and XLV), we navigate to the DPARs best machine learning model and further analyze the contribution of adding each factor.

Chapter 4

Financial Econometrics and Big Data: A Survey of Volatility Estimators and Tests for the Presence of Jumps and Co-Jumps

4.1 Introduction

The importance of integrated volatility, jumps and co-jumps in the financial econometrics literature and in terms of successful risk management by investors is quite obvious now, given the amount of research that has gone into this field. Measures of integrated volatility are crucial given the advent of numerous volatility based derivative products traded in financial markets while tests for jumps are essential in modeling and predicting volatility and returns. Tests of co-jumps on the other hand are meaningful indicators of transmission of financial shocks across different sectors, companies and markets. The rationale behind this chapter is to discuss some of recent advances in jump and co-jump testing methodology and measurement of integrated volatility, and the properties thereof, in a way which would help both researchers and practitioners in application of such econometric methods in finance. We begin by surveying the most widely used integrated volatility measures, jump and co-jump tests, followed by an empirical analysis using high frequency intra-day stock prices of DOW 30 companies and ETFs.

Daily integrated volatility is unobservable. Econometricians have developed numerous measures which estimate price fluctuations in a variety of ways. One of the earliest measures is the *Realized Volatility* in Andersen et al. (2001). However this measure does not separate jump variation from variation due to continuous components. Barndorff-Nielsen

and Shephard (2004) use the product of adjacent intra-day returns to develop jump robust measures *Bipower* and *Tripower Variations*. One of the more recent techniques of separating out the jump component is the truncation methodology which essentially eliminates returns which are above a given threshold as in Corsi et al. (2010) & Aït-Sahalia et al. (2009). One important caveat of high-frequency data is the existence of market microstructure noise which creates a bias in the estimation procedure. Zhang et al. (2005), Zhang et al. (2006) and Kalnina and Linton (2008) solved this problem with noise robust volatility estimators.

In Duong and Swanson (2011), the authors find that 22.8% of the days during the 1993-2000 period had jumps while 9.4% of the days during the 2001-2008 period had jumps. The existence of jumps in financial markets is obvious, which has led many researches to develop techniques which can test for jumps. Jump diffusion is pivotal in analyzing asset movement in financial econometrics and developing jump tests to identify jumps has been the focus for many theoretical econometricians in past few years. Using the ratio of *Bipower Variation* and estimated quadratic variation, Barndorff-Nielsen and Shephard (2006) construct a non parametric test for the existence of jumps. Lee and Mykland (2007) on the other hand propose tests to detect the exact timing of jumps at the intra-day level while Jiang and Oomen (2008) provide a "swap variance" approach to detect the presence of jumps. Instead of the more widely use "fixed time span" tests, Corradi et al. (2014) and Corradi et al. (2018) develop "long time span" jump test, building on earlier work by Aït-Sahalia (2002).

Co-jump tests which are instrumental in identifying systemic risk across multiple sectors and markets are relatively new in the literature. Co-jumps reflect market correlation and have important implication for portfolio management and risk hedging. There are tests which utilize univariate jump tests to identify co-jumps among multivariate processes

(Gilder et al. (2014)), while co-jump tests can also be directly applied to multiple price processes (see, e.g., Jacod and Todorov (2009), Bandi and Reno (2016), Bibinger and Winkelmann (2015) and Caporin et al. (2017)). Gnabo et al. (2014) propose a co-jump test based on bootstrapping methods, Bandi and Reno (2016) develop a nonparametric infinitesimal moments method to detect co-jumps between asset returns and volatilities and Caporin et al. (2017) build a co-jump test based on the comparison between smoothed realized variance and smoothed random realized variation.

As an illustration of the aforementioned testing methodologies and estimation procedures, an empirical analysis is carried out using high frequency intra-day stock prices of six DOW 30 companies and ETFs which include The Boeing Company (BA), Exxon Mobile Corporation (XOM), Johnson & Johnson (JNJ), JPMorgan Chase & Co. (JPM), Microsoft Corporation (MSFT) and Walmart Inc. (WMT) and two SPDR sector ETFs XLE & XLK. We use three jump tests; ASJ test (Aït-Sahalia et al. (2009)), BNS test Barndorff-Nielsen and Shephard (2006) and LM test (Lee and Mykland (2007)). In terms of co-jump tests we use, JT test (Jacod and Todorov (2009)), BLT test (Bollerslev et al. (2008)) and GST coexceedance rule (Gilder et al. (2014)). For estimation of integrated volatility we make use of *Realized Volatility* (Andersen et al. (2001)), *Bipower Variation* and *Tripower Variation* (Barndorff-Nielsen and Shephard (2004)), *Truncated Realized Volatility* (Aït-Sahalia et al. (2009)), *MedRV* and *MinRV* (Andersen et al. (2012)). In our findings, we report the volatility movement of the different stocks and ETFs, percentage of days identified as having jumps and co-jumps, kernel density plots of the different jump and co-jump test statistics as well the proportion of jump variation to the total variation in the asset prices.

The important empirical findings can be summarized as follows. Over the entire sample period JPMorgan has the highest and Johnson & Johnson has the lowest mean estimated integrated volatility. Amongst all the volatility measures, *Bipower Variation* reports the

lowest mean volatility estimate while *Realized Volatility* reports the highest mean volatility estimate for any given stock or ETF. This can be explained by the fact that in the presence of frequent jumps, *Realized Volatility* overestimates integrated volatility. All individual stocks achieve their highest volatility in the fourth quarter of 2008 during the financial crisis. XLK sector ETF has the largest percentage of jump days (38%) and ratio of jump to total variation (45%) among all other ETFs and individual stocks. BNS jump test detected more jumps and reported a lager percentage of jump days when compared with the other two jump tests. When the sampling frequency is reduced from 1-minute to 5-minute, the ASJ jump test reports lesser number of jumps as well as smaller proportion of jump to total variation in the sample data. We detect co-jumps between Exxon & JPMorgan, Exxon & Microsoft, Exxon & XLE, JPMorgan & Microsoft, Microsoft & XLK and XLE & XLK through JT co-jump test and the GST co-exceedance rule. The results show that the percentage of co-jump days range from 0.4%-2.5% for JT co-jump test and from 2.8%-9.5% for the GST co-exceedance rule. The higher percentage of co-jump days in case of the co-exceedance rule, which uses the results at the intersection of BNS and LM jump tests, could be because the test has a large false rejection rate. We use BLT co-jump test to detect co-jumps among six stocks including Boeing, Exxon, Johnson&Johnson, JPMorgan, Microsoft and Walmart. The percentage of co-jumps days is 0.2% during financial crisis period and 0.1% after financial crisis period.

The rest of the paper is organized as follows. Section 4.2 gives the theoretical background and setup. Sections 4.3, 4.4 and 4.5 give detailed descriptions of the different integrated volatility measures, jump tests and co-jump tests respectively. Section 4.6 discusses the empirical methodology and reports the findings. Finally Section 4.7 concludes.

4.2 Setup

We represent the log-price of a financial asset at continuous time t, as Y_t. It is assumed that the log-price is a Brownian semimartingale process with jumps and it can be denoted as[1]:

$$Y_t = Y_0 + \int_0^t \mu_s ds + \int_0^t \sigma_s dW_s + J_t \tag{4.1}$$

In (4.1) μ_s the drift term is a predictable process, σ_s the diffusion term is a cádlág process, W_s is a standard Brownian motion and J_t is a pure jump process. J_t can be defined as the sum of all discontinuous log price movements up to time t,

$$J_t = \sum_{s \leq t} \Delta Y_s \tag{4.2}$$

When this jump component is a finite activity jump process, i.e. a compound poisson process (CPP), then

$$J_t = \sum_{j=1}^{N_t} \xi_j \tag{4.3}$$

where N_t is a poisson process with intensity λ, the jumps occur at the corresponding times given as $(\tau_j)_{j=1,..,N_t}$ and ξ_j refers to $i.i.d$ random variables measuring the size of jumps at time τ_j. The finite activity jump assumption has been widely used in financial econometrics literature. Log-price Y_t can be decomposed into a continuous Brownian component Y_t^c and a discontinuous component Y_t^d (due to jumps). The "true variance" of process Y_t can be given as,

$$QV_t = [Y,Y]_t = [Y,Y]_t^c + [Y,Y]_t^d \tag{4.4}$$

where QV stands for quadratic variation. The variation due to the continuous component is

$$[Y,Y]_t^c = \int_0^t \sigma_s^2 ds, \tag{4.5}$$

[1]We follow the setup and notation as in Corradi et al. (2011) and Mukherjee and Swanson (2018)

and the variation due to the discontinuous jump component is

$$[Y,Y]_t^d = \sum_{j=1}^{N_t} \xi_j^2 \tag{4.6}$$

Integrated volatility which is the continuous part of QV is denoted as

$$IV_t = \int_{t-1}^{t} \sigma_s^2 ds, \quad t = 1, ..., T \tag{4.7}$$

where IV is the (daily) integrated volatility at day t. Since IV is unobservable, different realized measures of integrated volatility are used as its substitute. The presence of market frictions in high frequency financial data has been documented in recent literature. To take care of this, the observed log price process X can then be given as

$$X = Y + \epsilon \tag{4.8}$$

where Y is the latent log price and ϵ captures market microstructure noise. We consider M equi-spaced intradaily observations for each of T days for process X which leads to a total of MT observations, i.e.

$$X_{t+j/M} = Y_{t+j/M} + \epsilon_{t+j/M}, \qquad t = 0, .., T \ \ \& \ \ j = 1, .., M \tag{4.9}$$

where ϵ follows a zero mean independent process. The intradaily return or increment of process X follows,

$$\Delta_j X = X_{t+(j+1)/M} - X_{t+j/M} \tag{4.10}$$

The noise containing realized measure, RM of the integrated volatility is computed using process X given in (4.9) and can be expressed as the sum of IV and measurement error N, i.e.

$$RM_{t,M} = IV_t + N_{t,M} \tag{4.11}$$

RM can be used to estimate IV if k^{th} moment of the measurement error decays to zero at a fast enough rate or there exists a sequence b_M with $b_M \to \infty$ such that $E(|N_{t,M}|^k) = O(b_M^{-K/2})$, for some k $\geq$2.

4.3 Realized Measures of Integrated Volatility

Volatility measures variation in the asset prices and thus can be regarded as an indicator of risk. Accurate volatility estimation is very important in both asset allocation and risk management. Since volatility is inherently unobservable, the first two types of parametric models developed to estimate the latent volatility were continuous time (e.g. stochastic volatility) and discrete time models (e.g. ARCH-GARCH models). However, these parametric models have been proven to be misspecified in capturing volatilities implied by option pricing and other financial return variables. With the availability of high frequency data, a series of nonparametric models have been proposed to examine integrated volatility at intra-day level. Andersen et al. (2001) first introduce a nonparametric volatility measure, termed *Realized Volatility* by summing over intra-day squared returns. The authors showed that *Realized Volatility* is an error free estimator of integrated volatility in the absence of noise and jumps. When the sampling frequency of the data is relatively high, microstructure noise creates a bias in the volatility estimation procedure. Zhang et al. (2005), Zhang et al. (2006) and Kalnina and Linton (2008) solve this problem with microstructure noise robust estimators based on sub-sampling with multiple time scales. Barndorff-Nielsen et al. (2008) and Barndorff-Nielsen et al. (2011) on the other hand, use kernel based estimators to account for the microstructure noise in finely sampled data. When estimating integrated volatility in the presence of jumps within the underlying price process, jump components should be separated from the quadratic variation. Barndorff-Nielsen et al. (2003), Barndorff-Nielsen and Shephard (2004) provide asymptotically unbiased integrated volatility estimators, the bipower and tripower variations, which are robust to the presence of jumps. Aït-Sahalia et al. (2009) propose a threshold method to identify and truncate jumps and further develop a consistent non-parametric jump robust estimator of the integrated volatility. Corsi et al. (2010) introduce threshold bipower variation by

combining the concepts from Barndorff-Nielsen et al. (2003) and Mancini (2009). Jacod et al. (2014) estimate local volatility by using the empirical characteristic function of the return and then remove bias due to jump variation. When combining both jumps and microstructure noise in the price process, Fan and Wang (2007) propose a wavelet-based multi-scale approach to estimate integrated volatility. Podolskij et al. (2009) design modulated bipower variation, an estimator that filters the impact of microstructure noise then use bipower variation for volatility estimation. Andersen et al. (2012) use the concept of "nearest neighbor truncation" to establish jump and noise robust volatility estimators. On the other hand Brownlees et al. (2016) create truncated two scaled realized volatility by adopting a jump signaling indicator as in Mancini (2009) and noise robust sub-sampling as in Zhang et al. (2005). In addition to the above mentioned work, discussion regarding nonparametric estimation of integrated volatility and functionals of volatility can also be found in Barndorff-Nielsen et al. (2006), Mykland and Zhang (2009), Todorov and Tauchen (2012), Hautsch and Podolskij (2013), Jacod et al. (2013), Jing et al. (2014) and Jacod et al. (2017). What follows in the next section, is a detailed review of *12* of the most commonly used integrated volatility measures.[2]

4.3.1 Realized Volatility (RV)

Realized Volatility or RV as developed in Andersen et al. (2001) is one of the first empirical measures that used high-frequency intra-day returns to compute daily return variablility without having to explicitly model the intra-day data. The authors show that under suitable conditions RV is an unbiased and highly efficient estimator of QV as in (4.4). By extension it can be shown that in the absence of jumps or when jumps populate the data infrequently, RV converges in probability to IV as $M \longrightarrow \infty$. It should also be noted that

[2]We follow the notation and description as in Mukherjee and Swanson (2018)

RV has been used widely as part of the HAR-RV forecasting models. Here

$$RV_{t,M} = \sum_{j=1}^{M-1} (X_{t+(j+1)/M} - X_{t+j/M})^2 \tag{4.12}$$

4.3.2 Realized Bipower Variation (BPV)

In Barndorff-Nielsen and Shephard (2004), the authors demonstrate that they could untangle the continuous component of quadratic variation from its discontinuous component (jumps). This led them to develop *Realized Bipower Variation* (BPV), one of the first asymptotically unbiased estimators of IV which was robust to the presence of price jumps. It takes the following form

$$BPV_{t,M} = (\mu_1)^{-2} \sum_{j=2}^{M-1} |\Delta_j X||\Delta_{j-1} X| \tag{4.13}$$

where $\Delta_j X$ is the same as in (4.10) and $\mu_1 = 2^{\frac{1}{2}} \frac{\Gamma(1)}{\Gamma(\frac{1}{2})}$.

4.3.3 Tripower Variation (TPV)

The *Realized Bipower Variation* does not allow the consistency of the IV estimate to be impacted by finite activity jumps. However it is subject to finite sample jump distortions or upward bias. To counter this problem, BPV is generalized to *Tripower Variation* in Barndorff-Nielsen and Shephard (2004), by utilizing products of the (lower order) power of three adjacent intra-day returns. Theoretically speaking, although *Tripower Variation* (TPV) is more efficient, it is also more vulnerable to microstructure noise of the high frequency return data compared to BPV. TPV can be given as

$$TPV_{t,M} = (\mu_{\frac{2}{3}})^{-3} \sum_{j=3}^{M-1} |\Delta_j X|^{2/3} |\Delta_{j-1} X|^{2/3} |\Delta_{j-2} X|^{2/3} \tag{4.14}$$

where $\Delta_j X$ is the same as in (4.10) and $\mu_{\frac{2}{3}} = 2^{\frac{1}{3}} \frac{\Gamma(\frac{5}{6})}{\Gamma(\frac{1}{2})}$.

4.3.4 Two Scale Realized Volatility (TSRV)

It is found that when the sampling interval of the asset prices is small, microstructure noise issues become more prominent and *Realized Volatility* ceases to function as a robust volatility estimator. Due to the bias introduced by the market microstructure noise in the finely sampled data, initially longer time horizons are preferred by econometricians. It is found that ignoring microstructure noise works well for intervals more 10 minutes. However sampling over lower frequencies does not quantify and correct the noise effect on volatility estimation. As a solution, *Two Scale Realized Volatility* ($TSRV$) is introduced in Zhang et al. (2005) by combining estimators obtained over two time scales, avg and M. It forms an unbiased and consistent, microstructure noise robust estimator of IV in the absence of jumps. It takes the following form

$$TSRV_{t,M} = [X,X]^{avg} - \frac{1}{K}[X,X]^{M} \tag{4.15}$$

where

$$[X,X]^{m_i} = \sum_{j=1}^{m_i-1} (X_{t+((j+1)K+i)/M} - X_{t+(jK+i)/M})^2, \;\; i = 1,..,K \;\; \& \;\; m_i = \frac{M}{K} \tag{4.16}$$

$$[X,X]^{avg} = \frac{1}{K}\Sigma_{i=1}^{K}[X,X]^{m_i} \tag{4.17}$$

$$[X,X]^{M} = \sum_{j=1}^{M-1} (X_{t+(j+1)/M} - X_{t+j/M})^2 \tag{4.18}$$

$K = cM^{2/3}$ is the number of subsamples, $\frac{M}{K}$ is subsmaple size, $c > 0$ is a constant and M is the number of equispaced intra daily observations.

4.3.5 Multi Scale Realized Volatility (MSRV)

The $TSRV$ estimator though has many desirable properties, is not efficient. The rate of convergence for $TSRV$ is not satisfactory, it converges to the true volatility (IV in the

absence of jumps) only at the rate of $M^{-1/6}$. The *Multi Scale Realized Volatility* ($MSRV$) is proposed in Zhang et al. (2006). This is a microstructure noise robust measure which converged to IV (in the absence of jumps) at the rate of $M^{-1/4}$. While $TSRV$ uses two time scales, $MSRV$ on the other hand uses N different time scales. $MSRV$ takes the following form

$$MSRV_{t,M} = \sum_{n=1}^{N} a_n [X,X]^{(M,K_n)}, \;\; n = 1,..,N \tag{4.19}$$

where

$$a_n = 12\frac{n}{N^2}\frac{n/N - 1/2 - 1/(2N)}{1 - 1/N^2}, \;\; \sum_{n=1}^{N} a_n = 1 \;\; \& \;\; \sum_{n=1}^{N} a_n/n = 0 \tag{4.20}$$

$$[X,X]^{(M,K_n)} = \frac{1}{K_n}\sum_{l=1}^{K_n}\sum_{j=1}^{m_{n,l}-1}(X_{t+((j+1)K_n+l)/M} - X_{t+(jK_n+l)/M})^2 \tag{4.21}$$

Here $l = 1,..,K_n$ & $m_{n,l} = \frac{M}{K_n}$. We take $N = 3, K_1 = 1, K_2 = 2, K_3 = 3$.

4.3.6 Realized Kernel (RK)

Barndorff-Nielsen et al. (2008) introduce Realized Kernel (RK) which as the name suggests is a realized kernel type consistent measure of IV in the absence of jumps. It is robust to endogenous microstructure noise and for particular choices of weight functions it can be asymptotically equivalent to $TSRV$ and $MSRV$ estimators, or even more efficient. RK can be given as

$$RK_{t,M} = \gamma_0(X) + \sum_{h=1}^{H}\kappa(\frac{h-1}{H})\{\gamma_h(X) + \gamma_{-h}(X)\} \tag{4.22}$$

where

$$\gamma_h(X) = \sum_{j=1}^{M-1}(X_{t+(j+1)/M} - X_{t+j/M})(X_{t+(j+1-h)/M} - X_{t+(j-h)/M}) \tag{4.23}$$

Here c is a constant. For our analysis we take a Turkey-Hanning$_2$ kernel which gives $\kappa(x) = sin^2\{\pi/2(1-x)^2\}$ and $H = cM^{1/2}$.

4.3.7 Truncated Realized Volatility (TRV)

Truncated Realized Volatility (TRV) is one of the first volatility measures that tried to estimate IV by identifying when price jumps greater than an adequately defined threshold occurred as in Aït-Sahalia et al. (2009). The truncation level for the jumps are chosen in a data-driven manner; the cutoff level α (given below) is set equal to a particular number times estimated standard deviations of the continuous part of the semimartingale. The price jump robust measure can be given as

$$TRV_{t,M} = \sum_{j=1}^{M-1} |\Delta_j X|^2 1_{\{|\Delta_j X| \leq \alpha \Delta_M^{\varpi}\}} \tag{4.24}$$

where

$$\alpha = 5\sqrt{\sum_{j=1}^{M-1} |\Delta_j X|^2 1_{\{|\Delta_j X| \leq \Delta_M^{1/2}\}}} \tag{4.25}$$

Here $\varpi = 0.47$. $\Delta_M = 1/M$

4.3.8 Modulated Bipower Variation (MBV)

Modulated Bipower Variation (MBV) as in Podolskij et al. (2009) consistently estimates IV and is robust to both market microstructure noise and finite activity jumps. It takes the following form

$$MBV_{t,M} = \frac{(c_1 c_2/\mu_1^2) mbv_{t,M} - \vartheta_2 \hat{\omega}^2}{\vartheta_1} \tag{4.26}$$

where

$$\vartheta_1 = \frac{c_1(3c_2 - 4 + max((2-c_2)^3, 0))}{3(c_2-1)^2}, \;\; \vartheta_2 = \frac{2min((c_2-1), 1)}{c_1(c_2-1)^2} \tag{4.27}$$

$$mbv_{t,M} = \Sigma_{b=1}^{B} |\bar{X}_b^{(R)}||\bar{X}_{b+1}^{(R)}| \tag{4.28}$$

$$\bar{X}_b^{(R)} = \frac{1}{M/B - R + 1} \Sigma_{j=(b-1)M/B}^{bM/B-R} (X_{t+(j+R)/M} - X_{t+j/M}) \tag{4.29}$$

Here $c_1 = 2$, $c_2 = 2.3$, $R \approx c_1 M^{0.5}$, $B = 6$, $\mu_1 = 0.7979$, $\hat{\omega}^2 = \frac{1}{2M} RV_{t,M}$, $RV_{t,M}$ is given by (4.12).

4.3.9 Threshold Bipower Variation (TBPV)

Corsi et al. (2010) introduce a jump robust measure, *Threshold Bipwer Variation* ($TBPV$) which is constructed by combining the concepts of *Realized Bipower Variation* and *Threshold Realized Variance* (Mancini (2009). The authors show that $TBPV$ is robust to the choice of threshold function (υ as given below).

$$TBPV_{t,M} = \mu_1^{-2} \sum_{j=2}^{M-1} |\Delta_{j-1}X||\Delta_j X| I_{\{|\Delta_{j-1}X|^2 \leq \upsilon_{j-1}\}} I_{\{|\Delta_j X|^2 \leq \upsilon_j\}} \tag{4.30}$$

where

$$\upsilon_j = c_\upsilon^2 \hat{V}_j \tag{4.31}$$

$$\hat{V}_j^z = \frac{\Sigma_{i=-L}^{L} \kappa(\frac{i}{L})(\Delta_{j+i}X)^2 I_{\{(\Delta_{j+i}X)^2 \leq c_\upsilon^2 \hat{V}_{j+i}^{z-1}\}}}{\Sigma_{i=-L}^{L} \kappa(\frac{i}{L}) I_{\{(\Delta_{j+i}X)^2 \leq c_\upsilon^2 \hat{V}_{j+i}^{z-1}\}}}. \tag{4.32}$$

and $\Delta_j X$ is given by (4.10). Here we take $L = 25, c_\upsilon = 3, \hat{V}^0 = +\infty$. υ_j is the threshold for removal of large returns at each j. $\hat{V}_j^z$ gives estimated local variance in the presence of jumps at each iteration z for any j. Large returns are removed at each iteration according to $\{(\Delta_j X)^2 \leq c_\upsilon^2 \hat{V}_j^{z-1}\}$ and the estimated variance at that iteration is multiplied by c_υ^2 to get the threshold for the next iteration. When large returns cannot be removed any more, the iterations stop. Typically z is taken to be 2.

4.3.10 Subsampled Realized Kernel (SRK)

Barndorff-Nielsen et al. (2011) constructed *Subsampled Realized Kernel* (SRK) by combining the concepts of subsmapling (Zhang et al. (2005)) and realized kernels (Barndorff-Nielsen et al. (2008)). The main benefit of subsampling in this context is that it can overpower the inefficiency that stems from the poor selection of kernel weights that might be the case in *Realized Kernel*. SRK takes the following form

$$SRK_{t,M} = \frac{1}{S} \sum_{s=1}^{S} K^s(X) \tag{4.33}$$

where

$$K^s(X) = \gamma_0^s(X) + \sum_{h=1}^{H} \kappa(\frac{h-1}{H})\{\gamma_h^s(X) + \gamma_{-h}^s(X)\} \tag{4.34}$$

$$\gamma_h^s(X) = \sum_{j=1}^{\frac{M}{S}} x_j^s x_{j-h}^s \tag{4.35}$$

$$x_j^s = X_{t+(j+\frac{s-1}{S})/M} - X_{t+(j+\frac{s-1}{S}-1)/M} \tag{4.36}$$

Here the smooth Turkey-Hanning$_2$ kernel function gives $\kappa(x) = sin^2\{\pi/2(1-x)^2\}$, $S = 13$ and $H = 3$.

4.3.11 MedRV & MinRV

As alternatives to *Realized Bipower Variation* and *Tripower Variation*, Andersen et al. (2012) provide two alternative measures $MedRV$ and $MinRV$ which are robust to jumps and/or microstructure noise by using "nearest neighbor truncation". The basic concept behind these new measures is that the neighboring returns control the level of truncation of absolute returns. On one hand where $MinRV$ compares and takes the minimum of two adjacent absolute returns, $MedRV$ takes the median of three adjacent absolute returns and carries out two-sided truncation. Unlike the typical truncated realized measures as in Corsi et al. (2010), these new measures do not have to deal with the selection of an ex-ante threshold.

$$MinRV_{t,M} = \frac{\pi}{\pi - 2}(\frac{M}{M-1}) \sum_{j=1}^{M-1} min(|\Delta_j X|, |\Delta_{j+1} X|)^2 \tag{4.37}$$

$$MedRV_{t,M} = \frac{\pi}{6 - 4\sqrt{3} + \pi}(\frac{M}{M-2}) \sum_{j=2}^{M-1} med(|\Delta_{j-1} X|, |\Delta_j X|, |\Delta_{j+1} X|)^2 \tag{4.38}$$

where $\Delta_j X$ is given by (4.10).

4.4 Jump Testing

Jump diffusion has been increasingly important in characterizing dynamic movement of asset prices. Early studies about jump diffusions can be seen in Andersen et al. (2002), Chernov et al. (2003), Pan (2002), and Eraker et al. (2003). Differentiating jumps from continuous process is particularly useful because it has implications for both researchers and practitioners in financial econometrics. Thus, a strand of literature has addressed the methodologies to identify jumps in the discretely sampled financial data. Aït-Sahalia (2002) rely on the transition density to test the existence of jumps under the option pricing model. Focusing on the risk-neutral dynamics of the underlying option prices, Carr and Wu (2003) propose a method to use the convergence rates of option prices to distinguish jumps from continuous process. Johannes (2004) propose a jump test to identify jump-induced misspecification. However, these tests only use limited low frequency data. With availability of high frequency data, the mechanism behind jump testing methodology has evolved. Barndorff-Nielsen and Shephard (2006) use the ratio of bipower variation and realized quadratic variation to construct a nonparametric test for the existence of jumps. Huang and Tauchen (2005) design extensive Monte Carlo experiments to evaluate the properties of newly proposed jump tests (see Andersen et al. (2003a), Barndorff-Nielsen and Shephard (2004), and Barndorff-Nielsen and Shephard (2006)). Lee and Mykland (2007) propose tests to detect the exact timing of jumps at the intra-day level while Jiang and Oomen (2008) provide a "swap variance" approach to detect the presence of jumps. Mancini (2009) and Corsi et al. (2010) devise unique threshold or truncation techniques in their testing methodology. Aït-Sahalia et al. (2009) compare two higher order realized power variations to develop a test statistic for the null hypothesis of no jumps. On the other hand Podolskij and Ziggel (2010) combine the concepts truncated power variation and wild boostrap to propose a threshold-based jump test. In most of the above mentioned

papers, the presence of realized jumps is tested over a "fixed time span". Corradi et al. (2014) and Corradi et al. (2018) proposed a "long time span" jump test instead, building on earlier work by Aït-Sahalia (2002). More related work on jump tests, self-excitation and mutual excitation in realized jumps can be found in Lee et al. (2013), Dungey et al. (2016), and Boswijk et al. (2018). In the next section we discuss six different jump tests which arise from different branches of the jump testing literature.

4.4.1 Barndorff-Nielsen and Shephard Test (BNS)

To test for the existence of jumps in the sample path of asset prices, Barndorff-Nielsen and Shephard (2006) propose non-parametric Hausman (1978) type tests using the difference between *Realized Quadratic Variation*, an estimator of integrated volatility which is not robust to jumps, and *Realized Bipower Variation*, which is a jump robust estimator of integrated volatility. *Realized Quadratic Variation* is considered to be the same as *Realized Volatility* (RV). The adjusted jump ratio test statistic can be given as:

$$BNS = \frac{M^{1/2}}{\sqrt{\vartheta max(1, \frac{QPV}{(\mu_1^2 BPV)^2})}}(1 - \frac{BPV}{RV}) \xrightarrow{d} N(0,1) \tag{4.39}$$

where BPV is the same as in (4.13), RV is the same as in (4.12), ϑ =$((\pi^2/4) + \pi$ - 5) $\approx$ 0.6090. The realized quadpower variation QPV is used to estimate integrated quarticity ($\int_0^t \sigma_s^4 ds$) and can be given as:

$$QPV = M \sum_{j=4}^{M} |\Delta_j X||\Delta_{j-1} X||\Delta_{j-2} X||\Delta_{j-3} X| \xrightarrow{d} \mu_1^4 \int_0^t \sigma_s^4 ds \tag{4.40}$$

The authors show that the null hypothesis of no jumps is rejected if the test statistic BNS is significantly positive.

4.4.2 Lee and Mykland Test (LM)

Lee and Mykland (2007) use the ratio of realized return to estimated instantaneous volatility, and further construct a nonparametric jump test to detect the exact timing of jumps at the intra-day level. The test statistic which identifies whether there is a jump during $(t + j/M, t + (j + 1)/M]$ can be given as:

$$L_{(t+(j+1)/M)} = \frac{X_{t+(j+1)/M} - X_{t+j/M}}{\widehat{\sigma_{t+(j+1)/M}}} \tag{4.41}$$

where

$$\widehat{\sigma_{t+(j+1)/M}}^2 \equiv \frac{1}{K-2} \sum_{i=j-K+1}^{j-2} |X_{t+(i+1)/M} - X_{t+i/M} \,||\, X_{t+i/M} - X_{t+(i-1)/M}| \tag{4.42}$$

Here K is the window size of a local movement of the process. It is chosen in a way such that the effect of jumps on volatility estimation is eliminated. The authors suggest a value of K = 10 when the sampling frequency is 5-minute. Thus, it can be asymptotically shown that

$$\frac{max_{j\in\bar{A}_M}|L_{(t+(j+1)/M)}| - C_M}{S_M} \to \varepsilon, \quad as \;\; \Delta t \to 0, \tag{4.43}$$

where ε has a cumulative distribution function $P(\varepsilon \leq x) = exp(-e^{-x})$,

$$C_M = \frac{(2logM)^{1/2}}{c} - \frac{log\pi + log(logM)}{2c(2logM)^{1/2}} \quad and \quad s_M = \frac{1}{c(2logM)^{1/2}} \tag{4.44}$$

M is the number of intradaily observations, c ≈ 0.7979 and $\bar{A}_M$ is the set of $j \in \{0, 1, ..., M\}$ so that there are no jumps in $(t + j/M, t + (j + 1)/M]$.

4.4.3 Jiang and Oomen Test (JO)

Jiang and Oomen (2008) compare a jump sensitive variance measure to realized volatility in order to test for jumps. Their idea is based on the fact that in the absence of jumps the

accumulated difference between the simple return and log return (called the swap variance) captures one-half of the integrated volatility in the continuous time limit. Consequently it can be stated, in the absence of jumps the difference between swap variance and realized volatility should be zero, while in the presence of jumps the same difference reflects the replication error of variance swap thus detecting jumps. The swap variance can be given as

$$SV_{t,M} = 2\sum_{j=1}^{M-1}(\Delta_j P - \Delta_j X) \tag{4.45}$$

where $Y = log(P)$ and Y is the same as in (4.1). $\Delta_j P = \frac{P_{t+(j+1)/M}}{P_{t+j/M}} - 1$ and $\Delta_j X$ is the same as in (4.10). The three different swap variance tests proposed by the authors can be given as

(i) The difference test:

$$\frac{M}{\Omega_{SV}}(SV_{t,M} - RV_{t,M}) \xrightarrow{d} N(0,1) \tag{4.46}$$

(ii) The logarithmic test:

$$\frac{BPV_{t,M}M}{\Omega_{SV}}(log(SV_{t,M}) - log(RV_{t,M})) \xrightarrow{d} N(0,1) \tag{4.47}$$

(iii) The ratio test:

$$\frac{BPV_{t,M}M}{\Omega_{SV}}(1 - \frac{RV_{t,M}}{SV_{t,M}}) \xrightarrow{d} N(0,1) \tag{4.48}$$

where $\Omega_{SV} = \frac{\mu_6}{9}\frac{M^3\mu_{6/p}^{-p}}{M-p+1}\sum_{j=1}^{M-p}\prod_{k=0}^{p}|\Delta_{j+k}X|^{6/p}$ for $p \in \{1,2,...\}$, $\mu_z = E(|x|^z)$ for $z \sim N(0,1)$.

4.4.4 Aït-Sahalia and Jacod Test (ASJ)

In Aït-Sahalia et al. (2009), the authors develop a testing methodology for jumps in the (log) price process by comparing two higher order realized power variations with different sampling intervals, $k\Delta$ and Δ respectively. In this context $\Delta = \frac{1}{M}$, M is the number of

intra-daily observations and k is a given integer. The pth order realized power variation can be given as

$$\widehat{B}(p,\Delta) = \sum_{j=1}^{M-1} |X_{t+(j+1)/M} - X_{t+j/M}|^p \tag{4.49}$$

The ratio of the two realized power variations with different sampling intervals takes the following form

$$\widehat{S}(p,k,\Delta) = \frac{\widehat{B}(p,k\Delta)}{\widehat{B}(p,\Delta)} \tag{4.50}$$

The corresponding jump test statistic can then be defined as,

$$ASJ = \frac{k^{(p/2)-1} - \widehat{S}(p,k,\Delta)}{\sqrt{V_{t,M}}} \xrightarrow{d} N(0,1) \tag{4.51}$$

where $V_{t,M}$ can be estimated using either a truncation technique as in

$$\widehat{V}_{t,M} = \Delta \frac{\widehat{A}(2p,\Delta)M(p,k)}{\widehat{A}(p,\Delta)^2} \tag{4.52}$$

where

$$\widehat{A}(2p,\Delta) = \frac{\Delta^{1-p/2}}{\mu_p} \sum_{j=1}^{M-1} |X_{t+(j+1)/M} - X_{t+j/M}|^p 1_{\{|X_{t+(j+1)/M} - X_{t+j/M}| \leq \alpha\Delta^{\varpi}\}} \tag{4.53}$$

or using multipower variation as in

$$\widehat{V}_{t,M} = \Delta \frac{M(p,k)\bar{A}(p/([p]+1), 2[p]+2, \Delta)}{\bar{A}(p/([p]+1), [p]+1, \Delta)^2} \tag{4.54}$$

where

$$\bar{A}(r,q,\Delta) = \frac{\Delta^{1-qr/2}}{\mu_r^q} \sum_{j=q}^{M-q+1} \prod_{i=0}^{q-1} |X_{t+(j+i)/M} - X_{t+(j+i-1)/M}|^r, \tag{4.55}$$

$$M(p,k) = \frac{1}{\mu_p^2}(k^{p-2}(1+k)\mu_{2p} + k^{p-2}(k-1)\mu_p^2 - 2k^{p/2-1} - \mu_{k,p}) \tag{4.56}$$

and $\mu_r = E(|U|^r)$ and $\mu_{k,p} = E(|U|^p|U + \sqrt(k-1)V|^p|)$ for $U, V \sim N(0,1)$. The null hypothesis of no jumps is rejected when the test statistic ASJ is significantly positive.

4.4.5 Podolskij and Ziggel Test (PZ)

In Podolskij and Ziggel (2010) the concept of truncated power variation is used to construct test statistics which diverge to infinity if jumps are present and have a normal distribution otherwise. The jump testing procedure in this paper is valid (under weak assumptions) for all semi-martingales with absolute continuous characteristics and general models for the noise processes. The methodology followed by the authors is a modification of that proposed in Mancini (2009). In particular they consider,

$$T(X,p) = M^{\frac{p-1}{2}} \sum_{j=1}^{M-1} |X_{t+(j+1)/M} - X_{t+j/M}|^p (1 - \eta_i 1_{\{|X_{t+(j+1)/M} - X_{t+j/M}| \leq \alpha \Delta^{\varpi}\}}) \quad (4.57)$$

where $\{\eta_i\}_{i\in[1,1/\Delta]}$ is a sequence of positive $i.i.d$ random variables. The test statistic has the following form

$$PZ = \frac{T(X,p)}{Var^*(\eta)\widehat{A}(2p,\Delta)} \xrightarrow{d} N(0,1) \quad (4.58)$$

where $\widehat{A}(2p,\Delta)$ is the same as in (4.53).

4.4.6 Corradi, Silvapulle and Swanson Test (CSS)

Building on previous work by Aït-Sahalia (2002), Corradi et al. (2018) design "long time span" jump tests based on realized third moments or "tricity" for the the null hypothesis that the probability of a jump is zero. This jump testing methodology is used to detect jumps by examining the "jump intensity" parameter in the data generating process rather than realized jumps over a "fixed time span". This test is of immense value when one is interested in using jump diffusion processes for valuation problems like options pricing and

default modeling. Let,

$$\widehat{\mu}_{3,T,\Delta} = \frac{1}{T}\sum_{j=1}^{n-1}(X_{t+(j+1)/M} - X_{t+j/M} - \frac{X_{t+n/M} - X_{t+1/M}}{n})^3 \\ - \frac{1}{T^+}\sum_{j=1}^{n^+-1}(X_{t+(j+1)/M} - X_{t+j/M} - \frac{X_{t+n^+/M} - X_{t+1/M}}{n^+})^3 1\{|X_{t+(j+1)/M} - X_{t+j/M}| \leq \tau(\Delta)\} \tag{4.59}$$

where we have n^+ observations over an increasing time span of T^+, a shrinking discrete sampling interval $\Delta = \frac{1}{M}$, so that $n^+ = \frac{T^+}{\Delta}$, $T^+ \to \infty$ and $\Delta \to 0$. $\tau(\Delta)$ is the truncation parameter and one example for the choice of such truncation can be given as follows. If σ_s as in (4.1) is a square root process, so that all moments exist, we can set $\tau(\Delta) = c\Delta^\eta$ with $\frac{2}{7} < \eta < \frac{1}{2}$. The authors define $n = \frac{T}{\Delta} = n^+ - \frac{T^+ - T}{\Delta}$, with $T^+ > T$ and $\frac{T^+}{T} \to \infty$. Then, the test statistic for the null hypothesis of no jumps can be given as

$$CSS = \frac{T^{1/2}}{\Delta}\widehat{\mu}_{3,T,\Delta} \xrightarrow{d} N(0, \omega_0) \tag{4.60}$$

where ω_0 is defined in Corradi et al. (2018). Since, under the alternative hypothesis of positive jump intensity, the variance of the statistic is of larger order, it is difficult to construct a variance estimator which is consistent under all hypotheses. The authors use a threshold variance estimator, which removes the contribution of the jump component thus developing an estimator for the variance of CSS which is consistent under the null hypothesis of no jumps. Thus we have

$$\widehat{\sigma}^2_{CSS} = \frac{1}{\Delta^2}\sum_{j=0}^{n-1}(X_{t+(j+1)/M} - X_{t+j/M} - \frac{X_{t+n/M} - X_{t+1/M}}{n})^3 1\{|X_{t+(j+1)/M} - X_{t+j/M}| \leq \tau(\Delta)\} \tag{4.61}$$

Thus the t-statistic version of the jump test is

$$t_{CSS} = \frac{CSS}{\widehat{\sigma}_{CSS}} \tag{4.62}$$

4.5 Co-jump Testing

While univariate jump tests have been researched extensively, the study of co-jump tests has started growing only recently. One branch of literature proposes co-jump tests through identifying jumps in a portfolio. For example, Bollerslev et al. (2008) use observed return product to construct a test statistic for detecting co-jumps in an equiweighted index constructed from 40 stocks. Their co-jump test detects the modest-sized common jumps ignored in the Barndorff-Nielsen and Shephard (2004) jump test approach. Another branch uses univariate jump tests to identify co-jump among multivariate process. For example, Gilder et al. (2014) propose a co-exceedance rule to identify co-jumps by using univariate jump tests. Their Monte Carlo results show that the co-exceedance rule has similar power to the co-jump test proposed by Bollerslev et al. (2008). The third strand develops co-jump tests which can be directly applied to multiple price processes (see, e.g., Jacod and Todorov (2009), Bandi and Reno (2016), Bibinger and Winkelmann (2015) and Caporin et al. (2017)). Jacod and Todorov (2009) propose co-jump tests based on two null hypotheses: (i) there are common jumps in a bivariate process; (ii) there are disjoint jumps in a bivariate process. Mancini and Gobbi (2012) construct threshold estimators for integrated covariation from the realized covariation and show that the central limit theorem and robustness to nonsynchronous data still hold under different scenarios. Gnabo et al. (2014) propose a co-jump test based on bootstrapping methods. Bandi and Reno (2016) develop a nonparametric infinitesimal moments method to detect co-jumps between asset returns and volatilities. Bibinger and Winkelmann (2015) propose a spectral estimation method to detect co-jumps in multivariate high-frequency data in the presence of market microstructure noise and asynchronous observations. Caporin et al. (2017) build a co-jump test on the comparison between smoothed realized variance and smoothed random realized variation. More related literature about co-jumps can also be seen in Lahaye et al.

(2011) and Dungey et al. (2011). In the following section, we discuss five most widely used co-jump tests in details. [3]

4.5.1 BLT Co-jump Testing

Bollerslev et al. (2008) propose a mcp test to detect co-jumps in a large ensemble of stocks. They develop a theoretical foundation which shows how only co-jumps (not idiosyncratic jumps) can be detected in a large equiweighted index. Let n denote the total number of assets under co-jump detection. The mcp mean cross-product test statistic is defined as:

$$mcp_{t,j} = \frac{2}{n(n-1)} \sum_{i=1}^{n-1} \sum_{l=i+1}^{n} \Delta_j X^i \Delta_j X^l, j = 1, ..., M-1, t = 1, ..., T \tag{4.63}$$

where

$$\Delta_j X^i = X^i_{t+(j+1)/M} - X^i_{t+j/M}, \quad for \quad i = 1, ..., n \tag{4.64}$$

Since the mcp-statistic has nonzero mean and is analogous to a U-statistic, the studentized test statistic is:

$$z_{mcp,t,j} = \frac{mcp_{t,j} - \overline{mcp_t}}{s_{mcp,t}}, \quad for \quad j = 1, ..., M-1 \quad and \quad t = 1, ..., T. \tag{4.65}$$

where

$$\overline{mcp_t} = \frac{1}{M-1} mcp_t = \frac{1}{M-1} \sum_{j=1}^{M-1} mcp_{t,j} \tag{4.66}$$

and

$$s_{mcp,t} = \sqrt{\frac{1}{M-1} \sum_{j=1}^{M-1} (mcp_{t,j} - \overline{mcp_t})^2} \tag{4.67}$$

The null distribution under the null hypothesis of no jump is derived from bootstrapping the test statistics $z_{mcp,t,j}$ under Monte Caro simulations.

---

[3] We follow the notation and description as in Peng (2018)

4.5.2 JT Co-jump Testing

Jacod and Todorov (2009) construct two test statistics to identify co-jumps under two different null hypothesis: i. There is at least one common jump under the null hypothesis; ii. There is at least one disjoint jump under the null hypothesis. The test statistics are proposed for detecting co-jumps on bivariate processes for the path of $s \longrightarrow X_s$ on $[0, t]$. Co-jumps among multivariate processes can be detected from the combination of bivariate processes. The test statistics of the common jump $\Phi_n^{(j)}$ and disjoint jump $\Phi_n^{(d)}$ are defined as:

$$\Phi_n^{(j)} = \frac{V(f, k\Delta_n)_t}{V(f, \Delta_n)_t} \tag{4.68}$$

$$\Phi_n^{(d)} = \frac{V(f, \Delta_n)_t}{\sqrt{V(g_1, \Delta_n)_t V(g_2, \Delta_n)_t}} \tag{4.69}$$

where k is an integer greater than 1, and $\Delta_n = \frac{t}{M}$ is the length of equispaced intra-daily time interval. $V(f, k\Delta_n)_t$ is defined as:

$$V(f, k\Delta_n)_t = \sum_{j=1}^{[t/k\Delta_n]} f(X_{(j+1)k/M} - X_{jk/M}) \tag{4.70}$$

Where the functions for $f(x)$, $g_1(x)$ and $g_2(x)$ are defined as:

$$f(x) = (x_1 x_2)^2, g_1(x) = (x_1)^4, g_2(x) = (x_2)^4 \tag{4.71}$$

They propose asymptotic properties and central limit theorems of these two test statistics when the mesh Δ_n approaches 0. They show that the test statistics for the null hypothesis with disjoint jumps $\Phi_n^{(d)}$ converges stably in law to 0 on $\Omega_T^{(d)}$ and the null hypothesis with common jumps $\Phi_n^{(j)}$ converges stably in law to 1 on $\Omega_T^{(d)}$. Here $\Omega_T^{(j)}$ and $\Omega_T^{(d)}$ are defined as:

$$\Omega_T^{(j)} = \{\omega\text{: on } [0,t] \text{ the process } \Delta_j X^1 \Delta_j X^2 \text{ is not identically } 0\} \tag{4.72}$$

$$\Omega_T^{(j)} = \{\omega\text{: on } [0,t] \text{ the processes } \Delta_j X^1 \text{ and } \Delta_j X^2 \text{ are} \tag{4.73}$$
$$\text{not identically 0, but the process } \Delta_j X^1 \Delta_j X^2 \text{ is}\}$$

Where $\Delta_j X^i = X^i_{(j+1)/M} - X^i_{j/M}$, for $i = 1, 2$ and $j = 1, ..., M-1$. The authors construct critical regions of the two statistics as:

$$C_n^{(j)} = \{|\Phi_n^{(j)} - 1| \geq c_n^{(j)}\} \tag{4.74}$$

$$C_n^{(d)} = \{\Phi_n^{(d)} \geq c_n^{(d)}\} \tag{4.75}$$

4.5.3 MG Threshold Co-jump Test

Mancini and Gobbi (2012) use a threshold r_h to estimate each co-jump as:

$$\Delta_j X^1 \Delta_j X^2 - \Delta_j X^1 1_{\{(\Delta_j X^1)^2 \leq r_h\}} \Delta_j X^2 1_{\{(\Delta_j X^2)^2 \leq r_h\}}, \tag{4.76}$$

Where h is the length of observations interval and $h = \frac{t}{M}$ for every $j = 1, ..., M$. Threshold r_h is defined by a deterministic function from $h \to r_h$, with the following properties:

$$\lim_{h \to 0} r_n = 0 \quad and \quad \lim_{h \to 0} (h log \frac{1}{h}) / r_h = 0.$$

The threshold r_h depends on an unknown realized instantaneous volatility path. Monte Carlo simulations are used under different models to select a reasonable threshold. For example, in the model of stochastic volatility and finite compound Poisson jump part, the optimal choice of threshold is $r_h = 0.33\widehat{IC_{t,M}} h^{0.99}$, where the integrated covariation estimator $\widehat{IC_{t,M}}$ is derived by Mancini (2001):

$$\widehat{IC_{t,M}} = \tilde{v}_{1,1}^{(M)}(X^1, X^2)_t, \tag{4.77}$$

where

$$\tilde{v}_{1,1}^{(M)}(X^1, X^2)_t = h^{-3} \sum_{j:t_j \leq t} \Delta_j X^1 1_{\{(\Delta_j X^1)^2 \leq r_h\}} \Delta_j X^2 1_{\{(\Delta_j X^2)^2 \leq r_h\}}, \tag{4.78}$$

4.5.4 GST Co-exceedance Rule

Gilder et al. (2014) propose a co-exceedance based co-jump detection method by applying univariate jump tests to individual stocks to identify co-jumps. They select three univariate jump tests in Barndorff-Nielsen and Shephard (2006), Lee and Mykland (2007) and Andersen et al. (2010). The co-jumps are detected as intersection between ABD jump test results and BNS jump test results (ABD∩BNS), intersection between ABD jump test results and LM jump test results (ABD∩LM), intersection between BNS jump test results and LM jump test results (BNS∩LM), and the intersection among three jump tests results (ABD∩LM∩BNS).

The nonparametric BNS jump test and LM jump test have been discussed in subsection 4.4.1 and subsection 4.4.2 respectively. The ABD jump test in Andersen et al. (2010) is the sequential BNS test which first identifies jump days through BNS test and then calculates the maximum intra-day return as the jump level. Gilder et al. (2014) modified the maximum intra-day return during jump days into:

$$max\big(\mid \Delta_j X \mid / \sqrt{\widehat{s_{WSD,j}}^2 \cdot \Delta \cdot BPV_t} \big), \quad forj = 1, ..., M-1 \tag{4.79}$$

where $\Delta_j X = X_{t+(j+1)/M} - X_{t+j/M}$ for $t = 1, ..., T$ and $\Delta = \frac{1}{M}$. Here $\widehat{s_{WSD,j}}^2$ is the weighted standard deviation (WSD) estimator proposed by Boudt et al. (2011).

Comparisons between co-exceedance rule for co-jump detection and BLT co-jump test are made under extensive Monte Carlo simulations. The results show that intra-day co-exceedance based detection method has similar power to that of the BLT co-jump test both on large and small co-jumps.

4.5.5 CKR Co-jump Testing

The test statistics in Caporin et al. (2017) is derived from the difference between smoothed realized variance ($\widetilde{SRV}$) and smoothed randomized realized variance ($SRRV$). The SRRV is denoted as:

$$SRRV(X^i) = \sum_{j=1}^{M} \mid \Delta_j X^i \mid^2 \cdot K\left(\frac{\Delta_j X^i}{H^i_{\Delta_j,M}}\right) \cdot \eta^i_j, \tag{4.80}$$

$$i = 1, ..., n, \tag{4.81}$$

where $K(\cdot)$ is a differentiable kernel function with bounded first derivative almost everywhere in R having the following properties:

$$K(0) = 1, 0 \leq K(\cdot) \leq 1, \quad and \quad \lim_{x\to\infty} K(\mid x \mid) = 0 \tag{4.82}$$

And H is the bandwidth which is denoted as:

$$H^i_{\Delta_j,M} = h_M \cdot \widehat{\sigma_{\Delta_j}}^i \sqrt{\frac{t}{M}} \tag{4.83}$$

where h_M is the bandwidth parameter and $\widehat{\sigma_{\Delta_j}}^i$ is the point estimator of the local standard deviation of ith asset. η^i_j is an $n \times M$ matrix independent and identically distributed variable such that $E[\eta^i_j] = 1$ and $Var[\eta^i_j] = V_\eta \leq \infty$. V_η is set to 0.0025 in the application of the test.

Another estimator ($\widetilde{SRV}$) is written in the form as:

$$\widetilde{SRV}^n(X^i) = \sum_{j=1}^{M} \mid \Delta_j X^i \mid^2 \cdot \left(K\left(\frac{\Delta_j X^i}{H^i_{\Delta_j,M}}\right) + \pi^n_{k=1}\left(1 - K\left(\frac{\Delta_j X^k}{H^k_{\Delta_j,M}}\right)\right)\right) \tag{4.84}$$

The proposed test statistics takes the form:

$$S_{M,n} = \frac{1}{V_\eta} \sum_{i=1}^{M} \frac{\left(SRRV(X^i) - \widetilde{SRV}^n(X^i)\right)^2}{SQ(X^i)}, \tag{4.85}$$

where

$$SQ(X^i) = \sum_{j=1}^{M} \mid \Delta_j X^i \mid^4 \cdot K^2 \left(\frac{\Delta_j X^i}{H^i_{\Delta_j, M}} \right), \quad i = 1, ..., n \tag{4.86}$$

The asymptotic behavior of the $S_{n,N}$ is described as:

$$S_{M,n} \xrightarrow{d} \chi^2(n), \quad on \quad \overline{\Omega}^n_T$$
$$S_{M,n} \xrightarrow{p} +\infty, \quad on \quad \overline{\Omega}^{MJ,n}_T$$

Where $\overline{\Omega}^n_T$ and $\overline{\Omega}^{MJ,n}_T$ is defined as:

$$\overline{\Omega}^{MJ,n}_T = \left\{ \omega \in \Omega \mid \Pi^n_{i=1} (\Delta X^j)_t \text{ is not identically } 0 \right\},$$
$$\overline{\Omega}^n_T = \Omega / \overline{\Omega}^{MJ,n}_T$$

4.6 Empirical Experiments

4.6.1 Data Description

The empirical experiments are conducted with six stocks and two ETFs. The six individual stocks which include the Boeing Company (BA), Exxon Mobile Corporation (XOM), Johnson & Johnson (JNJ), JPMorgan Chase & Co. (JPM), Microsoft Corporation (MSFT) and Walmart Inc.(WMT), have the highest weight in their corresponding SPDR market sector ETFs such as XLI (industrial sector), XLE (energy sector), XLV (healthcare sector), XLF (finance sector), XLK (technology sector) and XLP (consumer staples sector). The two SPDR sector ETFs chosen are the energy and technology sector ETFs, XLE & XLK. The dataset is obtained from the Trade and Quote Database (TAQ) of Wharton Research Data Service (WRDS) and it covers the period from January 1st, 2006 to December 31st, 2013 for a total of 2013 days. We select trade data ranging from 9:30 am to 4 pm on regular trading days. Overnight transactions are excluded from our dataset. We mainly

use a 5-minute sampling frequency to eradicate the effect of market microstructure noise in the data which yields 78 total observations per day. We also use a 1-minute sampling frequency in specific cases which yields 390 observations per day. It should be noted that all empirical experiments are carried out on the logarithmic values of the stock and ETF prices.

4.6.2 Methodology

Our empirical experiment consists of three sections; (i) integrated volatility measures, (ii) jump tests and (iii) co-jump tests. For each of the different parts, we conduct analysis involving the most widely used measures and tests respectively. A detailed description of the different measures & tests used and the empirical methodologies thereof is given as follows.

Firstly we use six different measures to estimate Integrated Volatility for all the stocks and ETFs; (1) Realized Volatility (4.3.1), (2) Bipower Variation (4.3.2), (3) Tripower Variation (4.3.3), (4) Truncated Realized Volatility (4.3.7), (5) MedRV & (6) MinRV (4.3.11). Secondly to test for price jumps in the data three different jump tests are used; (1) ASJ jump test (4.4.4), (2) BNS jump test (4.4.1), (3) LM jump test (4.4.2). Lastly co-jump tests are carried out using (1) JT co-jump test (4.5.2), (2) BLT co-jump test (4.5.1) and (3) GST coexceedance rule (4.5.4).

Estimation of integrated volatility, BNS and LM jump tests as well as all the co-jump tests are carried out using 5 minute data where Δ is set to $\frac{1}{78}$. However for the ASJ jump test, both 1-minute ($\Delta = \frac{1}{390}$) and 5-minute frequencies are used as a basis for comparative study.

When conducting analysis using jump tests, we calculate the percentage of days identified as having jumps. For both the BNS and ASJ tests, it can be given as:

$$\text{Percentage of Jump Days} = \frac{100 \sum_{i=1}^{T} I(Z_i > c_\alpha)}{T}\% \tag{4.87}$$

where $I(\cdot)$ is the jump indicator function, c_α is the critical value at α significance level and Z_i is the BNS or ASJ jump test statistics. For the LM jump test on the other hand it can be derived as:

$$\text{Percentage of Jump Days} = \frac{100 \sum_{i=0}^{T} I(\exists t \in i, \mid L_t \mid > c_\alpha)}{T}\% \tag{4.88}$$

where L_t is the LM jump test statistic at the intra-day level within a particular day, t refers to the 78 intra-day intervals and c_α is the critical value at α significance level.

Once jumps are detected, we follow Andersen et al. (2007) and Duong and Swanson (2011) to construct risk measures by separating out the variation due to daily jump component and the continuous components. This is done by using volatility measures RV and TPV. It can be given as

$$\text{Variation due to Jump Component} = JV_t = max[RV_t - TPV_t, 0] * I_{jump,t} \tag{4.89}$$

Consequently the ratio of jump to total variation for all three jump tests can be calculated as,

$$\text{Ratio of Jump Varitaion to Total Variation} = \frac{JV_t}{RV_t} \tag{4.90}$$

For BLT co-jump test, the percentage of days identified as having co-jumps is calculated using,

$$\text{Percentage of Co-Jump Days} = \frac{100 \sum_{i=0}^{T} I(\exists j, z_{mcp,i,j} < c_{mcp,\alpha,l} \cup z_{mcp,i,j} > c_{mcp,\alpha,r})}{T}\% \tag{4.91}$$

where $c_{mcp,\alpha,l}$ and $c_{mcp,\alpha,r}$ are left and right tail critical values derived from bootstrapping the null distribution. α is the significance level. For the JT co-jump test, the percentage

of days identified as having co-jumps is calculated as:

$$\text{Percentage of Co-Jump Days} = \frac{100 \sum_{i=0}^{T} I(\Phi_n^{(d)} \geq c_n^{(d)})}{T}\% \tag{4.92}$$

In the co-exceedance rule proposed by Gilder et al. (2014), we use the BNS jump test and the LM jump test to identify co-jumps. The percentage of days identified as having co-jumps can be given as:

$$\text{Percentage of Co-Jump Days} = \frac{100 \sum_{i=0}^{T} I(\mid Z_i \mid \geq \Phi_\alpha) * I(\exists t \in i, \mid L_t \mid > c_\alpha)}{T}\% \tag{4.93}$$

where Z_i is the BNS jump test statistic and L_t is the LM jump test statistic.

In addition to reporting the findings of our empirical experiment on the entire sample, we also conduct analysis after splitting the data set into two periods. The first sample consists of the period from January 2006 to June 2009 and the second sample consists of the period from July 2009 to December 2012. This is done to inspect whether the jump activity in the stocks and the ETFs changes considerably over time. The break date of our sample (June 2009) roughly corresponds to the end of the business cycle contraction after the financial crisis as given by NBER.

4.6.3 Findings

Table 4.1 gives the summary statistics for integrated volatility which is estimated using six volatility measures RV, BPV, TPV, $MedRV$, $MinRV$ and TRV. The sample period considered for the six stocks and the two ETFs is January 2006 - December 2013. The mean, standard deviation, minimum and maximum values are all in terms of 10^{-4}. Amongst all the stocks and ETFs, JPMorgan seems to have undergone maximum price fluctuations across the sample period as it displays the highest mean and max values across all the volatility measures. On the other hand Johnson & Johnson and XLK appear to be tied in terms of having undergone least amount of price fluctuations as they display the lowest

mean and max volatility estimates. Amongst all the volatility measures, *Bipower Variation* reports the lowest mean volatility estimate while *Realized Volatility* reports the highest mean volatility estimate for any given stock or ETF. This can be explained by the fact that in the presence of frequent jumps, *Realized Volatility* overestimates integrated volatility. To get a clearer idea of how volatility differs across the stocks and ETFs, we turn to figures (4.1) - (4.2) which display the estimated volatility for the stocks Boeing and Exxon with respect to the six aforementioned volatility measures. Similar figures for 4 other stocks and 2 ETFs have not been given for the purpose of brevity and can be provided upon request. In general stocks and ETFs achieve their highest volatility in the fourth quarter of 2008 during the financial crisis with a few exceptions. For XLE, in case of all four volatility measures apart from TPV and TRV, volatility reaches its peak in the second quarter of 2009. For XLK on the other hand, only in case RV the volatility peak is reached in the first quarter of 2008 while for the other measures it is the fourth quarter of 2008.

We now look at tables (4.2 - 4.5) which display the descriptive statistics of the three jump tests. For the ASJ jump test we consider both 5-minute and 1-minute frequencies while for the BNS and the LM jump tests we only consider 5-minute frequency. Panel A in the tables refers to the pre-financial crisis sample period, January 2006 - June 2009 and Panel B refers to the post crisis period July 2009 - December 2012. In case of the ASJ jump tests, we find noticeable differences between 5-minute (table 4.2) and 1 minute (table 4.3) frequencies. Overall the mean value of the statistics is higher for the 1-minute data compared to the 5 minute frequency suggesting that more jumps would be identified in the 1-minute case. The skewness values are all negative irrespective of the sample period, type of stock and frequency of sampling suggesting that the ASJ test statistics are left-skewed. Panel A for both frequencies appear to have overall higher mean and max values again suggesting more jump activity in the financial crises period. In case of the BNS test (4.4) the skewness values are all positive, which suggests all BNS test statistics are right-skewed

and have a long right tail. The kurtosis values are all above 3, which indicates the empirical distribution of BNS test statistics is leptokurtic. For the LM test (table 4.5), a window size of $k = 50$ is chosen. The mean of LM test statistics is around 0, while the max and min value of test statistics are far from 0, even reaching 1726.992 and -2124.609.

Tables (4.6 - 4.8) denote the percentage of days identified as having jumps for the ASJ, BNS and LM jump tests. For all jump tests $\alpha = 0.1$ and 0.05 significance levels are considered. In case of the ASJ jump test (table 4.6), it appears that Johnson & Johnson has the largest percentage of jump days for post-June 2009 period (panel B). However for the pre-June 2009 period (panel A), only with 5-minute frequency, Johnson & Johnson attains the highest jump day percentage. While for 1-minute frequency XLK seems to lead the race. XLE on the other hand has the lowest percentage of jump days across all significance levels, sample periods and sampling frequencies. In case of the BNS jump test (table 4.7) XLK has the largest percentage of jump days for the crisis (panel A) period while Microsoft displays the highest percentage in the post-crisis (panel B) period. Overall for all the stocks and ETFs for both ASJ and BNS tests, panel A displays relatively higher jump activity than panel B which shows that jumps happen more frequently during financial crisis period, when compared with post financial crisis period. Table (4.8) shows the percentage of jump days and jump proportions for the LM test. The percentage of jump days is very large, reaching 90% in some cases. This is because LM jump test detects whether there is jump at each interval per day[4] and a day is classified as a jump day if a jump occurs on any of the 5-minute (78 observations) intervals. The jump proportion is calculated by the total number of test statistics which indicate jumps divided by the total number of test statistics across all intra-day intervals for the entire sample period. The jump proportions are much lower, close to 1%. It is noteworthy that both percentage of

[4]Refer to equation (93)

jump days and jump proportions are larger during post financial crisis period (panel B). One reason for this may be, the fact that the LM test detects more small and moderate jumps when compared with the ASJ and BNS tests and these types of jumps are more likely to happen during post financial crisis period.

To graphically illustrate the level of jump activity we turn to figures (4.3 - 4.5), which display the ASJ and BNS test statistic values for the days identified as having jumps for Boeing and Exxon across the sample period January 2006 - December 2013. Once again similar figures for other stocks and ETFs have not been given for the purpose of brevity and would be available upon request. The significance level considered is 5%. For the ASJ test, the analysis is carried out for both 5 (figure 4.3) and 1 minute (figure 4.4) frequencies. As is evident from the figures, with a higher sampling frequency of 1-minute, more jumps are detected across all stocks and ETFs in comparison to 5-minute frequency. In case of the BNS test both XLK and Johnson & Johnson appear to have the relatively higher degree of jump activity compared to the other stocks in the pre-June 2009 period, a result which evidently aligns with what we deduced from table (4.7).

Figures (4.6 - 4.8) contain the kernel density plots of ASJ, BNS and LM test statistics. In case of the ASJ test statistics (4.6), it appears that the distribution is left-tailed or negatively skewed. On the other hand the underlying distribution for the BNS test statistic (4.7) appears to be skewed right. The LM test statistics (4.8) display a high kurtosis and a long tail. All these results are consistent with what we found from tables (4.2-4.5).

When analyzing the average ratio of jump variation to total variation, we compare the results between the ASJ test, BNS test and LM test. For all three tests given in tables 4.9, 4.10 and 4.11, ratio of jump variation to total variation is larger during financial crisis than post financial crisis and this result is robust across all significance levels. The tech sector ETF XLK has the largest jump variation ratio amongst all stocks. The BNS jump

test is more likely to detect large jumps, especially during financial crisis period which is why the jump variation ratio reported by it is larger than the other tests.

Table (4.12) contains percentage of days identified as having co-jumps under both JT co-jump test and the co-exceedance rule between BNS jump test and LM jump test. Co-jumps are detected in case of each of the following pairwise stock combinations, including Exxon & JPMorgan, Exxon & Microsoft, Exxon & XLE, JPMorgan & Microsoft, Microsoft & XLK and XLE & XLK. The range of percentage of co-jump days in JT co-jump test is from 0.454% to 2.955%, while the range for the co-exceedance rule is from 2.838% to 9.545%. One reason for the larger percentage range in co-exceedance rule could be the fact, that the intersection results between two jump tests lead to a large false rejection rate. The percentage of co-jump days in JPMorgan & Microsoft, Microsoft & XLK and XLE & XLK is larger during the financial crisis period than post financial crisis period and this result is robust across the different significance levels and types of co-jump tests. In Table (4.13), we detect co-jumps among the six stocks (Boeing, Exxon, Johnson&Johnson, JPMorgan, Microsoft and Walmart), using the BLT co-jump test as in Bollerslev et al. (2008). As is clear from the table, the percentage of co-jump days as per the BLT test is small, ranging from 0.114% to 0.454%.

We now turn to discuss graphical representation of co-jumps. Figures have only been given for co-jumps between pairs Exxon & JPMorgan, Exxon & Microsoft. Figures involving co-jumps between other stock combinations are available upon request. Figure (4.9) denotes the kernel density plot of JT co-jump test. Overall the distribution of the test statistics appears to be heavily right tailed. Figure (4.11) shows the JT test statistics of co-jump days from year 2006 to 2013. It is clear that co-jumps are less densely populated when compared with jump days. When comparing how co-jumps are scattered

between financial crisis period and post financial crisis period, there is no significant difference amongst Exxon & JPMorgan, Exxon & Microsoft. On the other hand more frequent co-jumps are visible during the financial crisis period in Microsoft & XLK and XLE & XLK. Figure (4.12) shows the days which have co-jumps as per the co-exceedance rule. The results show there is not much significant difference on how co-jumps are distributed between financial crisis and post financial crisis period.

Finally, figures (4.10) and (4.13) show the empirical findings from BLT co-jump tests. Figure (4.10) denotes the kernel density plot of empirical BLT test statistics. The distribution of the test statistics is evidently positively skewed. Figure (4.13) shows the daily return, daily closing price, realized variance, bipower variation and co-jump days for equi-weighted stock index. In Bollerslev et al. (2008), the authors show that detection of co-jumps among multiple stocks is equivalent to detecting co-jumps in an equi-weighted index composed by the same underlying stocks. Here we test co-jumps among six stocks, including Boeing, Exxon, Johnson&Johnson, JPMorgan, Microsoft and Walmart. The last panel of figure 4.13 shows the number of co-jump days at $\alpha = 10\%$ significance level. There are only 9 co-jump days among six stocks from year 2006 to 2013.

4.7 Conclusion

In this chapter, we review some of the most recent literature on integrated volatility measures, jump and co-jump tests. We then select a small subset of these measures and tests to conduct an empirical investigation with intra-day TAQ data of six individuals stocks and two ETFs. This study helps to reveal how the general volatility movement, jump and co-jump activity amongst the stocks vary across different types of tests and sampling frequencies.

We find that the occurrence of jumps is more frequent during and before the financial

crisis period, i.e. January 2006 - June 2009 compared to the post financial crisis period, i.e. July 2009 - December 2013. All individual stocks apart from the ETFs reach their peak volatility in the fourth quarter of 2008. Overall, the incidence of co-jumps is lesser compared to jumps over the entire sample period i.e. January 2006 - December 2013. Additionally there is not much significant difference in terms of distribution of co-jumps between financial crisis and post financial crisis period.

Table 4.1: Descriptive Statistics of Integrated Volatility Measures: Sample period Jan 2006 - Dec 2013

	Volatility Measures	RV	BPV	TPV	MedRV	MinRV	TRV
Boeing	Mean	2.68	1.24	2.29	2.38	2.46	2.60
	Standard Deviation	4.35	2.10	3.95	4.10	4.29	4.32
	Min	0.21	0.10	0.15	0.19	0.20	0.21
	Max	60.05	28.47	58.80	62.83	65.26	60.05
	Skewness	6.50	6.66	6.81	7.13	7.00	6.63
	Kurtosis	61.54	62.81	66.26	73.91	70.90	63.35
Exxon	Mean	2.15	1.01	1.89	1.98	2.02	2.10
	Standard Deviation	5.30	2.65	4.94	5.47	5.75	5.08
	Min	0.10	0.04	0.07	0.08	0.09	0.10
	Max	131.00	72.39	140.95	156.49	166.62	131.00
	Skewness	12.17	14.05	15.01	15.47	15.91	12.89
	Kurtosis	223.33	301.42	346.86	357.84	374.71	254.66
Johnson & Johnson	Mean	1.05	0.47	0.85	0.90	0.93	1.00
	Standard Deviation	2.37	1.06	1.94	2.07	2.12	2.30
	Min	0.07	0.02	0.03	0.05	0.05	0.07
	Max	52.86	22.84	46.48	42.82	43.33	52.86
	Skewness	11.36	10.44	11.25	10.99	10.61	11.76
	Kurtosis	186.83	157.67	195.54	173.99	162.96	203.20
JP Morgan	Mean	5.85	2.76	5.11	5.26	5.41	5.80
	Standard Deviation	13.99	65.23	12.00	12.24	12.49	13.96
	Min	0.13	0.05	0.09	0.11	0.10	0.13
	Max	244.81	118.46	213.02	214.80	235.11	244.81
	Skewness	8.06	7.74	7.48	7.34	7.42	8.10
	Kurtosis	100.06	94.76	88.59	85.07	90.95	101.07
Microsoft	Mean	2.29	1.07	1.95	2.07	2.12	2.24
	Standard Deviation	3.71	1.82	3.49	3.62	3.67	3.69
	Min	0.16	0.06	0.10	0.13	0.14	0.14
	Max	62.08	34.69	66.05	54.42	65.94	62.08
	Skewness	7.32	7.98	8.14	7.44	7.76	7.44
	Kurtosis	82.10	99.39	10.17	79.17	91.30	83.96
Walmart	Mean	1.57	0.71	1.31	1.37	1.40	1.51
	Standard Deviation	2.95	1.32	2.53	2.53	2.48	2.86
	Min	0.13	0.57	0.10	0.12	0.11	0.13
	Max	71.09	31.41	63.15	60.95	53.54	71.09
	Skewness	10.74	10.07	10.93	10.19	8.76	11.02
	Kurtosis	190.00	172.43	205.05	180.79	130.01	204.82
XLE	Mean	2.82	1.35	2.49	2.70	2.74	2.72
	Standard Deviation	7.35	3.45	5.77	8.52	8.42	6.00
	Min	0.10	0.04	0.08	0.08	0.08	0.10
	Max	193.76	80.53	123.39	278.12	266.10	129.66
	Skewness	14.29	12.30	10.14	20.21	18.81	10.39
	Kurtosis	296.35	215.74	151.36	577.77	511.09	161.29
XLK	Mean	1.46	0.65	1.19	1.28	1.30	1.38
	Standard Deviation	3.18	1.41	2.72	2.69	2.78	2.81
	Min	0.07	0.02	0.04	0.06	0.05	0.07
	Max	61.21	24.11	49.50	40.78	41.31	49.62
	Skewness	8.88	7.92	8.53	7.52	7.72	7.83
	Kurtosis	117.31	87.29	103.04	76.99	79.80	89.51

*Notes: Table 4.1 gives the descriptive statistics of the different integarted volatility measures. Mean, standard deviation, min and max values are all in terms of 10^{-4}.

Table 4.2: Descriptive Statistics of ASJ Jump Test: 5-minute sampling frequency

		Boeing	Exxcon	Johnson&Johnson	JP Morgan	Microsoft	Walmart	XLE	XLK
Panel A	Mean	0.042	0.177	0.256	0.088	0.149	0.185	0.016	0.164
	st.dev	1.239	1.118	1.166	1.229	1.189	1.188	1.243	1.113
	skewness	-1.129	-1.149	-1.293	-1.236	-1.150	-1.340	-1.182	-1.134
	kurtosis	4.120	4.459	4.739	4.814	4.253	4.752	4.612	4.583
	max	2.413	2.648	2.330	2.427	2.530	2.666	2.938	2.526
	min	-5.374	-4.383	-4.681	-5.833	-4.319	-4.363	-5.746	-4.361
Panel B	Mean	-0.053	0.093	-0.009	-0.056	0.109	0.0541	-0.018	0.063
	st. dev	1.291	1.168	1.302	1.273	1.182	1.146	1.192	1.158
	Skewness	-1.074	-1.216	-1.211	-1.009	-1.079	-0.840	-1.150	-1.195
	Kurtosis	3.743	4.465	4.342	3.636	4.046	3.402	4.535	4.808
	Max	2.210	2.301	2.431	2.300	2.563	2.367	2.783	2.495
	Min	-5.095	-4.495	-5.685	-4.624	-4.437	-3.963	-5.770	-5.658

*Notes: Table 4.2 gives the descriptive statistics of ASJ jump test at 5-minute frequency. Panel A covers the financial crisis period from Jan 2006 - June 2009 and Panel B covers the post fiancial crisis period from July 2009 - Dec 2012.

Table 4.3: Descriptive Statistics of ASJ Jump Test: 1-minute sampling frequency

		Boeing	Exxcon	Johnson&Johnson	JP Morgan	Microsoft	Walmart	XLE	XLK
Panel A	Mean	0.399	0.404	0.587	0.391	0.612	0.453	0.125	0.756
	st. dev	1.455	1.345	1.414	1.315	1.300	1.358	1.371	1.385
	Skewness	-0.896	-0.776	-1.627	-1.035	-1.05	-0.845	-0.347	-1.071
	Kurtosis	4.378	5.219	10.193	6.531	5.650	4.770	3.682	9.357
	Max	4.723	5.138	4.538	4.105	5.457	4.998	4.548	6.183
	Min	-6.235	-6.387	-11.076	-8.702	-5.554	-5.755	-4.864	-8.529
Panel B	Mean	0.236	0.348	0.430	0.249	0.532	0.317	0.066	0.643
	st. dev	1.400	1.281	1.504	1.335	1.247	1.503	1.321	1.111
	skewness	-1.100	-1.122	-0.884	-1.294	-1.029	-1.279	-0.711	-0.568
	Kurtosis	5.678	7.305	4.546	7.522	5.3471	7.099	3.819	4.707
	Max	4.244	4.867	5.120	4.198	4.684	3.505	4.265	5.429
	Min	-8.733	-9.165	-6.190	-9.994	-5.867	-10.974	-4.813	-3.816

*Notes: Table 4.3 gives the descriptive statistics of ASJ jump test at 1-minute frequency. See notes of Table 4.2.

Table 4.4: Descriptive Statistics of BNS Jump Test

		Boeing	Exxcon	Johnson&Johnson	JP Morgan	Microsoft	Walmart	XLE	XLK
Panel A	Mean	0.878	0.771	1.098	0.854	0.867	0.859	0.599	1.415
	st.dev	1.511	1.327	1.665	1.434	1.320	1.401	1.327	1.693
	Skewness	1.030	0.618	1.151	0.951	0.602	0.801	0.780	1.315
	Kurtosis	4.903	3.749	4.851	4.518	3.500	4.068	4.169	6.395
	Max	7.791	6.631	8.661	7.352	5.811	6.662	6.947	10.731
	Min	-2.513	-2.341	-2.693	-2.364	-2.299	-2.505	-2.640	-2.695
Panel B	Mean	0.688	0.667	0.876	0.558	0.880	0.918	0.572	0.814
	st.dev	1.406	1.328	1.450	1.249	1.406	1.535	1.228	1.275
	Skewness	0.983	0.572	0.837	0.574	0.647	0.925	0.615	0.525
	Kurtosis	5.400	3.557	3.646	3.652	3.428	4.215	3.711	3.530
	Max	9.340	6.964	7.128	5.486	7.008	7.549	5.807	6.909
	Min	-2.485	-2.546	-2.006	-2.750	-2.417	-2.137	-2.225	-2.244

*Notes: Table 4.4 gives the descriptive statistics of BNS jump test at 5-minute frequency. See notes of Table 4.2.

Table 4.5: Descriptive Statistics of LM Jump Test

		Boeing	Exxcon	Johnson&Johnson	JP Morgan	Microsoft	Walmart	XLE	XLK
Panel A	Mean	0.595	4.436	-1.662	-0.676	3.987	0.181	2.202	2.347
	st.dev	42.865	50.142	101.707	47.879	66.636	52.002	37.687	72.997
	Skewness	0.911	2.909	0.675	0.850	1.267	-0.146	2.714	0.316
	Kurtosis	15.591	31.900	16.875	25.186	13.907	10.491	41.367	14.882
	Max	386.170	602.678	1008.160	525.995	585.419	314.852	472.919	509.147
	Min	-309.16	-185.941	-615.524	-354.424	-289.795	-343.618	-189.563	-570.747
Panel B	Mean	-0.110	0.295	0.076	0.137	0.097	0.636	-0.051	0.042
	st.dev	42.450	47.158	67.736	33.483	42.875	61.795	43.314	54.955
	Skewness	-0.465	-0.251	-0.635	1.958	1.035	0.138	-0.451	0.128
	Kurtosis	67.346	29.672	49.711	165.139	92.97	76.991	48.134	30.865
	Max	1047.900	1192.159	1455.508	1320.357	1726.992	1529.471	1288.848	1571.141
	Min	-1275.319	-764.818	-1789.208	-1399.492	-1064.302	-2124.609	-881.903	-881.418

*Notes: Table 4.5 gives the descriptive statistics of LM jump test at 5-minute frequency. See notes of Table 4.2.

Table 4.6: Percentage of days identified as having jumps - ASJ Jump Test

Name	Panel A: Jan 2006 - Jun 2009				Panel B: July 2009 - Dec 2012			
	1 min		5 min		1 min		5 min	
Significance level	0.05	0.10	0.05	0.10	0.05	0.10	0.05	0.10
Boeing	15.79	27.95	3.29	10.79	10.89	23.38	2.27	9.98
Exxon	12.61	22.84	3.63	11.47	9.76	21.11	2.72	8.74
Johnson & Johnson	19.88	32.04	4.77	14.09	16.00	27.80	3.40	10.44
JP Morgan	12.38	24.20	3.52	11.36	10.32	18.84	3.06	8.05
Microsoft	17.04	31.70	3.52	11.36	14.18	25.42	4.08	11.12
Walmart	15.11	27.61	3.52	11.59	13.16	24.85	3.74	9.53
XLE	10.22	17.84	3.06	9.43	7.60	13.96	2.27	7.94
XLK	20.45	34.31	3.63	10.68	15.20	26.44	2.83	9.19

*Notes: Table 4.6 gives the percentage of days identified as having jumps by the ASJ test at both 5 minute and 1 minute sampling frequencies. Jumps are tested at $\alpha = 0.05$ and $\alpha = 0.1$ significance level. Percentage of days is calculated using the equation 4.87 in section 4.6.2. Panel A covers the financial crisis period from Jan 2006 - June 2009 and Panel B covers the post fiancial crisis period from July 2009 - Dec 2012.

Table 4.7: Percentage of Days Identified as having Jumps - BNS Jump Test

Name	Panel A: Jan 2006 - Jun 2009		Panel B: July 2009 - Dec 2012	
Signifiance Level	0.05	0.10	0.05	0.10
Boeing	20.68	27.73	16.69	23.04
Exxcon	17.95	26.25	15.78	23.27
Johnson&Johnson	24.09	30.23	20.43	25.88
JP Morgan	19.89	25.23	12.83	19.64
Microsoft	18.86	25.23	21.45	27.70
Walmart	19.77	27.38	20.66	26.67
XLE	15.11	21.36	12.71	19.41
XLK	30.00	38.18	17.93	25.54

*Notes: Table 4.7 shows percentage of days identified as having jumps by BNS test at 5 minute sampling frequency. See notes of Table 4.6.

Table 4.8: Percentage of days identified as having jumps and Jump Proportion - LM Jump Test

Name	Panel A: Jan 2006 - Jun 2009				Panel B: July 2009 - Dec 2012			
	Jump proportion		% of Jump days		Jump proportion		% of Jump days	
Signifiance Level	0.05	0.10	0.05	0.10	0.05	0.10	0.05	0.10
Boeing	1.06	1.07	82.39	83.41	1.14	1.15	88.99	89.56
Exxcon	1.10	1.11	85.45	86.36	1.17	1.17	90.92	91.49
Johnson&Johnson	1.15	1.15	89.55	89.89	1.21	1.21	94.32	94.55
JP Morgan	1.03	1.04	80.45	80.91	1.11	1.12	86.83	87.29
Microsoft	1.15	1.15	89.66	89.66	1.16	1.17	90.47	91.15
Walmart	1.11	1.12	86.36	87.05	1.19	1.19	92.51	92.74
XLE	1.03	1.05	80.45	81.93	1.17	1.18	91.60	92.30
XLK	1.06	1.07	82.84	83.41	1.14	1.14	88.88	89.22

*Notes: Table 4.8 shows percentage of days identified as having jumps and jump proportion as per the LM test at 5 minute sampling frequency. Percentage of days is calculated using the equation 4.88 in section 4.6.2. See notes of Table 4.6.

Table 4.9: Average Ratio of Jump Variation to Total Variation - ASJ Jump Test

Name	Panel A: Jan 2006 - June 2009				Panel B: July 2009 - Dec 2012			
	1 min		5 min		1 min		5 min	
Significance level	0.05	0.10	0.05	0.10	0.05	0.10	0.05	0.10
Boeing	3.74	6.14	0.70	2.38	2.14	4.08	0.32	1.68
Exxon	2.86	4.28	0.44	1.63	1.55	3.02	0.26	1.03
Johnson & Johnson	5.21	8.09	0.99	2.87	3.49	5.96	0.64	2.17
JP Morgan	2.97	5.21	0.55	2.16	1.56	2.90	0.42	1.14
Microsoft	4.59	8.05	0.50	2.07	3.30	5.47	0.96	2.20
Walmart	3.50	6.30	0.53	2.18	2.93	5.33	0.86	1.81
XLE	2.08	3.35	0.34	1.39	1.44	2.40	0.24	1.05
XLK	10.78	16.96	1.27	3.40	4.69	7.88	0.54	1.74

Notes*: Table 4.9 gives the average ratio of jump varaition to total variation as per the ASJ test using both 5 minute and 1 minute sampling frequencies. Jump ratio is calculated using the equation 4.90 in section 4.6.2. Panel A covers the financial crisis period from Jan 2006 - June 2009 and Panel B covers the post fiancial crisis period from July 2009 - Dec 2012.

Table 4.10: Average Ratio of Jump Variation to Total Variation - BNS Jump Test

Name	Panel A: Jan 2006 - Jun 2009		Panel B: July 2009 - Dec 2012	
Signifiance Level	0.05	0.10	0.05	0.10
Boeing	37.87	34.36	6.10	8.58
Exxcon	32.00	28.44	6.93	7.67
Johnson&Johnson	42.46	39.93	9.30	11.09
JP Morgan	36.81	33.75	5.99	8.13
Microsoft	36.44	33.26	8.92	9.76
Walmart	36.60	33.43	7.91	8.87
XLE	33.00	30.08	4.37	5.64
XLK	44.63	41.78	12.75	14.70

*Notes: Table 4.10 shows average ratio of jump variation to total variation as per the BNS test using 5 minute frequency. See notes of Table 4.9.

Table 4.11: Average Ratio of Jump Variation to Total Variation - LM Jump Test

Name	Panel A: Jan 2006 - Jun 2009		Panel B: July 2009 - Dec 2012	
Signifiance Level	0.05	0.10	0.05	0.10
Boeing	17.72	17.79	14.59	14.87
Exxcon	14.65	14.58	12.59	12.62
Johnson&Johnson	21.53	21.53	19.34	19.4
JP Morgan	17.41	17.36	13.92	13.93
Microsoft	17.57	17.57	15.59	15.60
Walmart	17.68	17.56	15.22	15.23
XLE	13.58	13.56	10.98	11.17
XLK	25.45	25.35	21.33	21.41

*Notes: Table 4.11 shows the average ratio of jump variation to total variation as per the LM test using 5 minute frequency. See notes of Table 4.9.

Table 4.12: Percentage of Days Identified as having Co-jumps - GST Co-exceedance Rule

	Panel A: Jan 2006 - Jun 2009				Panel B: July 2009 - Dec 2012			
	JT Test		LM&BNS Test		JT Test		LM&BNS Test	
Significance Level	0.05	0.10	0.05	0.10	0.05	0.10	0.05	0.10
Exxon&JPMorgan	1.364	1.818	3.864	7.159	1.703	1.816	2.838	5.335
Exxon & Microsoft	0.795	0.909	3.295	6.818	1.022	1.476	3.519	5.675
Exxon & XLE	1.136	1.59	3.977	7.386	1.93	2.497	3.746	8.059
JPMorgan & Microsoft	1.136	1.363	3.409	5.682	1.135	1.249	2.951	5.335
Microsoft & XLK	2.500	2.955	6.136	9.545	1.022	1.362	4.767	7.491
XLE & XLK	2.045	2.386	4.773	8.295	0.454	0.568	3.065	6.129

*Notes: Table 4.12 shows the percentage of days identified as having co-jumps. Co-jumps are detected at $\alpha = 0.05$ and $\alpha = 0.1$ significance level. Both JT co-jump test and co-exceedance rule between BNS test and LM test are used to test co-jumps. Panel A covers the financial crisis period from Jan 2006 - June 2009 and Panel B covers the post fiancial crisis period from July 2009 - Dec 2012. The test statistics are calculated at 5-minute frequency.

Table 4.13: Percentage of Days Identified as having Co-jumps - BLT test

	Panel		Panel B	
Significance Level	0.05	0.1	0.05	0.1
BLT Test	0.227	0.341	0.114	0.454

*Notes: See notes to Table 4.12. Table 4.13 shows the percentage of days identified as having co-jumps from BLT co-jump tests. Co-jumps are detected among six stocks: Boeing, Exxon, JohnsonJohnson, JPMorgan, Microsoft and Walmart.

Figure 4.1: Integrated Volatility Measures - Boeing

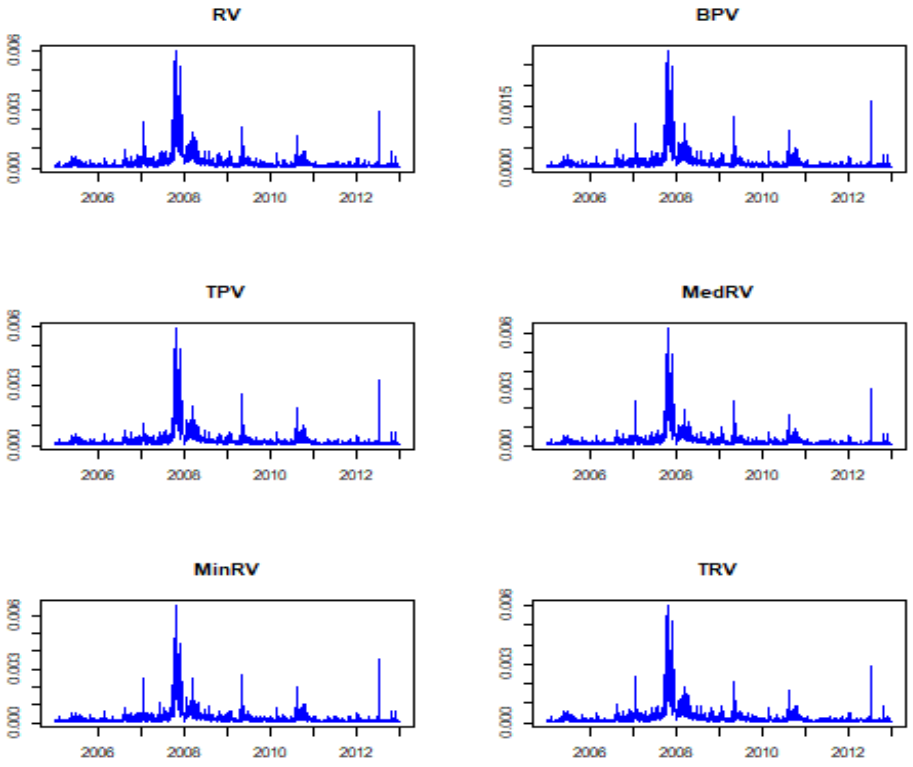

Notes*: Figure 4.1 displays volatility of Boeing across the sample period Jan 2006 - Dec 2013 using 5-minute sampling frequency with respect to six different integrated volatility measures which include RV, BPV, TPV, MedRV, MinRV and TRV.

Figure 4.2: Integrated Volatility Measures - Exxon

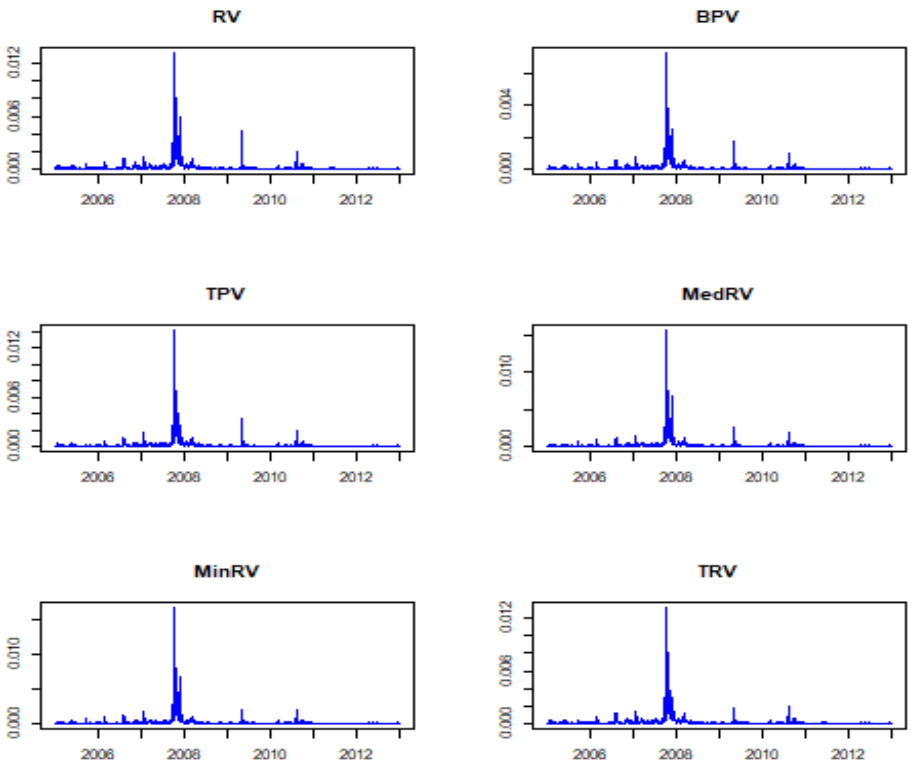

Notes*: Figure 4.2 displays volatility movement of Exxon. See notes of Figure 4.1.

Figure 4.3: ASJ Jump Test Statistics of Days Identified as having Jumps: 5-minute sampling frequency

*Notes: Figure 4.3 displays the scatter plot for ASJ test statistics for days identified as having jumps using 5-minute sampling frequency. We consider the following stocks and ETFs: Boeing & Exxon for the sample period Jan 2006 to Dec 2013.

Figure 4.4: ASJ Jump Test Statistics of Days Identified as having Jumps: 1-minute sampling frequency

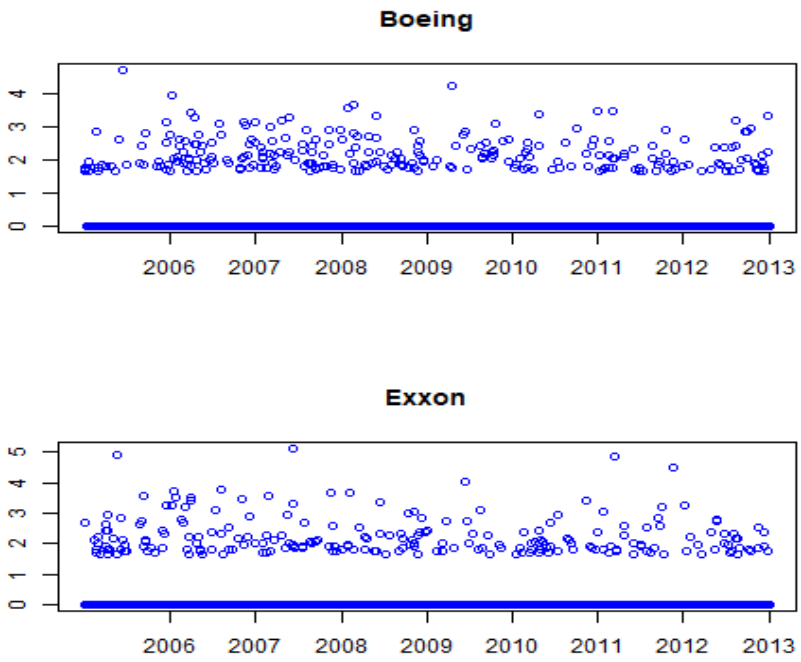

*Notes: Figure 4.4 displays the scatter plot for ASJ test statistics for days identified as having jumps using 1-minute sampling frequency. See notes of figure 4.3.

Figure 4.5: BNS Jump Test Statistics of Days Identified as having Jumps

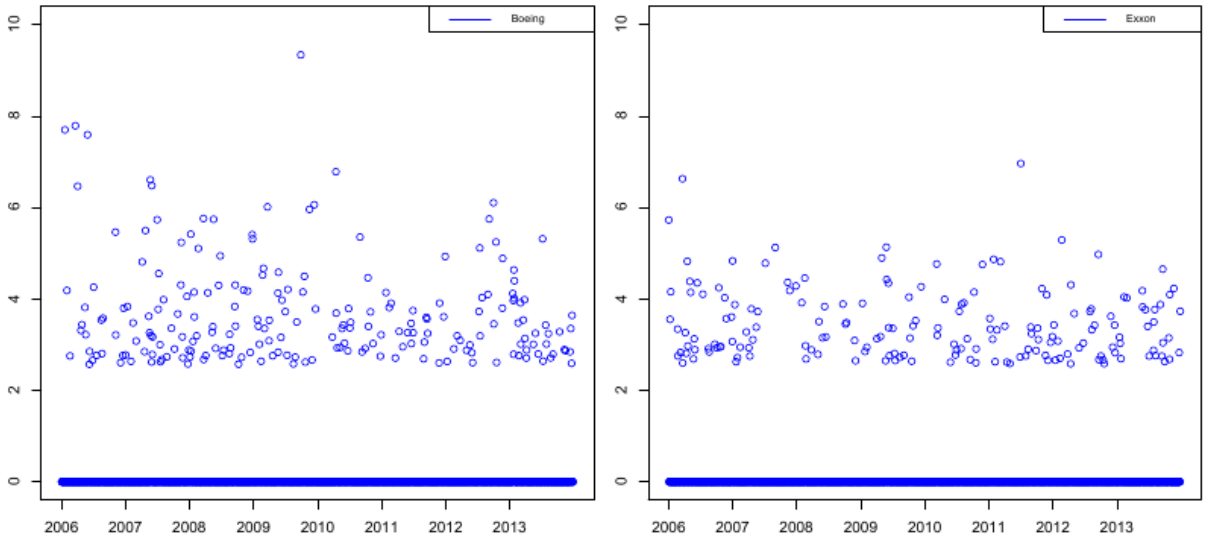

*Notes: Figure 4.5 displays the scatter plot for BNS test statistics for days identified as having jumps using 5-minute sampling frequency. See notes of figure 4.3.

Figure 4.6: Kernel Density Plots for ASJ Test Statistics

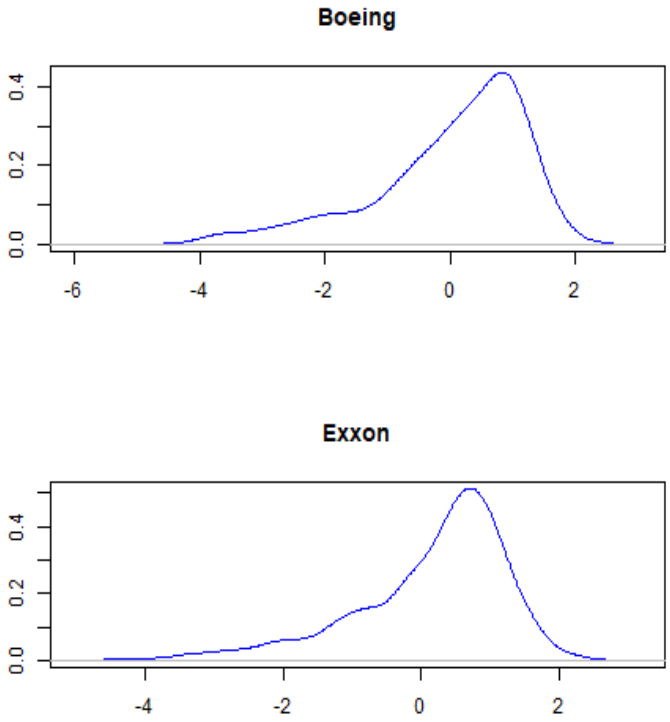

Notes*: Figure 4.6 displays the kernel density plot of ASJ jump test statistics using 5-minute sampling frequency. See notes of figure 4.3.

Figure 4.7: Kernel Density Plot of BNS Jump Test Statistics

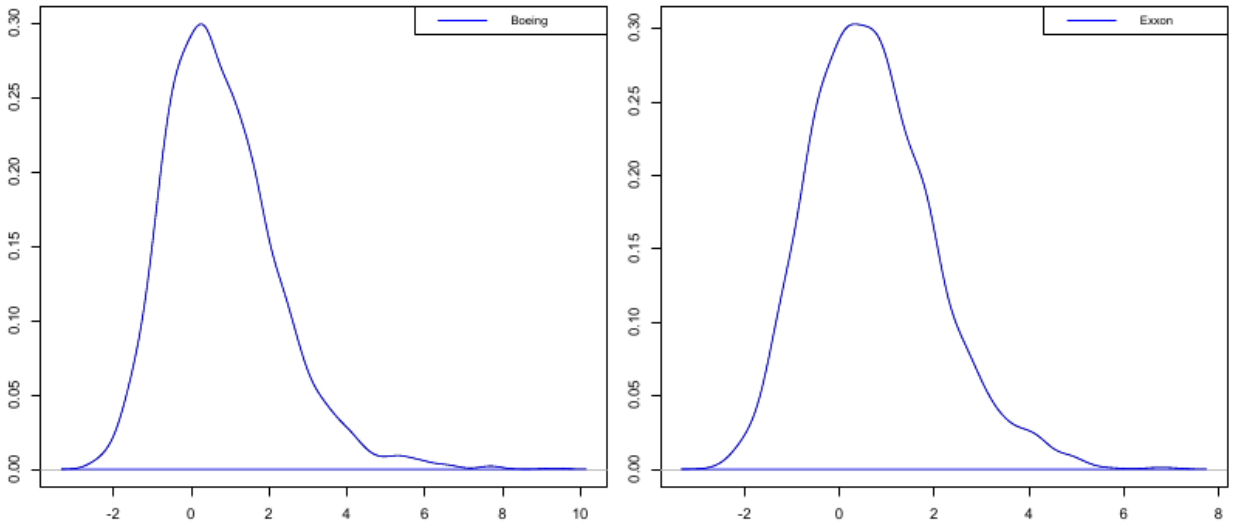

Notes*: Figure 4.7 displays the kernel density plot of BNS jump test statistics using 5-minute sampling frequency. See notes of figure 4.3.

Figure 4.8: Kernel Density Plot of LM Jump Test Statistics

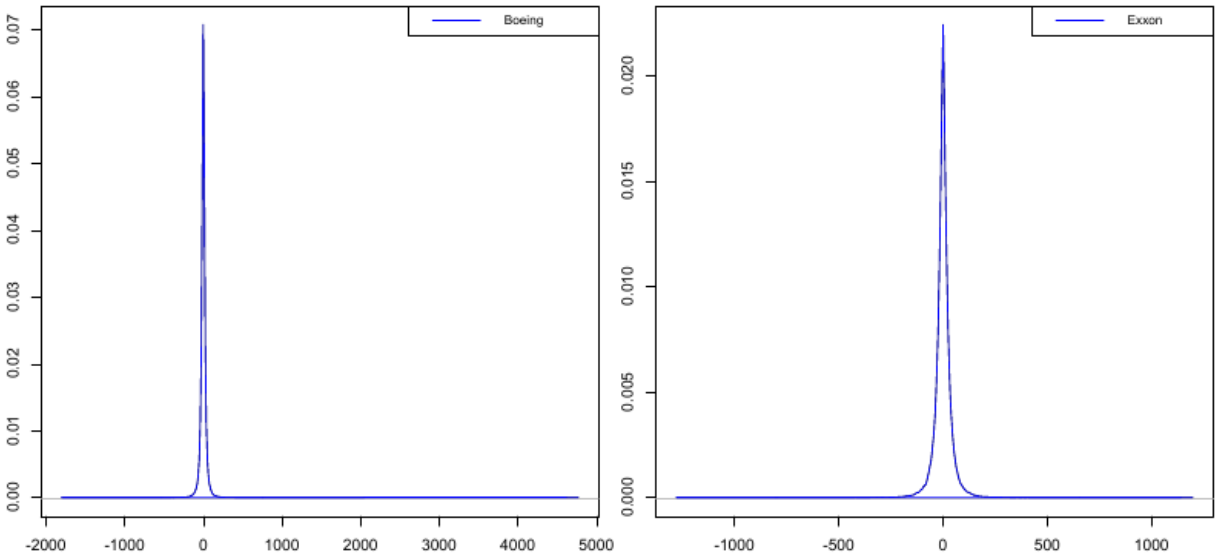

Notes*: Figure 4.8 displays the kernel density plot of LM jump test statistics using 5-minute sampling frequency. See notes of figure 4.3.

Figure 4.9: Kernel Density Plot of JT Co-jump Test Statistics

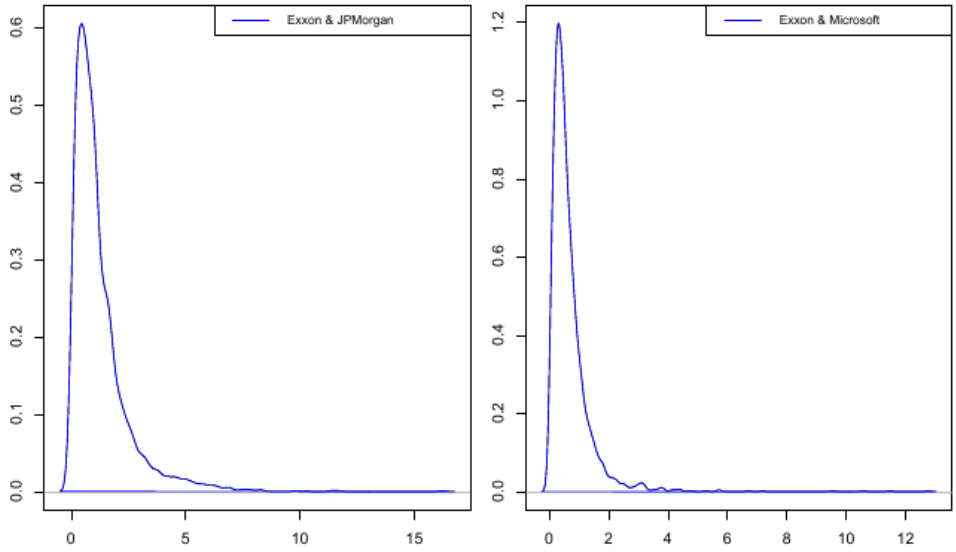

*Notes: Figure 4.9 displays the kenel density plot of JT co-jump test using 5-minute sampling frequency. The co-jumps are tested for the pairs Exxon & JPMorgan and Exxon & Microsft for the sample period Jan 2006-Dec 2013.

Figure 4.10: Kernel Density Plot of empirical observed BLT Statistics

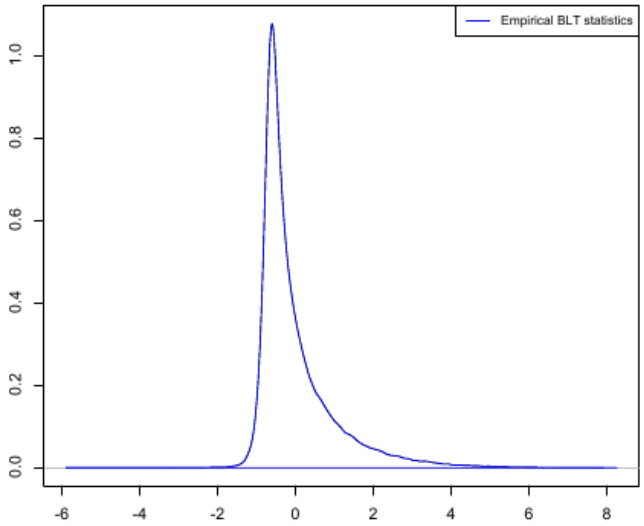

*Notes: Figure 4.10 displays the kernel density plot of the empirical observed BLT co-jump test statistics using 5-minute sampling frequency for the sample period Jan 2006-Dec 2013.

Figure 4.11: JT Co-jump Test Statistics of Days Identified as Having Co-jumps

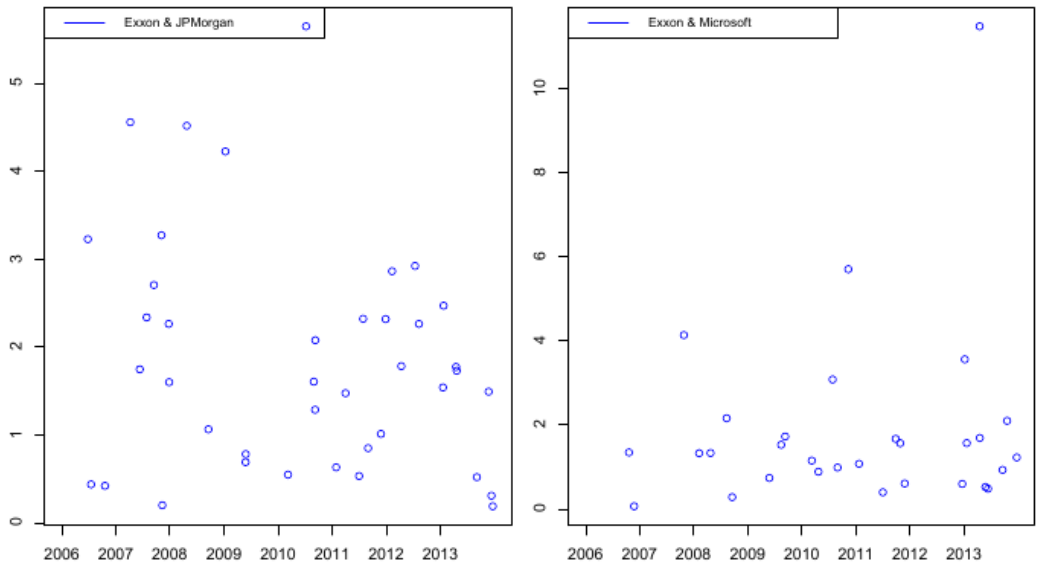

*Notes: Figure 4.11 displays the co-jump days test statistics of JT test for the sample period Jan 2006 to Dec 2013 using sampling frequency of 5-minute.

Figure 4.12: LM & BNS Test Statistics for Days Having Co-jumps

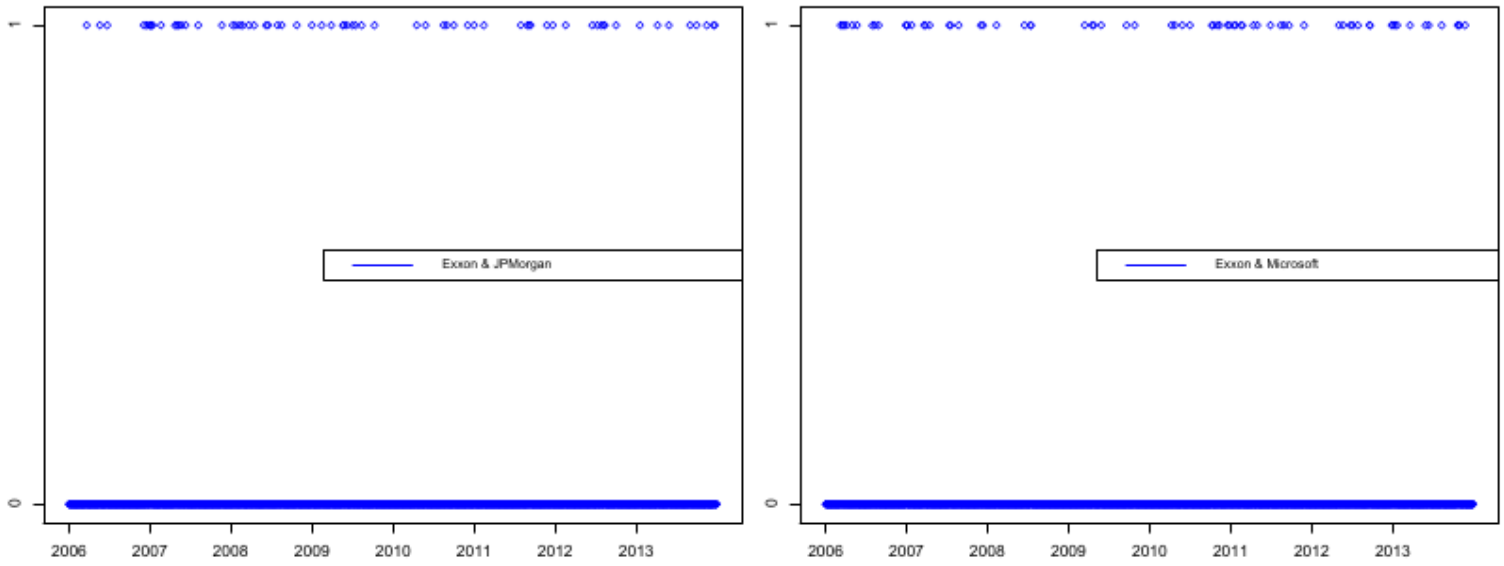

*Notes: Figure 4.12 displays the co-jump days identified from co-exceedance rule between LM jumps test and BNS jump test for the pairs Exxon & JPMorgan and Exxon & Microsoft. 5-minute sampling frequency is considered for sample period Jan 2006-Dec 2013.

Figure 4.13: Daily Return, Daily Closing Price, Realized Variance, Bipower Variation and Co-jump Days for Equi-weighted Stock Index

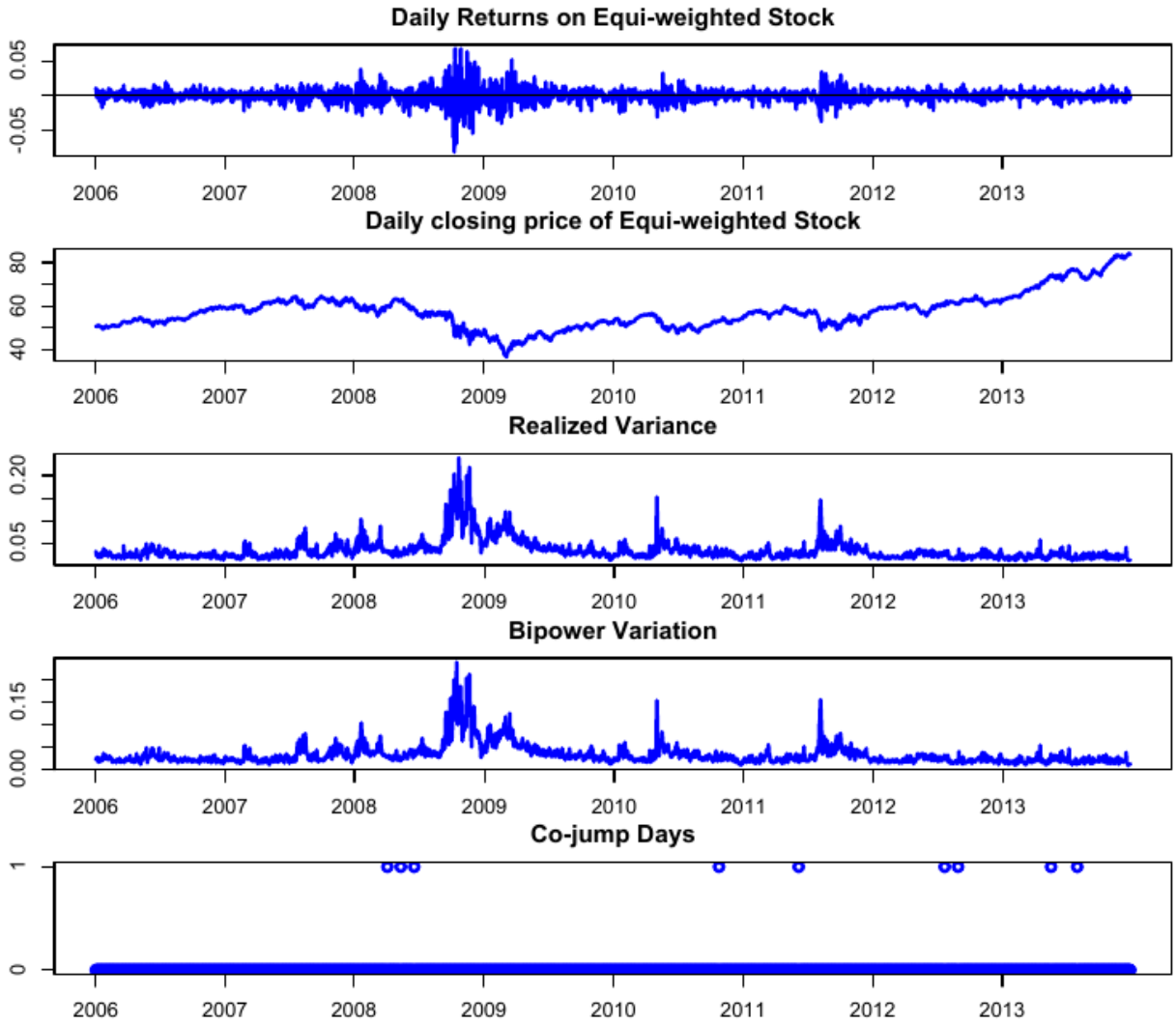

*Notes: Figure 4.13 displays the daily return, daily closing price, realized variance, bipower variation and co-jump days for equi-weighted stock index. The co-jump days in the last panel are detected through BLT co-jump tests at $\alpha = 0.1$ significance level from Jan 2006 to Dec 2013. The equi-weighted stock index is composed of six stocks (Boeing, Exxon, JohnsonJohnson, JPMorgan, Microsoft and Walmart) with equal weights.

Bibliography

Aït-Sahalia, Y. 2002. Telling from discrete data whether the underlying continuous-time model is a diffusion. *The Journal of Finance* 57:2075–2112.

Aït-Sahalia, Y. and Jacod, J. 2014. High Frequency Financial Econometrics. Princeton University Press.

Aït-Sahalia, Y., Jacod, J., et al. 2009. Testing for jumps in a discretely observed process. *The Annals of Statistics* 37:184–222.

Aït-Sahalia, Y. and Xiu, D. 2016. Increased correlation among asset classes: Are volatility or jumps to blame, or both? *Journal of Econometrics* 194:205–219.

Andersen, T. G., Benzoni, L., and Lund, J. 2002. An empirical investigation of continuous-time equity return models. *The Journal of Finance* 57:1239–1284.

Andersen, T. G., Bollerslev, T., and Diebold, F. X. 2003a. Some like it smooth, and some like it rough: Untangling continuous and jump components in measuring, modeling, and forecasting asset return volatility. *CFS Working Paper Series 2003/35, Center for Financial Studies (CFS)* .

Andersen, T. G., Bollerslev, T., and Diebold, F. X. 2007. Roughing it up: Including jump components in the measurement, modeling, and forecasting of return volatility. *The review of economics and statistics* 89:701–720.

Andersen, T. G., Bollerslev, T., Diebold, F. X., and Labys, P. 2001. The distribution of realized exchange rate volatility. *Journal of the American statistical association* 96:42–55.

Andersen, T. G., Bollerslev, T., Diebold, F. X., and Labys, P. 2003b. Modeling and forecasting realized volatility. *Econometrica* 71:579–625.

Andersen, T. G., Bollerslev, T., Frederiksen, P., and Ørregaard Nielsen, M. 2010. Continuous-time models, realized volatilities, and testable distributional implications for daily stock returns. *Journal of Applied Econometrics* 25:233–261.

Andersen, T. G., Dobrev, D., and Schaumburg, E. 2012. Jump-robust volatility estimation using nearest neighbor truncation. *Journal of Econometrics* 169:75–93.

Aruoba, S. B., Diebold, F. X., and Scotti, C. 2009. Real-time measurement of business conditions. *Journal of Business & Economic Statistics* 27:417–427.

Bandi, F. M. and Reno, R. 2016. Price and volatility co-jumps. *Journal of Financial Economics* 119:107–146.

Bandi, F. M. and Russell, J. R. 2008. Microstructure noise, realized variance, and optimal sampling. *The Review of Economic Studies* 75:339–369.

Barndorff-Nielsen, O. E., Graversen, S. E., Jacod, J., Podolskij, M., and Shephard, N. 2006. A central limit theorem for realised power and bipower variations of continuous semimartingales, pp. 33–68. *In* From stochastic calculus to mathematical finance. Springer.

Barndorff-Nielsen, O. E., Hansen, P. R., Lunde, A., and Shephard, N. 2008. Designing realized kernels to measure the ex post variation of equity prices in the presence of noise. *Econometrica* 76:1481–1536.

Barndorff-Nielsen, O. E., Hansen, P. R., Lunde, A., and Shephard, N. 2011. Subsampling realised kernels. *Journal of Econometrics* 160:204–219.

Barndorff-Nielsen, O. E. and Shephard, N. 2004. Power and bipower variation with stochastic volatility and jumps. *Journal of Financial Econometrics* 2:1–37.

Barndorff-Nielsen, O. E. and Shephard, N. 2006. Econometrics of testing for jumps in financial economics using bipower variation. *Journal of financial Econometrics* 4:1–30.

Barndorff-Nielsen, O. E., Shephard, N., et al. 2003. Realized power variation and stochastic volatility models. *Bernoulli* 9:243–265.

Bibinger, M. and Winkelmann, L. 2015. Econometrics of co-jumps in high-frequency data with noise. *Journal of Econometrics* 184:361–378.

Bloom, N. 2009. The impact of uncertainty shocks. *Econometrica* 77:623–685.

Bollerslev, T., Law, T. H., and Tauchen, G. 2008. Risk, jumps, and diversification. *Journal of Econometrics* 144:234–256.

Boswijk, H. P., Laeven, R. J., and Yang, X. 2018. Testing for self-excitation in jumps. *Journal of Econometrics* 203:256–266.

Boudt, K., Croux, C., and Laurent, S. 2011. Robust estimation of intraweek periodicity in volatility and jump detection. *Journal of Empirical Finance* 18:353–367.

Breiman, L. 2001. Random forests. *Machine learning* 45:5–32.

Bridle, J. S. 1990. Probabilistic interpretation of feedforward classification network outputs, with relationships to statistical pattern recognition. pp. 227–236.

Brock, W., Lakonishok, J., and LeBaron, B. 1992. Simple technical trading rules and the stochastic properties of stock returns. *The Journal of finance* 47:1731–1764.

Brownlees, C. T., Nualart, E., and Sun, Y. 2016. A truncated two-scales realized volatility estimator.

Caporin, M., Kolokolov, A., and Renò, R. 2017. Systemic co-jumps. *Journal of Financial Economics* 126:563–591.

Carr, P. and Wu, L. 2003. What type of process underlies options? a simple robust test. *The Journal of Finance* 58:2581–2610.

Chernov, M., Gallant, A. R., Ghysels, E., and Tauchen, G. 2003. Alternative models for stock price dynamics.

Christoffersen, P. F. and Diebold, F. X. 2006. Financial asset returns, direction-of-change forecasting, and volatility dynamics. *Management Science* 52:1273–1287.

Clark, T. E. and McCracken, M. W. 2009. Improving forecast accuracy by combining recursive and rolling forecasts. *International Economic Review* 50:363–395.

Clements, A., Liao, Y., et al. 2014. The role in index jumps and cojumps in forecasting stock index volatility: Evidence from the dow jones index. Technical report, National Centre for Econometric Research.

Corradi, V., Distaso, W., and Swanson, N. R. 2011. Predictive inference for integrated volatility. *Journal of the American Statistical Association* 106:1496–1512.

Corradi, V., Silvapulle, M., and Swanson, N. 2014. Consistent pretesting for jumps.

Corradi, V., Silvapulle, M. J., and Swanson, N. R. 2015. Testing for jumps and jump intensity path dependence.

Corradi, V., Silvapulle, M. J., and Swanson, N. R. 2018. Testing for jumps and jump intensity path dependence. *Journal of Econometrics* 204:248–267.

Corradi, V. and Swanson, N. R. 2006. Predictive density evaluation. *Handbook of economic forecasting* 1:197–284.

Corsi, F. 2004. A simple long memory model of realized volatility. *Available at SSRN 626064* .

Corsi, F., Pirino, D., and Reno, R. 2010. Threshold bipower variation and the impact of jumps on volatility forecasting. *Journal of Econometrics* 159:276–288.

Cortes, C. and Vapnik, V. 1995. Support-vector networks. *Machine learning* 20:273–297.

Cover, T. and Hart, P. 1967. Nearest neighbor pattern classification. *IEEE transactions on information theory* 13:21–27.

Cox, D. R. 1966. Some procedures associated with the logistic qualitative response curve.

Diebold, F. X. and Mariano, R. S. 1995. Com paring predictive accu racy. *Journal of Business and Economic Statistics* 13:253–263.

Duda, R. O., P. E. H. 1973. Pattern classification and scene analysis.

Dungey, M., Henry, Ó. T., and Hvozdyk, L. 2011. The impact of thin trading and jumps on realized hedge ratios. *manuscript, CFAP, University of Cambridge* .

Dungey, M. H., Erdemlioglu, D., Matei, M., and Yang, X. 2016. Financial flights, stock market linkages and jump excitation.

Duong, D. and Swanson, N. R. 2011. Volatility in discrete and continuous-time models: A survey with new evidence on large and small jumps, pp. 179–233. *In* Missing Data Methods: Time-Series Methods and Applications.

Duong, D. and Swanson, N. R. 2015. Empirical evidence on the importance of aggregation, asymmetry, and jumps for volatility prediction. *Journal of Econometrics* 187:606–621.

Eraker, B., Johannes, M., and Polson, N. 2003. The impact of jumps in volatility and returns. *The Journal of Finance* 58:1269–1300.

Fama, E. F. and Blume, M. E. 1966. Filter rules and stock-market trading. *The Journal of Business* 39:226–241.

Fama, E. F. and French, K. R. 1992. The cross-section of expected stock returns. *the Journal of Finance* 47:427–465.

Fama, E. F. and French, K. R. 2015. A five-factor asset pricing model. *Journal of financial economics* 116:1–22.

Fan, J. and Wang, Y. 2007. Multi-scale jump and volatility analysis for high-frequency financial data. *Journal of the American Statistical Association* 102:1349–1362.

Fan, R.-E., Chang, K.-W., Hsieh, C.-J., Wang, X.-R., and Lin, C.-J. 2008. Liblinear: A library for large linear classification. *Journal of machine learning research* 9:1871–1874.

Fisher, R. A. 1936. The use of multiple measurements in taxonomic problems. *Annals of eugenics* 7:179–188.

Frale, C., Marcellino, M., Mazzi, G. L., and Proietti, T. A monthly indicator of the euro area gdp. *European University Institute; Series/Number: EUI ECO; 2008/32* .

Friedman, J., Hastie, T., and Tibshirani, R. 2001. The elements of statistical learning, volume 1. Springer series in statistics New York.

Friedman, J. H. 2001. Greedy function approximation: a gradient boosting machine. *Annals of statistics* pp. 1189–1232.

Friedman, N., Geiger, D., and Goldszmidt, M. 1997. Bayesian network classifiers. *Machine learning* 29:131–163.

Gençay, R., Dacorogna, M., Muller, U. A., Pictet, O., and Olsen, R. 2001. An introduction to high-frequency finance. Academic press.

Ghysels, E., Sinko, A., and Valkanov, R. 2007. Midas regressions: Further results and new directions. *Econometric Reviews* 26:53–90.

Gilder, D., Shackleton, M. B., and Taylor, S. J. 2014. Cojumps in stock prices: Empirical evidence. *Journal of Banking & Finance* 40:443–459.

Gnabo, J.-Y., Hvozdyk, L., and Lahaye, J. 2014. System-wide tail comovements: A bootstrap test for cojump identification on the s&p 500, us bonds and currencies. *Journal of International Money and Finance* 48:147–174.

Gu, S., Kelly, B., and Xiu, D. 2018. Empirical asset pricing via machine learning. Technical report, National Bureau of Economic Research.

Hansen, P. R. and Lunde, A. 2006. Realized variance and market microstructure noise. *Journal of Business & Economic Statistics* 24:127–161.

Harvey, C. R. and Liu, Y. 2018. Lucky factors. *Available at SSRN 2528780* .

Hausman, J. 1978. Specification tests in econometrics. *Econometrica* 46:1251–1271.

Hautsch, N. and Podolskij, M. 2013. Preaveraging-based estimation of quadratic variation in the presence of noise and jumps: theory, implementation, and empirical evidence. *Journal of Business & Economic Statistics* 31:165–183.

He, K., Zhang, X., Ren, S., and Sun, J. 2016. Deep residual learning for image recognition. *In* Proceedings of the IEEE conference on computer vision and pattern recognition, pp. 770–778.

Hoerl, A. E. and Kennard, R. W. 1970. Ridge regression: Biased estimation for nonorthogonal problems. *Technometrics* 12:55–67.

Hornik, K., Stinchcombe, M., and White, H. 1989. Multilayer feedforward networks are universal approximators. *Neural networks* 2:359–366.

Huang, X. and Tauchen, G. 2005. The relative contribution of jumps to total price variance. *Journal of financial econometrics* 3:456–499.

Hutchinson, J. M., Lo, A. W., and Poggio, T. 1994. A nonparametric approach to pricing and hedging derivative securities via learning networks. *The Journal of Finance* 49:851–889.

Jacod, J., Li, Y., and Zheng, X. 2017. Estimating the integrated volatility with tick observations. Technical report.

Jacod, J. and Protter, P. 2011. Discretization of Processes. Springer.

Jacod, J., Rosenbaum, M., et al. 2013. Quarticity and other functionals of volatility: efficient estimation. *The Annals of Statistics* 41:1462–1484.

Jacod, J. and Todorov, V. 2009. Testing for common arrivals of jumps for discretely observed multidimensional processes. *The Annals of Statistics* pp. 1792–1838.

Jacod, J., Todorov, V., et al. 2014. Efficient estimation of integrated volatility in presence of infinite variation jumps. *The Annals of Statistics* 42:1029–1069.

Jiang, G. J. and Oomen, R. C. 2008. Testing for jumps when asset prices are observed with noise–a "swap variance" approach. *Journal of Econometrics* 144:352–370.

Jing, B.-Y., Liu, Z., and Kong, X.-B. 2014. On the estimation of integrated volatility with jumps and microstructure noise. *Journal of Business & Economic Statistics* 32:457–467.

Johannes, M. 2004. The statistical and economic role of jumps in continuous-time interest rate models. *The Journal of Finance* 59:227–260.

Jurado, K., Ludvigson, S. C., and Ng, S. 2015. Measuring uncertainty. *American Economic Review* 105:1177–1216.

Kalnina, I. and Linton, O. 2008. Estimating quadratic variation consistently in the presence of endogenous and diurnal measurement error. *Journal of Econometrics* 147:47–59.

Kim, H. H. and Swanson, N. R. 2016. Mining big data using parsimonious factor, machine learning, variable selection and shrinkage methods. *International Journal of Forecasting* .

Lahaye, J., Laurent, S., and Neely, C. J. 2011. Jumps, cojumps and macro announcements. *Journal of Applied Econometrics* 26:893–921.

Langley, P. 1993. Induction of recursive bayesian classifiers. *In* European Conference on Machine Learning, pp. 153–164. Springer.

Lee, S. S. and Mykland, P. A. 2007. Jumps in financial markets: A new nonparametric test and jump dynamics. *The Review of Financial Studies* 21:2535–2563.

Lee, T., Loretan, M., and Ploberger, W. 2013. Rate-optimal tests for jumps in diffusion processes. *Statistical Papers* 54:1009–1041.

Mancini, C. 2001. Disentangling the jumps of the diffusion in a geometric jumping brownian motion. *Giornale dell'Istituto Italiano degli Attuari* 64:44.

Mancini, C. 2009. Non-parametric threshold estimation for models with stochastic diffusion coefficient and jumps. *Scandinavian Journal of Statistics* 36:270–296.

Mancini, C. and Gobbi, F. 2012. Identifying the brownian covariation from the co-jumps given discrete observations. *Econometric Theory* 28:249–273.

Marcellino, M., Porqueddu, M., and Venditti, F. 2016. Short-term gdp forecasting with a mixed-frequency dynamic factor model with stochastic volatility. *Journal of Business & Economic Statistics* 34:118–127.

Mariano, R. S. and Murasawa, Y. 2003. A new coincident index of business cycles based on monthly and quarterly series. *Journal of Applied Econometrics* 18:427–443.

Masters, T. 1993. Practical neural network recipes in C++. Morgan Kaufmann.

McCracken, M. W. 2000. Robust out-of-sample inference. *Journal of Econometrics* 99:195–223.

McCulloch, W. S. and Pitts, W. 1943. A logical calculus of the ideas immanent in nervous activity. *The bulletin of mathematical biophysics* 5:115–133.

Mukherjee, A. and Swanson, N. 2018. New direction for volatility confidence interval prediction: Evidence from an experimental and empirical study. *Working Paper,* Rutgers University.

Müller, U. A., Dacorogna, M. M., Davé, R. D., Olsen, R. B., Pictet, O. V., and von Weizsäcker, J. E. 1997. Volatilities of different time resolutions?analyzing the dynamics of market components. *Journal of Empirical Finance* 4:213–239.

Müller, U. A., Dacorogna, M. M., Davé, R. D., Pictet, O. V., Olsen, R. B., and Ward, J. R. 1993. Fractals and intrinsic time: A challenge to econometricians. *Unpublished manuscript, Olsen & Associates, Zürich* .

Mykland, P. A. and Zhang, L. 2009. Inference for continuous semimartingales observed at high frequency. *Econometrica* 77:1403–1445.

Neely, C. J., Rapach, D. E., Tu, J., and Zhou, G. 2014. Forecasting the equity risk premium: the role of technical indicators. *Management Science* 60:1772–1791.

Pan, J. 2002. The jump-risk premia implicit in options: Evidence from an integrated time-series study. *Journal of financial economics* 63:3–50.

Peng, W. 2018. Co-jumps, co-jump tests and sector level s&p500 volatility prediction. *Working Paper, Rutgers University* .

Pesaran, M. H. and Timmermann, A. 1992. A simple nonparametric test of predictive performance. *Journal of Business & Economic Statistics* 10:461–465.

Podolskij, M., Vetter, M., et al. 2009. Estimation of volatility functionals in the simultaneous presence of microstructure noise and jumps. *Bernoulli* 15:634–658.

Podolskij, M. and Ziggel, D. 2010. New tests for jumps in semimartingale models. *Statistical inference for stochastic processes* 13:15–41.

Rapach, D. and Zhou, G. 2013. Forecasting stock returns, pp. 328–383. *In* Handbook of economic forecasting, volume 2. Elsevier.

Rapach, D. E., Strauss, J. K., and Zhou, G. 2013. International stock return predictability: what is the role of the united states? *The Journal of Finance* 68:1633–1662.

Rosenblatt, F. 1958. The perceptron: a probabilistic model for information storage and organization in the brain. *Psychological review* 65:386.

Rossi, B. and Inoue, A. 2012. Out-of-sample forecast tests robust to the choice of window size. *Journal of Business & Economic Statistics* 30:432–453.

Swanson, N. R. and White, H. 1997. A model selection approach to real-time macroeconomic forecasting using linear models and artificial neural networks. *Review of Economics and Statistics* 79:540–550.

Swanson, N. R. and Xiong, W. 2017. Big data analytics in economics: What have we learned so far, and where should we go from here?

Tibshirani, R. 1996. Regression shrinkage and selection via the lasso. *Journal of the Royal Statistical Society: Series B (Methodological)* 58:267–288.

Todorov, V. and Tauchen, G. 2012. The realized laplace transform of volatility. *Econometrica* 80:1105–1127.

Vapnik, V. and Chervonenkis, A. 1964. A note on class of perceptron. *Automation and Remote Control* 24.

Welch, I. and Goyal, A. 2007. A comprehensive look at the empirical performance of equity premium prediction. *The Review of Financial Studies* 21:1455–1508.

Yao, C. 2019. Measuring uncertainty using mixed frequency macroeconomic and financial volatility risk factors. *Working Paper, Rutgers University.* .

Zhang, L. et al. 2006. Efficient estimation of stochastic volatility using noisy observations: A multi-scale approach. *Bernoulli* 12:1019–1043.

Zhang, L., Mykland, P. A., and Aït-Sahalia, Y. 2005. A tale of two time scales: Determining integrated volatility with noisy high-frequency data. *Journal of the American Statistical Association* 100:1394–1411.